Distribution Agreement

In presenting this thesis or dissertation as a partial fulfillment of the requirements for an advanced degree from Emory University, I hereby grant to Emory University and its agents the non-exclusive license to archive, make accessible, and display my thesis or dissertation in whole or in part in all forms of media, now or hereafter known, including display on the world wide web. I understand that I may select some access restrictions as part of the online submission of this thesis or dissertation. I retain all ownership rights to the copyright of the thesis or dissertation. I also retain the right to use in future works (such as articles or books) all or part of this thesis or dissertation.

Signature:

_____ _____

Olivia Ann Moody Date

Pharmacologically targeting the $GABA_A$ receptors in neurological disease

By

Olivia Ann Moody
Doctor of Philosophy

Graduate Division of Biological and Biomedical Sciences
Neuroscience

Andrew Jenkins, PhD
Advisor

Paul S. García, MD PhD
Committee Member

Donald G. Rainnie, PhD
Committee Member

David B. Rye, MD PhD
Committee Member

Yoland Smith, PhD
Committee Member

Accepted:

Lisa A. Tedesco, Ph.D.
Dean of the James T. Laney School of Graduate Studies

Date

Pharmacologically targeting the $GABA_A$ receptors in neurological disease

By

Olivia Ann Moody
B.A., Bates College, 2012

Advisor: Andrew Jenkins, PhD

An abstract of
A dissertation submitted to the Faculty of the
James T. Laney School of Graduate Studies of Emory University
in partial fulfillment of the requirements for the degree of
Doctor of Philosophy.

Graduate Division of Biological and Biomedical Sciences,
Neuroscience

2017

Abstract

Pharmacologically targeting the $GABA_A$ receptors in neurological disease

By Olivia Ann Moody

Altering $GABA_A$ receptor activity can shift the balance of inhibition and excitation in the brain, leading to neurological diseases. Two examples where $GABA_A$ receptor activity can be impaired are the daytime sleepiness characteristic of idiopathic hypersomnia (IH) and the increased seizure susceptibility in epilepsy. In both diseases, drugs that target the benzodiazepine site on the $GABA_A$ receptor have been used to modulate symptoms, but further study of this site could help develop novel drugs treatments with fewer side effects. The mechanisms by which $GABA_A$ receptor activity is altered in IH and by rare mutations of the *GABR* genes in epilepsy remain incompletely understood.

In the first part of this thesis, I examined the structure-function relationship of the benzodiazepine binding site on $GABA_A$ receptors. Mutations were created in loop A, loop B, and loop C of the benzodiazepine site across the six different α subunits. Effects were measured using midazolam. Results from whole-cell patch clamp recording of mutated $\alpha_x\beta_2\gamma_{2s}$ receptors revealed that mutating loop A dramatically conferred or abolished the efficacy of midazolam. Surprisingly, mutating loop C also moderately altered the efficacy of midazolam depending on the α subunit mutated.

Second, I assessed the role of the high-affinity benzodiazepine site in mediating the positive allosteric modulator (PAM) actions of cerebrospinal fluid (CSF) taken from hypersomnia patients experiencing IH. Whole-cell patch clamp recording found that hypersomnolent CSF samples enhanced the activity of $\alpha_x\beta_2\gamma_{2s}$ $GABA_A$ receptors, even in receptors without a functional benzodiazepine site. Furthermore, CSF enhanced whole-cell current responses for extrasynaptic $\alpha_x\beta_2\delta$ receptors that are generally insensitive to benzodiazepines. Overall, the CSF results were not consistent with the active component of hypersomnolent CSF acting primarily through the high-affinity benzodiazepine site of the $GABA_A$ receptors.

Third, three rare, novel *GABR* mutations identified in pediatric patients with severe early-onset epilepsy were characterized. Whole-cell patch clamp recording showed that the mutations in the M2 and M2-M3 linker domains can alter the gating, desensitization and GABA apparent-affinity of receptors. Results offer insight into which GABAergic treatments may or may not be beneficial to patients with rare variants.

Understanding the pharmacology of $GABA_A$ receptors as they relate to neurological diseases will offer new insights for better treating diseases.

Pharmacologically targeting the $GABA_A$ receptors in neurological disease

By

Olivia Ann Moody
B.A., Bates College, 2012

Advisor: Andrew Jenkins, PhD

A dissertation submitted to the Faculty of the
James T. Laney School of Graduate Studies of Emory University
in partial fulfillment of the requirements for the degree of
Doctor of Philosophy.

Graduate Division of Biological and Biomedical Sciences,
Neuroscience

2017

Table of contents:

List of Figures and Tables by Chapter

Chapter 1:

Chapter 2:

Chapter 3:

Chapter 4:

Chapter 5:

Chapter 1: Introduction

Chapter 1: Introduction

To maintain proper brain function and prevent disease, a balance between excitation and inhibition is necessary. Excitation drives neurons to fire, whereas inhibition suppresses neuronal activity. In the brain, excitatory input is most often mediated by glutamatergic neurotransmission, while inhibition is mediated by GABAergic neurotransmission. Inhibition helps tune the timing of neural circuits across the brain, playing a role in neuroplasticity and rhythmic oscillations (Knoflach, Hernandez, & Bertrand, 2016) When GABAergic inhibition is disrupted, diseases can occur. Seizure disorders are a physiological phenomena where the balance of excitation and inhibition is disrupted. When neurons become overexcited and start firing in synchrony, a seizure can begin (Scharfman, 2007). On the other hand, enhancing GABAergic inhibition can suppress neural activity, as seen when sedatives and general anesthetics suppress consciousness (Franks & Zecharia, 2011). Disorders associated with changes in GABAergic inhibition include autism spectrum disorders, Down syndrome, schizophrenia and neurodegenerative disorders (Kim & Yoon, 2017; Knoflach et al., 2016). Recently, early-onset epilepsies have been linked to mutations in the $GABA_A$ receptor genes (Moller et al., 2017). To better treat neurological diseases in which inhibition is altered, the molecular mechanisms underlying neuronal inhibition must be examined.

The $GABA_A$ receptors are a common target of therapies seeking to alter inhibition in the brain to treat diseases. The 19 different subunits that can make up $GABA_A$ receptors provide a multitude of different binding sites for exogenous and endogenous compounds. Examples of therapeutics targeting $GABA_A$ receptors are benzodiazepines, general anesthetics, barbiturates and ethanol. The following dissertation seeks to examine how $GABA_A$ receptor activity can be altered pharmacologically or through mutation to either increase or decrease GABAergic inhibition.

1.1 $GABA_A$ receptors and GABAergic neurotransmission in the brain

Gamma-aminobutyric acid (GABA) is an inhibitory neurotransmitter found throughout the central nervous system. GABA is formed the decarboxylation of the amino acid glutamate and is considered an amino acid neurotransmitter. In the brain, between 20-50% of the synapses use GABA as a neurotransmitter (Sieghart, 1995a). GABA synthesis has been shown across many organisms from bacteria to humans. It was first localized to inhibitory nerve terminals in the mammalian brain in the early 1970's (Bloom & Iversen, 1971; Owens & Kriegstein, 2002). GABA is synthesized when glutamate is converted to GABA via the enzyme glutamate decarboxylase (GAD). GAD65 and GAD67 are two isoforms expressed in GABAergic neurons (Owens & Kriegstein, 2002).

In the brain, GABA's actions are mediated primarily through the ionotropic $GABA_A$ receptors and metabotropic $GABA_B$ receptors. $GABA_A$ receptors mediate the majority of fast inhibitory transmission in the mammalian CNS (Olsen & Sieghart, 2008). $GABA_B$ receptors are heterodimeric G_i/G_o-coupled receptors. They suppress high-voltage-activated calcium channels ($Ca_v2.1$, $Ca_v2.2$) pre-synaptically or activate inwardly-rectifying potassium channels post-synaptically (Owens & Kriegstein, 2002). The $GABA_B$ receptors mediate slower inhibitory neurotransmission (Bormann, 1988). Modulators that bind $GABA_A$ receptors generally do not bind to $GABA_B$ receptors, and so the two receptors each have a distinct pharmacology (Olsen & Sieghart, 2008).

Aside from the CNS, $GABA_A$ receptors are also found outside the CNS in other tissues. They have been identified in tissue from the lung, pancreas, digestive tract, liver, chondrocytes, and testicular cells (Jin et al., 2008; Ong & Kerr, 1990; X. Zhang et al., 2013). Outside of the CNS, GABA signaling has been linked with cell proliferation (Labrakakis, Patt, Hartmann, & Kettenmann, 1998). The expression of *GABR* genes has also been seen in different types of cancers, including medulloblastoma (Sengupta et al., 2014), lung cancer (X. Zhang et al., 2013) and breast cancer (Sizemore, Sizemore,

Seachrist, & Keri, 2014). However, GABA's role in mediating a proper balance of inhibition and excitation in the brain depends on the $GABA_A$ and $GABA_B$ receptors in the CNS.

In the adult mammalian brain, the activation of $GABA_A$ receptors results in increased chloride permeability, hyperpolarizing the membrane potential (Figure 1.1A) (Olsen & Sieghart, 2008). This is because mature neurons generally have lower intracellular than extracellular chloride concentrations. The chloride equilibrium potential is closer to the resting membrane potential. When the channels open, the influx of chloride shifts the membrane potential of neurons towards the chloride equilibrium potentiation, hyperpolarizing the membrane potential (Olsen & Sieghart, 2008). Although $GABA_A$ receptors are commonly associated with chloride flux, the channel can also pass other anions, such as bicarbonate (HCO_3^-) (Bormann, Hamill, & Sakmann, 1987).

During development, $GABA_A$-mediated signaling instead causes depolarization. The increased expression of the $Na+/K^+/2Cl^-$ co-transporter (NKCC1) during development results in the accumulation of chloride intracellularly, leading to depolarization when the channels open (Hubner & Holthoff, 2013). The switch in the CNS from depolarizing to hyperpolarizing chloride signals occurs during development when NKCC1 expression decreases and the expression of the cation-chloride co-transporter 2 (KCC2) increases (Watanabe & Fukuda, 2015). KCC2 extrudes chloride from the neurons, leading to lower intracellular chloride levels found in mature neurons. This leads to the $GABA_A$ receptor-mediated hyperpolarizing signals found in the adult brain that reduce neuronal excitability and neuronal firing rates.

GABAergic neurotransmission can either be phasic or tonic (Figure 1.1B). Phasic GABAergic transmission is synaptic. Synaptic signals are neuron-to-neuron signals that are temporally-specific and cause inhibitory post-synaptic potentials (IPSPs). In synaptic GABAergic transmission, GABA is loaded into synaptic vesicles by the vesicular neurotransmitter transporter (VGAT) and then released into the synapse via calcium-

dependent exocytosis (Owens & Kriegstein, 2002). During a synaptic event, GABA reaches millimolar concentrations which are cleared rapidly from the synapse on the time scale of 100's of microseconds (Farrant & Nusser, 2005). Non-phasic GABAergic signals, also called tonic inhibition, are less spatially and temporally restricted signals. Tonic inhibition is due to a combination of GABA spillover from nearby synapses and ambient, extracellular GABA (Farrant & Nusser, 2005). Non-vesicular release of GABA plays an important role in the developing nervous system (Owens & Kriegstein, 2002). Non-vesicular release of GABA has also been measured from astrocytes, which may contribute to setting the tonic inhibition levels in the brain (Yoon & Lee, 2014). The subunit composition of both extrasynaptic and synaptic $GABA_A$ receptors affects their functional properties.

$GABA_A$ receptors are cys loop ligand-gated ion channels (LGICs). They belong to the pentameric cys loop LGIC family along with nicotinic acetylcholine receptors (nAChRs), ionotropic 5-hydroxytryptamine$_3$ ($5\text{-}HT_3$) receptors and glycine receptors (Cromer, Morton, & Parker, 2002). As pentameric channels, they are made up of five subunits around a central ion pore. Like other cys loop LGICs, the $GABA_A$ receptor subunits have a common secondary and tertiary structure (Cromer et al., 2002). Each subunit consists of a long extracellular N-terminal domain, four transmembrane domains (M1, M2, M3 and M4) and short extracellular C-terminal domain (Figure 1.2A) (Olsen & Sieghart, 2008). There is also a large and variable intracellular loop between the third and fourth transmembrane domains (M3-M4) called the cys loop. The cys loop plays a role in trafficking, binding accessory proteins and channel function (Bracamontes, Li, Akk, & Steinbach, 2014; O'Toole & Jenkins, 2011). The M2 domain from each subunit forms the pore of the channel (Miller & Aricescu, 2014). In $GABA_A$ receptors, GABA binds to a site in the extracellular domain. This leads to a conformational change that opens the channel in the transmembrane region, allowing chloride ions to move along their concentration

gradient (Kash, Trudell, & Harrison, 2004). A rotational conformational movement of all five M2 domains is responsible for gating (opening and closing) the channel (Bera & Akabas, 2005; Nigel Unwin, 1995; N. Unwin, 2005). The pre-M1 region and M2-M3 linker mediate the transduction of the signal from the GABA binding site to the opening of the channel (Michalowski, Kraszewski, & Mozrzymas, 2017). The M2-M3 linker region also mediates the gating of the channel (Kash, Jenkins, Kelley, Trudell, & Harrison, 2003). The structure of each subunit varies across isoforms and affects channel function.

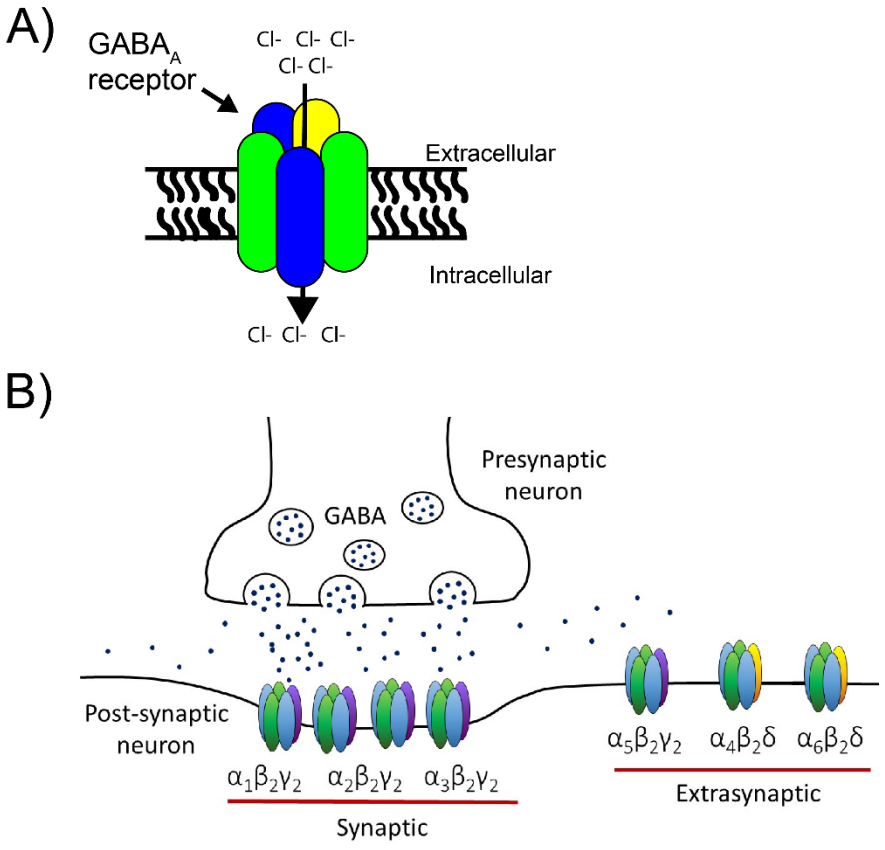

Figure 1.1. Structure of the GABA$_A$ receptor. A) GABA$_A$ receptors are pentameric anion channels that pass primarily chloride. B) Synaptic and extrasynaptic GABA$_A$ receptors expressed in the post-synaptic neuron. The most common predicted subunit assemblies are shown for each.

There is approximately 30% sequence homology among the cys loop ligand-gated ion channel superfamily. Further homology across the secondary and tertiary structures is also found (Olsen & Sieghart, 2008). Structural modeling of the other cys loop channels and related proteins has provided insight to the ligand-binding domains and structure of the $GABA_A$ receptor. The crystal structure of the acetylcholine binding protein (AChBP), a soluble protein found in the snail *Lymnaea stagnalis*, has been used to derive homology-driven models of the extracellular ligand-binding domains of nicotinic acetylcholine receptors (nAChRs) and the $GABA_A$ receptor (Brejc et al., 2001; Cromer et al., 2002). Recently, a crystal structure of a human beta homopentamer $GABA_A$ receptor at 3 Å resolution was achieved by Miller and Aricescu (Miller & Aricescu, 2014). This confirmed some of the predicted structures in the $GABA_A$ receptor, including the residues lining the pore and how certain epilepsy mutations disrupt receptor function. A heteropentamer crystal structure for the $GABA_A$ receptor continues to be sought to map specific allosteric binding sites on the receptor (Miller & Aricescu, 2014).

The 19 mammalian $GABA_A$ receptor subunits are coded by the *GABR* genes. The human *GABR* genes have been mapped to different chromosomes. The α1, α6, β2 and γ2 genes are located on chromosome locus 5q31.3-q33.2, while α5, β3 and γ3 genes are located at the 15q11-q13 locus. The α2, α4, β1 and γ1 are located at 4p13-4q11 locus (P. J. Whiting, McKernan, & Wafford, 1995). The α3 and δ are each located in isolation from other GABR subunits on Xq28 and 1p loci, respectively.

The $GABA_A$ receptors are differentially expressed across brain regions. The δ subunit's expression is expressed in the granule cells of the cerebellum, the thalamus, the dentate molecular layer, the subiculum and parts of the cerebral cortex and striatum (Pirker, Schwarzer, Wieselthaler, Sieghart, & Sperk, 2000). The γ2 subunit, on the other hand, is expressed throughout the brain, while γ1- and γ3- subunits are less abundant (Quirk, Gillard, Ragan, Whiting, & McKernan, 1994). The expression of specific $GABA_A$

subunits also changes over the course of development (Laurie, Wisden, & Seeburg, 1992). For example, in the thalamus, the α2, α3 and α5 subunits are present during embryonic development but have reduced mRNA levels in adult neurons when α1 and α4 become the most heavily expressed α subunits (Laurie et al., 1992). The *GABR* subunit expression in different brain regions determines the composition of different $GABA_A$ receptors in that region.

The expression of γ2 can alter the number of synaptic $GABA_A$ receptors. The loss of all γ2 in knock-out mice reduces the synaptic clustering of $GABA_A$ receptors. It also reduces gephyrin, a scaffolding protein that binds to γ2 and targets $GABA_A$ receptors to the synapse (Essrich, Lorez, Benson, Fritschy, & Luscher, 1998). Although $GABA_A$ receptors can diffuse within the cell membrane, the γ subunit and scaffolding proteins like gephyrin allow specific receptor assemblies to be more likely synaptic (αβγ) than extrasynaptic (αβδ). There are two γ slice variants for γ2, the long γ2 (γ2L) and the short γ2 (γ2s) found in the brain. These variants are created by RNA splicing. The long γ2 isoform has an eight amino acid insert into the intracellular loop (P. Whiting, McKernan, & Iversen, 1990). The insert contains a phosphorylation site for protein kinase C (PKC). Phosphorylation of the $GABA_A$ receptors is important for regulating receptor insertion into the cell membrane and so the regulation of endocytosis (Abramian et al., 2010; Comenencia-Ortiz, Moss, & Davies, 2014).

Heteropentameric $GABA_A$ receptors assemble from three subunits of 19 *GABR* gene products (α1-6, β1-3, γ1-3, δ, ε, θ, π, ρ1-3). With 19 different subunits, there are, in theory, hundreds of possible combinations, but only a limited number of specific combinations have been shown to specifically exist in the CNS (Olsen & Sieghart, 2008). The main subunit stoichiometry of $GABA_A$ receptors in the brain is 2:2:1 for α, β, and 1 auxiliary subunit (γ or δ) (Figure 1.2B) (Olsen & Sieghart, 2008). The $\alpha_1\beta_{2/3}\gamma_2$ receptor is

one of the most common synaptic $GABA_A$ receptor assemblies in the brain (Benke, Mertens, Trzeciak, Gillessen, & Mohler, 1991; Jean-Marc Fritschy & Hanns Mohler, 1995).The other assemblies that have been identified in the CNS with strong evidence are: $\alpha_1\beta_2\gamma_2$, $\alpha_2\beta\gamma_2$, $\alpha_3\beta\gamma_2$, $\alpha_4\beta\gamma_2$, $\alpha_4\beta_2\delta$, $\alpha_4\beta_3\delta$, $\alpha_5\beta\gamma_2$, $\alpha_6\beta\gamma_2$, $\alpha_6\beta_2\delta$, and $\alpha_6\beta_3\delta$ (Olsen & Sieghart, 2008). This does not exclude other subunit combinations from existing, but they most likely account for a smaller ratio of the total GABAergic inhibition in the brain.

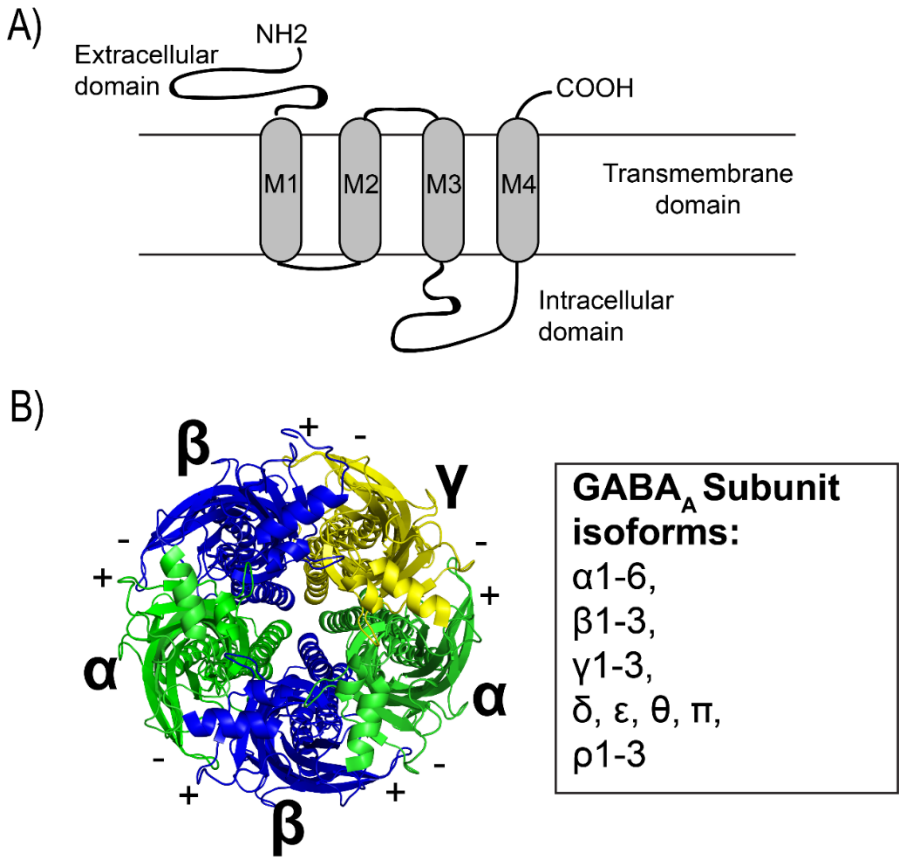

Figure 1.2. Subunit composition of pentameric $GABA_A$ receptors. A) Structural domains of a $GABA_A$ receptor subunit include the N-terminal extracellular domain, 4 transmembrane domains, an intracellular cys loop domain, and a C-terminal domain. B) The main subunit stoichiometry of a synaptic $GABA_A$ receptor is 2:2:1 for the α, β, and γ subunits. The interfaces of subunits are labeled + and – to help specify interfaces. There are 19 different $GABA_A$ receptor subunits coded for by the *GABR* genes.

Homomeric channels have also been studied. In *in vitro* recombinant studies, homomeric α and homomeric β channels can both form functional channels that pass current and are sensitive to picrotoxin and barbiturates (Blair, Levitan, Marshall, Dionne, & Barnard, 1988; Pritchett et al., 1988). However, homomeric channels form at lower efficiencies than heteropentamer channels (Pritchett et al., 1988). The αβ-only receptors may exist in the brain, but probably only contribute a small amount of inhibitory current relative to the αβγ receptors (Botzolakis et al., 2016; Eaton et al., 2014; Olsen & Sieghart, 2008; Sieghart et al., 1999). The subunit composition of the receptor also affects the kinetics and functional responses of the receptor.

The subunit composition of individual $GABA_A$ receptors affects their functional properties. These properties include the kinetics, desensitization, and the ability to be modulated by different drugs (A. Draguhn, T. A. Verdorn, M. Ewert, P. H. Seeburg, & B. Sakmann, 1990; Gingrich, Roberts, & Kass, 1995; Levitan, Blair, Dionne, & Barnard, 1988; McClellan & Twyman, 1999; Verdoorn, Draguhn, Ymer, Seeburg, & Sakmann, 1990). For example, the incorporation of the γ2s subunit into αβ receptors reduces desensitization and accelerates deactivation (Boileau, Li, Benkwitz, Czajkowski, & Pearce, 2003). In terms of modulatory properties, the αβ receptors are more sensitive to zinc inhibition while αβγ receptors are not (Andreas Draguhn, Todd A. Verdorn, Markus Ewert, Peter H. Seeburg, & Bert Sakmann, 1990; Trudell, Yue, Bertaccini, Jenkins, & Harrison, 2008). Also, the αβγ receptors can be modulated by benzodiazepines but αβδ receptors cannot (Barnard et al., 1998). Distinctive properties like these make the subunit composition of $GABA_A$ receptors highly relevant to their function.

There are six α $GABA_A$ subunit isoforms (α1-6), each of which contributes specific properties to receptor function. The alpha subunit is a major determinant of the pharmacological and kinetic properties of αβγ $GABA_A$ receptors. The α2 subunit slows the deactivation of inhibitory post-synaptic currents (Dixon, Sah, Lynch, & Keramidas, 2014).

The α3 subunit enhances the GABA apparent-affinity and slows the activation rate of $\alpha_3\beta_2\gamma_2$ receptors relative to $\alpha_1\beta_2\gamma_2$ receptors (Gingrich et al., 1995). The α6 subunit contributes a higher GABA sensitivity than α1 in $\alpha_x\beta_2\gamma_2$ receptors (Kleingoor, Wieland, Korpi, Seeburg, & Kettenmann, 1993). Finally, the α subunit also affects allosteric modulation, especially that of benzodiazepines for which the α subunit forms half of the binding site of (Benson, Low, Keist, Mohler, & Rudolph, 1998; Petroski et al., 2006; Puia, Vicini, Seeburg, & Costa, 1991). This will be further elaborated upon in later sections.

The expression patterns of each α subunit vary widely across the brain (Jean-Marc Fritschy & Hanns Mohler, 1995; Pirker et al., 2000). The α1 subunit is abundant in all brain regions (Jean-Marc Fritschy & Hanns Mohler, 1995). The α2 subunit is expressed in the limbic system, including the pyramidal cells of the cortex and hippocampus. Subcellularly, α2 is located on the axon initial segment, presumably controlling the output of the principal neurons (Low et al., 2000). The a3 subunit is expressed in the reticular activating system (Low et al., 2000). The highest concentrations of α4 exist in the thalamus but also in the striatum, nucleus accumbens and dentate gyrus (Pirker et al., 2000). The α5 subunit is expressed most highly in the pyramidal hippocampal cells but also in parts of the cerebral cortex and hypothalamus (Lee & Maguire, 2014; Pirker et al., 2000; Serwanski et al., 2006; Winsky-Sommerer, 2009). The α6 subunit is highly restricted to the granule cells of the cerebellum (Luddens et al., 1990). Although a few studies have shown the expression of two α isoforms within one neuron, most $GABA_A$ receptors are thought to have only one α isoform per receptor (Barnard et al., 1998). The expression patterns of $GABA_A$ subunits also vary across development (Laurie et al., 1992). Subunit composition plays an important role in conferring specific pharmacological properties to $GABA_A$ receptors.

1.2 Modulators of $GABA_A$ receptors

Modulators alter the activity of receptors. A multitude of exogenous and endogenous modulators can modulate $GABA_A$ receptors (Figure 1.3). The International Union of Basic and Clinical Pharmacology (IUPHAR) website lists many of the officially recognized ligands and modulators of $GABA_A$ receptors. In total, IUPHAR lists 5 agonists, 2 antagonists, 2 channel blockers, 3 endogenous allosteric modulators, 15 allosteric modulators, 5 selective allosteric modulators (subunit selective), and 8 labelled ligands that act at $GABA_A$ receptors. The endogenous allosteric modulators listed are zinc, 5α-pregnan-3α-ol-20-one, and tetrahydrodeoxycorticosterone. Non-endogenous allosteric modulators listed include flumazenil, clonazepam, flunitrazepam, diazepam, alprazolam, α3IA, α5IA, bretazenil, DMCM, MRK016, Ro15-4513, Ro19-4603, RO4938581, TP003, and TPA023. Although many of these compounds have behavioral effects or clinical utility, some of these ligands are research tools only used to study basic $GABA_A$ receptor function. Many more than the above modulators and ligands of the $GABA_A$ receptors exist and continue to be developed. $GABA_A$ receptors have many extracellular and transmembrane binding pockets for different modulators to bind (Figure 1.3)

The most commonly studied modulators of $GABA_A$ receptors are barbiturates, benzodiazepines, alcohol, general anesthetics, and neurosteroids. Barbiturates enhance $GABA_A$ receptor activity by lengthening the single channel opening time and at high concentrations they can directly open the channel (Study & Barker, 1981; Thompson, Whiting, & Wafford, 1996; P. J. Whiting et al., 1995). Benzodiazepines are allosteric modulators of $GABA_A$ receptors, acting at the α+/γ- interface (Cromer et al., 2002). They modulate receptor activity by increasing or decreasing the single channel opening frequency (Study & Barker, 1981). Ethanol enhances extrasynaptic $GABA_A$ receptor activity, particularly those containing the δ subunit. Alcohol depresses neuronal excitability in regions like the cerebellum, leading to behaviors such as impaired motor skills (Yoon &

Lee, 2014). Many general anesthetics enhance $GABA_A$ receptor activity, an important part of their mechanism of action in the brain (Franks, 2008). For example, propofol binds to the β subunit within the transmembrane domain (Krasowski, Nishikawa, Nikolaeva, Lin, & Harrison, 2001; Yip et al., 2013). Etomidate also enhances $GABA_A$ receptor activity with a transmembrane binding site between the α and β subunits (G. D. Li et al., 2006). The steroids 5α-pregnan-3α-ol-20-one (allopregnanolone) and 5α-pregnan-3α,21-diol-20-one can allosterically enhance $GABA_A$ receptor activity, and at high concentrations directly activate the receptor (P. J. Whiting et al., 1995). Understanding the molecular mechanisms of modulators acting at $GABA_A$ receptors will not only improve our understanding of existing drugs but also contribute new knowledge to the development of novel therapeutics.

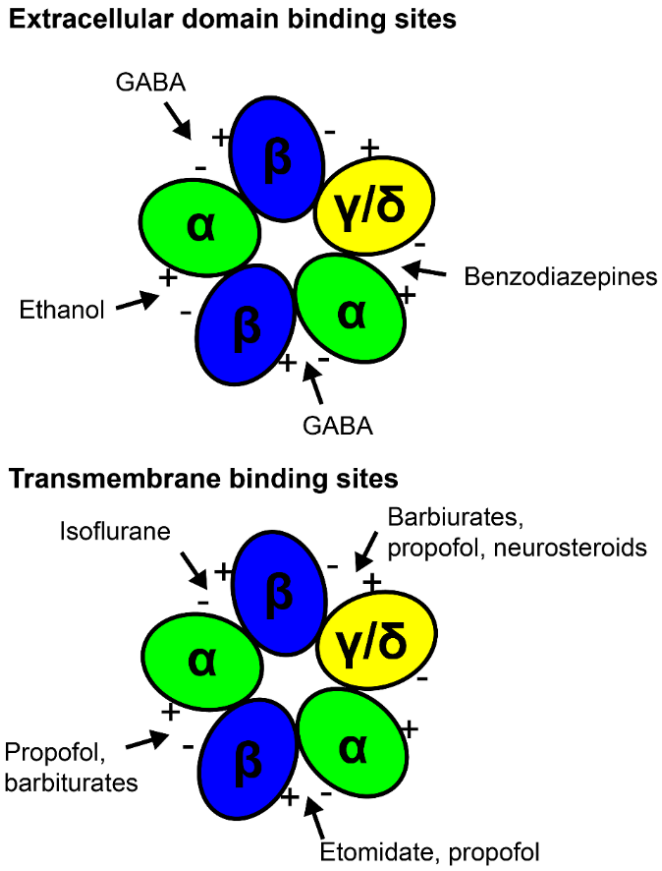

Figure 1.3. Proposed binding sites for various modulators of the $GABA_A$ receptor. Binding sites are shown for the extracellular domains and for the transmembrane domains. Binding sites based on information from review by Olsen, 2015.

1.3 Benzodiazepines act at $GABA_A$ receptors

1.3.1 Benzodiazepines

Benzodiazepines are one of the most prescribed drugs in the U.S. with estimates around 75-85 million prescriptions prescribed nationally in 2007-2008 (Olfson, King, & Schoenbaum, 2015). As a general drug class, benzodiazepines cause sedation, hypnosis, anxiolysis, anterograde amnesia, muscle relaxation and have anti-convulsive effects (Olkkola & Ahonen, 2008). In general, benzodiazepines are prescribed as mood regulators and anxiolytics for outpatients (Olfson et al., 2015). In clinical anesthesia, benzodiazepines are used for their sedative and anterograde amnesia effects (Olkkola & Ahonen, 2008). One of the earliest benzodiazepines developed was diazepam, often considered a "classic benzodiazepine." Diazepam was first synthesized in 1959 by Sternbac and Reeder and later marketed by Hoffman-LaRoche in 1963 as Valium®. Once developed, benzodiazepines began to replace barbiturates as sedative-hypnotics in clinical medicine due to their improved therapeutic index and the reduced risk of overdoses (Gravielle, 2016; Rudolph & Knoflach, 2011). In clinical anesthesia, the four commonly used benzodiazepines are midazolam, diazepam, lorazepam, and flumazenil (commonly referred to as a benzodiazepine antagonist) (Olkkola & Ahonen, 2008). Flumazenil is used to reverse benzodiazepine overdoses and benzodiazepine-induced sedation during general anesthesia (Olkkola & Ahonen, 2008). Benzodiazepines are also a first-line treatment for status epilepticus (Diviney, Reynolds, & Henshall, 2015). Novel benzodiazepines are continually being developed and as a group are one of the most prescribed oral medications in the western world (Malamed, 2010).

After benzodiazepines were introduced to medicine, the search for the "benzodiazepine receptor" began. In the 1980's and 1990's, $GABA_A$ receptors were a recognized target for benzodiazepines in the mammalian brain (Sigel, Stephenson, Mamalaki, & Barnard, 1983; Stephenson, Watkins, & Olsen, 1982). Initially, $GABA_A$

receptors were classified as benzodiazepine type I and benzodiazepine type II receptors depending on their binding affinity for diazepam (Barnard et al., 1998). Benzodiazepine type I receptors were found to be α1-containing $GABA_A$ receptors, while benzodiazepine type II receptors contained α2, α3 or α5 subunits (Luddens et al., 1990; Wingrove et al., 2002). This terminology was eventually replaced with more specific $GABA_A$ receptor terminology as the molecular genetics of $GABA_A$ receptor assemblies found in the mammalian brain revealed itself (Barnard et al., 1998). Although benzodiazepines can bind peripheral translocator protein receptors involved in cholesterol transport, these effects are not relevant to the sedative, anxiolytic, and amnestic effects mediated by the CNS (Jaremko, Jaremko, Jaipuria, Becker, & Zweckstetter, 2015).

$GABA_A$ receptors in the CNS are one of the primary sites of action for benzodiazepines (Rudolph et al., 1999; G. B. Smith & Olsen, 1995). Many benzodiazepines enhance $GABA_A$ receptor-mediated current, increasing the apparent-affinity of the receptor for GABA. They increase the frequency at which single $GABA_A$ receptors open (Rogers, Twyman, & Macdonald, 1994; Study & Barker, 1981). Therefore, less GABA is required to induce a given receptor response in the presence of benzodiazepines. At the synaptic level, benzodiazepines can increase the amplitude and prolong the decay of IPSPs (Martin & Olsen, 2000). Overall, this leads to increased GABAergic inhibition in the brain (Rudolph et al., 1999; G. B. Smith & Olsen, 1995).

Two important molecular properties of benzodiazepines make their pharmacology therapeutically useful in the clinic. First, the molecular actions of benzodiazepines at $GABA_A$ receptors are self-limiting. This means that benzodiazepines cannot increase the GABA conductance of the receptors beyond that caused by saturating GABA concentrations (Rudolph & Knoflach, 2011). Even at very high concentrations benzodiazepines cannot increase the activity of $GABA_A$ receptors beyond the physiologically-set range of activity. Second, benzodiazepines are allosteric modulators

of $GABA_A$ receptors and are unable to directly open the $GABA_A$ receptor in the absence of GABA. This also limits the actions of benzodiazepines at these receptors at excessively high concentrations because GABA.

1.3.2: Genetic knock-in mice & benzodiazepines

Transgenic knock-in mice with specific mutations in the $GABA_A$ receptors have provided important insights into the mechanisms of benzodiazepines. The first benzodiazepine-related $GABA_A$ receptor mutation knocked-into a mouse was the histidine-to-arginine point mutation (H101R) in the α1 $GABA_A$ subunit. This particular histidine is located in the high-affinity binding site for benzodiazepines and is found in the $GABA_A$ receptor subunits sensitive to diazepam and other positive benzodiazepines. When the α1(H101R) mutation was knocked-into a transgenic mouse it abolished the behavioral response of the mouse to the sedative and amnestic effects of diazepam (Rudolph et al., 1999). The anti-convulsant effects of diazepam were also partly reduced, while the anxiolytic and muscle relaxant effects remained unchanged. This α1(H101R) knock-in mouse model was useful for separating out the specific clinical effects of diazepam because the mutation did not alter the expression of the affected α1 subunit in the brain or the sensitivity of the receptor to GABA (Rudolph et al., 1999). The expression of the other $GABA_A$ receptor subunits in the brain was also not dramatically altered. Results from this transgenic mouse allowed researchers to conclude that the α1 subunit contributes to the sedative, amnestic and anti-convulsant effects of diazepam but not the anxiolytic and muscle relaxant effects (Rudolph et al., 1999). These results were also confirmed in a separate transgenic α1(H101R) knock-in mouse created by McKernan and colleagues (McKernan et al., 2000). These knock-in mice had normal $GABA_A$ receptor expression and responses to GABA, but with reduced diazepam binding and molecular potentiation of GABA responses by diazepam (Rudolph, Crestani, & Mohler, 2001).

As a result of the important mechanistic conclusions drawn from these transgenic mice, H101R mutation was subsequently knocked into other α $GABA_A$ receptor subunits individually into (α2(H101R), α3(H126R) and α5(H105R) mice. These mice were characterized behaviorally and different benzodiazepines tested, as with α1(H101R) mice. At the molecular level, binding assays confirmed the reduction of diazepam-insensitive $GABA_A$ receptors in the brains of α1(H101R), α2(H101R), α3(H126R), and α5(H105R) knock-in mice (Crestani et al., 2002; Low et al., 2000; Rudolph et al., 1999).

The α1(H101R), α2(H101R), α3(H126R) and α5(H105R) mutations have individually been knocked-into transgenic mice one at a time, revealing the following results about diazepam's clinical effects. These clinical effects can be separated into the sedative, anxiolytic and other effects of benzodiazepines which depend on the α subunit expressed. The sedative-hypnotic effects of diazepam and zolpidem are mediated by α1-containing $GABA_A$ receptor and not receptors expressing other α subunits like the α2 or α3 subunits (Kopp, Rudolph, Keist, & Tobler, 2003; Low et al., 2000; McKernan et al., 2000; Rudolph & Mohler, 2004). It is important to note that diazepam-induced sedation does not reflect natural sleep. Studies of the α2(H101R) and α3(H126R) knock-in mice revealed that the anxiolytic effects of diazepam are mediated through the α2 subunit and not α3 (Low et al., 2000). The anti-convulsive effects of diazepam and zolpidem are mediated through the α1 subunit and not the α2 or α3 subunits (Crestani, Martin, Mohler, & Rudolph, 2000; Low et al., 2000; Rudolph et al., 1999). The myorelaxant effect of benzodiazepines may be mediated by multiple subunits including the α2, α3, and α5 subunits (Crestani et al., 2001; Rudolph & Mohler, 2004). Another clinical feature of benzodiazepines that can occur with long-term use is the development of tolerance. The α5 subunit partly mediates this for diazepam (van Rijnsoever et al., 2004). The α5(H105R) knock-in mice also displayed improved performance in hippocampal-dependent tasks,

leading some to suggest that reducing α5-mediated GABAergic inhibition can improve cognitive performance (Yee et al., 2004).

The use of transgenic knock-in mice to dissect out the contributions of different α subunits to behavioral effects does have several limitations. Compensatory changes in the levels and expression of the remaining α-subunits remains a key limitation of these knock-in studies, even when general levels of the $GABA_A$ subunits remain unchanged. Another limitation is that if one mutation eliminates a response, it does not completely rule out the contributions of the other subunits. For example, two other subunits might contribute opposing effects to a drug (ex. sedative vs. arousing) that cancel each other out and cannot be detected. However, overall these knock-in studies have provided important information regarding the molecular mechanisms underlying benzodiazepine-mediated actions through the $GABA_A$ receptors.

1.3.3: Positive and negative allosteric modulators of benzodiazepines

The term benzodiazepine refers to the chemical structure of drugs which contain a benzene ring fused to a diazepine ring with two nitrogen atoms, usually located at the 1 and 4 positions (1,4 benzodiazepines) (Figure 1.4) (Rudolph & Knoflach, 2011).

Benzodiazepine site ligands are allosteric modulators. They alter the function of $GABA_A$ receptors by altering the binding and/or efficacy of GABA's actions at the receptor. Altering GABA's affinity would alter its tendency to form a receptor-ligand complex, while altering GABA's efficacy would alter the efficiency with which GABA elicits a biological response from the receptor once bound. Benzodiazepines can be positive, neutral or negative modifiers of $GABA_A$ receptor activity. Ultimately, positive and negative benzodiazepines stabilize different receptor conformations, leading to different levels of current being passed by the receptor (Rudolph & Knoflach, 2011). Positive benzodiazepines increase the activity of $GABA_A$ receptors, leading to enhanced

GABAergic neurotransmission in the brain. Commonly studied positive benzodiazepines include diazepam, zolpidem and midazolam. Zolpidem is a highly α1-specific imidazopyridine with less affinity for α2-, α3- and α5-containing receptors (Pritchett & Seeburg, 1990; Rudolph & Knoflach, 2011). Negative benzodiazepines bind the receptor and decrease the activity of $GABA_A$ receptors. They can also be called inverse agonists for the benzodiazepine site. Examples of negative benzodiazepine are the β-carbolines β-CCM (β-methyl-β-carboline-3-carboxylate), β-CCE (ethyl β-carboline-3-carboxylate), and DMCM (methyl 6,7-dimethoxy-4-ethyl-β-carboline-3-carboxylate). Beta-carbolines tend to bind α4- and α6-containing receptors (Stevenson, Wingrove, Whiting, & Wafford, 1995; Whittemore, Yang, Drewe, & Woodward, 1996). A neutral benzodiazepine would bind the benzodiazepine site and not alter the efficacy or binding of GABA to the receptor. However, its binding would prevent other benzodiazepine site ligands from binding that site. Flumazenil (also known as Ro 15-1788) is sometimes refered to as a competitive benzodiazepine antagonist and sometimes a neutral benzodiazepine, although its molecular pharmacology at $GABA_A$ receptors is complex depending on the concentration and the subunit composition of the receptors (Mohler, 2015; Rudolph & Knoflach, 2011; Safavynia et al., 2016).

Not all researchers prefer to use the terms positive benzodiazepine and negative benzodiazepine. However, these terms are helpful to discriminate the direction of allosteric modulation induced by a benzodiazepine. It can distinguish different benzodiazepines like β-CCM that can bind $\alpha_4\beta_2\gamma_2$ receptors but do not enhance receptor activity. For the rest of this dissertation, I will refer to positive benzodiazepines as positive allosteric modulators (PAMs) that enhance $GABA_A$ receptor activity, often through α1/α2/α3/α5-containing receptors and not through α4/α6-containing receptors. The term “negative benzodiazepine” will refer to benzodiazepine site ligands that often bind α4/α6-containing receptors and are negative allosteric modulators (NAMs).

A)

Example benzodiazepines:

Positive:
- diazepam
- flurazepam
- midazolam
- lorazepam
- flunitrazepam
- clonazepam
- zolpidem
- eszopiclone

Negative or inverse agonists:
- Ro 15-4513
- β- carbolines
- DMCM (methyl-6,7-dimethoxy-4-ethyl-beta- carboline-3-carboxylate)

Antagonists:
- Flumazenil (R0 15-1788)

1,4 benzodiazepine backbone:

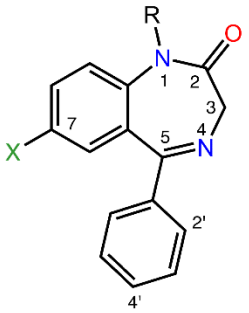

B) Positive Benzodiazeines:

Diazepam

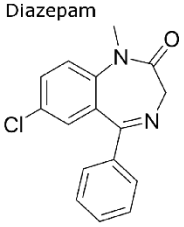

Lorazepam

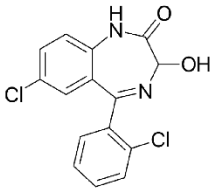

Flunitrazepam

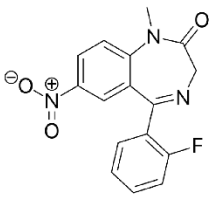

Imidazobenzodiazepines:

Midazolam

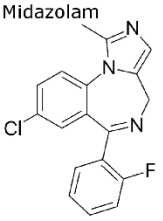

Flumazenil (Ro 15-1788)

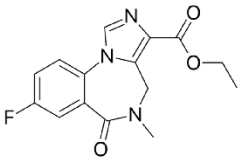

Ro 15-4513

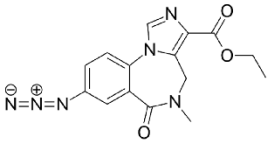

Negative Benzodiazepine:

DMCM

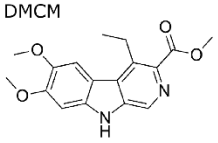

Non-Benzodiazepiones (Z-drugs):

Zolpidem

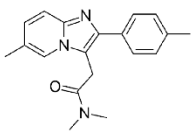

Imidazopyridine

Eszopiclone

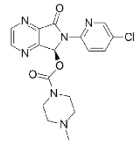

Cyclopyrrolone

Figure 1.4. Positive and negative benzodiazepines. A) Examples of commonly studied benzodiazepines. B) Benzodiazepine ligand structures. Benzodiazepines can be divided into multiple groups by efficacy (positive and negative benzodiazepines) but also by chemical structure (imidazobenzodiazepines and non-benzodiazepines (Z-drugs)). Classification is based on Whiting *et al.*, 1995.

1.3.4: The benzodiazepine binding site on the $GABA_A$ receptor

Benzodiazepines bind $GABA_A$ receptors at the high-affinity benzodiazepine site at the extracellular interface of the α and γ subunits (Rudolph et al., 1999; G. B. Smith & Olsen, 1995). Due to the 2:2:1 ratio of α, β, and γ subunits in the general synaptic $GABA_A$ receptor, there is only one high-affinity site (α+/γ-) per receptor. The γ2 subunit is important for forming the high-affinity benzodiazepine site on $GABA_A$ receptors. It has a higher affinity for benzodiazepines than receptors containing γ1- and γ3-subunits (Wafford et al., 1996). Benzodiazepines bind αβγ receptors, but not αβ only receptors (Pritchett, Sontheimer, et al., 1989). There are low-affinity sites on the $GABA_A$ receptor that may be activated by diazepam at high concentrations (above 10μM), but nanomolar concentrations of benzodiazepines are more therapeutically-relevant and bind the high-affinity site (Walters, Hadley, Morris, & Amin, 2000). The degree of benzodiazepine modulation measured depends on the subunit composition of the receptor. The beta subunit, although not directly contributing to the formation of the high-affinity benzodiazepine site, can affect that binding displacement of [^{3}H]flumazenil by flunitrazepam, βCCM, zolpidem and Cl 218,872 (Benke, Fritschy, Trzeciak, Bannwarth, & Mohler, 1994). The α and γ isoforms, as critical structural components of the binding site, affect the binding and efficacy of benzodiazepines at $GABA_A$ receptors.

1.3.5: Subunit composition affects benzodiazepine modulation

The specific α isoform expressed in $GABA_A$ receptors affects the binding and efficacy of benzodiazepine-site ligands (Benson et al., 1998; Hadingham et al., 1996; Knoflach et al., 1996; Puia et al., 1991; Wafford et al., 1996; H. A. Wieland & Luddens, 1994; Wingrove et al., 2002). The receptors expressing α1, α2, α3 or α5 subunits are generally more sensitive to positive benzodiazepines, though with different efficacies (Puia et al., 1991). Classic benzodiazepines, like diazepam, are thought to bind α1 greater than

α2, α3, and α5 subunits (T. A. Smith, 2001), but this varies for the newer benzodiazepine site ligands. However, binding affinity does not always match the efficacy of the drug. A drug with a high binding affinity might still have a low efficacy at a certain receptor. For example, the $\alpha_1\beta_2\gamma_2$ receptors can bind diazepam, clonazepam, CL 218-872, flunitrazepam, triazolam, Ro15-4513 and Ro 15-1788 (flumazenil) all bind to differing degrees (Luddens et al., 1990). However, functionally diazepam and clonazepam both showed greater efficacies for α2 and α3 than α1 or α5. This means that they enhanced GABA-evoked currents to a greater degree for $\alpha_{2,3}\beta_1\gamma_2$ receptors than $\alpha_{1,5}\beta_1\gamma_2$ receptors *in vitro* (Puia et al., 1991).

The α4 and α6 isoforms tend to form $\alpha_x\beta\gamma_2$ receptors insensitive to positive allosteric modulation, even at the concentrations above the nanomolar range (Hadingham et al., 1996; Luddens et al., 1990; Wafford et al., 1996; H A Wieland, Lüddens, & Seeburg, 1992; Wisden et al., 1991). Specifically, $\alpha_6\beta_2\gamma_2$ recombinant receptors are insensitive to binding diazepam, CL 218-872, clonazepam, flunitrazepam, triazolam but can bind Ro15-4513 (negative benzodiazepine or inverse agonist), bretazenil (a partial agonist), and flumazenil (Luddens et al., 1990). The benzodiazepine antagonist, flumazenil can competitively inhibit the response of bretazenil at $\alpha_4\beta_2\gamma_2$ and $\alpha_6\beta_2\gamma_2$ receptors (Knoflach et al., 1996). Receptors containing α4 and α6 subunits can bind negative benzodiazepines (Knoflach et al., 1996; Wafford et al., 1996). Overall, the α isoform specificity of different benzodiazepines has become an important pharmacological property because certain $GABA_A$ receptor assemblies mediate different clinical effects of benzodiazepines.

1.3.6: The high-affinity site is made up of structural loops A-F

The high-affinity benzodiazepine binding site is formed from six structural loops (loops A-F) (Figure 1.5) (Cromer et al., 2002; Michalowski et al., 2017; Miller & Aricescu,

2014). Sequence alignments of the major human $GABA_A$ receptor subunits show highly conserved regions for loops A-F (Figure 1.6). Loops A-C are on the α subunit and are connectors between β-strands. Loops D-F are on the γ subunit. Loops A-F are highly conserved across $GABA_A$ receptor subunits and form homologous GABA agonist binding sites at the β+/α- interfaces (Cromer et al., 2002; Miller & Aricescu, 2014). Loops A-C are sometimes referred to as loop 5 (loop A), loop 8 (loop B) and β-sheet 10 (loop C), based on nomenclature for the acetylcholine-binding protein (Brejc et al., 2001; Kash et al., 2004). Because loops A-F interact with the ligand, subtle differences across subunit isoforms (α1-6 and γ1-3) can affect the efficiency of the receptor-ligand interaction. Although we lack a crystal structure of the α+/γ- benzodiazepine site on $GABA_A$ receptors, key residues have been shown to be important in determining the efficacy and specificity of certain drugs for the benzodiazepine site (Hanson, Morlock, Satyshur, & Czajkowski, 2008; Morlock & Czajkowski, 2011).

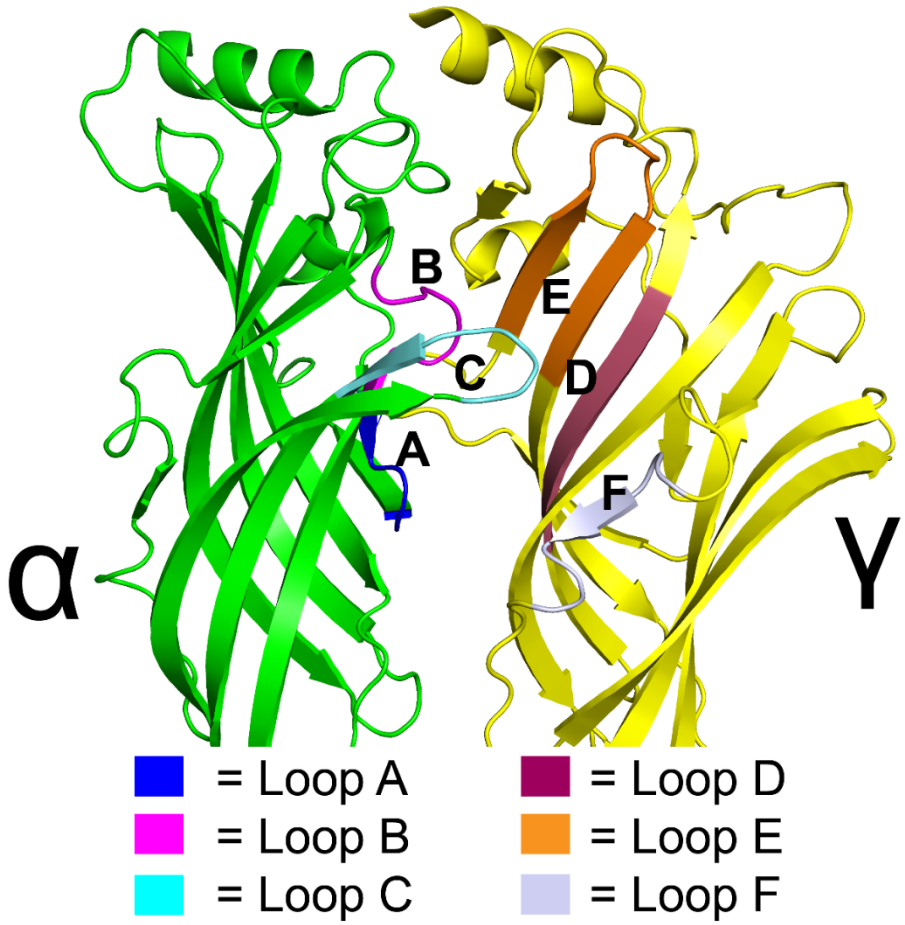

Figure 1.5. Structural loops A-F in high-affinity benzodiazepine site at the extracellular interface of the α and γ subunits of synaptic $GABA_A$ receptors. Loops A-C are on the α subunit (green), while loops D-F are on the γ (yellow). Figure based on the crystal structure of the beta homopentameric $GABA_A$ receptor from Miller *et al.,* 2014 (**DOI**: 10.2210/pdb4cof/pdb).

Previously, a combination of mutagenesis and functional or binding assays has been used to determine the role of specific amino acid residues within the structural loops A-F of the benzodiazepine site (Benson et al., 1998; Buhr, Schaerer, Baur, & Sigel, 1997; Hanson et al., 2008; Renard et al., 1999; Tan et al., 2007; H. A. Wieland & Luddens, 1994; M. Wieland & Hartig, 2007). As mentioned earlier, mutation the critical histidine in α1 (H101 in rodents and His102 in bovine and human cDNA) in loop A was the first point-mutation in the high-affinity benzodiazepine site shown to abolish sensitivity of the receptor to diazepam binding and modulation (H A Wieland et al., 1992). Histidine101 is present in the α1, α2, α3, and α5. In α4 and α6 isoforms an arginine (Arg101 in rodents and human cDNA) is present that makes the receptors insensitive to positive benzodiazepines (Kleingoor et al., 1993; Knoflach et al., 1996; Knoflach, Drescher, Scheurer, Malherbe, & Mohler, 1993; Luddens et al., 1990). The His101Arg mutation was first described by Wieland and colleagues (H A Wieland et al., 1992) It was noted that the $GABA_A$ receptors isolated from cerebellar granule tissue only bound benzodiazepine antagonists or inverse agonists (Ro 15-4513) but not classic benzodiazepine agonists like diazepam. This result could be mimicked by recombinant $\alpha_6\beta_2\gamma_2$ receptors (Luddens et al., 1990), leading researchers to look for sequence differences between α1 and α6. Wieland and colleagues eventually isolated the conserved histidine (His101 in rat cDNA) that when mutated to an arginine (α1(H101R)) failed to bind diazepam when expressed in $\alpha_x\beta_2\gamma_2$ receptors (H A Wieland et al., 1992). The H101R mutation abolished diazepam binding because the arginine sterically interfered with the diazepam binding site (H A Wieland et al., 1992; Wingrove et al., 2002). Functionally, α_1(H102R)$\beta_2\gamma_2$ recombinant receptors did not show diazepam potentiation of chloride currents like wildtype $\alpha_1\beta_2\gamma_2$ receptors do (Kleingoor et al., 1993). The opposite α6(R100H) mutation confered functional sensitivity for diazepam to α_6(R100H)$\beta_2\gamma_2$ recombinant receptors (Kleingoor et al., 1993). This created mutated receptors that could respond to diazepam like wildtype $\alpha_1\beta_2\gamma_2$ receptors.

As described above (**Section 1.3.2**), this mutation when knocked-into a transgenic mouse also inhibited certain therapeutic effects of diazepam at the behavioral level (Rudolph & Mohler, 2004). In summary, the conserved histidine present in loop A (FF**H**NG) is important for determining the molecular (Benson et al., 1998; Kleingoor et al., 1993; H A Wieland et al., 1992) and behavioral (Rudolph et al., 2001) effects of benzodiazepines. The presence of the histidine residue at this location in the benzodiazepine binding site is critical for the benzodiazepine-$GABA_A$ receptor interaction.

Other residues than His101 (His102 in human cDNA) in loops A-F of the benzodiazepine site are also important for the binding and interaction of benzodiazepines with the $GABA_A$ receptor. Mutagenesis studies have used proximity-accelerated irreversible chemical coupling (Tan et al., 2007), photoincorporation (Berezhnoy et al., 2004; Duncalfe, Carpenter, Smillie, Martin, & Dunn, 1996), binding assays (Amin, Brooks-Kayal, & Weiss, 1997; Hanson & Czajkowski, 2008; Renard et al., 1999) and patch clamp assays to study this (Amin et al., 1997; Benson et al., 1998; Morlock & Czajkowski, 2011). Because there is not a crystal structure of a heteropentameric $GABA_A$ receptor, these mutagenesis studies, along with molecular docking studies, provide vital information for how different benzodiazepines may be interacting with the receptor to have their positive or negative modulatory effects. The specific orientation of most ligands in the binding site remains incompletely understood (Hanson et al., 2008). Several key residues in loops A-F have been found to affect ligand selectivity, binding or efficacy of ligands acting at the benzodiazepine site.

Several studies have provided information specifically on how imidazobenzodiazepines interact with the benzodiazepine site. Imidazobenzodiazepines contain an imidazo ring, such as midazolam, flumazenil (Ro 15-1788) and Ro 15-4513 (P. Zhang et al., 1995). For example, the residues Gly157 (loop B), Val202 (loop C) and Val211 (loop C) within the α1 subunit are important for the imidazobenzodiazepine Ro 15-

4513 (a partial negative allosteric modulator) to interact with in the benzodiazepine site (Tan et al., 2007). Furthermore, the authors suggested that diazepam and imidazobenzodiazepines may orient in the binding pocket similarly with the Cl-group (diazepam) and azide group (Ro 15-4513) both aligning to interact with His101 residue (loop A). Another study showed that the γ2(Phe77) affects the binding affinity of diazepam, flunitrazepam and imidazobenzodiazepines (including flumazenil and midazolam) (Buhr & Sigel, 1997; Sigel, Schaerer, Buhr, & Baur, 1998). Other residues only affected imidazobenzodiazepine binding. The Ala79 residue within the γ2 subunit affected the binding affinities of Ro 15-4513 and flumazenil but had less effect on the binding affinity of flunitrazepam (Kucken et al., 2000). The γ2(Ala79) and γ2(T81) residues may line a part of the benzodiazepine site that specifically affects the interaction of the imidazo ring with the site (Kucken, Teissere, Seffinga-Clark, Wagner, & Czajkowski, 2003; Kucken et al., 2000). Although there are some overlaps in residues, α1(His101) and γ2(Phe77), in the benzodiazepine site that affect the binding of both classic benzodiazepines and imidazobenzodiazepines, other residues (γ2(Ala79) and γ2(T81)) appear to more specifically determine imidazobenzodiazepine binding.

Some residues have been shown to affect the α-specificity of benzodiazepines. This partly explains the different binding affinities between α1- and α4/6-containing receptors. Mutagenesis studies exchanged highly-conserved residues in the benzodiazepine site between different subunit isoforms. In one study, Derry and colleagues examined Ser205 in loop C that is homologous to the Asp204 in α6 and the Iso204 in α4 (rat cDNA) (Derry, Dunn, & Davies, 2004). The α4 and α6 subunits bind negative modulators like β-carbolines. This study confirmed that α4-containing receptors bind β-carbolines with a higher affinity than α6. The α6(N204I) mutation could confer higher α4- like binding affinity for β-carbolines (Derry et al., 2004). An α1(S205N) mutation reduced the receptor's affinity for β-CCE and DMCM to the level of α6-containing

receptors. However, α6(N204I) and α6(N204S) mutations had no large changes in binding affinity for Ro 15-4513 (an inverse imidazobenzodiazepine agonist) (Derry et al., 2004). This study showed that α6(Asn204)'s role in affecting binding affinity is α-specific for β-carbolines but less for Ro 15-4513.

Another mutagenesis study examined the role of loop C mutations on positive and negative benzodiazepines. Mutation of Thr206 (α1 rat) to a valine decreased the affinity of positive modulators (diazepam, flunitrazepam and zolpidem) and increased the affinity of flumazenil and negative modulators (Cl 218872 and the β-carboline, DMCM) (Sigel et al., 1998). These different effects may be caused by changes in steric interference of the substituted residue or by changes in the electronic charge interactions of side chains with the ligand. Positive and negative modulators likely interact with the binding site differently, affecting the direction of their modulation. Studies like this provide important details concerning the underlying mechanism by which benzodiazepines discriminate between different α subunits and also suggest potential residues that may contribute to the differential actions of positive and negative modulators.

Finally, mutagenesis experiments have revealed how specific loops and residues affect the ligand binding affinity *versus* the efficacy of benzodiazepine site ligands. A series of 24 cysteine mutations made across loops A-F in the benzodiazepine site revealed the different contributions of loops A-F to ligand affinity, selectivity and efficacy (Hanson & Czajkowski, 2008; Morlock & Czajkowski, 2011). Mutations in loops A, B and D altered the binding affinity of zolpidem, eszopiclone and other benzodiazepine ligands, suggesting that these loops are crucial for forming the physical structure of the binding pocket (Hanson & Czajkowski, 2008). Cysteine mutations in loops E and C affected the binding affinity for zolpidem and eszopiclone in different ways. For example, the mutations in loop C showed that Gly200, Val202 and Ser204 (all in rat α1) affected zolpidem affinity more than that of eszopiclone or flumazenil. Functional evaluation of these cysteine mutations

found that four mutated residues (Ala160 (loop B), Thr206 (loop C), Arg144 (loop E), Arg197 (loop F)) on the respective α1 and γ2 subunits, reduced the benzodiazepine efficacy but not binding of zolpidem, eszopiclone and flurazepam (Morlock & Czajkowski, 2011). Efficacy refers to the degree of maximum potentiation of GABA-evoked currents. Mutations of Val211 (loop C) and Glu198 (loop F) increased the efficacy of zolpidem only. Results indicated an unique effect on efficacy but not binding. Structure affected the coupling of benzodiazepine binding to GABA activation of the receptor, thereby affecting modulator's efficacy. On the other hand, the loop E mutations M130C, R132C, and R144C in γ2 affected the affinity of espizolpiclone, zolpidem and Ro 15-1788 but not their efficacy (Hanson et al., 2008). In general, loop C has more flexibility to shift upon ligand binding (Michalowski et al., 2017) and loop E is next to an unfilled space that may accommodate different ligands depending on their shape (Hanson & Czajkowski, 2008). This may account for the variable role loop C and E play in ligand binding and efficacy.

Studies like these provide important information about how different ligands might be interacting with the binding site. For example, knowing that the zolpidem ligand can orient in one of three different ways within the binding pocket is useful to drug developers who want to create α-isoform-specific drugs (Hanson & Czajkowski, 2008). It is also important to understand how certain structural loops play different roles in affecting ligand affinity and efficacy.

Existing drugs can be altered by changing the binding affinity, efficacy of both for certain receptor assemblies. Despite these and other mutagenesis studies of the benzodiazepine binding site, the role of specific loops and residues across multiple α and γ isoforms remains incompletely understood. Understanding how different residues when mutated can affect the degree or direction of benzodiazepine modulation across different α subunits will help understand drug action at this site.

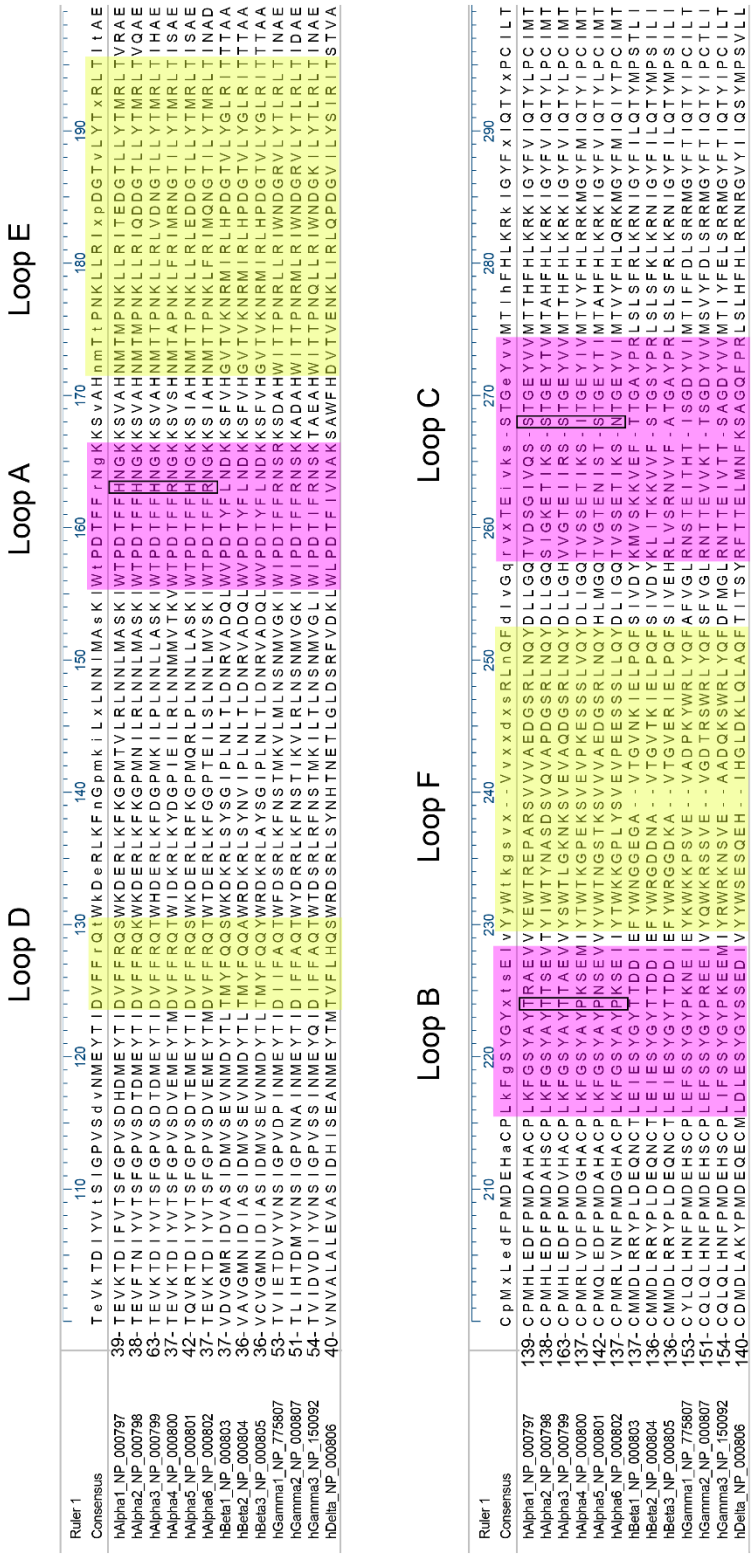

Figure 1.6. Sequence alignment of GABA$_A$ subunits (α1-6, β1-3, γ1-3, δ).

Figure 1.6. Sequence alignment of $GABA_A$ receptors subunits (α1-6, β1-3, γ1-3, δ) based on the human sequences. Loops A-F are highlighted in pink (loops A-C) and yellow (loops D-F). Smaller black boxes highlighted for α1-6 in loops A-C are the targeted residues mutated in midazolam studies described in *Chapter 3*. The numbering above uses the mature peptide numbering that does not include the signal peptide. Alignment was performed using Clustral Omega (MegaAlign Pro from DNASTAR, INC.). The length of signal peptides are: α1 = 27, α2 = 28, α3 = 28, α4 = 35, α5 = 31, α6 = 19, β1 = 24, β2 = 24, β3 = 25, γ1 = 35, γ2=39, γ3 = 17, δ = 24. The protein NCBI reference numbers are listed in the table.

1.3.7: Midazolam

Midazolam (8-chloro-6-(2-fluorophenyl)-1-methyl-4*H*-imidazo[1,5-a][1,4]benzodiazepine) is a positive imidazobenzodiazepine. It is also known as Versed®. It was first synthesized in 1975 by Hoffman-LaRoche and has a relatively rapid onset and duration of action (Olkkola & Ahonen, 2008). Midazolam is 1.5 times more potent than diazepam in humans (Malamed, 2010; Pieri, 1983). It is metabolized through the cytochrome P450 (CYP) enzymes in the liver or by gluconoride conjugation, but all three metabolites of midazolam lack bioactivity at $GABA_A$ receptors in humans (Olkkola & Ahonen, 2008; Pieri, 1983; Tobias & Leder, 2011).

Midazolam produces all the characteristic effects of classic benzodiazepines, like diazepam (Pieri, 1983). Midazolam causes sedation, anxiolysis, anticonvulsion and anterograde amnesia in a dose-dependent manner. It is frequently used for procedural sedation or the induction of anesthesia (Diviney et al., 2015; Olkkola & Ahonen, 2008; Tobias & Leder, 2011). The anxiolytic effects of midazolam are reliable but less pronounced than its sedative effects (Pieri, 1983). The clinical effects of midazolam make it a commonly used benzodiazepine. Midazolam has also been used off label in drug cocktails used for executions in the U.S. (Roche statement, Nov. 2015).

Plasma concentrations within the therapeutically-relevant range of midazolam are within the nanomolar range. Blood concentrations of midazolam measured in the clinic

showed that anesthetized patients have plasma concentrations around 350 ng/ml (966 nM) of midazolam (P. Persson, Nilsson, Hartvig, & Tamsen, 1987). Lower concentrations of 270 ng/mL produced a 50% chance of loss of consciousness (Glass et al., 1997). At even lower concentrations (75-150 ng/mL = 207 nM-414 nM), post-operative drowsiness was observed (M. P. Persson, Nilsson, & Hartvig, 1988; P. Persson et al., 1987). In terms of sedative-hyponotic effects of midazolam a 0.05mg/kg dose of midazolam (Versed) is equivalent to a blood alcohol concentration (BAC) of 0.1 alcohol. The concentrations that have sedative-hypnotic effects in people are equivalent at the molecular level to a 100% enhancement of the activity of $\alpha_1\beta_2\gamma_2$ $GABA_A$ receptors (Rye, et al., 2012).

Like other positive benzodiazepines, midazolam enhances GABAergic neurotransmission. It decreases firing rates of single neurons and multiunit activity in specific brain areas (Pieri, 1983). Midazolam interacts with the high-affinity benzodiazepine site on $GABA_A$ receptors. Previous studies have suggested that midazolam enhances the activity of $GABA_A$ receptors by enhancing the gating of GABA (Kristiansen & Lambert, 1996; Rusch & Forman, 2005; D. S. Wang, Lu, Hong, & Zhu, 2003). To date, there have been multiple studies of midazolam's actions at recombinant and native synaptic $GABA_A$ receptors. However, studies with full comparisons of most of the six alpha subunits in the same expression system remain rare. Studies comparing α1/α2/α3/α5-containing receptors used diazepam or flunitrazepam (Benson et al., 1998; Luddens, Seeburg, & Korpi, 1994; H. A. Wieland & Luddens, 1994). One study by Kilpatrick and colleagues tested a novel benzodiazepine site ligand, CNS-7056, and used midazolam as a comparison for its effects on $\alpha_1\beta_2\gamma_2$, $\alpha_2\beta_2\gamma_2$, $\alpha_3\beta_2\gamma_2$ and $\alpha_5\beta_2\gamma_2$ recombinant receptors expressed in Ltk cells (Kilpatrick et al., 2007). They found that midazolam had a higher efficacy at $\alpha_1\beta_2\gamma_2$ and $\alpha_3\beta_2\gamma_2$ recombinant receptors than $\alpha_2\beta_2\gamma_2$ and $\alpha_5\beta_2\gamma_2$, despite having similar pEC_{50} values (the negative log of the EC_{50}) (Kilpatrick et al., 2007).

However, midazolam's mechanism of modulation at $GABA_A$ receptors is partly based on binding assays. To our knowledge, no single study has measured the modulatory effects of midazolam across all six α $GABA_A$ subunits. Furthermore, the contributions of specific residues within the benzodiazepine binding pocket to the efficacy of midazolam across $GABA_A$ receptors with different α subunits remains to be understood.

1.3.8: Therapeutics of benzodiazepines

Benzodiazepines are an important therapeutic drug class that target $GABA_A$ receptors. Since the first benzodiazepines were developed, there have been dozens of benzodiazepines developed to target the sedative-hypnotic, anxiolytic, anticonvulsive, or cognitive modulator properties of these drugs (Mohler, 2015). One limitation has been that some benzodiazepine-site ligands lack subunit-specificity and so have multiple clinical effects. Benzodiazepines that bind and modulate multiple $GABA_A$ receptor assemblies can have undesirable side-effects, such as sedation during the day or a high risk of developing tolerance and physical dependence with long-term use (Rudolph & Knoflach, 2011). Subunit-selective benzodiazepines provide a more targeted method of modulating specific types of $GABA_A$ receptors. This can also target tonic or phasic inhibition in specific brain regions. Novel benzodiazepine-site ligands have been developed and studied to treat several important diseases and symptoms, including anxiety, sleep-disorders, cognitive disorders and more.

One example of a search for a specifically targeted benzodiazepine is research of non-sedative anxiolytics. The early benzodiazepines, like diazepam, had strong sedative effects which, made them less appropriate for daytime use. The development of a non-hypnotic anxiolytic would be a huge success for pharmacologists and patients. Researchers have been working for years to create the optimal non-sedative anxiolytic (Griebel et al., 2001; McKernan et al., 2000; Mohler, 2015; Rudolph et al., 2001). Then

researchers realized the sedative and anxiolytic effects of benzodiazepines could be separated based on the α isoform-specificity. Specifically α2 mediated anxiolytic effects (Low et al., 2000). They started generating benzodiazepine site ligands to target the $\alpha_2\beta_x\gamma_2$ $GABA_A$ receptors (See Mohler *et al.,* 2006 for a list of anxiolytic benzodiazepine site ligands)(Mohler, 2006). Ligands differentiating the α1/α2 subunits based on binding affinity were not as successful as predicted, but ligands with different efficacies for these α subunits have been more successful (Rudolph & Knoflach, 2011). TPA023 (also called MK-0777) is an example of a benzodiazepine-site ligand developed with a higher efficacy for α2/α3 subunits and has non-sedative anxiolytic properties in rats and squirrel monkeys (Atack et al., 2006; Rudolph & Knoflach, 2011). The role of α3-containing $GABA_A$ receptors in mediating anxiolytic effects is less clear. Data from H101R knock-in mice show no role of α3, but the compound TP003, an α3-specific benzodiazepine, had anxiolytic properties in mice (Dias et al., 2005).

New hypnotics are also an important direction drug development. Zolpidem and zaleplon (CL 284,846) are predominantly α1-specfic drugs that have primarily hypnotic effects but also anti-convulsive effects (Low et al., 2000; Sanger, Morel, & Perrault, 1996). These non-benzodiazepines (meaning they have a different chemical structure than classic benzodiazepines), also called Z-drugs, bind the high-affinity benzodiazepine site on the $GABA_A$ receptors. Many Z-drugs have higher α1-selectivity than other α subunits. Subunit selectivity often refers to the subunit that produces the greatest response, but it does not preclude a lower level of activity at other subunits.

Other benzodiazepines are being developed to treat cognitive impairments in different diseases like schizophrenia, autism, and age-related cognitive decline (Achermann et al., 2009; Atack, 2011; Han, Tai, Jones, Scheuer, & Catterall, 2014; Mohler, 2015; Rudolph & Knoflach, 2011). Both α2/α3-selective and α5-targeting modulators have been considered for their therapeutic value for treating cognitive

impairments in schizophrenia (Rudolph & Knoflach, 2011). Cognitive enhancers with α5-specificity have been developed using the principles of selective-efficacy to selectively reduce α5-mediated $GABA_A$ receptor activity. One example of a drug with low or antagonist efficacy at the α1, α2 and α3 subtypes and higher inverse agonism at α5-containing receptors is α5IA (Atack, 2011). The development of these novel compounds depends not only on modifying the chemical structure of existing benzodiazepine compounds, but also understanding the differences in the molecular mechanisms of different benzodiazepines at multiple $GABA_A$ receptor assemblies. Experiments in Chapter 3 will explore the relationship between subunit-specific, structure and benzodiazepine efficacy. Better understanding how benzodiazepine efficacy is altered across the six α subunits and in response to mutations in the benzodiazepine binding site will create the potential for new methods to target specific α-assemblies.

1.4.1: Altered $GABA_A$ receptor activity in neurological disease

It is not surprising that $GABA_A$ receptors, as major mediators of inhibition in the brain, are often involved in neurological diseases. In disease, altered $GABA_A$ receptor function can occur secondary to other changes or be a primary cause of disease, as in genetic mutations. Mutations within the *GABR* genes associated with disease include autism, epilepsy, schizophrenia and addiction (Yuan, Low, Moody, Jenkins, & Traynelis, 2015). As whole-exome and genome sequencing become more efficient and cost-effective, more diseases are being added to this list. Not surprisingly, diseases affecting GABAergic inhibition are often complex and multifaceted. Two examples of complex neurological disorders thought to involve disrupted GABAergic inhibition are idiopathic hypersomnia and epilepsy. Both will be discussed below in the context of the role altered GABAergic inhibition may play in disease.

Section 1.4.2. Idiopathic Hypersomnia:

Idiopathic hypersomnia (IH) is a rare neurological sleep disorder. Population statistics of the prevalence of IH remain scarce, but estimates based on narcolepsy statistics suggest less than 0.05% (Khan & Trotti, 2015). Patients with IH experience excessive daytime sleepiness that is not secondary to any medical or mental condition (Billiard & Sonka, 2016; Khan & Trotti, 2015). Many patients often sleep over 10 hours of a night, leaving the cause of daytime sleepiness unclear. Furthermore, there are no FDA-approved treatments (Rye et al., 2012). Many patients are prescribed stimulant medications, such as modafinil, a non-amphetamine wake-promoting agent (Khan & Trotti, 2015). Other stimulants like amphetamines (methylphenidate and dextroamphetamine) are also used to reduce daytime sleepiness. More recently, flumazenil and clarithromycin (macrolide antibiotic) have each provided some relief of daytime sleepiness to a subset of patients. In separate studies, 39% of patients treated with sublingual and transdermal flumazenil saw an improvement in symptoms, and 64% of patients treated with clarithromycin saw improvement (Trotti et al., 2014; Trotti et al., 2016). While an important step forward in seeking alternative treatments for excessive daytime sleepiness, many IH patients do not respond to medications, and the disease severely limits the quality of life of these patients.

IH is one of a group of central disorders of hypersomnolence. Other hypersomnolence disorders include type 1 and type 2 narcolepsy (Khan & Trotti, 2015). These disorders are characterized by an inability to stay awake during major waking periods (Anderson, Pilsworth, Sharples, Smith, & Shneerson, 2007; Khan & Trotti, 2015). Type 1 narcolepsy is defined by excessive daytime sleepiness, cataplexy, sleep paralysis and hallucinations (Khan & Trotti, 2015). Patients with type 2 narcolepsy have many of the above symptoms but lack the cataplexy. Patients with IH present symptoms similar to type 2 narcolepsy. IH patients are unrefreshed after naps and often experience sleep

drunkenness upon waking from sleep (Khan & Trotti, 2015). Patients with narcolepsy generally have reduced levels of hypocretin (also called orexin), a neuropeptide produced in the lateral hypothalamus. Hypocretin is important for regulating feeding, stress, the autonomic nervous system and the sleep/wake balance. Patients with IH generally have normal hypocretin levels in their cerebrospinal fluid (CSF) (Rye et al., 2012). The diagnosis of IH remains difficult due to the lack of a definitive biomarker and the need to rule out all other medical conditions, including type 2 narcolepsy (Billiard & Sonka, 2016; Khan & Trotti, 2015).

The research history surrounding idiopathic hypersomnia disorders has been eventful. IH was initially described by Bedrich Roth from a group of 642 patients seen over 30 years (Roth, 1976). He described a distinct hypersomnia disorder separate from narcolepsy and with marked sleepiness. Since there was no obvious cause for the hypersomnia, researchers continued to examine hypersomnia sleep disorders of unknown cause. One hypersomnia disorder occurring primarily in older men, “idiopathic recurring stupor,” was described in the early 1990’s. Researchers proposed that it was caused by “endozepines” in the brain binding $GABA_A$ receptors (Rothstein et al., 1992). Endozepines were thought to act like endogenous diazepam and to cause recurring episodes of stupor and coma in patients. These episodes could be reversed by flumazenil, the benzodiazepine antagonist. It was later revealed that certain cases of recurrent stupor were actually caused by wives giving their husbands benzodiazepines (lorazepam) without their knowledge (Granot et al., 2004). This revelation required researchers of idiopathic hypersomnia disorders to more rigorously question and test patients for exogenous medications. This misdiagnosis also slowed the research of idiopathic hypersomnia. The endozepine theory continued to be researched as researchers continued to search for an endogenous benzodiazepine-like compound in the brain (Cortelli et al., 2005).

Today the underlying mechanism of IH remains unknown. A biomarker of the disease would significantly advance research of IH. The search for a biomarker of IH started in the 1980's.To date, potential biomarkers suggested have ranged from monoamines to histamine to a peptide "somnogen" (Billiard & Sonka, 2016). Histamine was also found to be altered in some, but not other, hypersomnia studies (Bassetti et al., 2010; Dauvilliers et al., 2012; Kanbayashi et al., 2009). The difficulty in diagnosing IH and the heterogeneity across patients likely contributed to these opposing results. The most recent potential biomarker discovered was an endogenous peptide between 500-3000 Daltons that is found in the cerebral spinal fluid (CSF) of IH patients. This peptide enhances the activity of $GABA_A$ receptors and was predicted to bind to the benzodiazepine binding pocket (Rye et al., 2012). Its molecular actions could be blocked by flumazenil. Surprisingly, CSF samples from non-IH subjects also enhanced $GABA_A$ receptor activity, although to a lesser degree than hypersomnolent CSF.(Rye et al., 2012). Therefore, this peptide might represent a novel neuropeptide modulator expressed in all people.

The hypothesis of the endogenous peptide was that the peptide became more abundantly expressed or more potent in IH. The peptide enhanced GABAergic inhibition and led to excessive daytime sleepiness. One experiment supporting this "somnogen" based theory was that when hypersomnolent CSF was directly infused in the cerebral ventricles of rats, it increased the total length of sleep episodes (unpublished, Rye, et al.). This suggested that this somnogen might modulate sleep rather than directly promoting a wake-to-sleep transition. If the endogenous peptide does directly contribute too excessive sleepiness through its actions at the $GABA_A$ receptor, then it's $GABA_A$ receptor should reflect those receptor assemblies found in sleep centers of the brain.

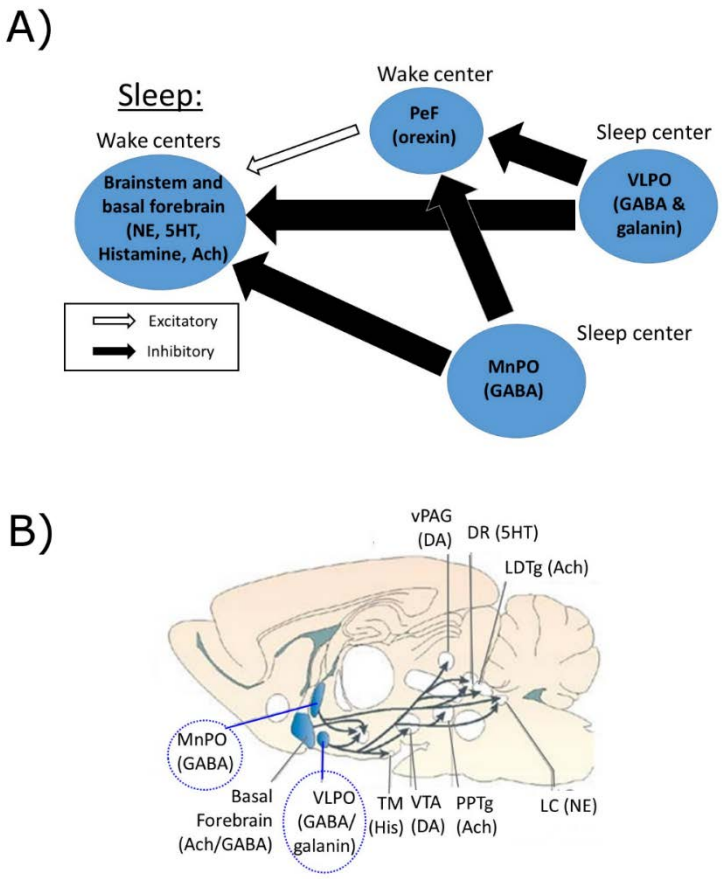

Figure 1.7: Sleep promotion in the brain. A) The sleep-wake balance is traditionally modeled as the reciprocal inhibition of the excitation/inhibition balance in the brain. Arousal is promoted by the release of wake-promoting neurotransmitters that activate wake centers (cortex, basal forebrain, hypothalamus, midbrain, brainstem) and inhibit sleep centers. Sleep is promoted by the release of GABA and galanin that inhibit the wake centers of the brain (shown above). B) Sleep-wake centers as portrayed in the rodent brain. Important sleep-promoting centers (circled in blue) inhibit the arousal-promoting centers. Brain regions: Sleep: MnPO = median preoptic area, VLPO = ventrolateral preoptic nucleus. Wake: DR = dorsal raphe, LC = locus coeruleus, LDTg = laterodorsal tegmental nucleus, PPTg = pedunculopontine tegmental nucleus, TM = tuberomammillary nucleus, vPAG = ventral periaqueductal grey, VTA = ventral tegmental area. Image adapted from Franks, NP., 2008 review.

Sleep is critical to maintaining biological functions and good health (Richter, Woods, & Schier, 2014). A simplified mechanism for sleep and arousal is based on specific "sleep centers" and "arousal centers" in the brain (Figure 1.7A). Sleep is thought to be triggered by a switch in which sleep centers actively suppress the activity of arousal centers. During waking periods, the opposite occurs with sleep centers being suppressed to produce arousal. The main sleep-promoting center in the brain is the ventrolateral preoptic area (VLPO) in the anterior hypothalamus that releases GABA and galanin (Figure 1.7B) (Harrison, 2007). Another sleep center is the median preoptic nucleus (MnPN), next to the third ventricle. Neurons in "sleep centers" of the brain actively inhibit "wake/arousal centers" in the basal forebrain, hypothalamus, midbrain and brainstem (Harrison, 2007; Richter et al., 2014). Both the VLPO and MnPN areas have a high density of GABAergic neurons that are active during sleep (Franks & Zecharia, 2011). Lesions of the VLPO reduced non-REM (NREM) sleep by 50-60% in rats (Pompeiano, Cirelli, Arrighi, & Tononi, 1995). This is consistent with GABAergic inhibition being critical for producing sleep. Important $GABA_A$ receptor assemblies are listed in **Table 1.1**.

Region	$GABA_A$ receptors expressed
Cortex – Layers 1-IV	$\alpha_1\beta_2\gamma_2$, $\alpha_2\beta_3\gamma_2$,
Cortex – Layer V & VI	$\alpha_3\beta_x\gamma_2$
Basal forebrain	$\alpha_1\beta_2\gamma_2$, $\alpha_3\beta_x\gamma_2$
Reticular nucleus of the thalamus	$\alpha_3\beta_3\gamma_2$
Hypothalamus	$\alpha_2\beta_3\gamma_2$, $\alpha_1\beta_2\gamma_{2,}$
Tuberomammillary nuclei	$\alpha_1\beta_2\gamma_2$, $\alpha_2\beta_3\gamma_2$
Dorsal raphe nucleus	$\alpha_3\beta_x\gamma_2$
Pedunculopontine tegmental nucleus & laterodorsal tegmental nucleus	$\alpha_1\beta_2\gamma_2$
Locus coeruleus	$\alpha_3\beta_x\gamma_2$
Hippocampus	$\alpha_2\beta_3\gamma_2$, $\alpha_5\beta_3\gamma_2$, $\alpha_4\beta_x\gamma_2$
Ventrolateral preoptic area (VLPO)	$\alpha_1\beta_2\gamma_2$

Table 1.1. Main $GABA_A$ receptor assemblies expressed in sleep and arousal-related brain regions. Other minor assemblies are also found in some of the above regions but they have lower expression levels. Receptor assemblies based on receptors listed in (Winsky-Sommerer, 2009).

Many drugs that enhance GABAergic inhibition in the brain also reduce consciousness or promote sleep. Examples are barbiturates, benzodiazepines and general anesthetics. A newer class of sleep drugs is the z-drugs (zolpidem, zaleplon, zopiclone and eszopiclone) that act at the benzodiazepine site of $GABA_A$ receptors. Given that flumazenil provides some clinical relief to IH patients and the molecular actions at $GABA_A$ receptors, the endogenous peptide in IH may enhance $GABA_A$ receptor function through the benzodiazepine site.

One central question about the endogenous peptide in CSF is its identity. Previous experiments narrowed the size range of the molecule to within 500-3000 Daltons (Rye et al., 2012). Trypsinization experiments showed that it was likely a peptide (Rye et al., 2012). Initial candidate molecules suggested from the literature were diazepam binding inhibitor (10,000 Da, DBI) and oleamides (300 Da).

DBI is also known as acyl-CoA binding protein (ACBP), a cytosolic protein (Farzampour, Reimer, & Huguenard, 2015). It can be cleaved into a family of smaller peptides, including triakontatetraneuropeptide, octadecaneuropeptide and octapeptide (Christian et al., 2013; Farzampour et al., 2015). DBI is strongly expressed by astrocytes and may be a downstream consequence of other signaling pathways (Farzampour et al., 2015). DBI was originally described as a negative allosteric modulator of $GABA_A$ receptors (Bormann, 1991). More recent experiments suggested that DBI or one of its fragments can act as a positive allosteric modulator of $GABA_A$ receptors in the thalamic reticular nucleus (Christian et al., 2013). At the behavioral level, DBI has been shown to suppress PTZ-induced seizures in one study and act as a proconvulsant in another study (Farzampour et al., 2015). DBI can also mediate $GABA_A$ receptor activity indirectly by binding to the peripheral benzodiazepine receptor (PBR) that is a cholesterol transporter (Farzampour et al., 2015). This could alter neurosteroids synthesis and neurosteroids that modulate $GABA_A$ receptor activity. Overall, the molecular and behavioral role of DBI remains complex, and its possible role as an endozepines require more research.

Oleamides are fatty acids that accumulate in sleep-deprived animals with sleep-inducing properties (Cravatt et al., 1995). Oleamides were found to enhance current of 5-$HT2_A$, 5-$HT2_C$ and $GABA_A$ receptors (Mendelson & Basile, 2001). Specifically, oleamides enhanced benzodiazepine-sensitive $GABA_A$ receptors, but there is not definitive evidence yet showing that oleamides act specifically through the benzodiazepine binding site (Yost et al., 1998). Both DBI and oleamides, while initially possible candidate molecules are outside the size 500-3000 Da range but fragments of DBI or similar molecules are still possible candidates.

Initial proteomic experiments of the endogenous somnogen were limited by the sensitivity of current mass spectrometer machines in 2012 (unpublished data, Nick Seyfried, *et al.*). Processing CSF for mass spectrometry requires one to first filter or digest

raw CSF to remove larger proteins (Gundry et al., 2009). Albumin is the most abundant protein in CSF (0.5 mg/mL), making up the majority of CSF proteins (Holewinski, Jin, Powell, Maust, & Van Eyk, 2013). Large proteins with high abundance can potentially mask the signals of smaller, less abundant proteins or peptides during mass spectrometry. Furthermore, we still do not know if the endogenous peptide in CSF from IH patients ("hypersomnolent CSF") is an undigested small peptide or if it is the product of cleavage from a larger protein. A common first step for processing human samples for mass spectrometry involves digesting samples with trypsin, a step known to remove CSF's biological activity at $GABA_A$ receptors (Rye et al., 2012). Also, new experiments running mass spectrometry of hypersomnolent CSF samples will require a large set of samples with $GABA_A$ receptor bioactivity ranging from low to high levels. Techniques to pre-process and filter CSF samples for mass spectrometry are currently being explored with collaborators at Emory University.

A second important question about the endogenous peptide is where it originates from. The CSF from patients with IH had a larger degree of biological activity at $GABA_A$ receptors than blood plasma from the same patients (Rye et al., 2012). This suggests that this endogenous peptide may originate in the CSF rather than the blood. CSF plays several roles cushioning the brain, circulating nutrients, maintaining the homeostasis of the interstitial fluid and clearing waste molecules (Sakka, Coll, & Chazal, 2011). The composition of CSF can vary but generally contains ions, vitamins, peptides from the blood, peptides and proteins from the choroid plexus, growth factors and small RNAs (Spector, Robert Snodgrass, & Johanson, 2015). The CSF contains 0.025 g/100mL of protein and the main protein is albumin. CSF is actively formed by the choroid plexus in the CNS and circulates the brain ventricles and subarachnoid space until its passively absorbed into the dural venous sinuses (Oreskovic & Klarica, 2010). The average volume

of CSF in the body is ~150 ml and has a turnover rate of 3-4 times a day (Sakka et al., 2011).

There are several ways CSF can interact with the CNS. First, the choroid plexus receives cholinergic, adrenergic, serotoninergic and peptidergic autonomic innervation that affects CSF secretion and circadian variations (Sakka et al., 2011). Second, the CSF is also a site of interaction between the immune system and the brain (Brinker, Stopa, Morrison, & Klinge, 2014). Third, CSF circulates the ventricles and fills the subarachnoid space around the brain tissue. Brain regions close to the ventricles may be in a location more accessible to interacting with large volumes of CSF. The locus coeruleus is an arousal center located in the pons close to the 4th ventricle. It receives GABAergic input and has $GABA_A$ receptors expressing α2, α3 and γ2 (Foote, Bloom, & Aston-Jones, 1983; Jean-Marc Fritschy & Hanns Mohler, 1995). If the endogenous peptide enhances GABAergic inhibition to increase sleep, then the peptide would likely be released around an arousal center that is suppressed during sleep. There are also circadian variations in CSF secretion mediated by the autonomic nervous system that might be disrupted during disease (Sakka et al., 2011). A patient with a disrupted circadian rhythm, as IH patients have, would likely also have altered levels of CSF production and/or elimination. It is possible a peptide could accumulate in the CSF over time if not properly cleared.

The CSF acts as a clearance system for waste molecules from the brain. These waste molecules include products of brain metabolism, peroxidation products and glycosylated proteins (Sakka et al., 2011). The endogenous peptide found in the CSF of hypersomnia patients could originate in the brain and its presence in the CSF could reflect its diffusion, transport or clearance from the brain into the CSF (Brinker et al., 2014).

Another way the peptide could interact with the brain is through the circumventricular organs. The circumventricular organs are located in seven midline locations around the ventricles of the brain. They are composed of specialized

ependymal cells and create regions with incomplete blood-brain barriers (Horsburgh & Massoud, 2013). In these regions, large molecules and polar substances can readily pass through the incomplete blood-brain barrier and expose the neurons to peripheral signals (Siso, Jeffrey, & Gonzalez, 2010). These regions could be another way through which peptides could get into the brain and modulate neuronal functions.

The most direct path to understanding this endogenous peptide is to identify it. However, research is on-going to isolate and characterizing this small endogenous peptide. Until then, functional data about the effects of hypersomnolent CSF on $GABA_A$ receptor activity will continue to shape and direct developing hypotheses of the mechanism of action.

Currently, most data about the endogenous peptide comes from patch clamp assays of its activity at $GABA_A$ receptors. Building on this, two areas remain understudied about to the functional effects of this endogenous peptide on $GABA_A$ receptors. First, the role that the high-affinity benzodiazepine binding site plays in CSF modulation of $GABA_A$ receptors remains incompletely understood. Second, the $GABA_A$ receptor assemblies important for conveying the functional enhancement of the endogenous peptide on $GABA_A$ receptors remain incompletely mapped. The effects of most $GABA_A$ receptor modulators showed subunit-specific differences in efficacy. The biological activity of the endogenous peptide has been shown to depend on the subunit composition of the $GABA_A$ receptor, where receptors containing α2 showed greater current potentiation than receptors with α1 (Rye, *et al.,* 2012). However, there are four other α subunits that haven't been studied and multiple other subunit combinations that make up $GABA_A$ receptor subtypes expressed in the brain and that are likely to be relevant to sleep and arousal. Understanding which $GABA_A$ receptor assemblies are sensitive to the peptide will help direct research efforts towards which brain regions might be most affected by it. Chapter 4 will discuss experiments meant to address these two questions.

1.4.3. Epilepsy

Epilepsy is a neurological disease of recurrent, unprovoked seizures. Seizures are periods of abnormal and synchronous brain activity (Scharfman, 2007). Epilepsy can either arise from a genetic predisposition or can arise from brain injury or disease. On average, 150,000 people are diagnosed with epilepsy each year in the U.S. (Epilepsy Foundation). There are many different types of epilepsy that range from febrile seizures to focal seizures to generalized epilepsy to temporal lobe epilepsy. Some neurological disorders have a seizure component or high degree of comorbidity. Examples are Angelman syndrome, Tuberous Sclerosis Complex, and Rett syndrome (Olson, Poduri, & Pearl, 2014). However, the exact cause of seizures is often unknown in 50% of cases (Macdonald, Kang, & Gallagher, 2012). As next-generation sequencing and whole-exome genome sequencing are improved and become more efficient and cheap, more genome data has become available from patients with different types of epilepsy.

Genetic abnormalities can be inherited or arise *de novo* in a patient. Some abnormalities, like certain missense mutations or deletions, have a clear deleterious effect on the affected gene product. Missense mutations occurring with a frequency less than 1% in the population are considered rare variants. Genetic epilepsies cover about 50% of epilepsy diagnoses made worldwide (Hernandez et al., 2016). Mutations in some genes, like *SCN1A,* are well-known to cause genetic forms of epilepsy like Dravet syndrome (Olson et al., 2014). Other genes, like the *GABR* genes, are only recently being linked to different forms of epilepsy. As of 2015, there were 27 *GABR* missense mutations associated with epilepsy and few with functional data (Table 1.2) (Yuan et al., 2015). Since then that number has grown quickly. Monogenic cases of genetic epilepsy associated with the *GABR* genes have been found in the *GABRA1, GABRB3* and *GABRG2* genes (Hernandez et al., 2016). The number of *GABR* epilepsy mutations with

functional data showing a loss-of-function, altered function or trafficking is increasing (Hernandez et al., 2016).

Table 1.2. Human GABAA receptor mutations in neurologic disorders

Gene	**Subunit**	**Total**	**RVIS[a]**	**AD**	**ASD**	**DD/MR**	**Epi**	**SZ**	**ADD**
GABRA1	α1	13	24	0	0	0	12	1	0
GABRA2	α2	11	34	0	1	1	0	0	9
GABRA6	α6	3	68	0	0	0	0	2	1
GABRB2	β2	7	15	0	2	0	0	5	0
GABRB3	β3	7	22	0	1	0	5	0	1
GABRG1	γ1	4	12	0	0	0	0	0	4
GABRG2	γ2	9	25	0	0	0	8	1	0
GABRG3	γ3	2	46	1	1	0	0	0	0
GABRR2	ρ2	6	59	0	1	0	0	0	5
GABRD	δ	2	59	0	0	0	2	0	0
Total		**64**		**1**	**6**	**1**	**27**	**9**	**20**

Table 1.2. Human GABAA receptor mutations in neurologic disorders. All missense mutations have a frequency of <1%. Stop codons and splice junction mutations are included. Total indicates the number of published *de novo* or inherited mutations in each subunit as of 2015. Many mutations have more than one phenotype. RVIS[a] is the residual variation intolerance score in percentile, for which lower numbers reflect genes less tolerant to mutation. Abbreviations: AD, Alzheimer's disease; ADD, addiction; ASD, autism spectrum disorder; DD, developmental delay; Epi, epilepsy; MR, mental retardation; SZ, schizophrenia. Based on table published in Yuan, Low, Moody, Jenkins & Traynelis, 2015.

In general, seizures are thought to occur from an imbalance in the inhibition and excitation in the brain. $GABA_A$ receptors, as major ion channels in the brain, are a predictable target in which mutations could alter the inhibition balance in the brain. A loss-of-function mutation can easily be related to increased hyperexcitability in the brain, but other mutations can have more subtle or complex effects. To date, several *GABR* mutations have been described from patients with epilepsy.

Mutations in the *GABRA1* gene have been associated with infantile epilepsies (Kodera et al., 2016). These *de novo* mutations in *GABRA1* include R112Q, P260L,

M263T, M263I, and V287L (Kodera et al., 2016). These mutations were found in patients with severe forms of infantile epilepsy, include early-onset epileptic encephalopathies (EOEEs). EOEEs begin early in life and are characterized by intractable seizures and developmental regression (Kodera et al., 2016). Examples of EOEE's include Ohtahara syndrome, West syndrome, Dravet syndrome, and early myoclonic encephalopathy.

Multiple *GABRG2* mutations have also been found and characterized in patients with epilepsy. Mutations in the *GABRG2* gene have been linked to familial febrile seizures (Boillot et al., 2015). For example, three truncated mutations in the *GABRG2* gene have been linked to familial febrile seizures (J. Wang et al., 2016). These truncated mutants (γ2(R136*), γ2(Q390*), γ2(W429*)) caused little to no surface expression of γ2. *De novo GABRG2* mutations that reduce $GABA_A$ receptor function have also been associated with epileptic encephalopathies (Shen et al., 2017). Decreased receptor function was caused by reduced cell surface expression, altered subunit stoichiometry or decreased GABA-evoked currents (Shen et al., 2017). Another mutation in the M2 domain, γ2(P302L), was found to reduce whole-cell GABA-evoked currents by increasing desensitization and reducing channel conductance (Hernandez et al., 2017; Moller et al., 2017). *GABRG2* mutations that reduce expression of disrupt receptor function appear to be deleterious to brain function and often associated with seizures.

Finally, multiple *GABRB3* mutations that reduced receptor function have been associated with a range of epilepsies from febrile seizures to epileptic encephalopathies (Janve, Hernandez, Verdier, Hu, & Macdonald, 2016; Moller et al., 2017). Many of these mutations occurred in or near the second transmembrane domain (M2) of the $GABA_A$ receptor subunit, a region important to forming the pore of the channel. A *GABRB3* mutation (β3(T287I)) in the 12' threonine M2 of the $GABA_A$ receptor subunit was found in a case of early infantile epileptic encephalopathy (Papandreou et al., 2016). A mutation in the second-to-third transmembrane region (M2-M3 linker) was found in two different

patients. The β3(Y302C) mutation was found in patients with focal epilepsy, and epileptic encephalopathy and Lennox-Gestaut syndrome (Moller et al., 2017). The β3(Y302C) mutation increased the GABA apparent-affinity and reduced receptor function (Moller et al., 2017). Another residue in the M2-M3 linker, β3(P301L), was also found in a case of focal epilepsy beginning at 15 months, but no functional data was presented (Moller et al., 2017). This recent data suggested that mutations of the *GABRB3* gene, while linked to a variety of different epilepsy syndromes, may be an important contributor to severe early-onset forms of epilepsy.

The increased functional data shows that *GABR* mutations can be extremely harmful to early development and the seizure threshold. The immature brain is more susceptible to seizures than the mature brain, but it is also more resistant to seizure-induced cell loss (Nardou, Ferrari, & Ben-Ari, 2013). GABAergic currents play an important role in the immature brain. During development, the high intracellular chloride gradient makes GABA excitatory, and at certain stages depolarizing GABA signals are an important drivers of neural development (Nardou et al., 2013). Deleterious mutations in the *GABR* genes could be more likely to cause seizures early in life because of their important role in the brain during development.

The amount of genome data being collected still outweighs the functional characterization of mutations found. To confirm a causative link between a mutation and a specific epilepsy syndrome, functional data is needed. Ideally, *in vitro* evidence would show altered function on the molecular level while *in vivo* data would show the behavioral and neural network consequences of that mutation. Since making a transgenic animal is costly and time-consuming, most functional data remains at the molecular level. Electrophysiology remains a gold-standard technique for measuring the effects of mutations on ion channel function. In Chapter 5, I will describe three missense mutations

in the *GABR* genes that electrophysiology data showed changes in receptor function that are predicted to impair synaptic GABAergic inhibition.

Section 1.5: Summary of background information and the rationale for the thesis

Often $GABA_A$ receptors, as major mediators of inhibitory neurotransmission, are disrupted by disease-causing mechanisms and become important targets of pharmacological therapies. Altering $GABA_A$ receptor function can have significant effects on the inhibitory signals in the brain. In diseases, treatments can seek to alter the inhibitory signals in the brain with drugs such as benzodiazepines. Although substantial work has been done previously to characterize the benzodiazepine mechanism at $GABA_A$ receptors, much remains to be understood in terms of the individual $GABA_A$ receptor subunits' contribution to benzodiazepine's actions on the brain. Understanding the specific roles of specific residues and subunits on the functional actions of benzodiazepines will improve the design of novel benzodiazepines with fewer side effects. Idiopathic Hypersomnia is a neurological sleep disorder in which altered $GABA_A$ receptor function may play a role. Here too, previous data suggests that hypersomnolent CSF has subunit-specific effects on $GABA_A$ receptor function that remain to be untangled to better understand which $GABA_A$ receptors may mediate the excessive daytime sleepiness patients experience. Finally, the growing functional data on epilepsy mutations in the *GABR* genes also seeks to understand how $GABA_A$ receptor function is altered to decrease the threshold for neuronal excitability and seizures. In this case, understanding the molecular mechanisms of these mutations can better direct physicians towards or away from certain GABAergic antiepileptic therapies. Taken together, there is a need for systematic experiments understanding the contribution of multiple $GABA_A$ receptor assemblies to pharmacologic treatments and disease-models.

The primary objective of studies in this thesis is to evaluate how $GABA_A$ receptor function was altered by pharmacologic treatments and mutational changes to the receptor. The rationale for this thesis was three-part. One, based on previous evidence of loops A-C affecting diazepam's actions at $GABA_A$ receptors, I initially predicted that mutations in loops A-C would alter the efficacy of midazolam. Two, based on preliminary evidence of a benzodiazepine-like mechanism, I predicted that hypersomnolent CSF would have a subunit-specific pattern of effects similar to that of diazepam. Three, based on previous research, *de novo* epilepsy mutations from early-onset epilepsy patients were predicted to be damaging to $GABA_A$ receptor function, most likely through a loss of function mechanisms. All three of these rationales are based on the principle that better understanding the biophysics of $GABA_A$ receptor function will improve research and the design of novel treatments for diseases in which inhibition in the brain is altered.

This thesis consists of six chapters. In Chapter 2, I present general methods and theory for performing whole-cell patch clamp experiments using transfected HEK293T cells. Further methods specific to each data chapter are presented in the abbreviated methods of Chapters 3, 4 and 5. In Chapter 3, I present data from 18 single mutations across the six α subunits in loops A-C of the benzodiazepine site. The aim was to systematically understand how specific residues in the benzodiazepine site contributed to midazolam's actions at $GABA_A$ receptors in a subunit-specific manner. In Chapter 4, the subunit-specific effects of hypersomnolent CSF were assayed across a range of $GABA_A$ receptor assemblies to map the assemblies sensitive to CSF modulation. The aim was to better understand the role of the benzodiazepine-sensitive receptor assemblies in mediating hypersomnolent CSF's effects. In Chapter 5, functional data showing altered $GABA_A$ receptor function is presented for three epilepsy *GABR* mutations not previously characterized. Chapter 6 presents a full discussion of the results chapters in the context of understanding the different roles $GABA_A$ receptors play in neurological disease and

pharmacological interventions. I will also present my predictions for how certain $GABA_A$ receptor assemblies can be targeted or may play a role in different neurological diseases.

Chapter 2: Methods

Chapter 2: Methods

Overview:

The goal of the experiments presented in this dissertation was to measure the effects of different positive allosteric modulators (PAMs) on wildtype and mutated $GABA_A$ receptor function. To achieve this, I used three main techniques: cell culture, site-directed mutagenesis and voltage-clamp electrophysiology. Human embryonic kidney type 293T cells were used as an *in vitro* expression system for $GABA_A$ receptors. Site-directed mutagenesis was used to introduce single residue amino acid substitutions in the cDNA of specified $GABA_A$ receptor subunits. Voltage-clamp electrophysiology was used to measure the whole-cell currents that passed through $GABA_A$ receptors in response to drug stimulation. In the following chapter, I will describe the fundamentals of each method and the design of protocols used to perform each. Further details specific to each data chapter are presented in methods sections for Chapters 3-5, but the main methods will be presented in Chapter 2.

2.1 Plasmids and Mutagenesis:

Human (*Homo sapiens*) $GABA_A$ subunits (α1-6, β2, β3, γ2s) were subcloned into pcDNA3.1+ vectors with a cytomegalovirus (CMV) promoter and ampicillin-resistance gene (Figure 2.1). Sequences matched the sequences of NM_000806 (α1), NM_000807 (α2), NM_000809 (α4), NM_000810 (α5), NM_000811 (α6), NM_000814 (β3), and NM_000816 (γ2s). The β2 and α3 sequences were humanized rat (*Rattus norvegicus*) cDNA, meaning that amino acid substitutions were made to match the rat peptide sequence to the human peptide sequence. In the case of rat β2 (NM_012957), a N323S mutation was made to convert it to the human β2 peptide sequence (NP_000804). The rat α3 sequence (NM_017069) had 3 amino acids mutated (I220V, A419G and V431I) to match the human α3 peptide sequence (NP_000799). The α1-3, α5, β2, and γ2s subunits

were a generous gift from Neil L. Harrison (Columbia University Medical Center, NY). The α4 and β3 subunits were obtained from GenScript (Piscataway, NJ). The α6 subunit was a generous gift from Robert L. McDonald (Vanderbilt University, TN). All purchased subunits were sequenced prior to use (Eurofins MWG Operon).

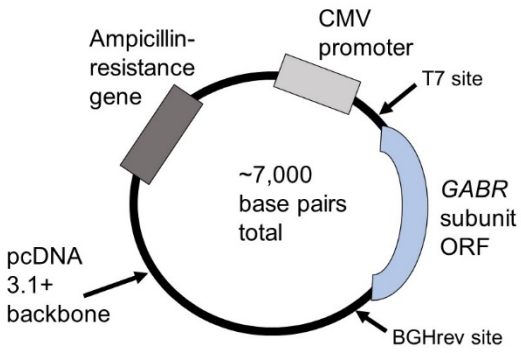

Figure 2.1. Plasmid vector map of pcDNA 3.1+ containing the *GABR* subunit open reading frame (ORF) inserted under the control of the cytomegalovirus (CMV) promoter. Vectors also contained an ampicillin-resistance gene. Primer sites included the T7 before the insert and the BGHrev after the insert.

All point mutations were introduced using the QuikChange Lightening site-directed mutagenesis kit (cat# 200521, Agilent Technologies, Santa Clara, CA) according to the manufacturer's instructions. Briefly, primers were designed using the directions in the QuikChange manual and with the help of their Primer Design Tool (http://www.genomics.agilent.com/primerDesignProgram.jsp). Primers generally were 25-45 bases long starting about 10-15 base pairs before the residue of interest. Ideal primers had a melting temperature of 78°C or above and a guanine and cytosine (%GC) content above 40%. Primers had a guanine or cytosine base at the 3' end in order for the polymerase enzyme to attach properly to the cDNA strand. For a list of forward primers used, see Table 2.1.

Table 2.1. Primers used for mutagenesis.

Mutation	WT = wildtype; MT=mutant	Peptide sequence	Forward primer (5'→3') with mutation change highlighted & capitalized
hα1(H102R)	WT	DTFFHNG	ccggacacatttttc cAc aatggaaagaagtcagtggc
	MT	DTFFRNG	Ccggacacatttttc cGc aatggaaagaagtcagtggc
hα1(T162P)	WT	GSYAYTR	cccactaaaatttggaagttatgcttat Aca agagcagaagttgtttatgaatggaccag
	MT	GSYAYPR	cccactaaaatttggaagttatgcttat Cca agagcagaagttgtttatgaatggaccag
hα1(S206I)	WT	SSTGEYV	gactctggaattgtccagtca aGt aca ggagaatatgttgttatgaca
	MT	SITGEYV	gactctggaattgtccag tca aTt aca ggagaatatgttgttatgac
hα2(H101R)	WT	FFHNG	gactccagatacctttttt cAc aatgggaaaaaatcagtagctc
	MT	FFRNG	gactccagatacctttttt cGc aatgggaaaaaatcagtagctc
hα2(T161P)	WT	GSYAYTT	cctctgaaatttggcagctatgcatat Aca acttcagaggtcacttatatttgg
	MT	GSYAYPT	cctctgaaatttggcagctatgcatat Cca acttcagaggtcacttatatttgg
hα2(S205I)	WT	SSTGEYT	ggaaaggagacaattaaatcc aGT aca ggtgaatatactgtaatgac
	MT	SITGEYT	ggaaaggagacaattaaatcc aTC aca ggtgaatatactgtaatgac
hα3(H126R)	WT	FFHNG	actccagataccttcttc cAc aacggtaaaaaatcagtg
	MT	FFRNH	actccagataccttcttc cGc aacggtaaaaaatcagtg
hα3(T187P)	WT	GSYAYTT	tgaagtttggaagctatgcctat Acc acagctgaag
	MT	GSYAYPT	tgaagtttggaagctatgcctat Ccc acagctgaag
hα3(S230I)	WT	SSTGEYV	tgggacagagataatccggtct agt acaggagaatatg
	MT	SITGEYV	tgggacagagataatccggtct att acaggagaatatg
hα4(R100H)	WT	FFRNG	gtggacccctgatactttcttc AGG aatggaaagaaatctgtctcac
	MT	FFHNG	gtggacccctgatactttcttc CAC aatggaaagaaatctgtctcac

hα4(P161T)	WT	GSYAYPK	gaaattcgggagttatgcctat Cca aagagtgagatgatctatac
	MT	GSYAYTK	gaaattcgggagttatgcctat Aca aagagtgagatgatctatac
hα4(I204S)	WT	SITGEYI	aaaccgtatcaagtgaaaccatcaaatca aTt acgggtgaatatatt
	MT	SITGEYS	aaaccgtatcaagtgaaaccatcaaatca aGt acgggtgaatatatt
hα5(H105R)	WT	FFHNG	accccagacacgttcttc cAc aacgggaagaagtccat
	MT	FFRNH	ccagacacgttcttc cGc aacgggaagaagtcc
hα5(P166T)	WT	GSYAYPN	aatttggcagctatgcgtac Cct aattctgaagtcgtttac
	MT	GSYAYTN	aatttggcagctatgcgtac Act aattctgaagtcgtttac
hα5(S209I)	WT	TSTGEYT	tgagaacatcagcacc aGc acaggcgaatacacaa
	MT	TITGEYT	tgagaacatcagcacc aTc acaggcgaatacacaa
hα6(R100H)	WT	FFRNG	aaatctggacgcctgacacctttttc AGA aatggtaaaaagtccattgct
	MT	FFHNH	aaatctggacgcctgacacctttttc CAC aatggtaaaaagtccattgct
hα6(P161T)	WT	GSYAYPK	actcaagtttgggagctatgcttat Ccc aaaagtgaaatcatatat
	MT	GSYAYTK	actcaagtttgggagctatgcttat Acc aaaagtgaaatcatatat
hα6(N204I)	WT	TNTGEYV	aacagtatctagtgagacaattaaatct aAc acaggtgaatacgtt
	MT	TITGEYV	aacagtatctagtgagacaattaaatct aTc acaggtgaatacgtt
Epilepsy Mutations			
hA5(V294L)	WT	FGVTT	ggacagtttttggg GTC accacggtgctg
	MT	FGLTT	ggacagtttttggg CTC accacggtgctg
hA2(T292K)	WT	VLTMT	tttggagtaacaactgtccta aCa atgacaactctaagcatcag
	MT	VLKMT	tttggagtaacaactgtccta aAa atgacaactctaagcatcag

hβ3(P301L)	WT	TLPKI	cttcgggagaccttg cCc aaaatcccctatgtc
	MT	TLLKI	cttcgggagaccttg cTc aaaatcccctatgtc

Table 2.1. Primers used for mutagenesis. Forward primers are shown for each point mutation made for experiments throughout this dissertation. Reverse primers were the reverse complement of the forward oligomer. Mutated bases are capitalized and in red. The wildtype *GABR* subunit served as a template cDNA for all constructs. WT = wildtype, MT = mutant.

The general mutagenesis protocol is described briefly below (Figure 2.2). Once primers were received, polymerase chain reaction (PCR) was performed using the template wildtype cDNA plasmid of interest and the primers (both forward and reverse primers). PCR consisted of 30 cycles in which the DNA reaction was heated to 95°C to denature the strands of DNA, then cooled to 60°C to allow the primers to anneal to the single DNA strands, and finally heated again to 68°C allow the polymerase enzyme to synthesize the new complementary DNA strand (extension/elongation) with the desired mutation. The PCR-product DNA was digested using the *Dpn I* enzyme to remove any methylated parental cDNA. The PCR-product cDNA was then replicated and amplified via a bacterial transformation using a dam+ *E. coli* strain of XL-10 Gold competent cells (Aligent Technologies) on LB agar plates containing 100 µL of a 100 mg/mL ampicillin. After 24 hours, single bacterial colonies were selected and DNA isolated using a minipreparation kit (cat#27106, QIAprep Spin Miniprep Kit, Qiagen). The final cDNA was sequenced and the desired mutation confirmed before use in electrophysiology experiments (Eurofins MWG Operon, Louisville, KY).

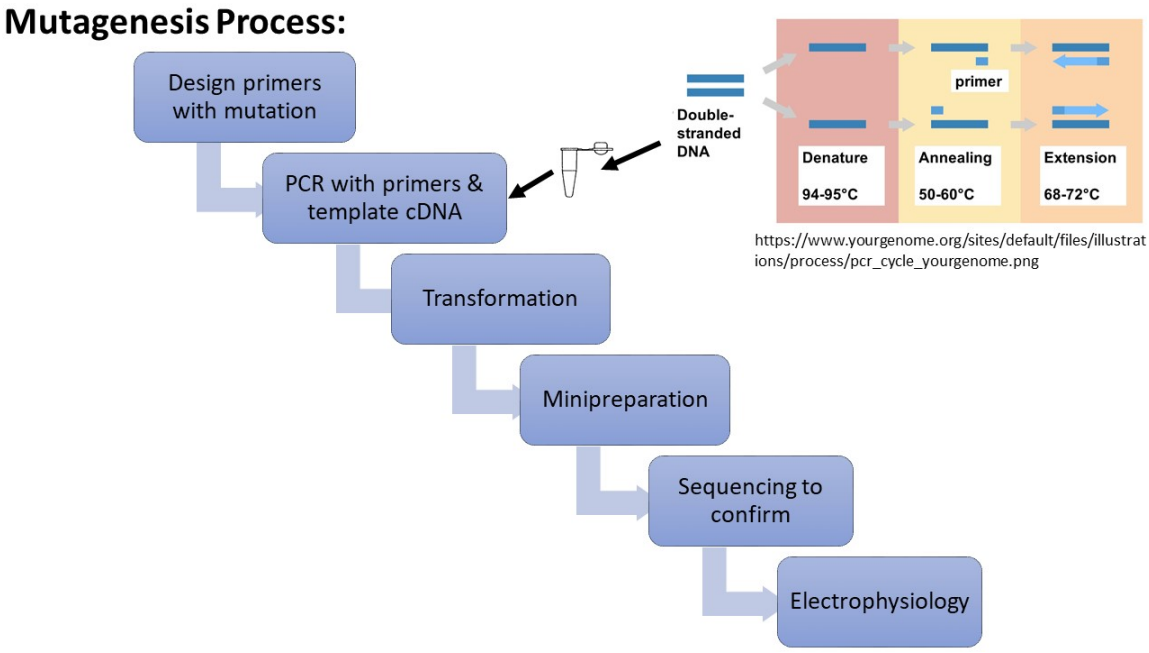

Figure 2.2. Mutagenesis was performed to introduce point mutations into plasmid vectors containing the selected *GABR* subunits. Mutagenesis was performed using the QuikChange Lightening site-directed mutagenesis kit. Minipreparation was performed using the Qiagen Miniprep Spin Kit. Sequencing was confirmed by Eurofins MWG Operon.

2.2 HEK293T cell properties and origin:

Human embryonic kidney cells containing the SV40 T-antigen (HEK293T) were acquired from American Type Culture Collection (ATCC®, Manassas, VA), catalogue number CRL3216. HEK293T cells are a heterologous expression system commonly used to study the function of ion channels. They can be passaged continuously for 20-30 times and still retain a high degree of fidelity (Thomas & Smart, 2012). For this reason, HEK293T were used for the all whole-cell patch clamp experiments described here.

The original HEK293 cell line was made into an immortalized cell line in the 1970's by exposing human embryonic kidney cells to sheared fragments of the adenovirus type 5 DNA (Graham, Smiley, Russell, & Nairn, 1977). HEK293 cells and their derivatives are

the second most common cell line used in cell biology after Chinese hamster ovary (CHO) cells (Lin et al., 2014). HEK293 cell morphology is similar to that of endothelial cells, although immunochemistry has revealed HEK cells display some neurofilament subunits (Thomas & Smart, 2012). Cells are 20-30 μm long which is large enough to patch with a microelectrode but small enough to receive sufficient drug perfusion to all sides of the cell during experiments (Thomas & Smart, 2012). The HEK293 cell line also express pseudotriplody chromosome features (Lin et al., 2014). Derivatives of the HEK293 cell line, like the 293T line, were created by expressing extra antigens. The HEK293T cell line expresses a SV40 T antigen that improves the expression of transiently transfected proteins (DuBridge et al., 1987; Rio, Clark, & Tjian, 1985).

Several features of HEK293 cell lines make them ideal for use in patch clamp experiments. First and foremost, HEK293 cells have a low level of expression of endogenous ion channels that could disrupt the measurements of the desired ion channel being expressed. Second, they have the necessary cellular machinery to take up exogenously introduced cDNA and translate and traffic it to the cell surface. For example, HEK293 cells can be transiently transfected with the ion channel protein of interest contained in a plasmid vector (ex. pcDNA3.1+), leading to strong protein expression for 1-3 days. Third, HEK293 cells are cultured easily and have low maintenance. Fourth, a low number of endogenous ion channels are expressed by HEK293 cell lines. These include human Na(v)1.7 sodium channels (creates a tetrodotoxin, TTX,-sensitive current) (He & Soderlund, 2010), endogenous potassium channels (Yu & Kerchner, 1998), and endogenous calcium channels (Berjukow et al., 1996). For measuring the activity of $GABA_A$ receptors, HEK293 cells do not express other ion channels that would infer with the signals measured from $GABA_A$ receptors.

In rare cases, certain *GABR* genes have also been reported in some lines of HEK293 cells. This includes the β3, γ3, and ε $GABA_A$ subunits (Thomas & Smart, 2012).

Most relevant to the following experiments performed here, the β3 *GABR* subunit can become endogenously expressed in certain HEK293 cell lines (Davies, Hoffmann, Carlisle, Tyndale, & Hales, 2000). Replicating this result has been inconsistent though and the expression of β3 may be linked to a very high passage number (Fuchs, Zezula, Slany, & Sieghart, 1995). This significance of β3 expression is that the β3 *GABR* subunit can form homopentameric channels that cause a tonic background leak current in patched cells. This is undesirable for patch clamp experiments of heteropentameric channels. The expression of the β3 *GABR* gene can be tested for using a simple picrotoxin inhibition assay. If beta homopentameric channels are being expressed endogenously by HEK293T cells, then untransfected cells will have a larger basal leak current when patched in the absence of GABA. This is because beta homopentameric channels form tonically open channels (Krishek, Moss, & Smart, 1996). Picrotoxin, a $GABA_A$ receptor channel blocker, can block this tonic current. If β3 is being endogenously expressed, picrotoxin exposure to patched cells will result in the block of leak current (see Figure 5.4 for an example of picrotoxin blocking tonic leak current) (Krishek et al., 1996). In our lab, HEK293T cells were tested for endogenous β3 expression each time a new frozen cell aliquot was resuscitated. For experiments described in this dissertation, no endogenous β3 was detected from HEK293T cells used.

When exogenous cDNA is introduced, the HEK293T cells efficiently express the desired protein above all other endogenous DNAs (Thomas & Smart, 2012). This process of introducing exogenous DNA is called *transfection* and is described below.

2.3 Cell culture and transfection:

HEK293T cells were maintained at 37°C and 5% CO_2 in Eagle Minimum Essential Medium (MEM) supplemented with 5% fetal bovine serum (Atlanta Biologicals Inc., Flowery Branch, GA), 40 μM *L*-glutamine, 100 U/ml penicillin and 0.1 mM streptomycin.

All reagents were purchased from Sigma-Aldrich (St. Louis, MO) unless otherwise stated. HEK293T cells grew in a monolayer until they become overly confluent (dense), when they began to form clumps. To avoid this, HEK293T cells were passaged weekly when they reached 70% confluency (Figure 2.3). “Passaging” meant that the cells were trypsinized to enzymatically remove them from the bottom of the flask they grew in. The cells were resuspended in supplemented MEM media and centrifuged (5 min at 1000 x g) down to a pellet. This pellet was then resuspended in media and a new flask with fresh supplemented MEM media was seeded with a low dilution of the HEK cells. Each round of passaging advanced the cell’s passage number by one (ex. p1 to p2). Cells were usually not passaged more than 22-25 times when used for patch clamp experiments.

When HEK293T cells reached a high passage number (>p22), a new frozen stock of HEK293T cells was resuscitated. Frozen HEK293T stocks were stored in liquid nitrogen and had a passage number of p2-4. Resuscitation of frozen cells involved thawing the cells gently in a 37°C water bath and then gently resuspending the cells in supplemented MEM media. After a gentle centrifugation cycle (8 min at 800 x g), the cells were seeded into a new flask with warmed media. Cells were then grown and passaged normally. As a side note, a previous genome sequencing study verified that HEK293T cells that are frozen in liquid nitrogen and then resuscitated retain the same genome sequence as new HEK293T cells produced (Lin et al., 2014).

Cells used for *in vitro* electrophysiology experiments were prepared over 2-4 days. First HEK293T cells were grown on glass coverslips (No.2, VWR, Radnor, PA) coated with 0.25 mg/ml of poly-D-lysine (#P7405-5MG, Sigma) until the cells reached 50-60% confluency. Then they were transiently transfected with α, β, and γ $GABA_A$ receptor subunits using X-tremeGENE (Roche Diagnostics, Indianapolis, IN). Briefly, 6 µL of X-tremeGENE reagent was added to 100 µL of ordinary MEM media. The mixture was incubated at room temperature for 5 minutes before the desired cDNAs were added to

give a total of 2 µg of cDNA (ratio of 6 µL:2µg cDNA). The ratio of α:β:γ subunit cDNAs was 1:1:1 (0.5 µg cDNA each). green fluorescent protein (GFP, 0.5 µg) cDNA of was also included in the transfection as an expression marker. Cells that fluoresced green after 24hrs were considered successfully transfected. Patch clamp experiments were performed on cells at 24-72 hours post-transfection. All *in vitro* electrophysiology experiments were performed at 22°C.

In most experiments performed for this dissertation, αβγ receptors were used. The successful incorporation of the γ subunit is important to confirm because αβ receptors have different pharmacology and kinetic properties than αβγ receptors (Angelotti & Macdonald, 1993; Verdoorn et al., 1990). Receptors expressing αβ only are sensitive to inhibition by Zn^{2+}, while αβγ receptors are insensitive to Zn^{2+} block (A. Draguhn et al., 1990; Trudell et al., 2008). In our system, γ2 incorporation into receptors was tested with zinc inhibition assays regularly and when testing a new receptor combination.

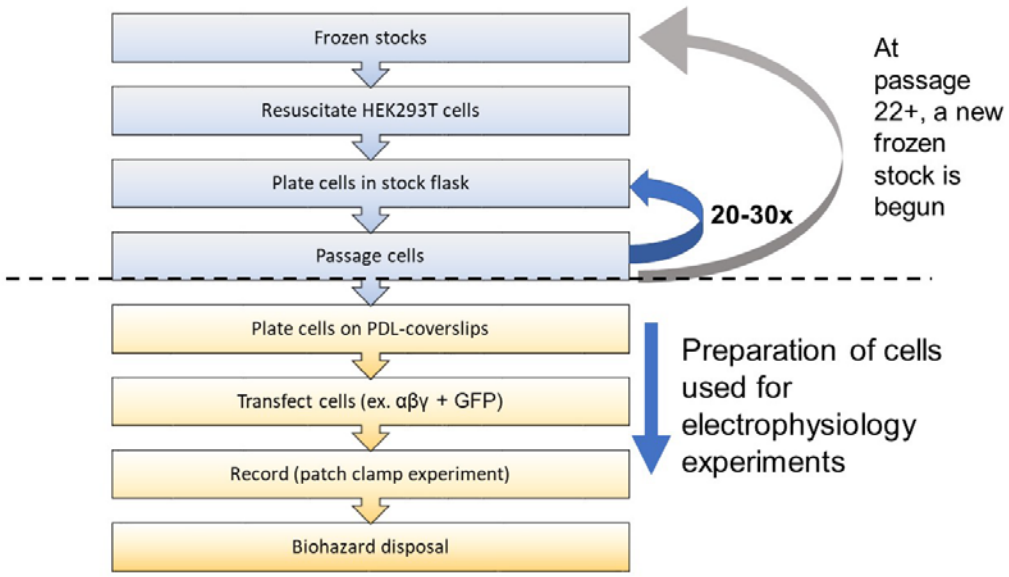

Figure 2.3. Flow chart describing how HEK293T cells were resuscitated, passaged, plated and transfected for *in vitro* patch clamp recording experiments. Specific details of how cells were resuscitated, passages and transfected are described in Section 2.3.

2.4. Theory and circuits of whole-cell patch clamp electrophysiology

$GABA_A$ receptors are ion channels that allow anionic current to pass when stimulated (Bormann et al., 1987). When ions flow across a membrane from one side of a gradient to another, it creates current (*I*). The permeability of the cell membrane to current is low when channels are closed (GABA not present). When GABA is present, the channels open and allow chloride ions to pass (conductance). In the adult mammalian brain, chloride flows into the cell, hyperpolarizing the cell membrane (Sieghart, 1995a). Because the state of ion channels set the cell membrane's degree of permeability to chloride ions, the ion channels can be thought of as resistors to ion flow. Conductance (*g*) of current (*I*) and resistance (*R*) are electrical properties of a circuit that are inversely related, as described in Ohm's Law:

$$\Delta V_{mem} = I_{mem} x R_{mem} = I_{mem}/g$$

The voltage across the membrane (V_{mem}) is also called the membrane potential. It is set by the difference in charge across the membrane which ion channels and other ion transporters set. The purpose of voltage-clamp electrophysiology is to measure the conductance of current across the cell membrane, basically how electrical charge passes from one point to another.

In the whole-cell patch clamp set up, the microelectrode is key to measuring a high-fidelity signal. Microelectrodes are pulled from glass capillary tubes to a point with a resistance of 3-8 MΩ when filled with intracellular solution and the tip placed in extracellular solution. When forming a patch with the cell membrane, several steps are followed. First, the electrode must be lowered down onto the membrane and light negative pressure applied until a gigaseal (>1GΩ) is formed. The gigaseal is crucial to forming stable patches with good signal-to-noise ratio. Once the gigaseal is formed, light negative pressure is applied to break open the cell membrane at the tip of the electrode. When this occurs, the intracellular solution inside the microelectrode becomes continuous with the

intracellular solution of the cell (**Figure 2.4**). When ions flow in or out of the ion channels, the electrode detects this current. To do this, the microelectrode contains a silver chloride wire continuous with the internal solution. The chloride ions (Cl^-) in solution can react with the silver ions (Ag^+) to form AgCl (s) on the wire, which releases an electron:

$$Ag^+ + Cl^- = AgCl + e -$$

The electron released is a current signal that can be transmitted through the rest of the system to the computer, as described below. As described below, the voltage-clamp system allows the researcher to measure the flow of ions across channels like $GABA_A$ receptors.

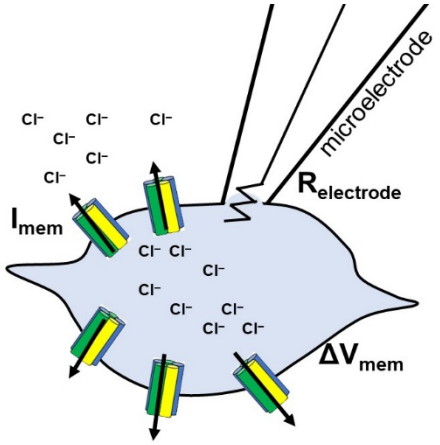

Figure 2.4. Schematic of whole-cell patch clamp recording from HEK293T cells expressing $GABA_A$ receptors. Current (I_{mem}) can flow across the cell membrane through ion channels. The ion channels, depending on how many are open, set the level of ion conductance for the cell. The membrane potential (V_{mem}) is set by the difference in electrical charge across the cell membrane. A microelectrode can measure the flow of this current through voltage-clamp recording. The electrode itself also acts as a resistor for the current signal being sent up the electrode to the computer. The arrows are pointing outwards to represent the flow of chloride ions in the HEK293T cell expressing $GABA_A$ receptors when the holding V_{mem} is set to -60 mV.

There are several important components of the voltage-clamp, whole-cell electrophysiology set up (Figure 2.5). The cell expressing ion channels is the center of the system. The microelectrode (or micropipette) measures the change in ion current as the channels are activated and deactivated. The inside of the microelectrode is constant with the inside of the cell (whole-cell). Because the changes in membrane potential are very small, the current flows through an amplifier to increase the amplitude of the signal. The signal is also sent through a digitizer that converts the signal from analogue to digital. The signal is then sent to the computer. In the voltage-clamp system, the computer calculates the difference between the set holding voltage ($V_{holding}$), also called the command voltage (V_{cmd}). To correct for the difference between the holding and membrane potential ($V_{holding} - V_{mem}$) a certain amount of current is injected back into the cell system to hold the voltage steady (voltage clamp). The amount of current injected is the signal recorded by the computer. This current signal represents the sum activity of the chloride current passing across all the ion channels in the HEK293T cell membrane (hence “whole-cell recording”).

In our HEK293T system, cells are clamped to -60 mV. This means that chloride current actually flows out of the $GABA_A$ receptors when the channels open. $GABA_A$ receptors are generally studied using a close to symmetrical chloride gradient to avoid the effects of Goldman rectification (Goldman 1943). When the cell membrane is clamped to -60 mV, chloride flows outwards (efflux). This is an accepted method because $GABA_A$ receptors have been shown to generally behave as simple ohmic pores that can conduct ions equally-well in both directions when activated (Bormann et al., 1987). There is some evidence that chloride currents rectify slightly outwardly at very low P_o values and the direction of current flow affects the degree of modulation measured by general anesthetics (O'Toole & Jenkins, 2012), but clamping HEK293 cells to -60mV is a common recording method used by multiple labs because -60 mV is sufficiently far from E_{Cl} to preclude

rectification. The HEK293 expression system is still one of the most sensitive and accurate methods for measuring $GABA_A$ receptor function *in vitro*.

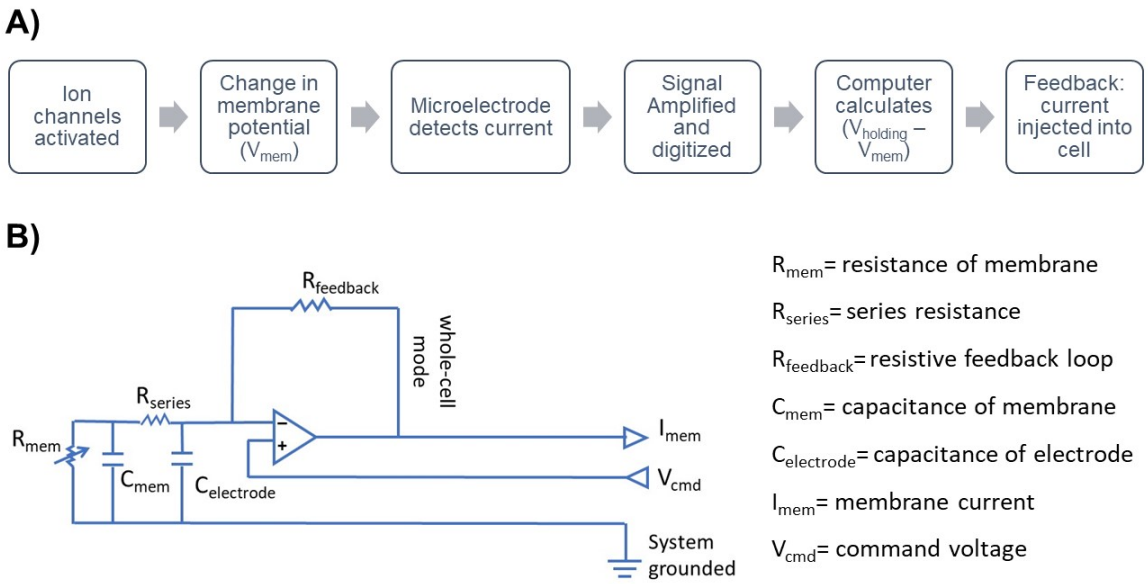

Figure 2.5. Schematic of how the voltage-clamp patch clamp electrophysiology works. A) The steps through which the signal (change in ion channel conductance) is detected and sent to the computer. Tthe difference in membrane potential (V_{mem}) is compared to the holding potential (V_{cmd} or $V_{holding}$). The difference in membrane potential is corrected for by injecting a specific amount of current back into the cell system to hold the membrane potential constant. The amount of current injected is the signal measured. B) Electrical circuit diagram of the whole-cell, voltage-clamp recording system for a patched cell expressing ion channels.

In this system, series resistance compensation was not used. Series resistance compensation corrects for the non-zero resistance the microelectrode adds to the system as the signal is transported from the cell to the computer. Ideally, the resistance of the patch microelectrode is zero and so measuring the changes in membrane current or when changing the membrane voltage would be limited to the speed of the electronics (a few microseconds). Series resistance compensation uses positive feedback to correct for the microelectrode resistance. A signal proportional to the measured current is added to the signal to increase the command potential to compensate for the potential drop across the microelectrode. Compensation is limited by two factors. First, as compensation approaches 100%, the command potential will saturate the limit of the electronics. Second, the positive feedback of the compensation can turn the compensation of the circuit into an oscillator, degrading the signal fidelity. Another way of thinking of series resistance is assuming 1 nA of current is passing up the electrode which is a 10 MΩ resistor. Using Ohm's Law, this creates 10 mV of current. If the cell is supposed to be clamped to -60 mV then the uncompensated series resistance means the cell is actually clamped to -50 mV. This means that only very large currents are attenuated, but only by 10%. In our GABA concentration-response curves, not using series resistance compensation would only attenuate the highest GABA concentration responses by about 10%, but the smaller responses would be minimally affected. For this reason, we did not use series resistance compensation in the following experiments.

The pipette offset compensation is applied to the electrode before patching a HEK293T cell. The pipette offset compensation is used to correct the pipette command potential in mV for the total liquid-liquid and liquid-metal junction potentials in the electrode on bath. Junction potentials occur when two mediums of different electrolyte composition meet, usually liquid-liquid. When the two meet, the ions move along there gradients, but some move faster than others. The difference in ion gradients creates a potential. Junction

potentials degrade the quality of the signal and so are corrected for with the pipette offset correction.

The ideal cell to patch for whole-cell voltage clamp experiments has a good cell morphology and moderate expression of the GFP reporter gene. Ideal cells are isolated or near no more than 1-2 other cells with no obvious connections between cells. Cells growing next to each other are more likely to be electrically coupled and the increased volume of the patch makes it harder to voltage clamp (Thomas & Smart, 2005). Round cells are unhealthy and overly flat cells are difficult to patch. Cells should form a strong gigaseal (≥1 GΩ) onto the tip of the electrode. When patch configuration goes whole-cell upon the application of negative pressure, there should be a minimal change in the series resistance and the leak current should be less than 200 pA (closer to 0 is ideal).

2.5. Bath and drug perfusion system:

Patch clamp experiments took place in a bath placed on an inverted Zeiss microscope (Axiovert 200). The microscope was mounted on a Micro-g-anti-vibration table (Technical Manufacturing Corp., 63-563). A handmade bath was mounted on the stage of the microscope. The bath consists of a plastic culture dish (10 cm diameter) onto which aquarium sealant has been applied to create a straight rectangular bath chamber for the solution. There were two inlets (shortened and beveled p200 pipette tips) on one side of the bath and two outlets (syringe needles, BD 21G 1 ½ , cat# 305167) on the other side that direct solution straight across the bath to be suctioned off (Figure 2.6A). The extracellular solution was gravity-driven and maintained at room temperature (22°C).

Drugs were applied to the system via a perfusion system. The drug perfusion system consisted of glass capillary tubes (borosilicate glass: O.D. 1.0 mm, I.D. 0.75mm, 10cm length; Sutter #B100-75-10) attached to a perfusion head controlled by a rapid solution changer (RSC-160, BioLogics Science Instruments). The tubes on the perfusion

head were connected with polyethylene tubing to a longer set of polytetrafluoroethylene (PTFE) tubing that was connected to a 10-channel infusion pump (KD Scientific Inc). Solutions were loaded in 10 mL syringes (BD 10 mL Luer-Lok tip, cat# 309604) that were loaded onto the infusion pump. The pump pushed solutions out at a rate of 1 mL/min over the patched cell placed in the middle of the flow (Figure 2.6B-C).

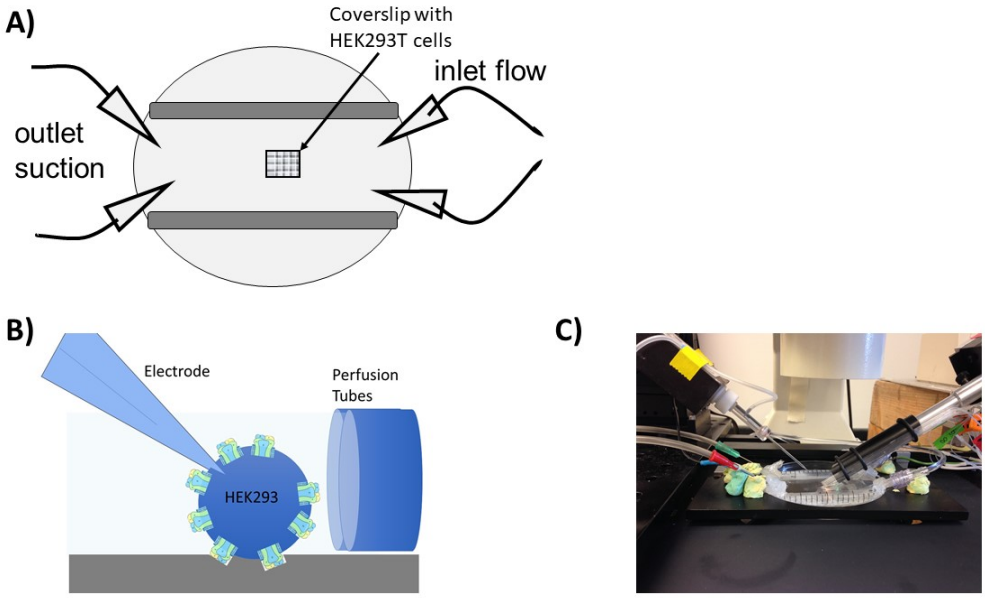

Figure 2.6. Whole-cell patch clamp setup in the recording bath. A) Top view schematic of the bath on the rig. Two inlets perfuse extracellular solution into the bath and two outlets suction off the liquid. The placement of the inlet/outlets pulls solution across the bath in an even flow so that the coverslip with HEK293T cells constantly receives fresh extracellular solution. B) Schematic of a HEK293 cells expressing $GABA_A$ receptors being patched with an electrode. Perfusion tubes apply the drug solutions and were controlled by the computer. C) Picture of an actual recording bath with the electrode on the left and perfusion tubes on the right.

In order to apply an even and consistent flow of drug solutions, the glass tubes of the perfusion system must be aligned with the cell to be patched. The perfusion system was calibrated daily on $\alpha_1\beta_2\gamma_{2s}$ receptors by measuring currents elicited by 5-10 μM GABA for each tube used in the pharmacology experiment (Figure 2.7). The goal was to have an even flow and equal responses from every tube with less than 20-40pA of variability (~10% or less). If a different drug protocol was used that day, then that protocol was used for the calibration.

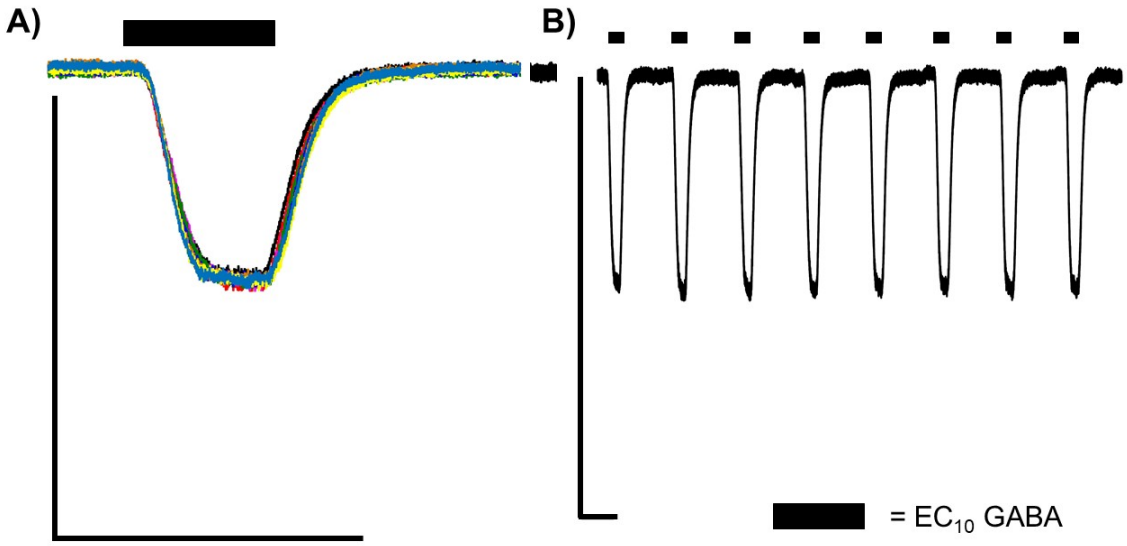

Figure 2.7. Example trace of GABA calibration performed daily to calibrate the drug perfusion system before starting experiments. A) Overlay of eight EC_{10} GABA responses. Scale bar: 2 sec, 500 pA. B) Trace of the eight EC_{10} GABA responses recorded with 8 sec of washout between exposures. Scale bar: 2 sec, 500 pA. Whole-cell patch clamp recording of HEK293T cells expressing $\alpha_1\beta_2\gamma_{2s}$ $GABA_A$ receptors.

2.6 Whole-cell patch clamp electrophysiology:

Two different electrophysiology rig setups were used to collect the data in this dissertation. One rig was called the “pharmacology rig” because its perfusion system was set up to best record modulator like benzodiazepines. The second rig was called the “CSF rig” and was set up to measure the effects of CSF on $GABA_A$ receptors. The CSF sample volumes loaded onto perfusion pumps were smaller than those typically used for other modulators (2 mLs instead of 10 mL). This required a separate setup than the “pharmacology rig”. Both are described below.

2.6.1 Pharmacology patch clamp rig setup

The “Pharmacology” rig used to measure GABA concentration-response assays, midazolam assays, and picrotoxin assays was setup as follows. A rapid solution changer (RSC-160, BioLogics Science Instruments) connected to a 10-channel infusion pump (KD Scientific Inc) was controlled by protocols written in pClamp 9 (Molecular Devices, LLC.) and used to deliver drugs. Whole cell currents were recorded at -60mV, filtered at 100 Hz and sampled at 200 Hz with a MultiClamp 700B amplifier and DigiData 1322A (Molecular Devices, LLC) digitizer. Data was acquired with pClamp 9.2 software (Molecular Devices).

The inverted Zeiss microscope (Axiovert 200) was mounted on a Micro-g-anti-vibration table (Technical Manufacturing Corp., 63-563). The microscope had a 10X and 40X objective (Zeiss), a HAL100 halogen lamp, a HBO100 FluoArc fluorescence source, and a LD condenser for phase contrast visualization.

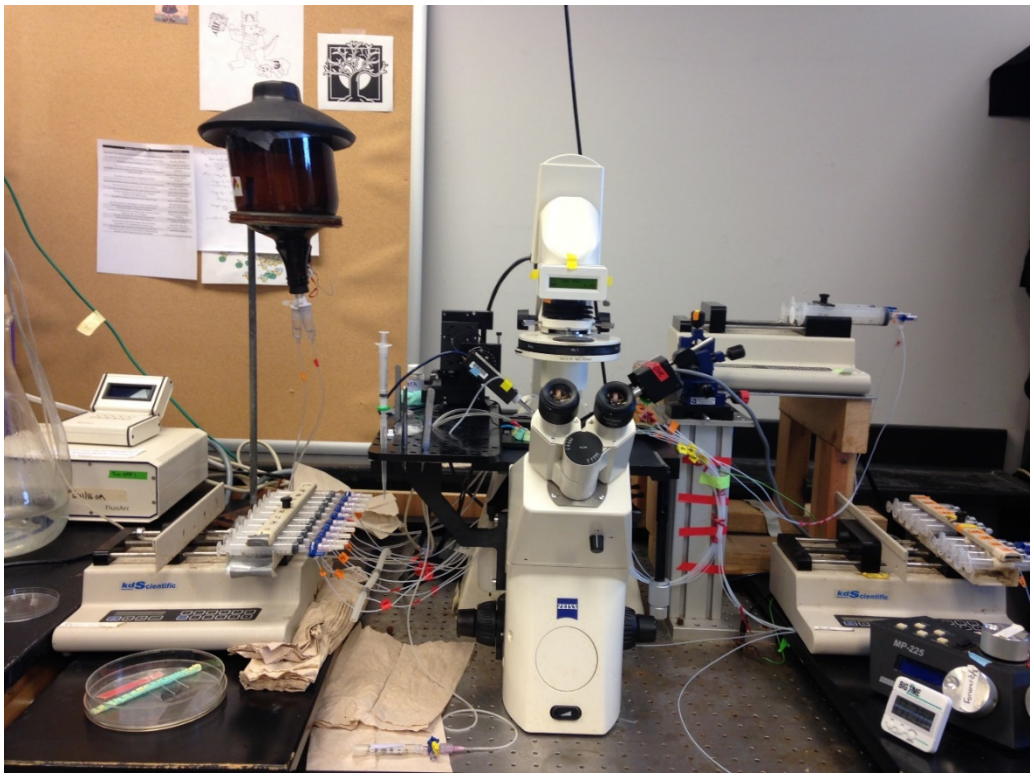

Figure 2.8. Whole-cell patch clamp recording rig used for pharmacology experiments. The rig set up includes two 10-channel infusion pumps, one 2-channel infusion pump, inverted microscope mounted on Micro-g-anti-vibration table, FluoArc fluorescence box, Sutter micromanipulator, rapid solution changer, MultiClamp 700B amplifier, DigiData 1322A. Data was acquired via a Dell computer running pClamp 9.2.

2.6.2 Patch clamp rig setup used for CSF assays

The patch clamp recording rig consisted of a rapid solution changer (RSC-160, BioLogics Science Instruments) connected to a 10-channel infusion pump (KD Scientific Inc) and two 2-channel infusion pumps (KD Scientific Inc) (Figure 2.9). The 10-channel infusion pump contained 10 mL plastic syringes. The 2-channel pumps held CSF samples 3mL plastic syringes (BD 3mL luer-lok syringe, cat# 309657). The tubing for the three different pumps was interconnected as shown in Figure 2.9. Drugs were perfused into the bath at a rate of 1 ml/min. The infusion pumps were connected to the glass perfusion capillary tubes on the rapid solution changer controlled by protocols written in pClamp 10.2 (Molecular Devices, LLC.). Whole-cell currents were recorded at -60mV, filtered at 100 Hz and sampled at 200 Hz with a Axopatch 200B, a Tuneable Activity Filter 900 (Frequency Devices INC) and a DigiData 1440A (Molecular Devices, LLC). The electrode holder was controlled by a Sutter MP-225. The recording bath was placed on the stage of an inverted Axiovert 200 microscope (Zeiss) with a 100W halogen bulb and a Zeiss HBO 50/ac microscope illuminator box (mbq52 ac, Zeiss) for fluorescence.

The CSF samples were always loaded onto a 2-channel infusion pump. This pump was only run when the CSF was directly being applied to the patched cell. The 10-channel infusion pump contained the extracellular washout solutions and GABA solutions. During CSF assays, the 10-channel pump was on continuously to provide the background solution flow necessary to wash the CSF solutions across the cell in a single direction before solutions were suctioned off. The 2-channel infusion pump was turned on manually 2-3 seconds before recording the CSF responses and then turned off 3 seconds after the CSF exposure finished. A GABA calibration (10 μM GABA in every tube) was run daily to confirmed that manually turning on and off the 2-channel pump did not disrupt the flow of solutions in the bath or the peak currents measured.

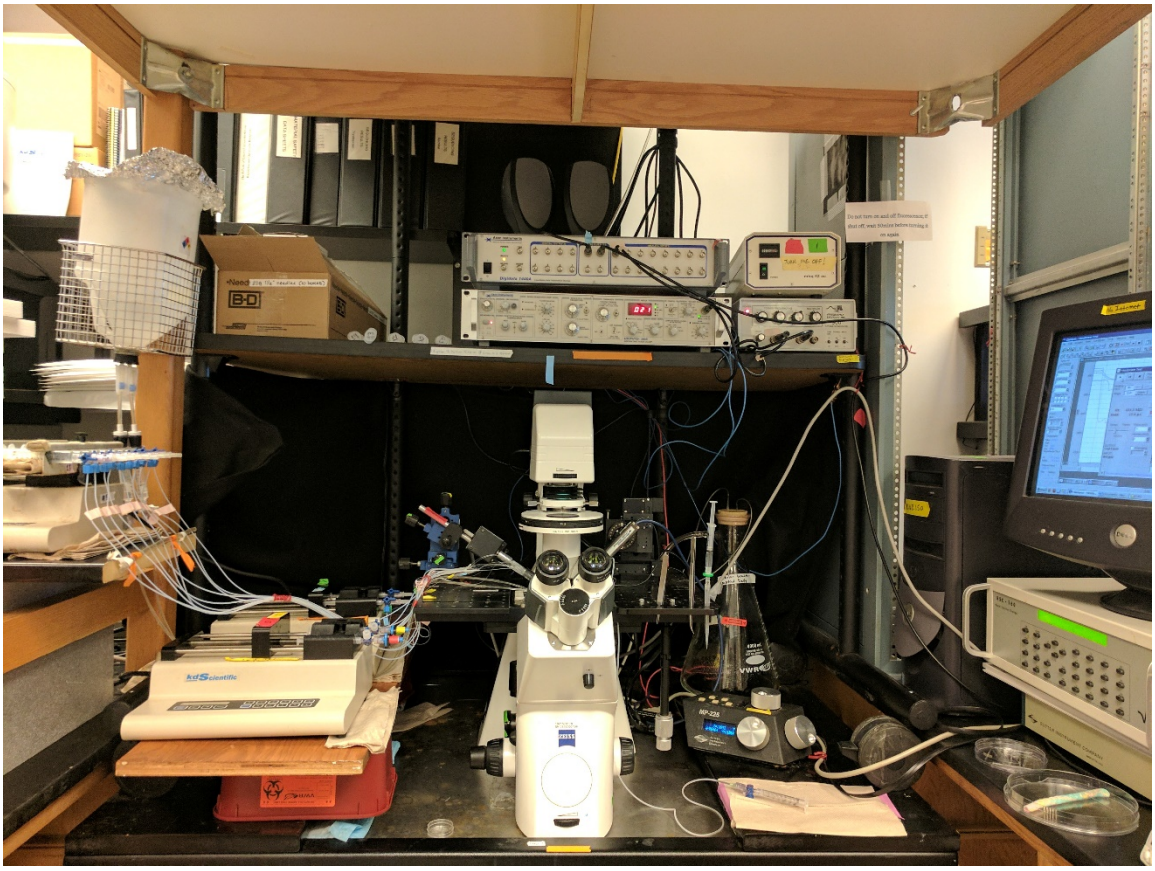

Figure 2.9. Patch clamp rig setup used for CSF assays. Whole-cell patch clamp recording rig used for CSF experiments. The rig set up includes one 10-channel infusion pump and two 2-channel infusion pumps. See Section 2.5.2 for further details.

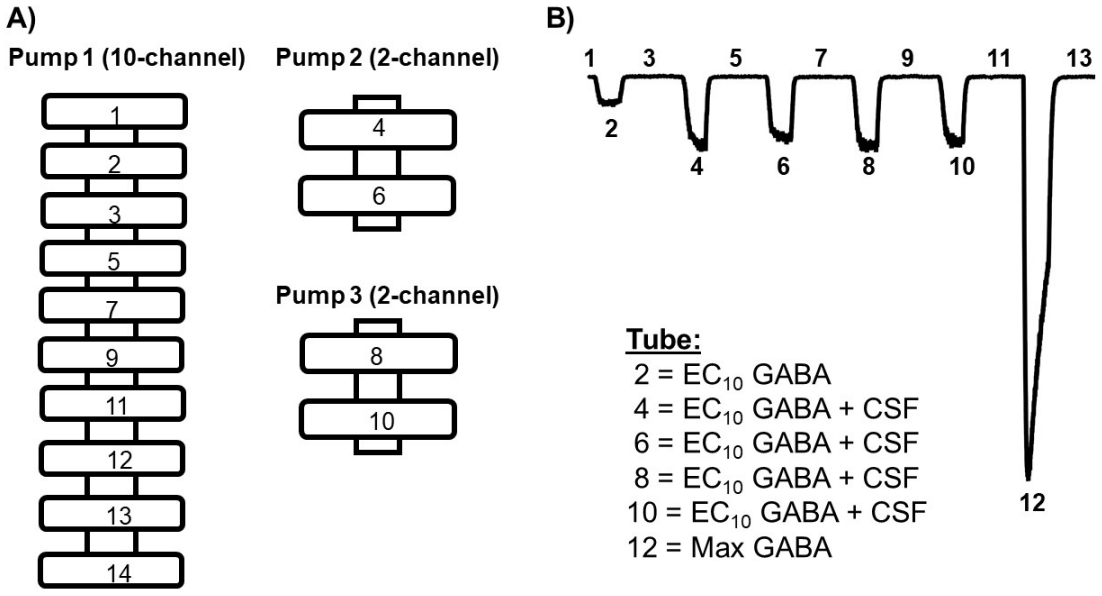

Figure 2.10. How drug perfusion pumps are set up for CSF assays. Three infusion pumps were connected to the rapid solution changer to measure CSF potentiation. CSF samples were loaded onto the 2-channel pumps. Extracellular solution and GABA solutions were loaded onto the 10-channel pump. Tubing from each infusion pump was interconnected onto the rapid solution changer. The numbers indicate the order in which the tubing was connected (#1-14 for pump channels). B) An example CSF trace which contained a control EC_{10} GABA response and maximum GABA (300 μM) response along with 4 different CSF dilutions (channels 4, 6, 8, 10).

2.6.3 Whole-cell voltage clamp recordings:

Whole-cell patch clamp recording experiments were performed using HEK293T cells expressing $\alpha_x\beta_2\gamma_{2s}$ $GABA_A$ receptors and GFP. Patch pipettes were created from thin-walled borosilicate glass (TW150F-4, World Precision Instruments, Inc.) using a horizontal puller (P-97, Sutter Instruments, Inc.) (Sutter protocol listed in Appendix C) to give a resistance of 2-8 MΩ when filled with intracellular solution (120 mM KCl, 2 mM $MgCl_2$, 10 mM EGTA, 10 mM HEPES and adjusted to pH 7.2 with NaOH, 315 mOsm). Extracellular solution contained 161 mM NaCl, 3 mM KCl, 1 mM $MgCl_2$, 1.5 mM $CaCl_2$, 10 mM HEPES and 6 mM D-Glucose, adjusted to pH 7.4 with NaOH (320-330 mOsm). Whole-cell currents were recorded at -60mV, filtered at 100 Hz and sampled at 200 Hz in pClamp 9.0 or 10.2. All experiments occurred at room temperature (22°C).

Whole-cell patch clamp experiments consisted of data collected from at least 10 cells per condition. To control for cell health and transfection efficiency, cells were recorded from at least 3 different days and at least 2 different transfections. On days when mutant receptors were recorded, an additional 3-5 wildtype cells were recorded to provide a time-matched expression control.

The details of each pClamp protocol used in this dissertation are listed in Appendix A. Below, the GABA concentration-response assay protocol is described in detail and was used most often in the following experiments.

2.6.4. GABA concentration-response assay protocol

GABA concentration-response assays were performed by exposing each whole-cell patch to 8 concentrations of GABA across a 3.5 logarithmic decade. Typically, each drug exposure was for 2 seconds with 8 seconds of washout between concentrations (Figure 2.8A). Each concentration-response assay consisted of 8 sweeps, one sweep per GABA concentration. Each sweep was made up of 2048 data points (10.24 seconds).

GABA concentrations for $\alpha_x\beta_2\gamma_{2s}$ receptors were: α1 = 0.3-1000 μM; α2-α3 = 0.01-300 μM; α4 = 0.03-100 μM; and α5-α6 = 0.01-30 μM.

.

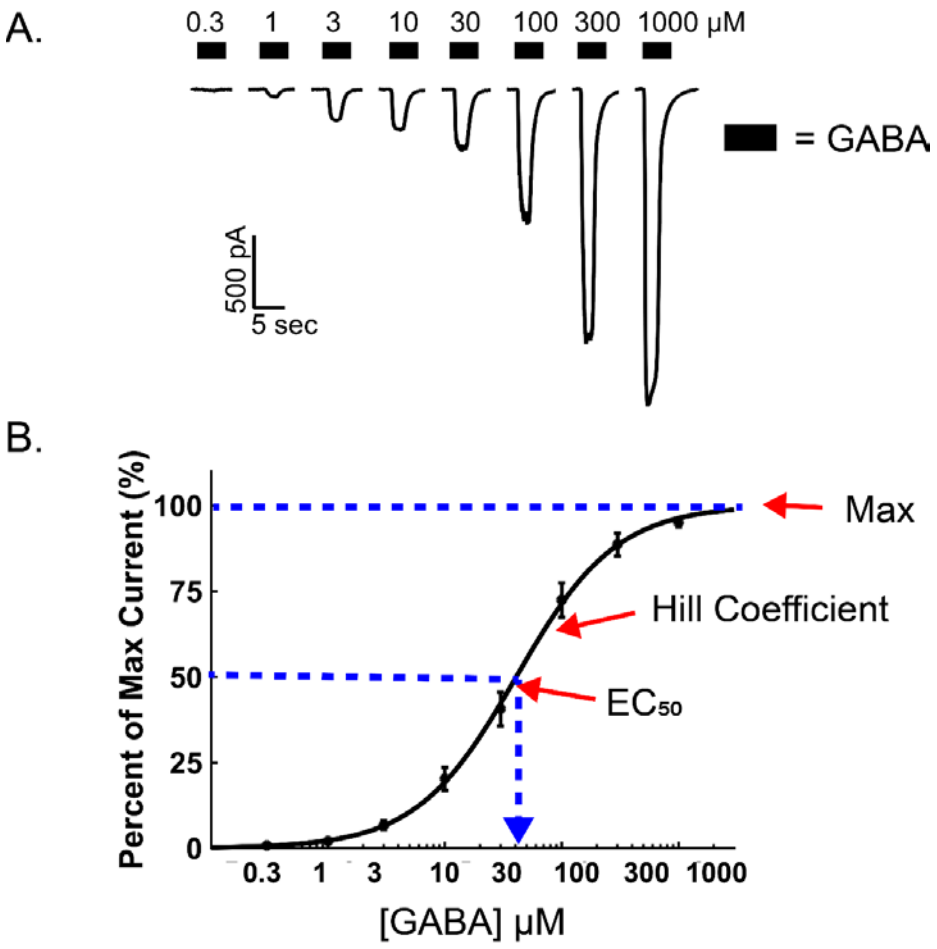

Figure 2.11. Example GABA concentration-response curve (0.3-1000 µM) measured from HEK293T cells expressing $\alpha_1\beta_2\gamma_{2s}$ $GABA_A$ receptors using whole-cell patch clamp recording. **A)** Example trace of a GABA concentration-response assay. **B)** Peak currents from example trace (A) plotted on semilogarithmic plot. Three parameters define this curve: the maximum response, slope (Hill coefficient), and EC_{50}. The Hill equation estimates these three parameters. The Hill equation is: $I = I_{max}\ x\ \frac{[G]^{nH}}{([G]^{nH}+EC_{50}{}^{nH})}$ where the peak current response (*I*) is defined by the maximal current response (I_{max}), GABA concentration (*[G]*), the concentration defining the half-maximal response (EC_{50}), and the Hill coefficient (*nH*).

2.7 Whole-Cell Analysis:

2.7.1. Analyzing whole-cell recordings:

Recordings were analyzed using MATLAB (Math Works, Inc.). Each data file of a single GABA concentration-response assay consisted of 8 sweeps, each 2048 points long. Recordings were baseline corrected in MATLAB to adjust for any baseline drift across each sweep of the recording. Baseline correction was performed using the linear equation: Y= mX + b. First, the first and last 21 points of each sweep were averaged (Startmean and Endmean). The slope (mgrad) and y-intersect (b) were calculated. Then the leak current was calculated for each point throughout the sweep. The leak current was then subtracted from every point in the raw current trace (all 2048 points).

$$mgrad = \frac{(Endmean - Startmean)}{2028}$$

$$b = Startmean - (mgrad\ x\ 10)$$

$$leak\ current = b + mgrad(1{:}2048)$$

$$Leak\ subtracted\ current = raw\ current - leak\ current$$

Each data file was baseline corrected for each sweep within the file. The MATLAB code was adjusted to fit different protocols when needed and is listed in Appendix B.

2.7.2 Analyzing GABA concentration-response curves:

Whole-cell peak currents (*I*) were measured from GABA exposures. The eight peak currents measured were fit using a least-of-squares non-linear regression based on the Hill equation (Figure 2.11):

$$I = I_{max} * [A]^{nH} / (EC_{50}^{nH} + [A]^{nH})$$

where *I* was current peak amplitude recorded, I_{max} was maximum current amplitude, EC_{50} was the half-maximal GABA concentration, *A* was agonist concentration and *nH* was the

Hill coefficient. The maximum peak current, EC_{50} and Hill coefficient were fit for each cell's run. The overall average for each parameter was calculated by averaging each estimated parameter from all of the cells measured from that condition.

Some labs average each GABA concentration response first and perform a single Hill fit through pooled data. This method can under- or overestimate the EC_{50} and other Hill parameters because it fails to take into account differences in receptor expression and cell size across cells. For this reason, our lab fits GABA concentration-response curves for each cell measured before averaging all the measurements to give an overall average value.

2.7.3 Interpretation of changes in Hill parameters:

When Hill parameters are estimated from whole-cell recordings, the natural variations in the Hill parameters can be explained by the following. The natural variations in the Hill parameters between cells expressing the same receptor combination can be caused by differences in cell volume and shape, receptor expression level and patch quality. Other differences in the Hill parameters between wildtype and mutated receptors can be explained by the following. Changes in maximum current can be due to changes in single-channel conductance or the rate of desensitization, but slight changes in cell surface receptor expression are often the cause of minor changes in maximum current. The maximum current also reflects the efficacy for the receptor condition tested. The Hill coefficient for $GABA_A$ receptors is usually between 1.0-2.0. Classically, changes in the Hill coefficient can be due to changes in altered GABA cooperativity, the loss of a GABA binding site or altered channel desensitization. Another situation in which the Hill slope can be underestimated is if the concentration-response curve has a bell-shaped curve. This causes the Hill fit to underestimate the maximum response and have a shallower Hill coefficient. More often minor changes in the Hill coefficient are attributed to the

homogeneity in the receptor population expressed by the HEK293T cell. For example, a shallower Hill coefficient can be caused by a shift in the population of receptors expressed from mostly αβγ receptors to a mixture of αβγ and αβ receptors. Apparent-affinity (EC_{50}) is a compound measure affected by the energetics of the binding affinity and channel gating (efficacy). Changes in GABA apparent-affinity can be due to changes in GABA's binding affinity, gating or both. Other explanations than the above are possible but less likely.

In theory, shifts in the GABA concentration-response relationship can be interpreted as changes in GABA binding affinity or efficacy. A parallel shift would have an altered GABA EC_{50} but with an unchanged Hill coefficient (slope). This could reflect a change in the binding affinity of GABA for the receptor. Alternatively, a change in the maximum response to saturating GABA concentrations could indicate a change in the gating of the receptor (efficacy of GABA). Each of these effects would need further experiments, including binding assays, to confirm the underlying mechanisms, especially if the binding was affected. Just comparing the EC_{50} of two conditions is not enough to definitively show an effect because the EC_{50} is a compound parameter of changes in the gating and binding. Most changes in the concentration-response relationship reflect a mixture of binding and gating effects, which is why further experiments would be needed to confirm a specific molecular mechanism.

A mutation made in an allosteric binding site (ex. benzodiazepine site) could alter the allosteric modulator's effect on the receptor in one or more of the following ways: 1) alter the modulator's ability to alter GABA's affinity, 2) alter the modulator's ability to alter the efficacy of GABA, 3) alter the modulator's binding affinity for the receptor, and/or 4) alter the coupling of the allosteric site to that of the GABA-binding site. When a mutation within an allosteric site changes the GABA apparent-affinity (EC_{50}), any of the above reasons might be the cause.

2.8. Statistics: The whole-cell Hill parameters compared statistically were the maximum current, the Hill coefficient, and the EC_{50}. The mean and standard error of the mean (S.E.M.) were calculated for each parameter. Differences were evaluated using a one-way ANOVA with repeated measures when there were 3 or 4 different receptor conditions. When a significant F statistics was found, Dunnett's post-hoc analysis was performed for multiple comparisons. An $\alpha = 0.05$ was used as a threshold for significance. When only two receptor conditions were present, a Student's t-test was performed ($\alpha = 0.05$) to assess significance. Statistical analysis was carried out using Prism 7.0 (Graphpad Software, Inc.).

Summary:

Using the above methods, I investigated the modulation of $GABA_A$ receptor function by positive allosteric modulators and mutation. Methods combined cell culture, site-directed mutagenesis and whole-cell voltage clamp electrophysiology to measure $GABA_A$ receptor function. While modest changes in these methods were made for specific experiments carried out in the following data chapters, these details are noted in the abbreviated methods sections for Chapters 3-5.

Chapter 3:

Chapter 3:

The molecular pharmacology of midazolam at $GABA_A$ receptors

Overview:

In this chapter, I address two questions about the molecular actions of benzodiazepines at $GABA_A$ receptors: 1) how does mutating the benzodiazepine binding site of the $GABA_A$ receptor affect the ability of the receptor to respond to midazolam's positive allosteric effects, and 2) does midazolam alter the GABA concentration-response relationship consistent with conventional benzodiazepine theory. In the first half of the chapter, I present data from single residue mutations of conserved residues in the α1-6 subunits within the benzodiazepine binding site. I hypothesized that substituting a residue present in α subunits sensitive to midazolam modulation (α1, α2, α3, α5) with the residues present in the α subunits insensitive to midazolam modulation (α4 and α6) would reduce the degree of receptor potentiation measured with midazolam. The opposite residue exchanges were also made in α4 and α6 subunits. These were predicted to increase the sensitivity of the receptor to midazolam. The three mutations were located in structural loop A, loop B and loop C of the α subunit half of the benzodiazepine binding site. There were 18 mutations in total. In loop A, mutating the conserved histidine to an arginine of α1, α2, α3 and α5 abolished midazolam potentiation as expected. The mutation of a threonine or proline in loop B of α1-6 had minimal effects on the efficacy of midazolam potentiation. The loop C mutations (serine to isoleucine) increased or decreased the efficacy of midazolam in a α-subunit-specific manner, dramatically increasing it in α3 and α5. The second half of the chapter compares midazolam's positive modulation of $GABA_A$ receptors to conventional benzodiazepine theory which is based on diazepam's actions. These experiments were based on the hypothesis that the presence of midazolam will shift the GABA concentration-response relationship leftwards in a parallel manner. The

results were not consistent with this hypothesis. Instead, a non-parallel leftwards shift was shown. This was consistent with more recent theories that positive benzodiazepines (i.e. midazolam) can affect both GABA's binding and gating of the receptor channel. Overall, this chapter describes data that extends the present knowledge about midazolam's actions at $GABA_A$ receptors.

3.1: Introduction

Diazepam is a classic benzodiazepine PAM. It binds and modulates synaptic $GABA_A$ receptors containing α1, α2, α3, or α5 subunits but not α4 or α6 (Benson et al., 1998; H A Wieland et al., 1992). It is often assumed that other positive benzodiazepines (ex. midazolam, lorazepam, flunitrazepam) follow the same pattern of α-subunit specificity as diazepam. Most studies looking at the underlying mechanisms of benzodiazepines have used diazepam over other benzodiazepines in studies of structural-function (Rogers et al., 1994).

The conventional theory underlying the mechanism by which benzodiazepines enhance $GABA_A$ receptor activity is based on changes in binding affinity and not gating. Diazepam was originally shown to shift GABA concentration-response relationships leftwards in a parallel manner based on binding assays and patch clamp studies (Lavoie & Twyman, 1996). Single channel studies showed that diazepam increased the single-channel opening frequency without altering the mean open duration (Rogers et al., 1994). These results were interpreted as diazepam increasing the affinity of GABA for the receptor. However, more recent studies have suggested that benzodiazepines alter GABA's gating of the receptor rather than its binding (Matt T. Bianchi, Botzolakis, Lagrange, & Macdonald, 2009; Kristiansen & Lambert, 1996; Rusch & Forman, 2005). Midazolam is a positive allosteric modulator (PAM) commonly used to induce anesthesia

and sedation (Olkkola & Ahonen, 2008). Midazolam has been less studied than diazepam, and one mechanism of action of midazolam that remains to be completely understood is how midazolam alters the binding and gating properties of $GABA_A$ receptors to enhance channel function. It is also less studied how different structures within the high-affinity benzodiazepine site play a role in the functional effects of midazolam.

There are three structural loops (loops A, B and C) on the α-subunit and three loops on the γ2 subunit (loops D, E and F) that form the structure of the benzodiazepine binding site (Figure 3.1). Loops A-C form connectors between sequential β-strands and are highly conserved across $GABA_A$ receptor subunits (Figure 1.6). Loops A-C are important for ligand binding. They form the benzodiazepine site at the α+/γ- interface, but also form a homologous GABA agonist binding site at the β+/α- interface (Cromer et al., 2002; Miller & Aricescu, 2014). Understanding how different parts of loops A-F affect the actions of benzodiazepines at $GABA_A$ receptors is important to improving the specificity of newer benzodiazepines being developed that will have few side effects.

Mutagenesis has been used to determine the role of specific residues within the structural loops A-C of the benzodiazepine site (Benson et al., 1998; Morlock & Czajkowski, 2011; Sancar, Ericksen, Kucken, Teissere, & Czajkowski, 2007; Tan et al., 2007; H. A. Wieland & Luddens, 1994; M. Wieland & Hartig, 2007). The conserved histidine in loop A (His101 in rodents and His102 in bovine and human cDNAs) was shown to be important for the molecular and behavioral actions of diazepam using *in vitro* experiments (Benson et al., 1998; H A Wieland et al., 1992) and knock-in mice (Rudolph et al., 1999; Rudolph & Mohler, 2004). Other residues in loops A-C have been studied. For example, the conserved threonine in loop B (GSYAY**T**R) and serine in loop C (S**S**TGEYV) differentially affect the potency and efficacy of benzodiazepine-site ligands, including that of zolpidem, eszopiclone, flumazenil and β-carbolines (Buhr et al., 1997;

Derry et al., 2004; Hanson et al., 2008; Morlock & Czajkowski, 2011; Renard et al., 1999). However, most mutagenesis experiments were constrained to mutating 1-2 α subunit isoforms. This limits the conclusions drawn, especially given that many benzodiazepine ligands bind to multiple $GABA_A$ receptor assemblies. It is less understood how specific residues in loop A-C (other than His102) affect the functional actions of benzodiazepines across all of the human α subunits (α1-6).

To better understand midazolam's mechanism, a mutagenesis study across the six α subunits was performed to determine the role of specific residues on midazolam's efficacy. In these experiments, I mutated the highly-conserved histidine in loop A (His102 in α1), threonine in loop B (Thr163 in α1) and serine in loop C (Ser206 in α1) in all six $GABA_A$ α subunits (Table 3.1). The α4 and α6 subunits have different residues (R100, P161 and I/N204) in these locations and tend to form $GABA_A$ receptors insensitive to positive benzodiazepines (Knoflach et al., 1996). I predicted that mutating these residues in α1-3 and α5 to the residues present in α4 a4/α6 would reduce the responsiveness of the receptor to midazolam and *vice versa* for mutations in α4 and α6. Whole-cell patch clamp recording was used to measure the actions of midazolam on mutated $\alpha_x\beta_2\gamma_{2s}$ $GABA_A$ receptors.

Results showed that mutating the threonine and serine in loop B and loop C altered the efficacy of midazolam less than the dramatic changes seen when mutating the histidine in loop A across α1-6. Surprisingly, mutating the serine in loop C altered the efficacy of midazolam potentiation in different directions depending on the α isoform. Particularly, midazolam efficacy was increased in α3 and α5. These subunit-selective observations have the potential to offer new strategies for the design of α3- and α5-selective benzodiazepines.

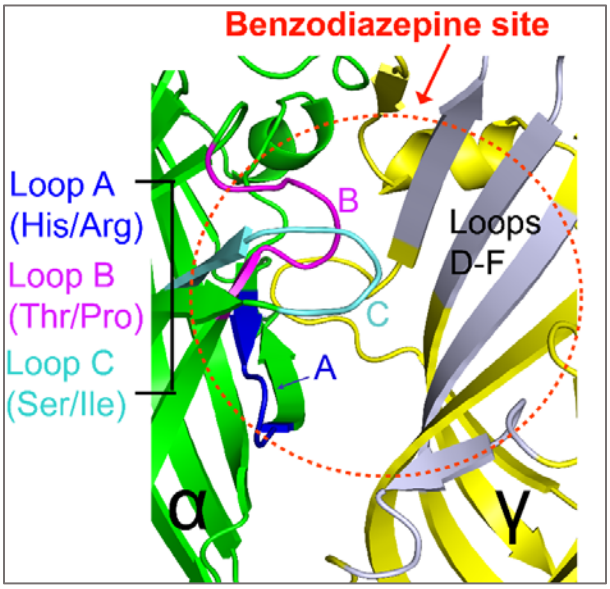

Figure 3.1. The structural loops A-C (blue, magenta, cyan) on the α subunit (green) and loops D-F (grey) on the γ subunit (yellow) form the benzodiazepine site (red dotted circle) on the $\alpha_x\beta_2\gamma_2$ $GABA_A$ receptor. Target residues used in this study noted under loops.

Subunit	Loop A	Loop B	Loop C
α1	FF**H**NG	GSYAY**T**R	S**S**TGEYV
α2	FF**H**NG	GSYAY**T**T	S**S**TGEYT
α3	FF**H**NG	GSYAY**T**T	S**S**TGEYV
α4	FF**R**NG	GSYAY**P**K	S**I**TGEYI
α5	FF**H**NG	GSYAY**P**N	T**S**TGEYT
α6	FF**R**NG	GSYAY**P**K	S**N**TGEYV

Table 3.1. The structural loops A-C are highly conserved across $GABA_A$ receptor α subunits. Location of the residues of interest within loops A-C across the six α subunits. The targeted residues are highlighted in **bold**. The numbering is based on the human mature peptide sequences not including the signal peptide (peptide sequences based on NP_000797, NP_000798, NP_000799, NP_000800, NP_000801, NP_000802).

3.2: METHODS:

3.2.1 Cell Culture

HEK293T cells were cultured and transfected according to the protocols described in Chapter 2.3.

3.2.2 Mutagenesis:

Human $GABA_A$ subunits (α1-6, β2, γ2s) are described in Chapter 2.1. Site-directed mutagenesis (QuikChange Lightening, Agilent Technologies) was performed to make the 18 single residue substitutions in α1-6 in Loops A-C (Table 3.2). Primers used for mutagenesis are listed in Chapter 2, Table 2.1. Mutations were confirmed by sequencing (Eurofins MWG Operon) before use.

3.2.3 In vitro electrophysiology

Recording: Whole-cell patch clamp recording was performed on HEK293T cells expressing $\alpha_x\beta_2\gamma_{2s}$ $GABA_A$ receptors and GFP, as described in Chapter 2.6.

GABA concentration-response assays were performed by exposing each whole-cell patch to 8 concentrations of GABA across a 3.5 logarithmic decade as described in Section 2.5. GABA concentrations for $\alpha_x\beta_2\gamma_2$ receptors were as follows: α1 = 0.3, 1, 3, 10, 30, 100, 300, 1000 μM; α2-3 = 0.01, 0.3, 1, 3, 10, 30, 100, 300 μM; α4 = 0.03, 0.1 0.3, 1, 3, 10, 30, 100 μM; and α5-6 = 0.01, 0.03, 0.1, 0.3, 1, 3, 10, 30 μM.

Selecting the EC_{10} GABA concentration for midazolam experiments: An EC_{10} GABA concentration was selected to maximize the range (10%-100% of receptor activity) in which potentiation of the receptor response could be measured (Moody et al., 2017). This GABA concentration was approximately 2-5 μM for receptors containing α1-3 and 0.3-0.8 μM for α4-6. The EC_{10} concentration was selected daily at the start of experiments

by patching 3-10 cells and testing a range of low GABA concentrations until at least three cells gave a consistent response that is around 10% of the maximal response.

Midazolam concentration-response assays were performed by exposing patches to two successive EC_{10} GABA exposures and then exposing patches to ascending concentrations of midazolam (10, 50, 100, 500, 1000 nM) + GABA (EC_{10}). Each drug exposure consisted of 3 seconds of GABA + midazolam (concentration) and then 2 seconds of GABA at the end of each midazolam exposure before washout in extracellular solution (8 sec). GABA pre- and post-control runs were performed before and after each midazolam assay for each cell to verify a consistent EC_{10} response and full washout of midazolam. GABA pre- and post-control runs consisted of 3 seconds of EC_{10} GABA with washout and then exposure to a saturating GABA concentration (100-300 μM depending on the α subunit) (see Figure 3.2A for midazolam protocol examples). Cells were recorded with the midazolam protocol no more than 2 times to avoid desensitization, incomplete deactivation, and incomplete washout (see Figure 3.2 for schematic diagram of the protocol).

GABA concentration-response + 1 μM midazolam assays were performed on $\alpha_1\beta_2\gamma_{2s}$ receptors in the presence of midazolam. The protocols for these assays were identical to GABA-concentration-response assays (0.3-1000 μM) described in Chapter 2.6.4 (***"GABA concentration-response protocol"***) except that 1 μM midazolam was added to each GABA solution.

1μM midazolam + saturating GABA: Maximum response to saturating GABA (1000 μM) in the presence and absence of 1 μM midazolam was measured using $\alpha_1\beta_2\gamma_{2s}$ receptors. Each drug exposure was 2 sec with 8 sec of washout in extracellular solution and 1-2 min washout between exposures containing saturating GABA. A pre- and post-control GABA response (EC_{10} GABA0 was recorded for each assay.

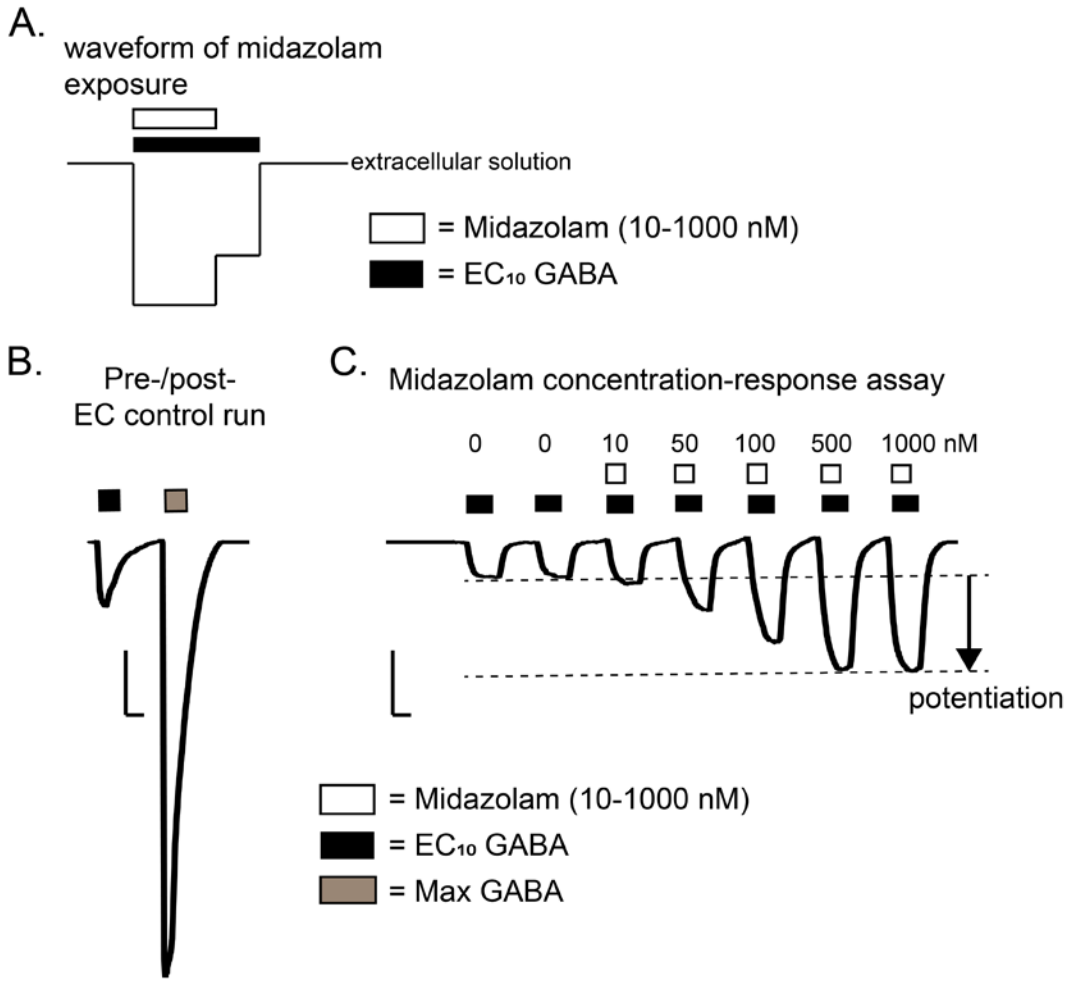

Figure 3.2. Example of whole-cell patch clamp recording protocols used for midazolam concentration-response assays. **A)** Example waveform of the GABA + midazolam drug exposure used for midazolam concentration-response assays. GABA and midazolam were co-applied for 3 seconds and then GABA was applied alone for 2 sec before washout in extracellular solution. **B)** Example trace of the "Pre/post EC run" that was used to ensure that the chosen EC_{10} GABA concentration gave a 10% of maximum current response for the cell patched. This consisted of one 3 sec exposure to EC_{10} GABA then a 3 sec exposure to a saturating GABA concentration (max GABA). This protocol was run before and after each midazolam concentration-response to ensure consistent EC_{10} GABA responses and complete washout of midazolam afterwards. Scale bar: 5 sec, 500 pA. **C)** Example trace of midazolam concentration-response assay (10-1000 nM) for $\alpha_3(S230I)\beta_2\gamma_2$ receptors. "Potentiation" is marked as arrow between dotted lines. Drug exposures were 5 seconds total before washout. See **Methods 3.2.3** for further details. *EC* = effective concentration. Scale bar: 5 sec, 500 pA.

3.2.4 Whole-Cell Analysis:

Recordings were baseline corrected and analyzed using MATLAB (Math Works, Inc.).

GABA concentration-response curves: Whole-cell peak currents (*I*) were measured from GABA exposures and fit using a non-linear regression analysis based on the Hill equation, as described in Chapter 2.7.

Midazolam concentration-response curves: The Pre-/Post-control runs for each cell were analyzed to ensure the EC_{10} GABA concentration gave a consistent response that was approximately 10% of the maximum (5-15% was considered acceptable). The midazolam potentiation (%) of each GABA-evoked response was calculated by the equation: $Pot = (I_{MDZ} - I_G)/I_G \; x \; 100\%$ where *Pot* is potentiation (%), and I_G and I_{MDZ} are the amplitude of peak currents for the EC_{10} GABA (average of two control peaks) and GABA + Midazolam responses, respectively. The potentiation points from midazolam concentration-response curves were fit using the Hill equation as:

$$P = P_{max} * [M]^{nH} / (EC_{50}^{nH} + [M]^{nH},$$

where *P* was potentiation, P_{max} was maximum potentiation, EC_{50} was the midazolam concentration producing the half-maximal response*, M* was midazolam concentration and *nH* was the Hill coefficient. Concentration-response relationships that were not described by a sigmoidal function were not included in our analysis (e.g. no response or a linear non-saturating response). The Hill equation was fit to each individual cell's concentration-response curve data.

GABA concentration-response + 1 μM midazolam: GABA concentration-response curves in the presence and absence of 1μM midazolam were analyzed the same as described above for *"**GABA concentration-response curves".***

1μM midazolam + saturating GABA: Peak current responses were averaged for each cell (1-3 replicates per cell). A two-way unpaired t-test (α=0.05) was used to compare 1000μM GABA peak current responses in the presence and absence of 1μM midazolam.

3.2.5 Statistics: Hill parameters (max response, Hill coefficient, EC_{50}) from concentration-response curves (GABA and midazolam each) were compared for significant differences within each α subunit (α1-6) and its loop A-C mutants using a one-way ANOVA (alpha=0.05). Where the results of the ANOVA were significant ($p<0.05$), a Dunnett's post-hoc test for multiple comparisons ($p<0.05$) was performed. Statistical analysis was carried out using Prism 7.0 (Graphpad Software, Inc.). For other comparisons in which there were only two groups, a two-way Student's t-test was performed (α=0.05).

Subunit	Loop A	Loop B	Loop C
α1	H102R	T163P	S206I
α2	H101R	T162P	S205I
α3	H126R	T187P	S230I
α4	R100H	P161T	I204S
α5	H105R	P166T	S209I
α6	R100H	P161T	N204I

Table 3.2. Eighteen mutations made across the human α1-6 $GABA_A$ receptor subunits within loops A-C of the benzodiazepine site. Peptide numbering based on mature peptide sequence. The mutations made in this study are referred to as “loop A”, “loop B” and “loop C” in subsequent figures and text.

3.3: RESULTS

3.3.1 GABA concentration-response curves with loop A-C mutations

The role of single residues in the benzodiazepine binding site on midazolam's efficacy was examined. The following mutations were made in the conserved regions of loops A-C of α1, α2, α3, and α5 subunits: histidine to arginine (loop A), threonine to proline (loop B), and serine to isoleucine (loop C) (Table 3.2). In α4 and α6 subunits, the opposite mutations were made: arginine to histidine (loop A) and proline to threonine (loop B). Loop C mutations were α4(I204S) and α6(N204I). This gave a total of 18 total mutations and 6 wildtype α subunits (total 24 conditions). Whole-cell patch clamp recording was used to measure the actions of GABA and midazolam on mutated $\alpha_x\beta_2\gamma_{2s}$ $GABA_A$ receptors. The benzodiazepine binding site is located away from the GABA binding site. Mutating single residues in the benzodiazepine binding-site was not predicted to have any dramatic effect on the ability of GABA to bind and activate the channel. To confirm this, GABA concentration-response curves were performed on all 18 mutant subunits and compared to wildtype $\alpha_x\beta_2\gamma_{2s}$ $GABA_A$ receptors (Figures 3.3-3.8).

Overall, the shifts in the GABA concentration curves were subtle for all mutations, except for three mutations. The loop A mutations, α5(H105R) and α2(H102R), and the loop C mutation, α6(N204I), had notable changes in the GABA apparent-affinity (EC_{50}). The α2(H102R) mutation caused a 2-fold increase in the GABA EC_{50} (α_2(H101R)$\beta_2\gamma_{2s}$ = 16.25 ± 2.20; $\alpha_2\beta_2\gamma_{2s}$ = 8.29 ± 0.78 μM, Figure 3.4). The α5(H105R) mutation caused a 3-fold increase in the GABA EC_{50} (α_5(H105R)$\beta_2\gamma_{2s}$ = 9.84 ± 3.29; $\alpha_5\beta_2\gamma_{2s}$ = 3.18 ± 0.71 μM, Figure 3.7). The third mutation, α6(N204I) (loop C), had a decrease in EC_{50} (α_6(N204I)$\beta_2\gamma_{2s}$ = 0.421 ± 0.061; $\alpha_6\beta_2\gamma_{2s}$ = 0.703 ± 0.078 μM, Figure 3.8), consistent with the receptor becoming more sensitive to GABA. Over all, the α5(H105R) and α2(H102R)

mutations made the receptors to less sensitive to GABA relative to wildtype receptors, while the α6(N204I) mutation increased GABA apparent-affinity.

Aside from changes in GABA apparent-affinity, minimal changes in maximum current and Hill coefficient were seen (Table 3.3). Of 18 mutations (loops A-C), five had significant changes in the maximum GABA-evoked responses (α1(T163P), α2(T162P), α2(S205I), α3(H126R) and α4(P161T) (Table 3.3). However, these changes in the absence of changes in EC_{50} were hard to distinguish as changes in receptor conductance or minor differences in protein level expression or cell health. Given that these receptors had no significant (p>0.05) changes in GABA apparent-affinity, the changes in maximal current were considered subtle changes. Overall, only 9 out of 18 mutations showed some significantly altered response for one of the Hill parameters, except α4(P161T) which was altered for two of the parameters (Hill coefficient and maximum current). None of the mutations dramatically altered both apparent GABA affinity and maximum current, suggesting that most of these changes were subtle, and the mutated receptors were functioning normally. Table 3.3 has the full comparisons of parameters in all mutations.

Another important comparison that the GABA concentration-response data provided was the relative GABA apparent-affinity for the wildtype α subunits (Figure 3.9). The GABA EC_{50}'s of $\alpha_x\beta_2\gamma_2$ receptors in rank-order from smallest-to-largest were: α6 < α5 ≈ α4 < α2 < α3 < α1. GABA Ec_{50} values for $\alpha_x\beta_2\gamma_{2s}$ receptors were as follows for α1-6: 45.10 ± 7.75 μM (α1), 8.29 ± 0.78 μM (α2), 15.53 ± 2.55 μM (α3), 3.00 ± 0.53 μM (α4), 3.18 ± 0.71 μM (α5) and 0.703 ± 0.078 μM (α6). All groups had data from at least 10 cells. Overall, the GABA apparent-affinity of $\alpha_x\beta_2\gamma_2$ $GABA_A$ receptors measured here was within the range previously reported in the literature (Bohme, Rabe, & Luddens, 2004; Ducic, Caruncho, Zhu, Vicini, & Costa, 1995; Mortensen, Patel, & Smart, 2011; Petroski et al.,

2006), suggesting measurements from this system will be relevant to whole-cell patch clamp recording data from other groups using HEK293 cells.

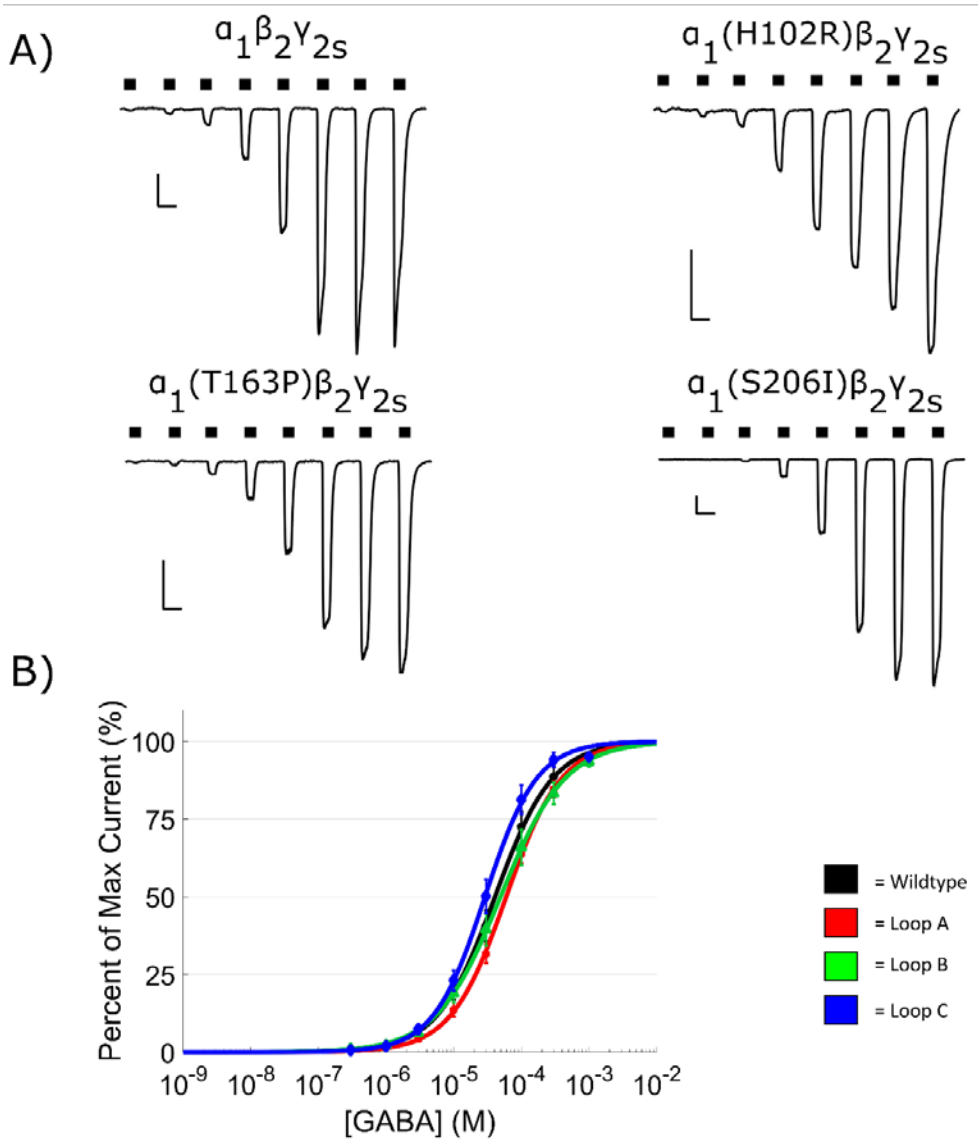

Figure 3.3. GABA concentration-response curves for $\alpha_1\beta_2\gamma_{2s}$ $GABA_A$ receptors with benzodiazepine-site mutations in loop A-C. **A)** Example traces of GABA concentration-response assays (black bars = GABA 0.3-1000 μM). Scale bars: 5 sec, 500 pA. **B)** GABA concentration-response curves for wildtype-α (black), loop A mutation (α1(H102R), red), loop B mutation (α1(T163P), green), and loop C mutation (α1(S206I), blue). Points are mean ± SEM and lines are drawn by eye and have no theoretical value. N=10 cells per group.

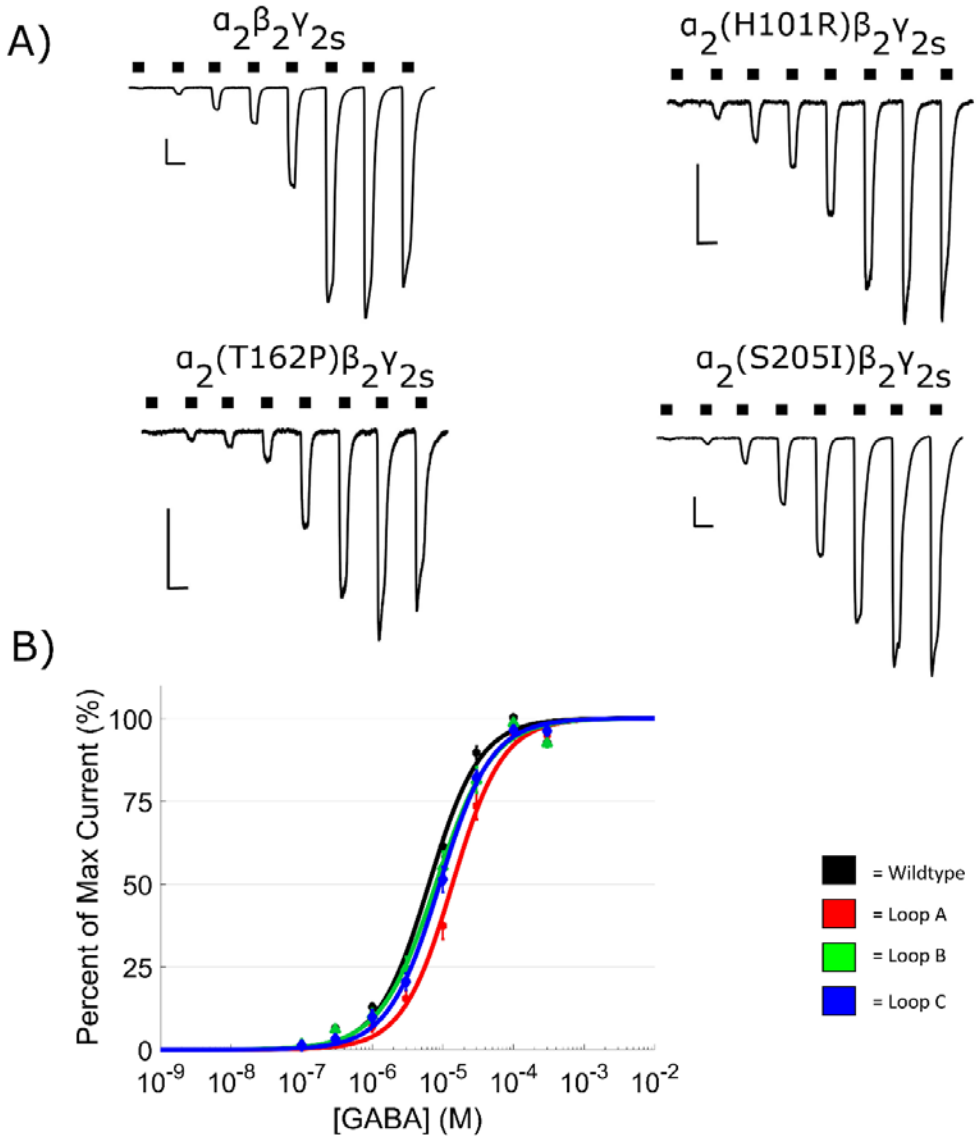

Figure 3.4 GABA concentration-response curves for $\alpha_2\beta_2\gamma_{2s}$ $GABA_A$ receptors with benzodiazepine-site mutations in loop A-C. **A)** Example traces of GABA concentration-response assays (black bars = GABA 0.1-300 μM). Scale bars: 5 sec, 500 pA. **B)** GABA concentration-response curves for wildtype-α (black), loop A mutation (α2(H101R), red), loop B mutation (α2(T162P), green), and loop C mutation (α2(S205I), blue). Points are mean ± SEM and lines are drawn by eye and have no theoretical value. N=9-40 cells per group.

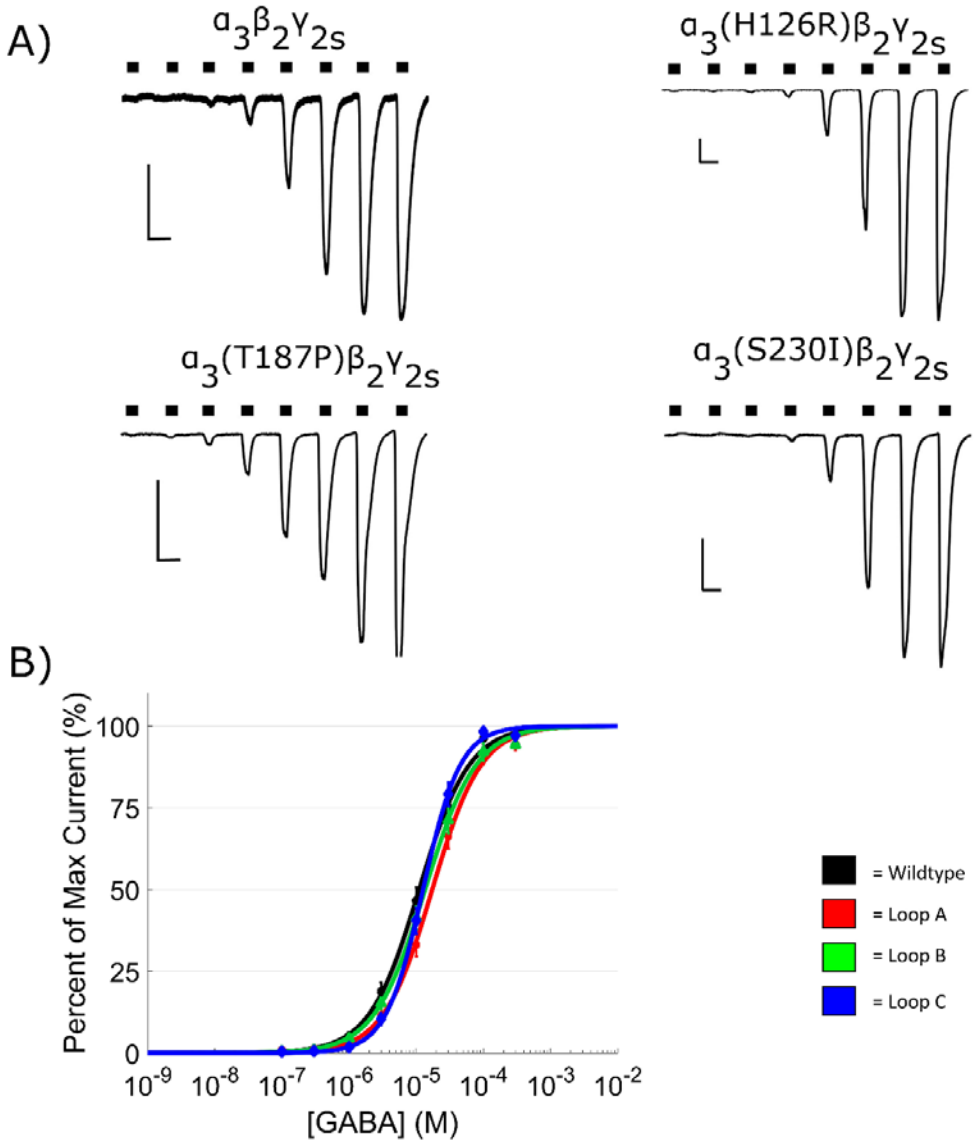

Figure 3.5 GABA concentration-response curves for $\alpha_3\beta_2\gamma_{2s}$ $GABA_A$ receptors with benzodiazepine-site mutations in loop A-C. **A)** Example traces of GABA concentration-response assays (black bars = GABA 0.1-300 μM). Scale bars: 5 sec, 500 pA. **B)** GABA concentration-response curves for wildtype-α (black), loop A mutation (α3(H126R), red), loop B mutation (α3(T187P), green), and loop C mutation (α3(S230I), blue). Points are mean ± SEM and lines are drawn by eye and have no theoretical value. N=11-16 cells per group.

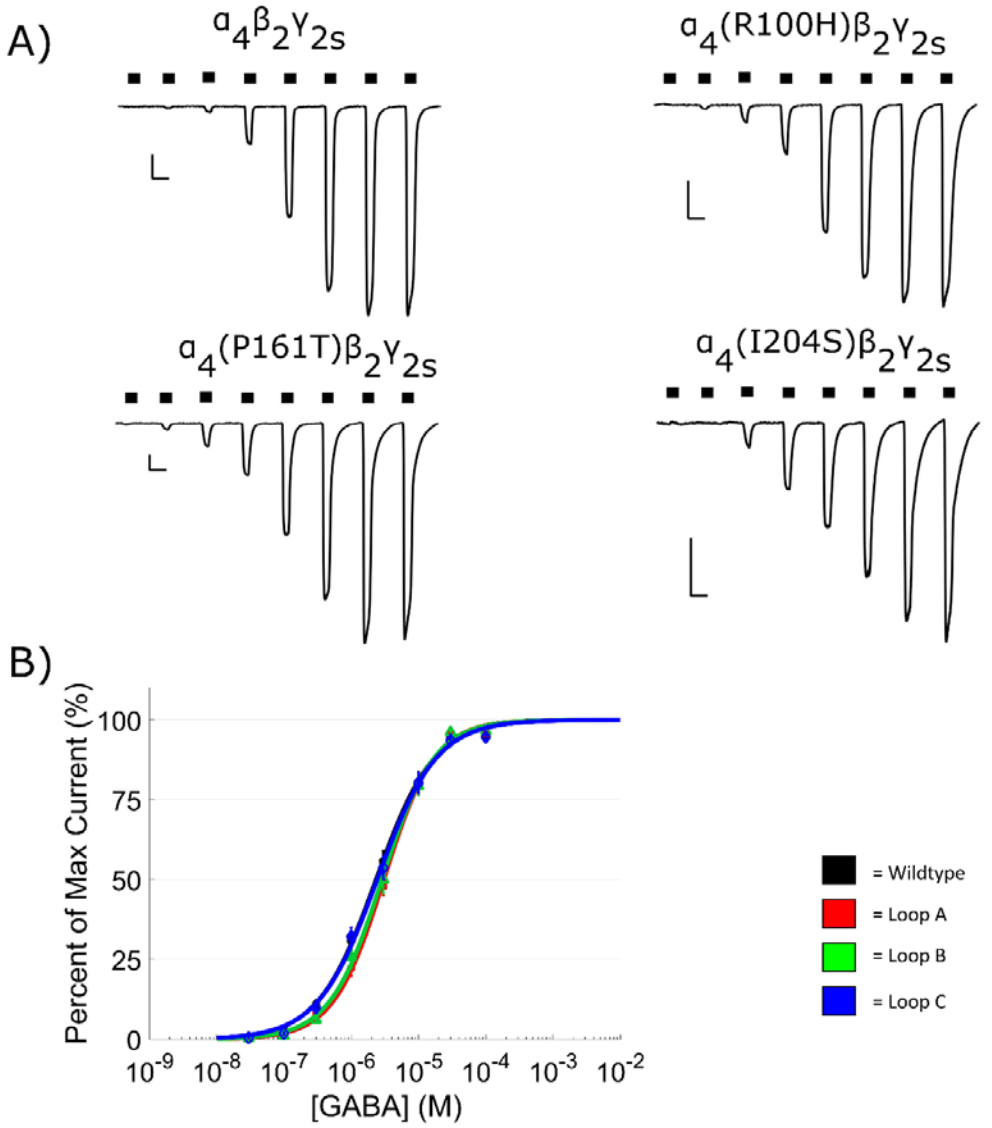

Figure 3.6 GABA concentration-response curves for $\alpha_4\beta_2\gamma_{2s}$ $GABA_A$ receptors with benzodiazepine-site mutations in loop A-C. **A)** Example traces of GABA concentration-response assays (black bars = GABA 0.03-100 μM). Scale bars: 5 sec, 500 pA. **B)** GABA concentration-response curves for wildtype-α (black), loop A mutation (α4(R100H), red), loop B mutation (α1(P161T), green), and loop C mutation (α4(I204S), blue). Points are mean ± SEM and lines are drawn by eye and have no theoretical value. N=12-14 cells per group.

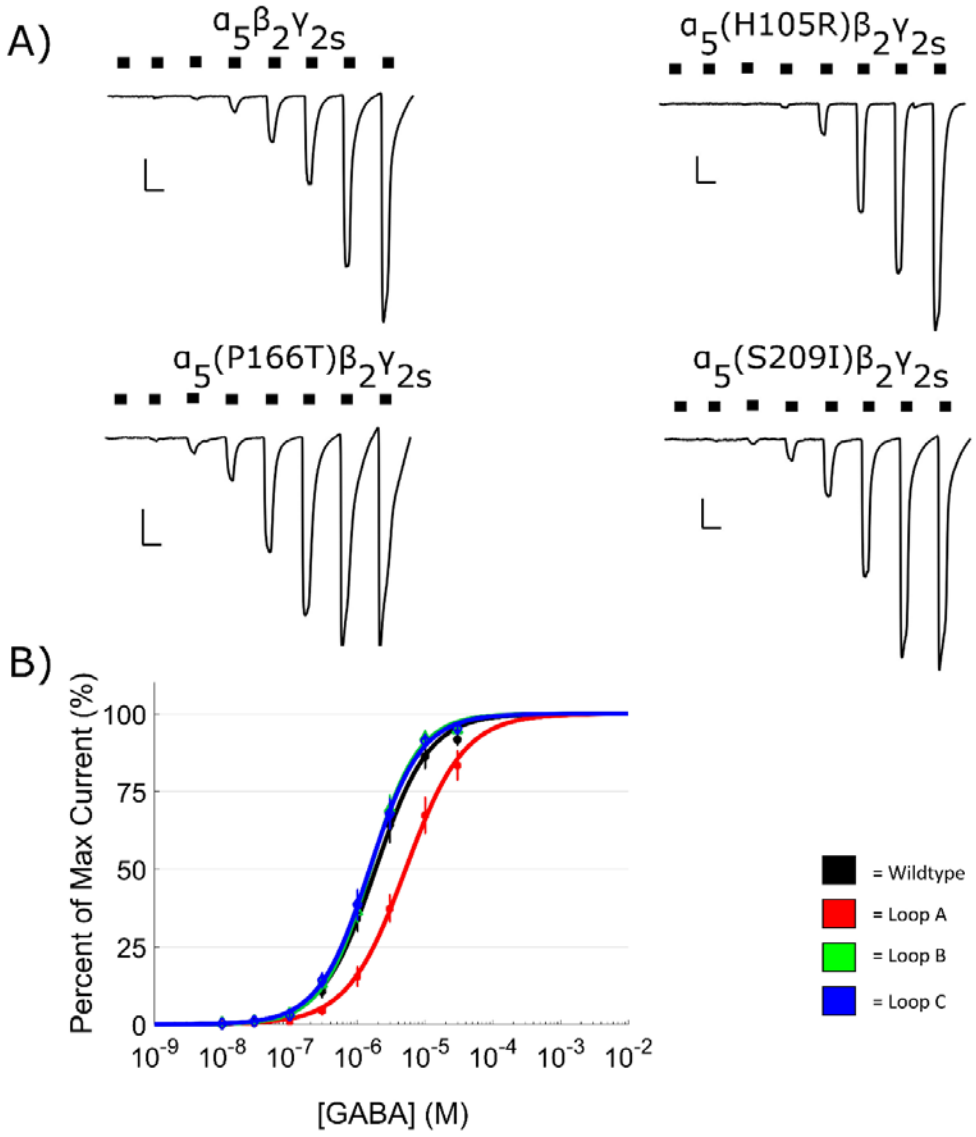

Figure 3.7 GABA concentration-response curves for $\alpha_5\beta_2\gamma_{2s}$ $GABA_A$ receptors with benzodiazepine-site mutations in loop A-C. **A)** Example traces of GABA concentration-response assays (black bars = GABA 0.01-30 μM). Scale bars: 5 sec, 500 pA. **B)** GABA concentration-response curves for wildtype-α (black), loop A mutation (α5(H105R), red), loop B mutation (α5(P166T), green), and loop C mutation (α5(S209I), blue). Points are mean ± SEM and lines are drawn by eye and have no theoretical value. N=10-12 cells per group.

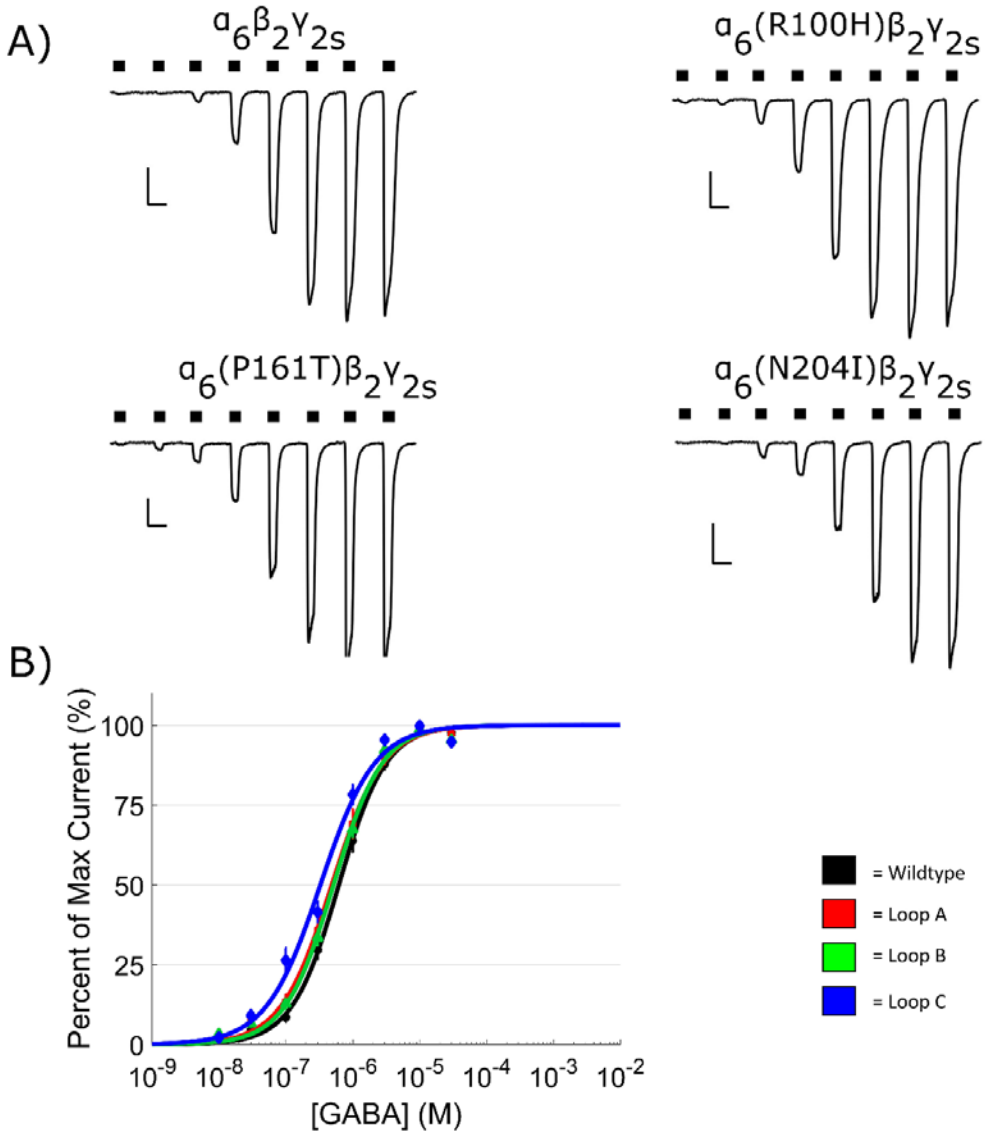

Figure 3.8 GABA concentration-response curves for $\alpha_6\beta_2\gamma_{2s}$ $GABA_A$ receptors with benzodiazepine-site mutations in loop A-C. **A)** Example traces of GABA concentration-response assays (black bars = GABA 0.01-30 μM). Scale bars: 5 sec, 500 pA. **B)** GABA concentration-response curves for wildtype-α (black), loop A mutation (α6(R100H), red), loop B mutation (α6(P161T), green), and loop C mutation (α6(N204I), blue). Points are mean ± SEM and lines are drawn by eye and have no theoretical value. N=7-15 cells per group.

Table 3.3. Hill parameters for GABA concentration-response assays

Conditions:	**Wildtype**	**Loop A**	**Loop B**	**Loop C**
	$\alpha_1\beta_2\gamma_2$	**α1(H102R)**	**α1(T163P)**	**α1(S206I)**
Max Current (pA)	-4218 ± 601.6	-3175 ± 444.3	-2449 ± 376.1**	-5007 ± 470.7
Hill coefficient	1.400 ± 0.102	1.255 ± 0.097	1.230 ± 0.049	1.444 ± 0.104
EC_{50} (μM)	45.10 ± 7.75	60.72 ± 5.23	56.81 ± 11.40	44.41 ± 10.66
N# (cells)	10	10	10	10
	$\alpha_2\beta_2\gamma_2$	**α2(H101R)**	**α2(T162P)**	**α2(S205I)**
Max Current (pA)	-3326 ± 356.7	-3186 ± 390.8	-1765 ± 246.0**	-7835 ± 763.5**
Hill coefficient	1.581 ± 0.074	1.443 ± 0.092	1.494 ± 0.101	1.452 ± 0.151
EC_{50} (μM)	8.29 ± 0.78	16.25 ± 2.20**	11.63 ± 1.85	9.60 ± 1.13
N# (cells)	40	11	16	9
	$\alpha_3\beta_2\gamma_2$	**α3(H126R)**	**α3(T187P)**	**α3(S230I)**
Max Current (pA)	-2535 ± 210.5	-3597 ± 343.6**	-1993 ± 189.7	-1724 ± 286.1
Hill coefficient	1.467 ± 0.065	1.519 ± 0.88	1.388 ± 0.155	1.796 ± 0.063**
EC_{50} (μM)	15.53 ± 2.55	24.39 ± 4.57	16.39 ± 2.23	14.46 ± 1.171
N# (cells)	16	16	12	11
	$\alpha_4\beta_2\gamma_2$	**α4(R100H)**	**α4(P161T)**	**α4(I204S)**
Max Current (pA)	-3039 ± 347.3	-3049 ± 378.6	-4487 ± 397.2**	-3424 ± 394.5
Hill coefficient	1.113 ± 0.063	1.215 ± 0.079	1.392 ± 0.073**	1.180 ± 0.072
EC_{50} (μM)	3.00 ± 0.53	3.58 ± 0.62	3.61 ± 0.46	3.41 ± 0.70
N# (cells)	12	12	14	13
	$\alpha_5\beta_2\gamma_2$	**α5(H105R)**	**α5(P166T)**	**α5(S209I)**
Max Current (pA)	-5115 ± 315.9	-6799 ± 919.2	-4543 ± 553.0	-6073 ± 742.0
Hill coefficient	1.547 ± 0.123	1.269 ± 0.084	1.420 ± 0.064	1.434 ± 0.059
EC_{50} (μM)	3.18 ± 0.71	9.84 ± 3.29**	1.94 ± 0.29	1.09 ± 0.57
N# (cells)	10	10	12	10

	$\alpha_6\beta_2\gamma_2$	α6(R100H)	α6(P161T)	α6(N204I)
Max Current (pA)	-3276 ± 578.1	-2902 ± 349.5	-3540 ± 290.2	-3549 ± 408.6
Hill coefficient	1.405 ± 0.074	1.277 ± 0.079	1.323 ± 0.063	1.260 ± 0.056
EC_{50} (μM)	0.703 ± 0.078	0.570 ± 0.110	0.575 ± 0.056	0.421 ± 0.061**
N# (cells)	11	7	15	14

Table 3.3. Hill parameters estimated from GABA concentration-response assays for benzodiazepine site mutations in loops A-C of the α subunit. Residues of interest were the histidine/arginine (loop A), the threonine/proline (loop B), and the serine/isoleucine (loop C). Measurements were performed using whole-cell patch clamp recording of HEK293T cells expressing $\alpha_x\beta_2\gamma_2$ receptors. Significance was determined using one-way ANOVA tests ($\alpha = 0.05$) for each α subunit and its loop A-C mutations (4 receptor conditions). Where significance was found, a Dunnett's post-hoc analysis for multiple comparisons was performed using the wildtype receptors as the control group. Asterisks denote $p<0.05$ significance.

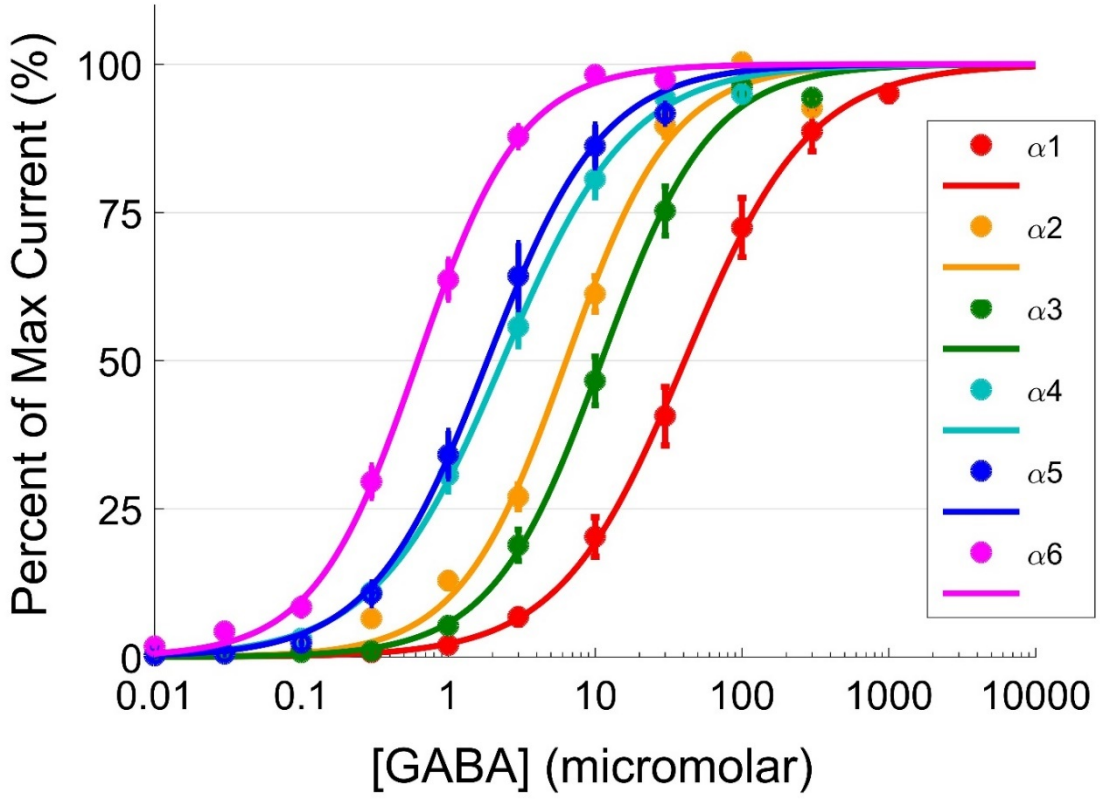

Figure 3.9. Combined GABA concentration-response curves for wildtype $\alpha_x\beta_2\gamma_{2s}$ $GABA_A$ receptors with α1-6. Averaged EC_{50}'s are as follows for α1-6: 45.10 ± 7.75 μM (α1), 8.29 ± 0.78 μM (α2), 15.53 ± 2.55 μM (α3), 3.00 ± 0.53 μM (α4), 3.18 ± 0.71 μM (α5) and 0.703 ± 0.078 μM (α6) with n ≥10 cells per group. Legend: α1 (red), α2 (orange), α3(green), α4(light blue), α5(dark blue), α6(magenta).GABA concentrations were: α1 = 0.3, 1, 3, 10, 30, 100, 300, 1000 μM, α2-3 = 0.01, 0.3, 1, 3, 10, 30, 100, 300 μM, α4 = 0.03, 0.1 0.3, 1, 3, 10, 30, 100 μM, and α5-6 = 0.01, 0.03, 0.1, 0.3, 1, 3, 10, 30 μM. Lines are fit by eye and have no theoretical value. Points are mean ± SEM and SEM is not visible where its smaller than the point.

3.3.2 Exposure protocol affects the degree of midazolam potentiation measured:

Two important aspects of the experimental design of midazolam assays were the concentrations of GABA and midazolam chosen. First, a low concentration of GABA was used when measuring midazolam potentiation of GABA-evoked responses. This maximized the range of receptor response in which potentiation could be measured without causing desensitization (Moody et al., 2017). Second, midazolam has been shown to produce a bell-shaped curve in the amplitude of potentiation of $GABA_A$ receptor activity. Previous patch clamp experiments found that midazolam potentiation increased with increasing midazolam concentration until 10 μM, when the degree of potentiation began decreasing (D. S. Wang et al., 2003; Yakushiji, Fukuda, Oyama, & Akaike, 1989). My preliminary data found that $\alpha_1\beta_2\gamma_{2s}$ receptors showed a plateau in the level of midazolam potentiation around 500-1000 nM. Concentrations above 1 μM did not produce increased potentiation for $\alpha_1\beta_2\gamma_{2s}$ receptors (Figure 3.10). Therefore, I chose the range 10-1000 nM midazolam for the following experiments. This corresponds to the physiologically-relevant range of plasma midazolam concentrations measured from sedated patients (Glass et al., 1997; M. P. Persson et al., 1988; P. Persson et al., 1987).

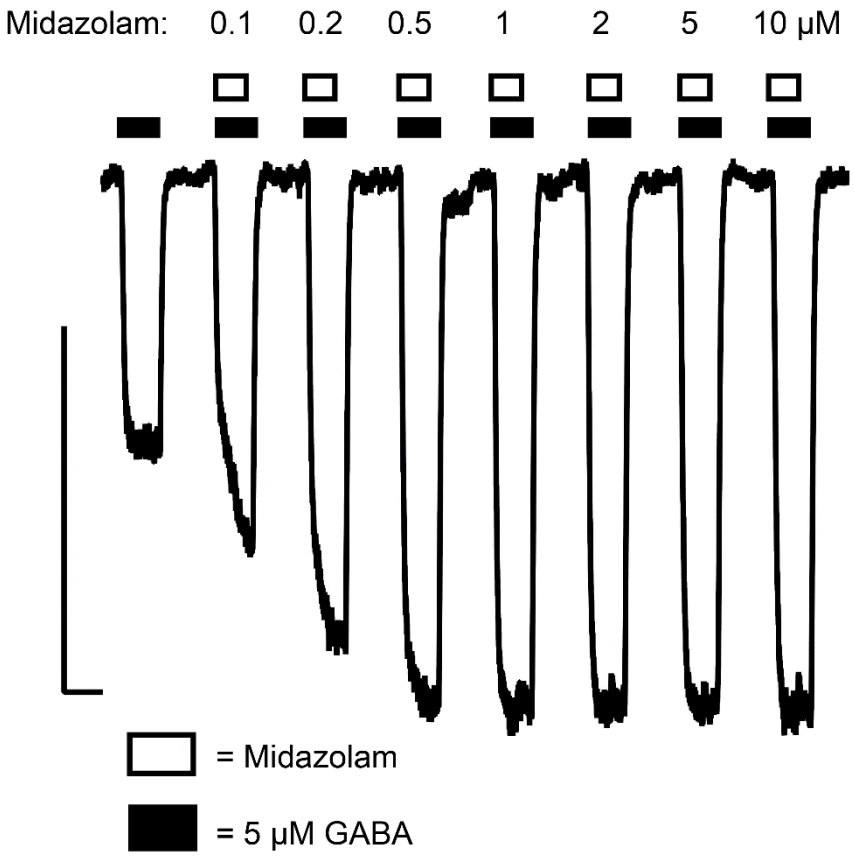

Figure 3.10. Midazolam concentration-response curve for $\alpha_1\beta_2\gamma_{2s}$ receptors from 0.1-10 μM midazolam. Notice how the degree of potentiation plateaus around 1000 nM Midazolam concentrations were 100, 200, 500, 1000, 2000, 5000, 10000 nM. Scale bare: 5 sec, 500 pA.

3.3.3 Midazolam concentration-response curves & loop A-C mutations

I hypothesized that mutating single residues in the conserved loops A-C of the benzodiazepine binding site would alter the modulation of $GABA_A$ receptors by midazolam. Whole-cell patch clamp recording of α1-6-containing $\alpha_x\beta_2\gamma_{2s}$ $GABA_A$ receptors was used to measure the degree of potentiation by midazolam within the therapeutically-relevant range of 10-1000 nM. Midazolam potentiation was measured as the percent of enhancement in non-saturating GABA-evoked currents. A 100% potentiation was a doubling in amplitude of the whole-cell current evoked by the control EC_{10} GABA-response. Overall, single residue mutations in loop B and loop C did not alter, abolish or confer midazolam sensitivity as dramatically as the histidine-to-arginine exchanges in loop A. Interestingly, we found that loop C mutations in α3 and α5 $GABA_A$ subunits increased the maximum potentiation by midazolam (Figures 3.13 and 3.15). The raw numbers for midazolam potentiation for all receptor conditions are listed in Table 3.4. The Hill fit parameters are reported in Tables 3.5.

Loop A mutations

Midazolam assays showed that the α1(H102R), α2(H102R), α3(H126R), α5(H105R) mutations abolished the ability of receptors to respond to midazolam potentiation, and Hill fits could not be performed on this data (Figures 3.11-3.16). The average potentiation measured for receptors at 1000 nM midazolam was: 28.87 ± 6.18 nM (α1(H102R)), 31.81 ± 11.79 nM (α2(H101R)), 10.78 ± 2.42 nM (α3(H126R)), and 8.17 ± 4.66 nM (α5(H105R)) (Table 3.4). This is consistent with previous reports using diazepam (Benson et al., 1998). The α4(R100H) and α6(R100H) mutations conferred the ability to receptors to be potentiated by midazolam (midazolam EC_{50}: α_4(R100H)$\beta_2\gamma_2$ = 73.99 ± 3.44 nM (n=8) and α_6(R100H)$\beta_2\gamma_2$ = 41.88 ± 6.02 nM (n=7), Fig. 3.14 and 3.16). The wildtype $\alpha_4\beta_2\gamma_2$ and $\alpha_6\beta_2\gamma_2$ receptors showed no notable midazolam potentiation. As

a result, no statistics could be performed to compare the midazolam potentiation of the R100H mutation to wildtype receptors. Overall, the histidine/arginine loop A mutations could confer (α4(R100H) and α6(R100H)) or abolish (α1(H102R), α2(H102R), α3(H126R), α5(H105R)) midazolam responsiveness in the receptor.

Loop B mutations

The receptors containing threonine-to-proline mutations failed to abolish the receptors' response to midazolam for α1(T163P), α2(T162P) and α3(T187P) mutants. The midazolam EC_{50} values of α1(T163P), α2(T162P) and α3(T187P) mutants remained unchanged relative to the wildtype receptors (p>0.05, Table 3.5). Only α_1(T163P)$\beta_2\gamma_2$ receptors had a significantly lower maximum potentiation compared to wildtype $\alpha_1\beta_2\gamma_2$ receptors (α_1(T163P)$\beta_2\gamma_2$: 133.8 ± 19.51%, n=11; $\alpha_1\beta_2\gamma_2$: 203.0 ± 17.6%, n=7, p=0.0092). The α5(P166T) mutation produced little change in midazolam potentiation, either maximum potentiation or midazolam EC_{50} (p>0.05, n=7 per group). The presence of a threonine residue failed to confer midazolam responsiveness to α_4(P161T)$\beta_2\gamma_2$ or α_6(P161T)$\beta_2\gamma_2$ receptors (Figure 3.14 and 3.16). Overall, the presence of a proline in this location caused only subtle changes in midazolam potentiation.

Loop C mutations

The loop C mutations (S**S**TGEYV) had more noticeable effects on the $\alpha_x\beta_2\gamma_{2s}$ receptors' response to midazolam, but the direction of change was α-isoform specific (Figure 3.11-16). As predicted, the α1(S206I) mutation decreased the amplitude of the maximum potentiation by midazolam by approximately 33% (α_1(S206I)$\beta_2\gamma_2$ = 135.8 ± 23.8% (n=6); $\alpha_1\beta_2\gamma_2$= 203.0 ± 17.6% (n=7), p=0.0403). The α2(S205I) mutation reduced the maximum midazolam potentiation by approximately 31% (α_2(S205I)$\beta_2\gamma_2$ = 116.4 ± 23.0%, n=8) compared to wildtype receptors ($\alpha_2\beta_2\gamma_2$ = 169.6 ± 49.9%, n=7), but this result was not significant (p=0.416). The α3(S230I) mutation had the largest alteration

in midazolam potentiation (Figure 3.13). It enhanced the degree of maximum midazolam potentiation by approximately 63% (α_3(S230I)$\beta_2\gamma_2$ = 436.0 ± 39.4% (n=7); $\alpha_3\beta_2\gamma_2$ = 267.8 ± 20.3% (n=7), *p*=0.0004), and it increased the midazolam EC_{50} by approximately 63% (α_3(S230I)$\beta_2\gamma_2$ = 73.6 ± 1.8 nM; $\alpha_3\beta_2\gamma_2$ = 46.4 ± 7.4 nM, *p*=0.0014). Similarly, the α5(S209I) mutation increased the maximum degree of midazolam potentiation by approximately 63%, although this difference was not statistically significant (α_5(S209I)$\beta_2\gamma_2$ = 175.1 ± 26.6% (n=6); $\alpha_5\beta_2\gamma_2$ = 107.9 ± 20.3% (n=7), *p*=0.1067). The α4(I204S) and α6(N204I) mutations failed to convey any notable midazolam potentiation to the receptors and no meaningful Hill parameters for midazolam concentration-response curves could be estimated (Figure 3.14 and 3.15). On the whole, loop C mutations showed that α_1(S206I)$\beta_2\gamma_2$ and α_2(S205I)$\beta_2\gamma_2$ receptors had a decreased maximal midazolam potentiation, and the α_3(S230I)$\beta_2\gamma_2$ and α_5(S209I)$\beta_2\gamma_2$ receptors had an increased maximal midazolam potentiation.

Wildtype $\alpha_x\beta_2\gamma_{2s}$ receptors

The degree of midazolam potentiation measured from wildtype $\alpha_x\beta_2\gamma_{2s}$ receptors is α-isoform specific (Figure 3.17). Wildtype $\alpha_x\beta_2\gamma_2$ receptors could broadly be separated into two categories: midazolam-responsive (up to ~280% potentiation; α1, α2, α3 and α5) or non-responsive (<23% potentiation at 1 μM midazolam; α4 and α6) (Figure 3.17). For the receptors that showed potentiation, the rank-order of smallest midazolam EC_{50} to largest was: α3 < α2 = α5 < α1 (in rank-order (nM): 46.39 ± 7.44 (α3), 52.09 ± 4.68 (α2), 52.84 ± 3.48 (α5), 71.43 ± 5.80 (α1)). In terms of the maximum midazolam potentiation (efficacy) evoked, the rank-order from greatest-to-smallest was: α3 > α1 > α2 > α5 (potentiation: 281.17 ± 24.73% (α3), 215.35 ± 26.71% (α1), 165.35 ± 48.98% (α2), 123.12 ± 26.08% (α5)). The maximum potentiation did not correlate to the maximum amplitude of GABA-evoked responses because α5-receptors had the largest GABA-induced currents (-5115

± 315.9 pA) but smallest degree of maximal midazolam potentiation (123.12 ± 26.08%) for wildtype $\alpha_x\beta_2\gamma_2$ receptors. Overall, the wildtype $\alpha_3\beta_2\gamma_2$ receptors were most sensitive to modulation by midazolam with the highest apparent-affinity for midazolam (EC_{50} = 46.39 ± 7.44 nM) and highest efficacy (281.17 ± 24.73%) relative to the other wildtype receptors (Figure 3.17). This is not due to a higher GABA potency because wildtype $\alpha_3\beta_2\gamma_2$ receptors had the second lowest GABA potency (15.53 ± 2.55 μM) relative to the other α1-6-containing receptors.

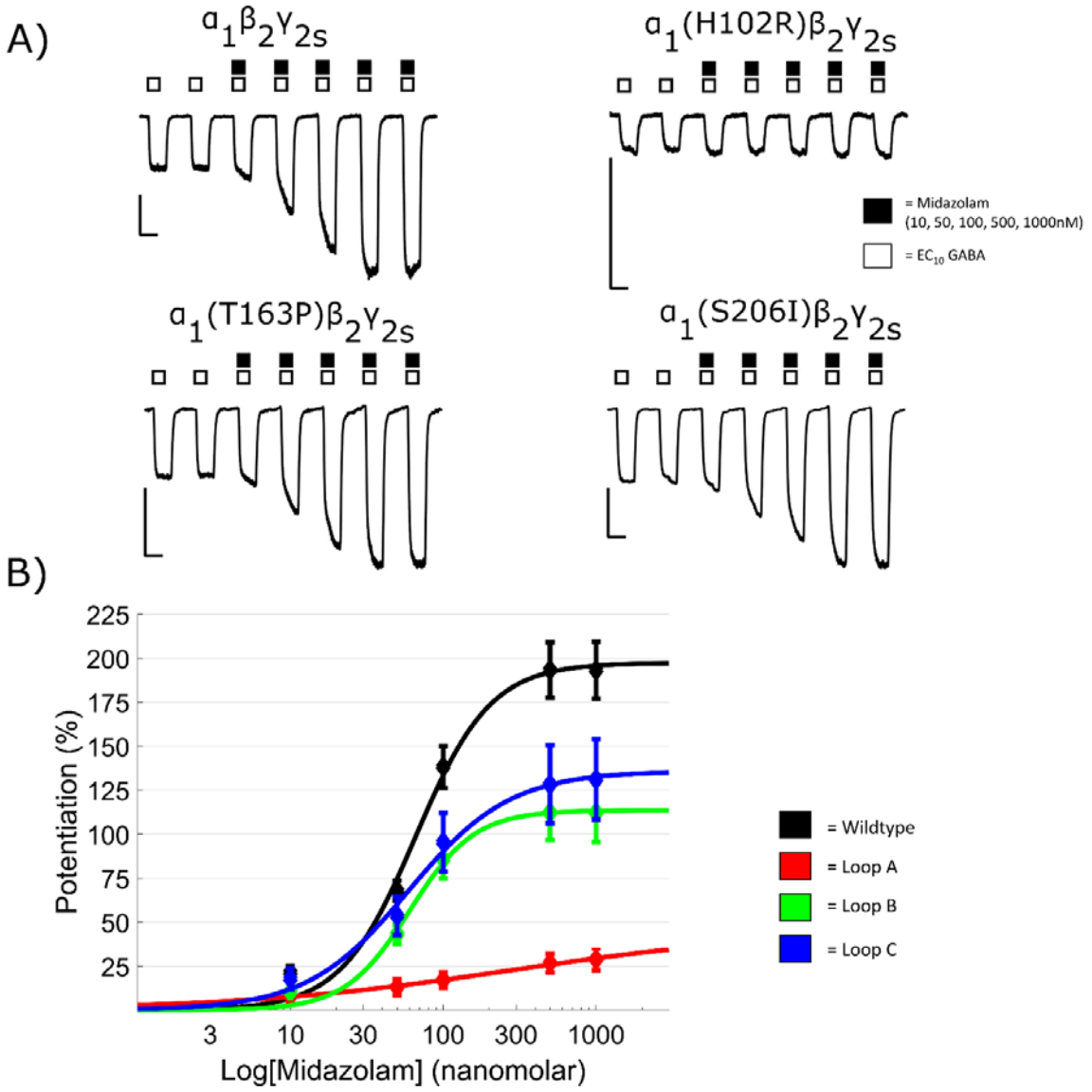

Figure 3.11. Midazolam concentration-response curves from $\alpha_1\beta_2\gamma_{2s}$ receptors containing Loop A-C mutations. **A)** Example traces from $\alpha_x\beta_2\gamma_{2s}$ mutated receptors. Scale bar: 5 sec, 500 pA. **B)** Midazolam concentration-response curves (10-1000 nM) for $\alpha_x\beta_2\gamma_{2s}$ mutated receptors. Potentiation (%) was measured as the enhancement of an EC_{10} GABA response with 10-1000nM midazolam. Mutations are α1(H102R) (loop A, red), α1(T163P) (loop B, green), α1(S206I) (loop C, blue). Points are mean ± SEM and where not visible SEM is smaller than points. Sample sizes are N=6-11 cells.

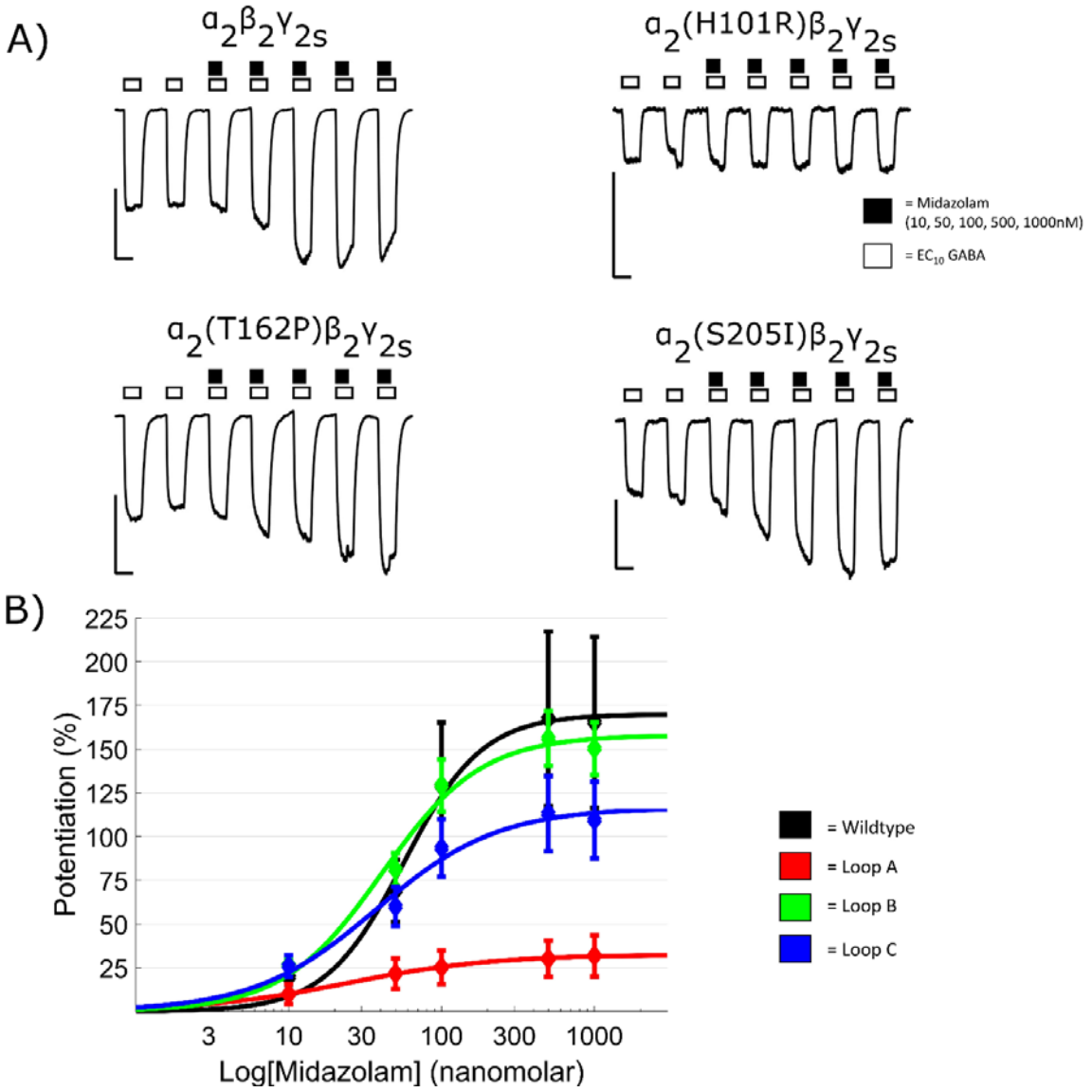

Figure 3.12. Midazolam concentration-response curves from $\alpha_2\beta_2\gamma_{2s}$ receptors containing Loop A-C mutations. **A)** Example traces from $\alpha_x\beta_2\gamma_{2s}$ mutated receptors. Scale bar: 5 sec, 500 pA. **B)** Midazolam concentration-response curves (10-1000 nM) for $\alpha_x\beta_2\gamma_{2s}$ mutated receptors. Potentiation (%) was measured as the enhancement of EC_{10} GABA with 10-1000nM midazolam. Mutations are α2(H101R) (loop A, red), α2(T162P) (loop B, green), α2(S205I) (loop C, blue). Points are mean ± SEM and where not visible SEM is smaller than points. Sample sizes are N=6-8 cells per group.

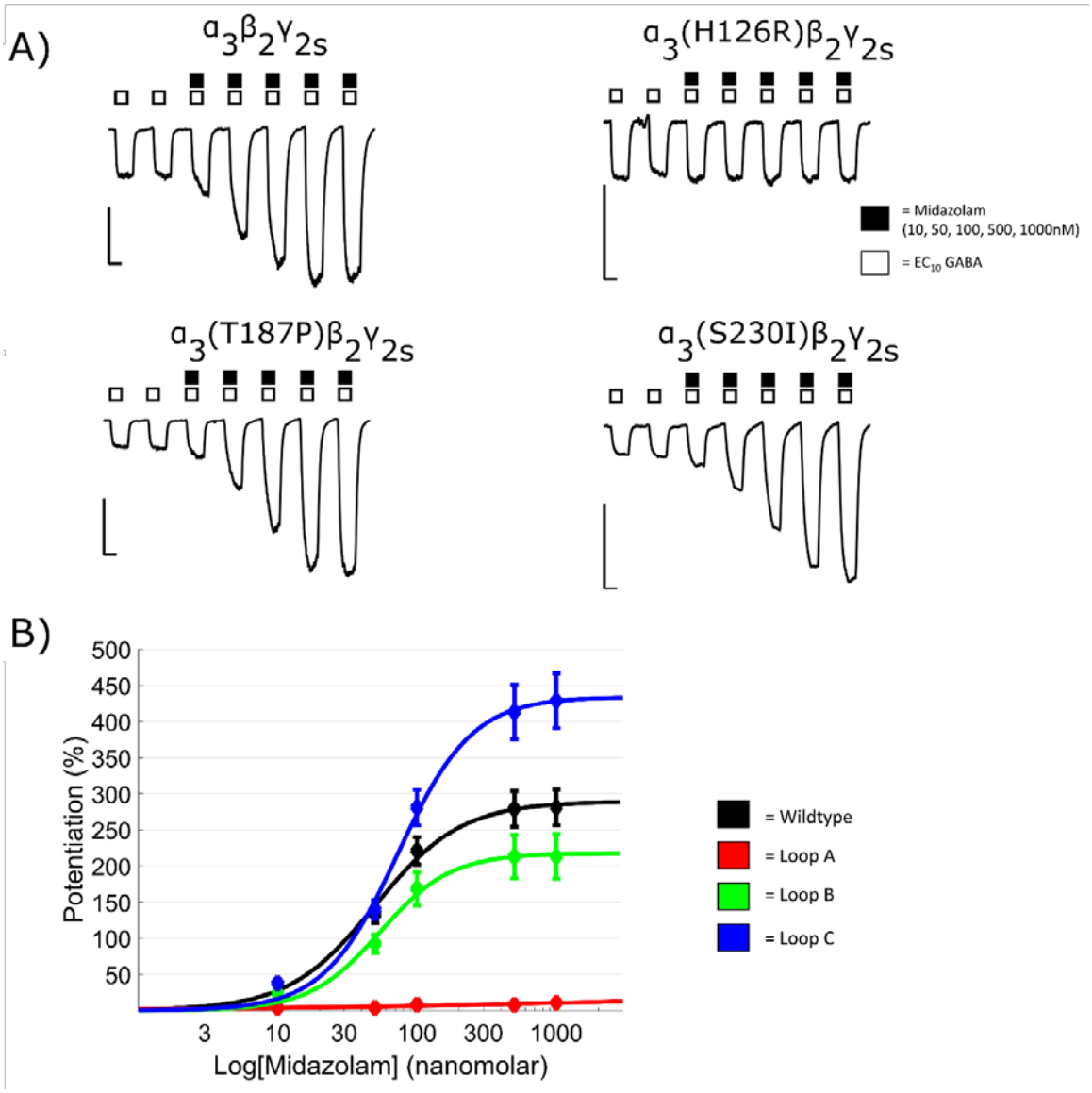

Figure 3.13. Midazolam concentration-response curves from $\alpha_3\beta_2\gamma_{2s}$ receptors containing Loop A-C mutations. **A)** Example traces from $\alpha_x\beta_2\gamma_{2s}$ mutated receptors. Scale bar: 5 sec, 500 pA. **B)** Midazolam concentration-response curves (10-1000nM) for $\alpha_x\beta_2\gamma_{2s}$ mutated receptors. Potentiation (%) was measured as the enhancement of EC_{10} GABA with 10-1000 nM midazolam. Mutations are α3(H126R) (loop A, red), α3(T187P) (loop B, green), α3(S230I) (loop C, blue). Points are mean ± SEM and where not visible SEM is smaller than points. Sample sizes are N=6-7 cells per group.

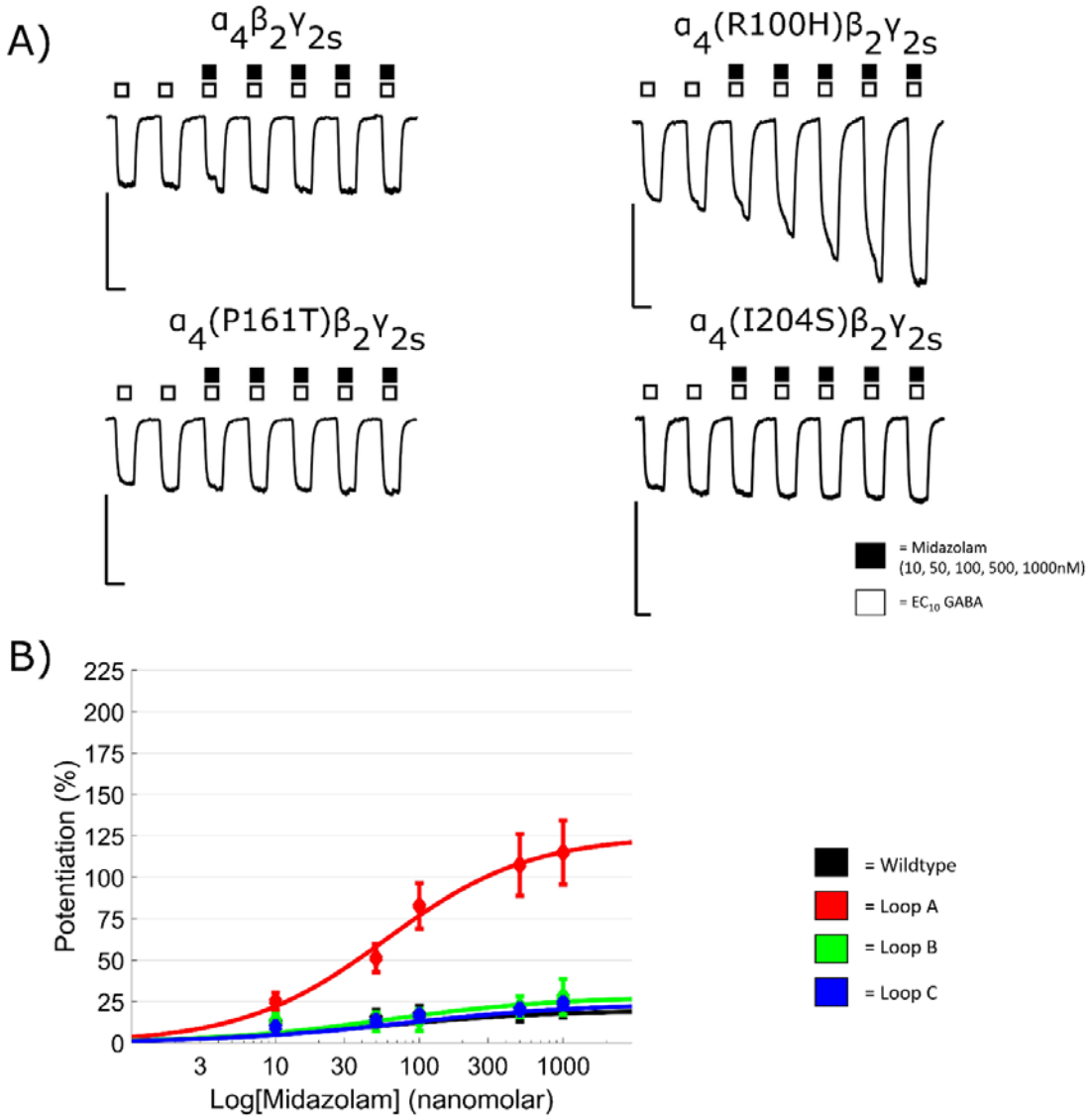

Figure 3.14. Midazolam concentration-response curves from $\alpha_4\beta_2\gamma_{2s}$ receptors containing Loop A-C mutations. **A)** Example traces from $\alpha_x\beta_2\gamma_{2s}$ mutated receptors. Scale bar: 5 sec, 500 pA. **B)** Midazolam concentration-response curves (10-1000nM) for $\alpha_x\beta_2\gamma_{2s}$ mutated receptors. Potentiation (%) was measured as the enhancement of EC_{10} GABA with 10-1000 nM midazolam. Mutations are α4(R100H) (loop A, red), α1(P161T) (loop B, green), α4(I204S) (loop C, blue). Points are mean ± SEM and where not visible SEM is smaller than points. Sample sizes are N=7-8 cells per group.

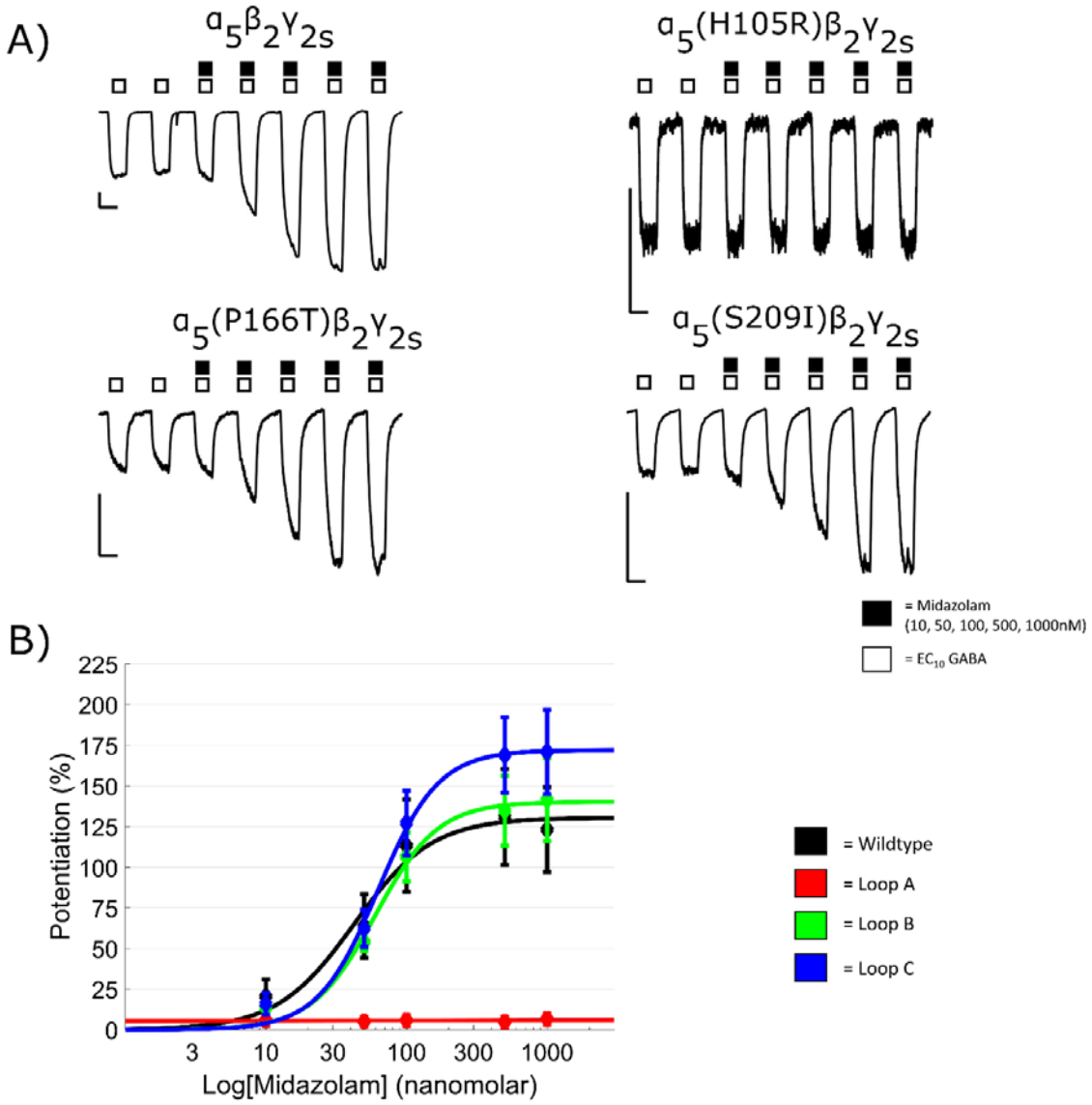

Figure 3.15. Midazolam concentration-response curves from $\alpha_5\beta_2\gamma_{2s}$ receptors containing Loop A-C mutations. **A)** Example traces from $\alpha_x\beta_2\gamma_{2s}$ mutated receptors. Scale bar: 5 sec, 500 pA. **B)** Midazolam concentration-response curves (10-1000nM) for $\alpha_x\beta_2\gamma_{2s}$ mutated receptors. Potentiation (%) was measured as the enhancement of EC_{10} GABA with 10-1000 nM midazolam. Mutations are α5(H105R) (loop A, red), α5(P166T) (loop B, green), α5(S209I) (loop C, blue). Points are mean ± SEM and where not visible SEM is smaller than points. Sample sizes are N=6-7 cells per group.

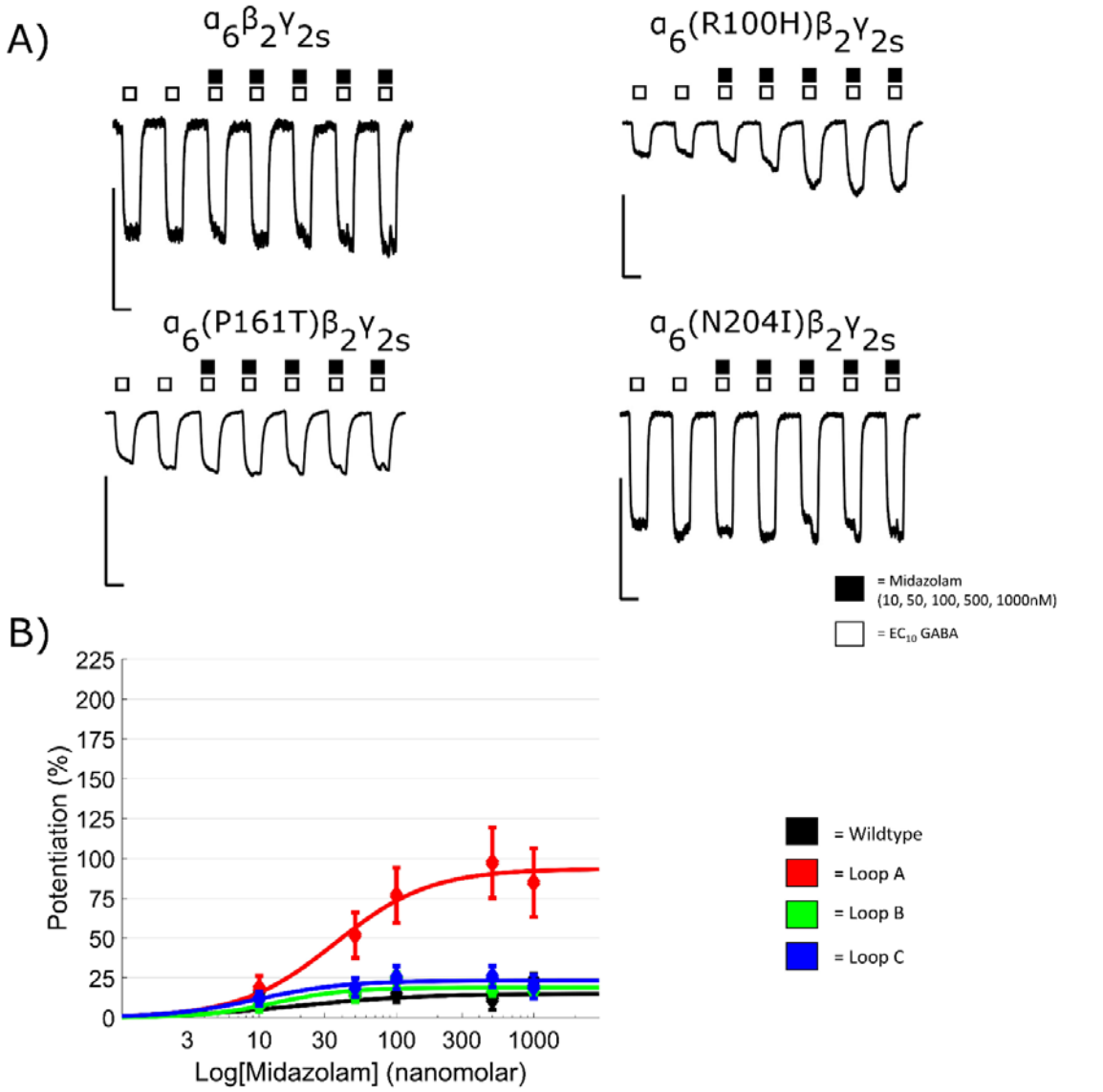

Figure 3.16. Midazolam concentration-response curves from $\alpha_6\beta_2\gamma_{2s}$ receptors containing Loop A-C mutations. **A)** Example traces from $\alpha_x\beta_2\gamma_{2s}$ mutated receptors. Scale bar: 5 sec, 500 pA. **B)** Midazolam concentration-response curves (10-1000nM) for $\alpha_x\beta_2\gamma_{2s}$ mutated receptors. Potentiation (%) was measured as the enhancement of EC_{10} GABA with 10-1000 nM midazolam. Mutations are α6(R100H) (loop A, red), α6(P161T) (loop B, green), α6(N204I) (loop C, blue). Points are mean ± SEM and where not visible SEM is smaller than points. Sample sizes are N=6-7 cells per group.

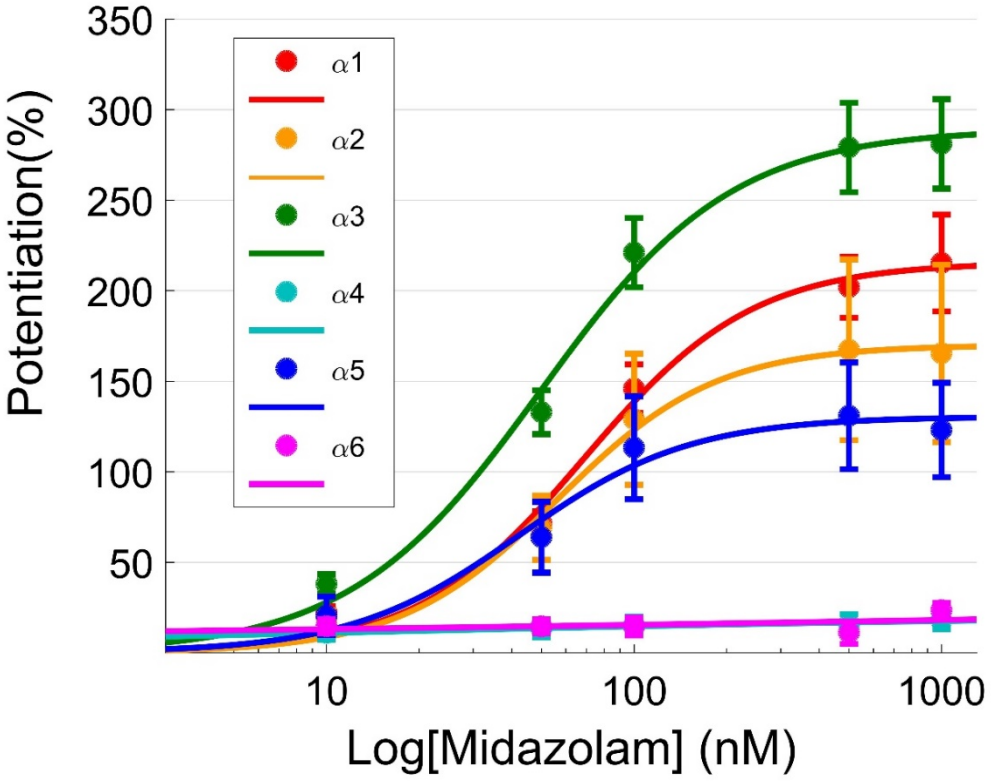

Figure 3.17. Comparison of midazolam potentiation for wildtype $\alpha_x\beta_2\gamma_{2s}$ $GABA_A$ receptors. Midazolam (10, 50, 100, 500, 1000 nM) concentrations-response curves were recorded using whole-cell patch clamp recording. Potentiation (%) was measured as the percent of enhancement in the GABA EC_{10} peak current response. Number of recordings per group (6-7 cells per group): α1=13, α2=10, α3=17, α4=9, α5=11, α6=17. Legend: α1 (red), α2 (orange), α3(green), α4(light blue), α5(blue), α6(magenta). Points are mean ± SEM and where not visible SEM is smaller than points.

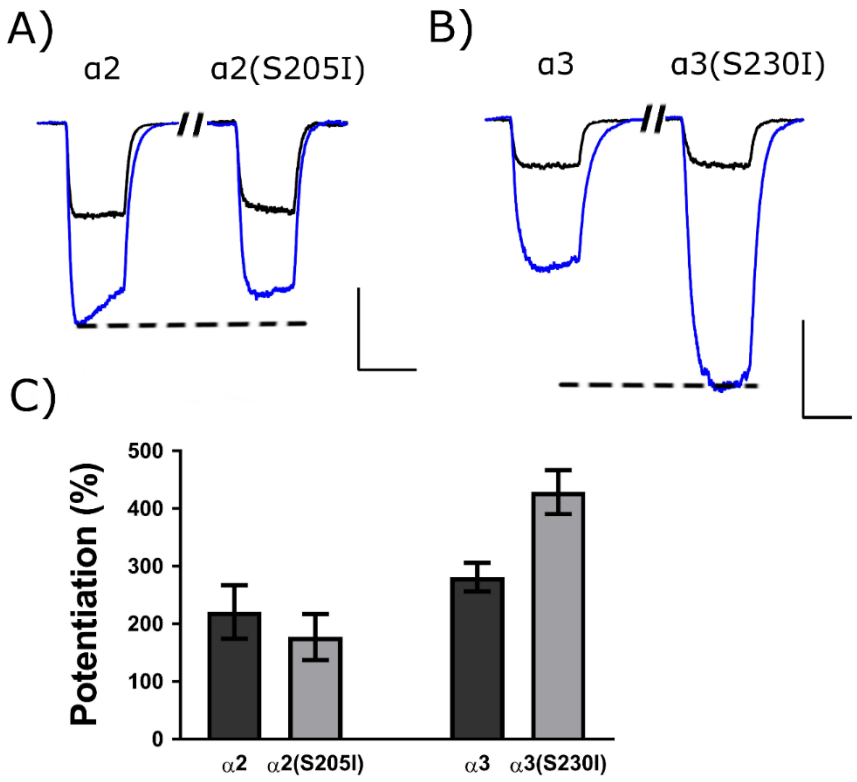

Figure 3.18. Although loop C mutations in α2 and α3 mutations had similar GABA apparent-affinities but showed different degrees of midazolam potentiation of $\alpha_x\beta_2\gamma_2$ receptors. A-B) Example traces of whole-cell responses to EC_{10} GABA (black) and EC_{10} GABA + 1 μM midazolam (blue) for: A) $\alpha_2\beta_2\gamma_2$ and α_2(S205I)$\beta_2\gamma_2$ receptors, and B) $\alpha_3\beta_2\gamma_2$ and α_3(S230I)$\beta_2\gamma_2$ receptors. The dotted line marks the highest degree of midazolam potentiation for each example. Scale bar in (A) is 5 sec, 500 pA for $\alpha_2\beta_2\gamma_2$ and α_2(S205I)$\beta_2\gamma_2$ receptors. Scale bar in (B) is 5 sec, 320 pA for $\alpha_3\beta_2\gamma_2$ and 5 sec, 500 pA for α_3(S230I)$\beta_2\gamma_2$ receptors. C) Quantifying the maximum potentiation measured with 1 μM midazolam for $\alpha_2\beta_2\gamma_2$, α_2(S205I)$\beta_2\gamma_2$, $\alpha_3\beta_2\gamma_2$ and α_3(S230I)$\beta_2\gamma_2$ receptors. *p<0.05 significance was determined using a two-way ANOVA and Sidak's post-hoc analysis. Bars are mean ± SEM from n=9-17 cells per group.

Table 3.4. Midazolam potentiation measurements for midazolam assays

	Midazolam Potentiation Values			
	Wildtype	**Loop A**	**Loop B**	**Loop C**
[MDZ] nM	**$\alpha_1\beta_2\gamma_2$**	**α1(H102R)**	**α1(T163P)**	**α1(S206I)**
10	22.06 ± 3.46	8.10 ± 3.48	14.19 ± 4.15	13.37 ± 5.70
50	71.67 ± 6.40	13.07 ± 4.69	49.96 ± 8.44	44.00 ± 10.96
100	145.94 ± 13.37	16.99 ± 4.42	96.68 ± 15.00	80.14 ± 17.04
500	201.94 ± 16.80	26.78 ± 5.31	124.27 ± 18.98	107.07 ± 22.95
1000	215.35 ± 26.71	28.87 ± 6.18	123.00 ± 18.99	108.21 ± 24.13
N	7 (13)	11 (15)	11 (18)	6 (11)
[MDZ] nM	**$\alpha_2\beta_2\gamma_2$**	**α2(H101R)**	**α2(T162P)**	**α2(S205I)**
10	19.47 ± 4.19	9.85 ± 5.77	26.45 ± 4.06	21.06 ± 6.24
50	69.08 ± 17.73	21.72 ± 8.75	81.24 ± 9.43	54.26 ± 10.25
100	128.98 ± 36.14	25.17 ± 9.58	129.24 ± 14.94	86.20 ± 14.74
500	167.38 ± 49.89	30.08 ± 10.31	156.21 ± 15.70	102.63 ± 19.49
1000	165.35 ± 48.98	31.81 ± 11.79	150.36 ± 15.00	97.62 ± 20.12
N	7 (10)	7 (11)	6 (9)	8 (13)
[MDZ] nM	**$\alpha_3\beta_2\gamma_2$**	**α3(H126R)**	**α3(T187P)**	**α3(S230I)**
10	37.98 ± 5.40	3.71 ± 1.31	23.71 ± 6.37	37.59 ± 4.12
50	132.92 ± 12.09	3.63 ± 2.06	92.47 ± 12.51	139.86 ± 12.63
100	221.10 ± 19.12	8.25 ± 1.64	168.56 ± 23.08	280.95 ± 24.73
500	279.18 ± 24.71	7.92 ± 2.84	212.97 ± 30.06	413.27 ±37.70
1000	281.17 ± 24.73	10.78 ± 2.42	213.30 ± 30.99	428.92 ± 38.09
N	7 (17)	6 (9)	6 (11)	7 (14)
[MDZ] nM	**$\alpha_4\beta_2\gamma_2$**	**α4(R100H)**	**α4(P161T)**	**α4(I204S)**
10	10.98 ± 3.61	26.12 ± 4.95	13.22 ± 3.76	9.47 ± 1.93
50	13.30 ± 4.65	54.65 ± 8.66	10.31 ± 5.64	13.23 ± 1.68
100	15.15 ± 4.85	87.48 ± 13.68	14.28 ± 5.87	16.59 ± 1.59
500	15.98 ± 5.42	117.13 ± 19.82	21.94 ± 5.61	20.16 ± 2.01

1000	17.89 ± 4.82	125.77 ± 21.01	26.43 ± 9.72	23.95 ± 2.33
N	6 (9)	8 (15)	7 (10)	7 (10)
[MDZ] nM	**$\alpha_5\beta_2\gamma_2$**	**α5(H105R)**	**α5(P166T)**	**α5(S209I)**
10	20.47 ± 10.62	8.59 ± 4.39	13.32 ± 1.68	15.95 ± 6.58
50	63.82 ± 19.54	7.73 ± 4.67	54.02 ± 5.66	62.43 ± 11.51
100	113.29 ± 28.44	8.00 ± 4.85	106.37 ± 15.09	127.16 ± 19.87
500	130.90 ± 29.52	5.65 ± 3.99	134.76 ± 21.59	168.94 ± 23.17
1000	123.12 ± 26.08	8.17 ± 4.66	141.51 ± 25.59	170.92 ± 25.92
N	7 (11)	7 (11)	7 (11)	6 (9)
[MDZ] nM	**$\alpha_6\beta_2\gamma_2$**	**α6(R100H)**	**α6(P161T)**	**α6(N204I)**
10	14.66 ± 3.92	14.39 ± 8.03	7.52 ± 3.56	11.98 ± 4.42
50	14.55 ± 3.86	45.91 ± 12.95	13.89 ± 3.99	19.07 ± 5.84
100	14.58 ± 4.87	71.31 ± 17.31	24.46 ± 3.86	25.21 ± 7.32
500	11.15 ± 6.25	85.96 ± 19.92	17.25 ± 3.52	25.85 ± 6.62
1000	23.34 ± 4.23	79.13 ± 19.87	16.98 ± 4.08	19.31 ± 7.32
N	7 (17)	7 (10)	6 (10)	6 (11)

Table 3.4. Midazolam (MDZ) potentiation (%) values measured from $\alpha_x\beta_2\gamma_2$ $GABA_A$ receptors containing mutations in the benzodiazepine site. Mutations in loops A-C were made across the α1-6 subunits. Potentiation was calculated as the percent of enhancement of EC_{10} GABA responses. Midazolam concentrations were from 10-1000 nM. Data was collected using whole-cell patch clamp recording of HEK293T cells expressing $\alpha_x\beta_2\gamma_2$ receptors. Sample sizes were from N cells with the total number midazolam assays run in parentheses. Values are mean ± S.E.M.

Table 3.5. Hill fit parameters for midazolam concentration-response curves

Conditions:	Wildtype	Loop A	Loop B	Loop C
	$\alpha_1\beta_2\gamma_2$	**α1(H102R)**	**α1(T163P)**	**α1(S206I)**
Max pot %	203.0 ± 17.6	h.n.f.	127.7 ± 16.0**	135.8 ± 23.78**
Hill coefficient	1.765 ± 0.165	h.n.f.	2.113 ± 0.154	1.568 ± 0.199
EC_{50} (nM)	71.43 ± 5.80	h.n.f.	61.08 ± 3.72	59.77 ± 4.11
N	7	11	11	6
	$\alpha_2\beta_2\gamma_2$	**α2(H101R)**	**α2(T162P)**	**α2(S205I)**
Max pot %	169.6 ± 49.9	h.n.f.	158.2 ± 15.8	116.4 ± 23.0
Hill coefficient	1.743 ± 0.133	h.n.f.	1.393 ± 0.073	1.362 ± 0.140
EC_{50} (nM)	50.90 ± 5.05	h.n.f.	42.03 ± 2.86	41.65 ± 4.99
N	7	7	6	8
	$\alpha_3\beta_2\gamma_2$	**α3(H126R)**	**α3(T187P)**	**α3(S230I)**
Max pot %	267.8 ± 20.3	h.n.f.	219.6 ± 32.3	436.0 ± 39.4**
Hill coefficient	1.503 ± 0.117	h.n.f.	1.963 ± 0.224**	1.655 ± 0.061
EC_{50} (nM)	46.39 ± 7.44	h.n.f.	55.21 ± 2.91	73.56 ± 1.81**
N	7	6	6	7
	$\alpha_4\beta_2\gamma_2$	**α4(R100H)**	**α4(P161T)**	**α4(I204S)**
Max pot %	h.n.f.	113.8 ± 21.6	h.n.f.	h.n.f.
Hill coefficient	h.n.f.	1.187 ± 0.150	h.n.f.	h.n.f.
EC_{50} (nM)	h.n.f.	73.99 ± 3.44	h.n.f.	h.n.f.
N	6	8	7	7
	$\alpha_5\beta_2\gamma_2$	**α5(H105R)**	**α5(P166T)**	**α5(S209I)**
Max pot %	107.9 ± 20.3	h.n.f.	140.7 ± 23.7	175.1 ± 26.6
Hill coefficient	2.632 ± 0.329	h.n.f.	3.661 ± 1.897	2.232 ± 0.334
EC_{50} (nM)	52.84 ± 3.48	h.n.f.	53.28 ± 5.54	65.44 ± 2.76
N	7	7	7	6
	$\alpha_6\beta_2\gamma_2$	**α6(R100H)**	**α6(P161T)**	**α6(N204I)**
Max pot %	h.n.f.	93.27 ± 22.84	h.n.f.	h.n.f.
Hill coefficient	h.n.f.	2.310 ± 0.56	h.n.f.	h.n.f.
EC_{50} (nM)	h.n.f.	41.88 ± 6.02	h.n.f.	h.n.f.
N	7	7	6	6

Table 3.5. Midazolam Hill fit parameters for $GABA_A$ receptors with loop A-C mutations in the benzodiazepine site of α1-6. Midazolam concentration-response relationships (10-1000 nM) were measured with whole-cell patch clamp recording of HEK293T cells expressing $\alpha_x\beta_2\gamma_2$ receptors. Midazolam concentration-response relationships not described by a sigmoidal function (h.n.f.= Hill Not Fit) were not included in this analysis (eg: no response or a linear non-saturating response). Significance was determined using one-way ANOVA with Dunnett's post hoc analysis for each α-subunit and its mutations. ***p*<0.05. Multiple comparisons were made relative to the wildtype $\alpha_x\beta_2\gamma_2$ receptor. Values are mean ± S.E.M. from N number of cells.

Summary of mutagenesis results with midazolam

Overall, loop A mutations altered the efficacy of midazolam's modulation most dramatically. Mutating the critical histidine in loop A could abolish (α1, α2, α3, α5) and confer (α4 and α6) midazolam sensitivity to $\alpha_x\beta_2\gamma_2$ receptors. Mutating the threonine (loop B) and serine (loop C) residues across α1-6 subunits failed to dramatically abolish or confer the ability of $\alpha_x\beta_2\gamma_2$ $GABA_A$ receptors to be modulated by midazolam. Loop C mutants caused modest changes in the maximum midazolam potentiation (efficacy), particularly in α3 and α5. A summary table of the statistically significant changes for mutations in both GABA concentration-response curves and midazolam concentration-response curves is reported in Table 3.6.

	GABA assays			Midazolam assays		
	Loop A (His-Arg)	**Loop B (Thr-Pro)**	**Loop C (Ser-Iso)**	**Loop A (His-Arg)**	**Loop B (Thr-Pro)**	**Loop C (Ser-Iso)**
α1	none	↓Max	none	↓P%	↓Max	↓Max
α2	↑EC_{50}	↓Max	↑Max	↓P%	none	none
α3	↑Max	none	↑Hill	↓P%	↑Hill	↑Max ↑EC_{50}
α4	none	↑Max ↑Hill	none	↑P%	n.p.	n.p.
α5	↑EC_{50}	none	none	↓P%	none	none
α6	none	none	↓EC_{50}	↑P%	n.p.	n.p.

Table 3.6. Summary of significant (p<0.05) changes in estimated Hill parameters for concentration-response curves with GABA and midazolam. Loop A-C mutations were made in $\alpha_x\beta_2\gamma_2$ $GABA_A$ receptors and parameters compared to that of wildtype receptors using one-way ANOVA's with Dunnett's post-hoc analysis. Legend of abbreviations: EC_{50} = concentration that gives half-maximal response; Hill = Hill coefficient; Max=maximum current; ↓P% = abolished sensitivity; ↑P% = conferred sensitivity; n.p. = no potentiation measured.

3.3.4: Effects of midazolam on the GABA concentration-response relationship for $\alpha_1\beta_2\gamma_2$ receptors

GABA (0.3-1000 μM) concentration-response assays in the presence and absence of 1 μM midazolam were performed on $\alpha_1\beta_2\gamma_2$ $GABA_A$ receptors. This concentration (1 μM) was considered a saturating concentration for the high-affinity benzodiazepine binding site. In the presence of 1 μM midazolam, the GABA concentration-response curve shifted leftwards, but contrary to conventional benzodiazepine theory, the shift was non-parallel (Figure 3.19). Supporting this, the Hill coefficient was significantly larger (1 μM midazolam: 1.435 ± 0.120; Control: 1.000 ± 0.102, $p<0.05$, $t=2.533$, $df=21$) in the presence of midazolam. The half-maximal (EC_{50}) concentration was significantly lower (1 μM midazolam: 35.9 ±8.3 μM; control: 76.8 ± 17.1 μM, $p<0.05$, $t=0.0260$, $df=21$) in the presence of midazolam. Maximum GABA-evoked current did not differ in the absence (-3288 ± 272 pA) or presence (-3817 ± 643 pA) of midazolam. A separate experiment was performed to confirm that midazolam was not enhancing saturating GABA responses. Results showed that 1 μM midazolam did not significantly alter whole-cell peak currents evoked by saturating (1000 μM) GABA (GABA: -6916 ± 640.2 pA, GABA + midazolam: -6172 ± 774.1 pA, $p=0.468$, n=10 cells per group) (Figure 3.20).

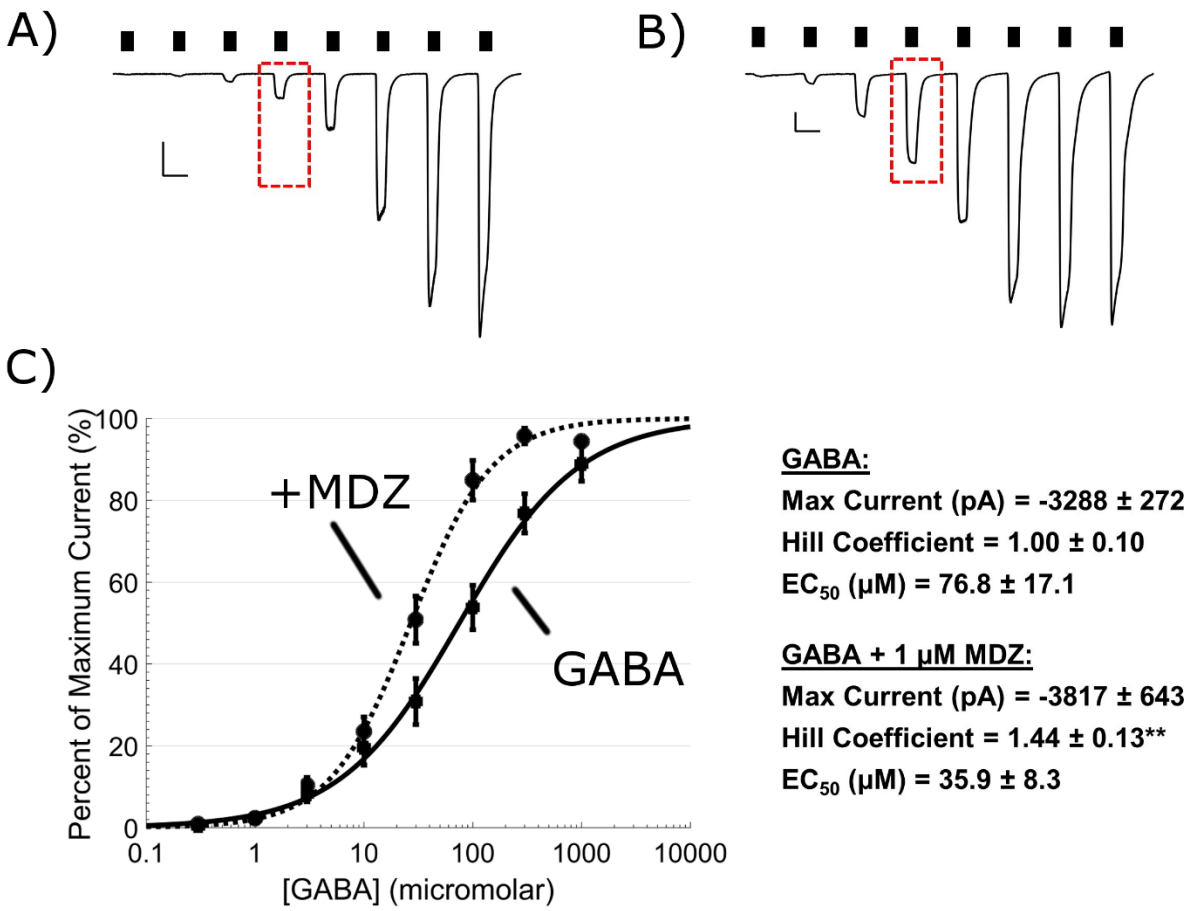

Figure 3.19. Saturating midazolam shifts the GABA concentration-response curve leftwards. **A-B)** Example traces of GABA concentration-response assays (0.3-1000 μM) in the absence (A) and presence of 1 μM midazolam (B) for $\alpha_1\beta_2\gamma_2$ receptors. The red box highlights the 10 μM GABA response and how much larger it is in the presence of 1 μM midazolam. Scale bar = 5 sec, 500 pA. **C)** GABA concentration-response curve in absence (black line) and presence of 1 μM midazolam (dotted line). N= 9-10 cells per group. Points are mean ± SEM.

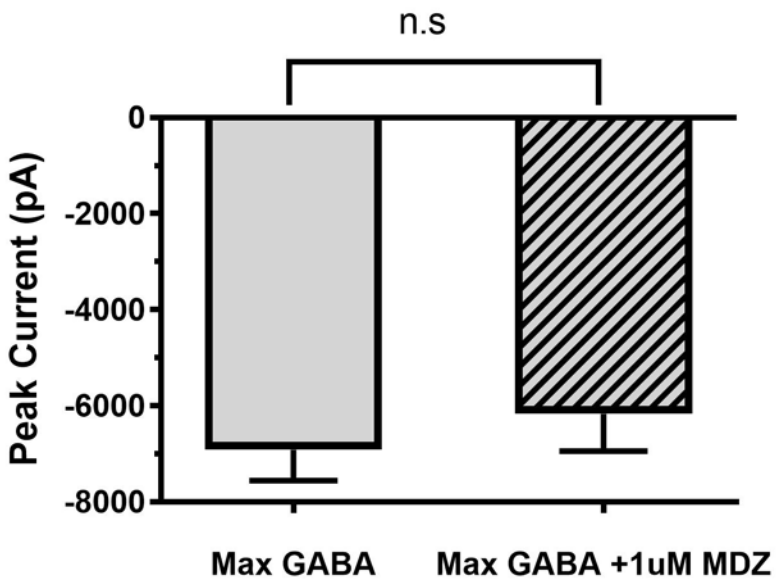

Figure 3.20. The presence of 1 μM midazolam does not significantly (p>0.05) alter the whole-cell maximum peak current response of $\alpha_1\beta_2\gamma_{2s}$ receptors to 1000 μM GABA. A two-way unpaired t-test (α=0.05) was used to compare 1000 μM GABA responses in the presence and absence of 1 μM midazolam. N=10 cells per group. n.s= non-significant. Mean ± SEM.

3.4: Discussion

Midazolam is a positive allosteric modulator (PAM) that enhances $GABA_A$ receptor activity. Midazolam binds the high-affinity benzodiazepine binding site on the $GABA_A$ receptor. The exact mechanism by which midazolam transmits its PAM effects from the benzodiazepine binding site to channel opening remains incompletely understood. Certain highly-conserved residues in the benzodiazepine binding site are predicted to play a direct role in either the binding of midazolam or the coupling midazolam binding to its allosteric effects on receptor activity. Loop A, loop B, and loop C within the α subunit contain several highly-conserved residues that may play one or both these roles. In this chapter, mutagenesis of three of these residues (His/Arg in loop A, Thr/Pro in loop B, and Ser/Ile in loop C) was performed across all six α subunits (Table 3.2 for mutation list). Whole-cell patch clamp recording of $\alpha_x\beta_2\gamma_{2s}$ $GABA_A$ receptors containing these mutations was performed to dissect the individual contributions of specific residues to midazolam's potentiation of $GABA_A$ receptor activity. Second, the modulatory effects of midazolam on GABA-evoked responses from $\alpha_1\beta_2\gamma_{2s}$ $GABA_A$ receptors was compared to conventional benzodiazepine theory that predicts how midazolam would shift the GABA concentration-response relationship. The following discussion will be divided into two parts: 1) a discussion of the results of the mutagenesis of loops A-C in the benzodiazepine site on midazolam's modulatory actions (section 3.5.1), and 2) a discussion of how midazolam shifts the GABA concentration-response curve (section 3.5.2).

3.4.1 *Mutation of single residues in loops A-C can alter the efficacy of midazolam*

In these experiments, I examined the role of the histidine in loop A, threonine in loop B, and serine in loop C within the α subunit and how these residues affected the allosteric potentiation of the $GABA_A$ receptor by midazolam. The histidine-to-arginine loop

A mutation provided an example of how a single residue mutation can dramatically alter the efficacy of midazolam potentiation. The loop B threonine and loop C serine are highly conserved across α subunits, except in α4 and α6 subunits, which are generally insensitive to classic benzodiazepines (Knoflach et al., 1996; Wafford et al., 1996). We predicted that the presence of a proline in loop B and isoleucine in loop C would decrease the degree of potentiation of the $\alpha_x\beta_2\gamma_2$ $GABA_A$ receptors by midazolam. Overall, the loop A mutations (histidine/arginine) had the most dramatic effect on midazolam efficacy. The mutation of the conserved threonine-to-proline in loop B had subtle effects on midazolam potentiation. Finally, the serine-to-isoleucine mutation in loop C altered the efficacy of midazolam potentiation, especially for α3 and α5-containing receptors.

Across the 18 mutations made in loops A-C within the benzodiazepine site, only subtle changes were seen in GABA apparent-affinity. The α_2(H101R) and α_5(H105R) mutations caused 2-fold and 3-fold reductions in GABA apparent-affinity, but these effects were relatively small. It was also similar to the 2-fold changes in GABA apparent-affinity reported by Benson (1998) for these mutations (Benson et al., 1998). Since the mutation was away from the GABA binding site, it is unlikely the mutations caused a large structural rearrangement of the extracellular domain that affected the channel's activation. The α6(N204I) mutant increased the GABA's apparently-affinity, but this was not sufficient to make the receptor any more responsive to midazolam than the wildtype α6-containing receptors. On the whole, the results were consistent with mutations that had minimal effects on GABA's normal actions at the mutated receptor.

It is well established that the conserved histidine present in loop A (FF**H**NG) of the α subunit is important in determining the molecular (Benson et al., 1998; Kleingoor et al., 1993; H A Wieland et al., 1992) and behavioral (Rudolph et al., 2001) effects of benzodiazepines (as described in section 1.6 of the Introduction). His102 is present in the

α subunits sensitive to positive benzodiazepines but not in α4 and α6 that are insensitive (Knoflach et al., 1996). This was initially described when $GABA_A$ receptors isolated from cerebellar granule tissue displayed similar pharmacology to $\alpha_6\beta_2\gamma_2$ recombinant receptors, binding only benzodiazepine antagonists and inverse agonists (e.g. Ro 15-4513) but not the PAM diazepam (Knoflach et al., 1996). Wieland and colleagues isolated the conserved histidine (His102) that when mutated to an arginine (α1(H102R)) impaired the binding of diazepam to $\alpha_x\beta_2\gamma_2$ receptors because the arginine sterically prevented benzodiazepines from interacting properly with the site (H A Wieland et al., 1992; Wingrove et al., 2002). The homologous H102R mutation also abolished diazepam's actions in α2, α3, and α5 subunits (Benson et al., 1998). However, most H102R mutations have not been studied beyond their effects on diazepam's actions.

In my experiments, I mutated the homologous H102R mutation across all six human α $GABA_A$ subunits. These mutations were α1(H102R), α2(H101R), α3(H126R), α4(R100H), α5(H105R), and α6(R100H). Replicating these mutations provided a reference for how altering a key residue in the benzodiazepine binding site can dramatically alter the efficacy of midazolam at $\alpha_x\beta_2\gamma_{2s}$ $GABA_A$ receptors. The homologous H102R mutation in α1-3 and α5 abolished midazolam potentiation, consistent with past results using diazepam (Benson et al., 1998). Conversely, mutating the conserved arginine-to-histidine in α4 and α6 conferred midazolam potentiation capabilities to α4(R100H)- and α6(R100H)-containing $\alpha_x\beta_2\gamma_2$ receptors (Figures 3.11-16). Based on previous literature, the elimination of midazolam sensitivity for α1(H102R), α_2(H101R), α_3(H126R) and α_5(H105R) mutant receptors was most likely due to reduced binding of midazolam to the receptor (Berezhnoy et al., 2004; Duncalfe et al., 1996; Tan et al., 2007; H. A. Wieland & Luddens, 1994; H A Wieland et al., 1992). Although the α_4(R100H) and α_6(R100H) mutations dramatically conferred midazolam responsiveness to the $\alpha_x\beta_2\gamma_2$

receptors, it was still less than the wildtype responses for the other α subunits (~170-270%). The maximum midazolam potentiation remained at only ~110% for α_4(R100H) and ~90% for α6(R100H) mutations. This suggests that other critical contact points exist for midazolam in the binding pocket and contribute to producing the increased efficacy of midazolam seen with receptors containing α1-3/5. Although it is unusual for single point mutations to be able to confer ligand sensitivity to a receptor in such a dramatic way, this residue appears to be an exception for midazolam. These results provided an example of how a single residue mutation could dramatically alter the efficacy of midazolam potentiation across receptors containing α1-6 isoforms.

The threonine (GSYAY**T**R, loop B) and serine (S**S**TGEYV, loop C) mutations had more subtle effects on midazolam potentiation than the H102R mutation. The serine and threonine have been studied previously in binding assays (Amin et al., 1997; Buhr et al., 1997; Renard et al., 1999; Sawyer, Chiara, Olsen, & Cohen, 2002; Schaerer, Buhr, Baur, & Sigel, 1998; Strakhova, Harvey, Cook, Cook, & Skolnick, 2000) but less often in functional assays. Binding studies suggested that these residues could alter benzodiazepine binding (threonine in loop B) and ligand selectivity (serine in loop C), but these studies used the non-benzodiazepines zolpidem and eszopiclone that have different chemical structures from midazolam (Hanson et al., 2008; Renard et al., 1999). The loop B results showed that only the α1(T163P) mutation decreased the maximum amplitude of midazolam potentiation as predicted. Of the other loop B mutations, α3(T187P) only slightly decreased the maximum potentiation and α5(P166T) slightly increased it. Previous binding studies showed that a proline-to-threonine mutation in α5 and α6 moderately increased the binding affinity of zolpidem (Renard et al., 1999) and diazepam (H. A. Wieland & Luddens, 1994). Prolines are known to induce turns in the secondary structure that could affect the global protein structure. The proline present in α5 might restructure

the benzodiazepine pocket to limited zolpidem's ability to interact efficiently with the benzodiazepine binding site compared to α1-containing receptors. My results were consistent with the threonine in loop B conferring only slightly higher midazolam efficacy to the receptor than the proline.

The loop C mutations had more obvious changes in the efficacy of midazolam potentiation. The wildtype α1, α2, α3 and α5 subunits all contain the homologous Ser233 (human α1) that I predicted would reduce midazolam potentiation when mutated to an isoleucine. Surprisingly, the results did not follow the predicted pattern. In the α1(S206I) and α2(S205I) mutants, the isoleucine decreased midazolam's maximum potentiation by 31-33%, but in α3(S230I) and α5(S209I), it increased midazolam's potentiation by approximately 63%. Only α3(S230I) significantly (p<0.05) altered midazolam's $EC_{50.}$ In the case of an allosteric modulator, an altered EC_{50} might be caused by changes in the modulator's ability to bind and interact with the receptor or the modulator's ability to alter GABA's binding and gating of the channel (Colquhoun, 1998). As mentioned above, only modest changes in GABA apparent-affinity were seen for loop C mutations, suggesting that changes in midazolam potentiation were caused by an altered midazolam-receptor interaction and not global alterations in structure that transmitted to the GABA binding site.

Loop C is important for ligand binding because it has more mobility than the other loops (Michalowski et al., 2017). Previous studies found that the α6(Asn204) and α4(Ile203) residues (both homologous to human α1(Ser206)) were important for distinguishing the binding of negative benzodiazepines (Derry et al., 2004). Ser206 was also shown to physically interact with a diazepam analogue in α1, α2 and α5, suggesting a critical role in benzodiazepine actions (Luscher, Baur, Goeldner, & Sigel, 2012). A neighboring mutation, α1(T206C), specifically altered benzodiazepine efficacy and not binding (Morlock & Czajkowski, 2011). I propose that the homologous Ser206 in loop C

may provide an important point of contact between the ligand and benzodiazepine site that affects the coupling of the benzodiazepine site to GABA activation, thereby affecting the benzodiazepine's efficacy. Because mutations in α3 and α5 were most dramatic, this serine may be more appropriately positioned in these subunits to alter midazolam's efficacy.

The α3 and α5 subunits have specific expression profiles in the brain that reflect their roles in cognitive- and limbic-related pathways. The α3 subunit is expressed in the cortex, amygdala, olfactory bulb and thalamic reticular nucleus, where $\alpha_3\beta_{2/3}\gamma_2$ receptors that mediate phasic inhibition. The α5 subunit is most highly expressed in the pyramidal hippocampal cells but also in the cortex and hypothalamus (Lee & Maguire, 2014; Pirker et al., 2000). The $\alpha_5\beta_3\gamma_2$ receptors contribute to tonic inhibition in the hippocampus (Farrant & Nusser, 2005).

In my results, the greatest increase in midazolam's efficacy was seen with the α3(S230I) loop C mutation. The wildtype α3-containing receptors were the most sensitive to modulation by midazolam with the lowest midazolam EC_{50} and highest maximum potentiation relative all the other α subunits. This is consistent with a previous study where diazepam bound $\alpha_3\beta_1\gamma_2$ receptors higher than $\alpha_1\beta_1\gamma_2$ and $\alpha_2\beta_1\gamma_2$ (Pritchett, Luddens, & Seeburg, 1989). Even with the higher wildtype levels of potentiation, the α3(S230I) loop C results were still notable. Both $\alpha_2\beta_3\gamma_2$ and $\alpha_3\beta_3\gamma_2$ receptors had similar GABA apparent-affinities. However, when compared to the α2(S205I) mutant in loop C, the α3(S230I) mutation dramatically increased the efficacy of midazolam potentiation (Fig. 3.18). This novel finding underlines the importance of better understanding the differences in allosteric modulation of $GABA_A$ receptors expressing α3 compared to other α subunits. For example, non-hypnotic drugs targeting the α2 and α3 subunits have been studied for their anxiolytic and analgesic effects (Lewter et al., 2017; Rudolph & Knoflach, 2011).

However, creating ligands that distinguish these two subunits remains difficult, as shown when an "α3-specific" PAM (SB-205384) was found to potentiate α6-containing $GABA_A$ receptors even more strongly than α3 (Heidelberg, Warren, & Fisher, 2013). Similarly, the α5 subunit is increasingly being studied for its role in cognition (Mohler, 2015; Rudolph & Knoflach, 2011) and anesthetic-induced neurotoxicity (Zurek et al., 2014). Based on our results, loop C might be a potential target for developing novel drugs that specifically modulate α3- and α5-containing $GABA_A$ receptors using PAMs targeting the allosteric benzodiazepine site.

3.5.2 *Midazolam shifts the GABA concentration-response relationship leftwards, inconsistent with conventional benzodiazepine theory.*

Conventional theory on the mechanism of action of benzodiazepines at $GABA_A$ receptors is based diazepam's actions. It says that benzodiazepines only alter GABA's binding affinity for the receptor and not gating (Lavoie & Twyman, 1996). Benzodiazepines are thought to enhance $GABA_A$ receptor activity by increasing the frequency of the channel opening and not the single channel conductance or open time (Sieghart, 1995b; Study & Barker, 1981). One study did measure increases in single channel conductance using diazepam (Eghbali, Curmi, Birnir, & Gage, 1997), but other studies have not supported this (Lavoie & Twyman, 1996; Rogers et al., 1994). When measuring the effects of diazepam on the GABA concentration-response relationship, diazepam shifts the curve leftwards in a parallel manner (Kemp, Marshall, Wong, & Woodruff, 1987; Sigel & Baur, 1988). These leftwards shifts are often described with increases in the GABA apparent-affinity (EC_{50}) in the presence of diazepam.

In this chapter, midazolam's ability to shift the GABA concentration-response relationship was examined. GABA (0.3-1000 μM) concentration-response curves in the

presence and absence of 1 μM midazolam were performed on $\alpha_1\beta_2\gamma_{2s}$ $GABA_A$ receptors expressed in HEK293T cells. 1 μM midazolam was considered saturating for the high-affinity benzodiazepines site (Figure 3.10). In the presence of 1μM midazolam, the concentration-response curve shifted leftwards. Contrary to conventional benzodiazepine theory, the shift was non-parallel with an increased Hill coefficient (slope) in the presence of midazolam (Figure 3.19). Midazolam also increased the apparent-affinity for GABA by 2-fold. Midazolam did not alter the maximum GABA-evoked current at saturating GABA concentrations (Figure 3.20). Although EC_{50} is a compound measure of binding and gating changes, these results were consistent with midazolam enhancing $\alpha_1\beta_2\gamma_{2s}$ $GABA_A$ receptor activity by enhancing gating.

More recent studies of midazolam's actions on $GABA_A$ receptor activity suggest midazolam alters receptor gating. One study by Kristiansen and Lambert (1996) measured the potentiation of 5-(4-piperidyl)isoxazol-3-ol (4-PIOL) by midazolam using cultured rat hippocampal neurons. 4-PIOL is a partial agonist for $GABA_A$ receptors. At a saturating 4-PIOL (1mM) concentration, responses were potentiated by 0.1 μM midazolam (Kristiansen & Lambert, 1996). Given that 1 mM 4-PIOL should have activated the full receptor occupancy, the only way to increase current responses was by enhancing gating. These responses were measured both with and without midazolam pretreatment to the neurons, but both conditions had similar responses when tested with 4-PIOL, consistent with enhanced gating.

A second patch clamp study examined another partial agonist, piperidine-4-sulfonic acid (P4S) to study the effects of midazolam on gating (Rusch & Forman, 2005). They found that 1 μM midazolam potentiated the responses evoked by 10 mM P4S, a saturating concentration (Rusch & Forman, 2005). This was consistent with midazolam enhancing gating of the receptor to increase the efficacy of P4S. When expressed in

oocytes, $GABA_A$ receptors containing an α1(L264T) pore mutation were constitutively active in the absence of GABA or other agonists. The $\alpha_1(L264T)\beta_2\gamma_{2L}$ receptors could also be directly activated by diazepam and midazolam, a result not seen with wildtype $\alpha_1\beta_2\gamma_{2L}$ receptors (Rusch & Forman, 2005). Since there was no GABA or other agonist present for midazolam to increase the binding of, the receptor's gating must have been enhanced to produce larger current responses. The authors used an allosteric co-agonism model based on the Monod-Wyman-Changeux model of benzodiazepine's actions via the high-affinity benzodiazepine site to explain these findings (Rusch & Forman, 2005). Their model estimated that midazolam bound the receptor approximately 3-times more tightly in the open state than the closed state. This explained why benzodiazepines need GABA or another agonist to active the receptor before their modulatory effects could take place. In the context of the more recent studies and data shown here, midazolam most likely enhances $GABA_A$ receptor activity by enhancing the gating of the receptor when GABA binds.

3.5.5 Conclusions and future directions:

Data in this chapter presented a systematic review of the effect of benzodiazepine site mutations across all six α subunits and the molecular actions of midazolam at $\alpha_x\beta_2\gamma_{2s}$ $GABA_A$ receptors. Few studies have systematically measured the effects of a single mutation across all six α subunits, and to our knowledge, none using midazolam. Midazolam potentiated the GABA-evoked responses of $\alpha_x\beta_2\gamma_{2s}$ receptors containing α1, α2, α3, and α5. At the synaptic level, this enhancement would result in enhanced postsynaptic inhibitory currents. Slice electrophysiology experiments have shown that midazolam increased the current decay time constants of $GABA_A$ receptors in brain slices (Otis & Mody, 1992; Poncer, Durr, Gahwiler, & Thompson, 1996; Rovira & Ben-Ari, 1999). A future experiment might be to dissect the contributions of the different α subunits to this lengthened decay time constant in brain slice recordings.

Mutations altering only drug efficacy are difficult to confirm. They require both binding assays and functional assays. The mutagenesis results presented should be explored further using binding assays to dissect which loop A-C mutations, if any, alter midazolam efficacy alone. Only a few groups have systematically done this for residues in the benzodiazepine binding site of the $GABA_A$ receptor (Morlock & Czajkowski, 2011). Understanding how different structures, like loops A-C, can affect drug efficacy will help develop novel ligands with specific effects. Developing new benzodiazepine site ligands with different drug efficacies rather than different binding affinities for the various α subunits has produced novel drugs with better clinical effects (Rudolph & Knoflach, 2011). However, there is still much room for improvement in current benzodiazepines, especially those with minimized sedative effects. Producing a new benzodiazepine site ligand that selectively interacts with loop C of the α subunit might help improve the α-selectivity of the drug. This might also help distinguish α3- and α5-containing receptors.

Chapter 4:

Chapter 4:

The allosteric modulation of $GABA_A$ receptors by cerebrospinal fluid from patients with idiopathic hypersomnia

Overview:

Idiopathic hypersomnia (IH) is a complex neurological sleep disorder. Patients primarily display unexplained excessive daytime sleepiness that impairs their quality of life. The hypersomnia cannot always be controlled with standard amphetamine sleep medications. Flumazenil and clarithromycin, both newer non-FDA-approved treatments work for a subset of IH patients, but new alternative treatments for IH patients continue to be sought. One important breakthrough in the study of IH came when cerebrospinal fluid (CSF) from IH patients was shown to act as a PAM at $GABA_A$ receptors, enhancing receptor activity (Rye et al., 2012). The hypothesis was that an endogenous peptide in CSF enhanced $GABA_A$ receptors' activity by acting through the high-affinity benzodiazepine binding site. To assess this hypothesis, I measured the CSF modulation of HEK293T cells expressing $\alpha_x\beta_2\gamma_{2s}$ $GABA_A$ receptors using patch clamp recording. Based on the α subunit expressed, I predicted that the degree of CSF modulation measured would be higher for receptors containing α1-3,5 and lower for α4/6, based on the α-subunit-specificity of benzodiazepines. Surprisingly, CSF potentiation (>100%) was measured at all $\alpha_x\beta_2\gamma_{2s}$ $GABA_A$ receptors containing α1-6. CSF potentiation was also measured at extrasynaptic δ-containing receptors, which normally do not respond to benzodiazepines. Overall, patch clamp results were not consistent with mechanism acting purely through the high-affinity benzodiazepine-site site. This suggests that the molecular component within hypersomnolent CSF may enhance $GABA_A$ receptor activity through a site other than the high-affinity benzodiazepine site.

4.1. Introduction

Primary idiopathic hypersomnia (IH) is a rare neurological sleep disorder characterized by excessive daytime sleepiness not explained by any other medical or psychiatric conditions (Billiard & Sonka, 2016; Khan & Trotti, 2015). While some hypersomnia patients respond to stimulant medications like modafinil (Mayer, Benes, Young, Bitterlich, & Rodenbeck, 2015), between 17-38% IH patients remain refractory to standard sleep treatments (Khan & Trotti, 2015). Newer treatments include sublingual flumazenil and clarithromycin that alleviate sleepiness in a subset of patients (Trotti et al., 2014; Trotti et al., 2016). For example, nearly two-thirds of IH patients initially prescribed clarithromycin for hypersomnia reported improvement in sleepiness (Trotti et al., 2013). However, many patients do not achieve adequate control over their symptoms and continue to seek other treatments. Further research is needed to better understand this disorder and develop new treatments for patients with refractory hypersomnia.

There are several challenges to the research of IH. First, making a clinical diagnosis of IH remains difficult because there is no definitive biomarker for IH. The physician must rule out all other medical conditions, including other hypersomnia disorders like Narcolepsy-2 that look very similar clinically (Billiard & Sonka, 2016; Khan & Trotti, 2015). The second challenge to studying IH has been the lack of a definitive biological mechanism. Most theories for idiopathic hypersomnia disorders have revolved around an unknown molecule or pathway in the brain that enhances sleep or suppresses arousal to cause excessive daytime sleepiness (Farzampour et al., 2015). If there is a single molecule enhancing sleepiness, then it could also potentially be used as biomarker for the disease, decreasing the diagnostic time for patients. Discovering a molecular biomarker for IH would also open up avenues for where to direct research efforts. Different potential biomarkers have been suggested for IH, including monoamines, histamine, endozepines, and a peptide somnogen (Billiard & Sonka, 2016).

A recent breakthrough in IH research occurred when the CSF from IH patients was found to enhance the activity of synaptic $\alpha_1\beta_2\gamma_{2s}$ $GABA_A$ receptors (Rye et al., 2012). CSF enhanced (also called *potentiation*) $\alpha_1\beta_2\gamma_{2s}$ $GABA_A$ receptor activity by 82% (Rye et al., 2012). CSF samples from IH patients will be called “hypersomnolent CSF” samples in further sections. Surprisingly, control CSF samples also enhanced $GABA_A$ receptor activity by 31% (Rye et al., 2012). Preliminary analysis of CSF suggested that an endogenous peptide, between 500-3000 Daltons, existed in CSF samples which enhanced $GABA_A$ receptor activity. It was hypothesized that the endogenous peptide may also exist in normal people without excessive daytime sleepiness. In IH, the endogenous peptide may become expressed more abundantly or may exist in a different isoform that becomes more potent to cause excessive daytime sleepiness.

Hypersomnolent CSF samples robustly enhance $\alpha_1\beta_2\gamma_{2s}$ $GABA_A$ receptor activity (Figure 4.1). Initial studies suggested the endogenous peptide may act like an endogenous benzodiazepine at $GABA_A$ receptors. Two types of evidence, molecular and clinical, supported this. First, the molecular actions (receptor enhancement) of CSF samples from IH patients displayed similar pharmacology to benzodiazepines. For example, the CSF potentiation at $\alpha_1\beta_2\gamma_{2s}$ receptors could be largely blocked by flumazenil (Rye et al., 2012). Flumazenil is a benzodiazepine antagonist and is used in the clinic to reverse benzodiazepine overdoses (Olkkola & Ahonen, 2008). Also, CSF potentiation was reduced by 60% at $\alpha_1(H102R)\beta_2\gamma_{2s}$ receptors. This is the same mutation that abolished diazepam (Kleingoor et al., 1993) and midazolam’s (Chapter 3) potentiation. The second piece of evidence was that some IH patients given flumazenil, by an oral or topical route, showed improved vigilance and reduced daytime sleepiness (Rye et al., 2012). Together the molecular and clinical evidence supported a benzodiazepine-centered hypothesis for the molecular actions hypersomnolent CSF at $GABA_A$ receptors.

For this chapter, the starting hypothesis was that the endogenous peptide in hypersomnolent CSF was acting through the high-affinity benzodiazepine binding site on the $GABA_A$ receptor to enhance receptor activity. Based on this hypothesis, $\alpha_x\beta_2\gamma_{2s}$ receptors that showed little to no potentiation with midazolam (i.e. α_1(H102R)$\beta_2\gamma_{2s}$, $\alpha_4\beta_2\gamma_{2s}$ and $\alpha_6\beta_2\gamma_{2s}$) were predicted to also have reduced potentiation by hypersomnolent CSF. Extrasynaptic $GABA_A$ receptors ($\alpha_4\beta_2\delta$ and $\alpha_4\beta_2\delta$) were also predicted to not respond to modulation by hypersomnolent CSF because they are normally insensitive to benzodiazepines.

To test the high-affinity benzodiazepine site hypothesis, I created a single pool of CSF from five patients suspected of having IH. This pooled CSF was filtered through a 10 kDa filter to remove the proteins above 10 kDa in the hypersomnolent CSF. The degree of CSF potentiation was measured using whole-cell patch clamp recording of HEK293T cells expressing $\alpha_x\beta_2\gamma_{2s}$ or $\alpha_x\beta_2$X $GABA_A$ receptors. The α subunit specificity of hypersomnolent CSF potentiation at $\alpha_x\beta_2\gamma_{2s}$ receptors was measured, along with potentiation at extrasynaptic $\alpha_x\beta_2\delta$ receptors. The results showed that hypersomnolent CSF potentiation (>100%) could be measured at α1-6-containing $GABA_A$ receptors, including receptor assemblies normally insensitive to benzodiazepine modulation (α_1(H102R)$\beta_2\gamma_{2s}$, $\alpha_4\beta_2\gamma_{2s}$, $\alpha_6\beta_2\gamma_{2s}$, $\alpha_4\beta_2\delta$ and $\alpha_6\beta_2\delta$). This was consistent with the active component of CSF enhancing $GABA_A$ receptor activity through a site other than the high-affinity benzodiazepine site.

A second set of experiments, measured the degree of potentiation measured by hypersomnolent CSF at different GABA concentrations (10-300 μM) at $\alpha_1\beta_2\gamma_{2s}$ receptors. I predicted that the degree of CSF potentiation measured would be inversely related to the GABA concentration used. These experiments confirmed that the degree CSF potentiation measured at $\alpha_1\beta_2\gamma_{2s}$ receptors decreased as the underlying GABA concentration increased, as expected for positive modulator.

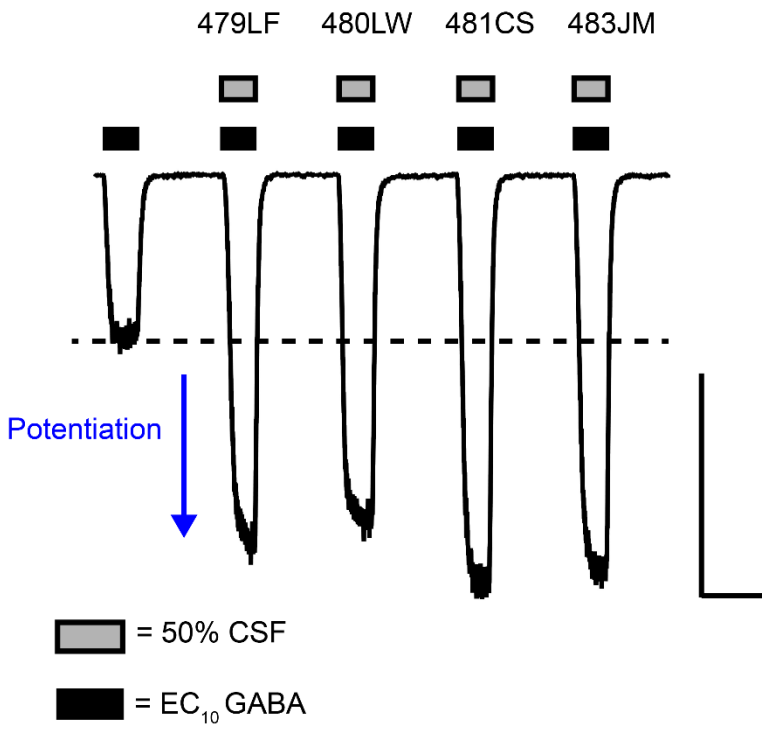

Figure 4.1. Hypersomnolent CSF potentiates $\alpha_1\beta_2\gamma_{2s}$ $GABA_A$ receptor activity. Whole-cell patch clamp recording was used to measure the potentiation of an EC_{10} GABA-evoked response by a 50% dilution of hypersomnolent CSF. Average potentiation measurements for each CSF samples were 142.1% (479LF), 133.9% (480LW), 162.6% (481CS), and 149.8% (483JM). Scale bar is 5 sec, 500 pA.

4.2 Methods:

4.2.1 Cell Culture, cDNA plasmids and transfections

HEK293T cells were cultured and transfected according to the protocols described in Chapter 2 (Section 2.3). The human cDNA $GABA_A$ subunits used were hα1, hα2, hα3, hα4, hα5, hα6, hβ2, hγ2s, and hδ. $GABA_A$ receptors ($\alpha_x\beta_2\gamma_{2s}$ or $\alpha_x\beta_2\delta$) were transiently transfected into HEK293T cells along with GFP using X-tremeGENE transfection reagent.

4.2.2 Cerebrospinal fluid (CSF) sample preparation

Cerebrospinal fluid (CSF) samples were taken from patients seen at the Emory Sleep Clinic who reported excessive daytime sleepiness and who underwent a lumbar puncture procedure for suspected Idiopathic Hypersomnia (IH). Patients provided informed consent for lumbar punctures to determine an etiology for their sleepiness. Patients were not taking any sedative-hypnotic medications at the time of lumbar puncture. Samples were collected by a member of the Emory Sleep Clinic (Dr. David Rye or Dr. Lynn Marie Trotti, Atlanta, GA). Samples were obtained by lumbar puncture with a 22-gauge sterile needle entered at the L4–5 or L3–4 lumbar level, with the average volume of CSF obtained being 12 mL (SD +/- 3.9). Samples were collected between 8 am and 6 pm and were immediately refrigerated. They were aliquoted into 1 mL portions within 1–4 hours of collection and transferred to a -80°C freezer for long-term storage. When samples were transferred from the Rye lab to the Jenkins lab, they were transferred on dry ice and then stored at -20°C until use in electrophysiology assays.

Individual patient CSF samples used in the following experiments were from patients suspected of having IH. Other than the aliquoting into 1 mL tubes at the time of collection, these samples received no other filtration or treatments before electrophysiology analysis.

A pooled CSF sample (Pool C_{om}) was composed of equal 1:1:1:1:1 ratios of five different patient CSF samples from patients suspected of having IH. Patient samples were 453 ME, 459 MM, 474 BC, 477 DG, and 503 CS. Samples were selected randomly from the list of CSF samples provided from patients experiencing hypersomnolence and that had 4 mL's of available CSF. Both patient samples 453 ME and 503 CS had been previously run by Olivia Moody and had 83.5% and 74.4% potentiation measured respectively at $\alpha_1\beta_2\gamma_{2s}$ receptors. Patient samples were a 2:3 mix of male and female samples from individuals age 20-56. The pooled 20 mL of CSF was split into 10 different 2 mL aliquots that were each run through a 10 kDa centrifugal filter (Amicon Ultra-2 Centrifugal Filter Device,10 kDa, cat# UFC201024). Samples were filtered according to the manufacturer's instructions. Briefly, 2 mL pooled CSF samples were placed in the filter column centrifuged at 4,000 x g for 20 minutes at room temperature (21-22°C). The flow-through was collected and labeled as 10 kDa-filtered sample. Afterwards, the pooled and filtered CSF sample was aliquoted into 1 mL samples that were stored at -20°C until use (within 5 weeks of being filtered).

The day of electrophysiology assays, frozen hypersomnolent CSF samples were thawed on ice. Samples were then spun down in a mini benchtop centrifuge for 30 seconds. Samples were diluted 1:1 in a GABA solution twice the final GABA concentration. For example, 1 mL of CSF was diluted with 1 mL of 10 μM GABA to give final concentrations of 50% CSF and 5 μM GABA. The final sample volume of 50% CSF was 2 mL. The GABA solution was made up in extracellular solution (161 mM NaCl, 3 mM KCl, 1 mM $MgCl_2$, 1.5 mM $CaCl_2$, 10 mM HEPES and 6 mM D-Glucose at pH 7.4 and 320-330 mOsm). The CSF dilution (2 mL volume) was then kept on ice until it was loaded onto the drug infusion pump for the assay. When loaded onto the pump, the CSF sample was

at room temperature and the sample was used up in the assay within 3-4 hours of being loaded onto the pump.

4.2.3 *In vitro* electrophysiology

4.2.3.1: Whole-cell patch clamp recording was performed on HEK293T cells expressing $\alpha_x\beta_2\gamma_{2s}$ $GABA_A$ receptors and GFP, as described in Chapter 2 (Section 2.5). The patch clamp rig used to perform CSF assays was described in Chapter 2.5.2. Before preparing the CSF samples, a brief GABA concentration-response assay was performed (ex. 0.3, 0.5, 1, 3, 5 μM). The data was analyzed from 3-5 cells. Based on the results, a GABA concentration was selected that gave a 10% response of the maximum (defined as an "EC_{10} concentration"). This pre-CSF assay step allowed a more accurate estimation of an EC_{10} GABA concentration for the $\alpha_x\beta_2\gamma_{2s}$ receptors to be used that day. Once an EC_{10} GABA concentration was selected, the CSF sample preparation and experiments were started.

4.2.3.2 CSF potentiation assays: CSF samples were assayed using a similar protocol as described in **Chapter 3.2.3** for midazolam samples. Briefly, CSF samples were thawed for use the day of the recording experiment. CSF samples (2 mL volume) were loaded onto the 2-channel infusion pump in fresh 3mL syringes. Once whole-cell patch was achieved, an EC Protocol (Figure 4.2C) was run with 2 sec exposures to EC_{10} GABA and then 300 μM GABA (maximum). This confirmed that the cell patched had an ~EC_{10} response before testing the CSF sample. Next the CSF assay was run. The CSF assay always began with a control response to 3 sec of EC_{10} GABA. Five seconds of washout occurred between each drug exposure. Then CSF and EC_{10} GABA were co-perfused for 3 seconds before washout (Figure 4.2A-B). The CSF assay always ended with a post-control GABA response to EC_{10} GABA or saturating GABA (300 μM). After the CSF assay was complete, a post-EC Protocol was run to confirm that CSF potentiation was washed

out and that the cell retained an EC_{10} GABA response. See Figure 4.2 for examples of the two CSF protocols used.

4.2.3.3 ECn & CSF assay: Whole-cell current responses were recorded at four different GABA concentrations (10, 30, 100, 300 μM) in the absence and presence of CSF (50% dilution). Each drug exposure was 3 seconds long with 7 seconds of washout in extracellular solution between drug exposures. Drugs were always applied by ascending GABA concentration. Each cell patched was measured at all four GABA concentrations in the presence and absence of CSF.

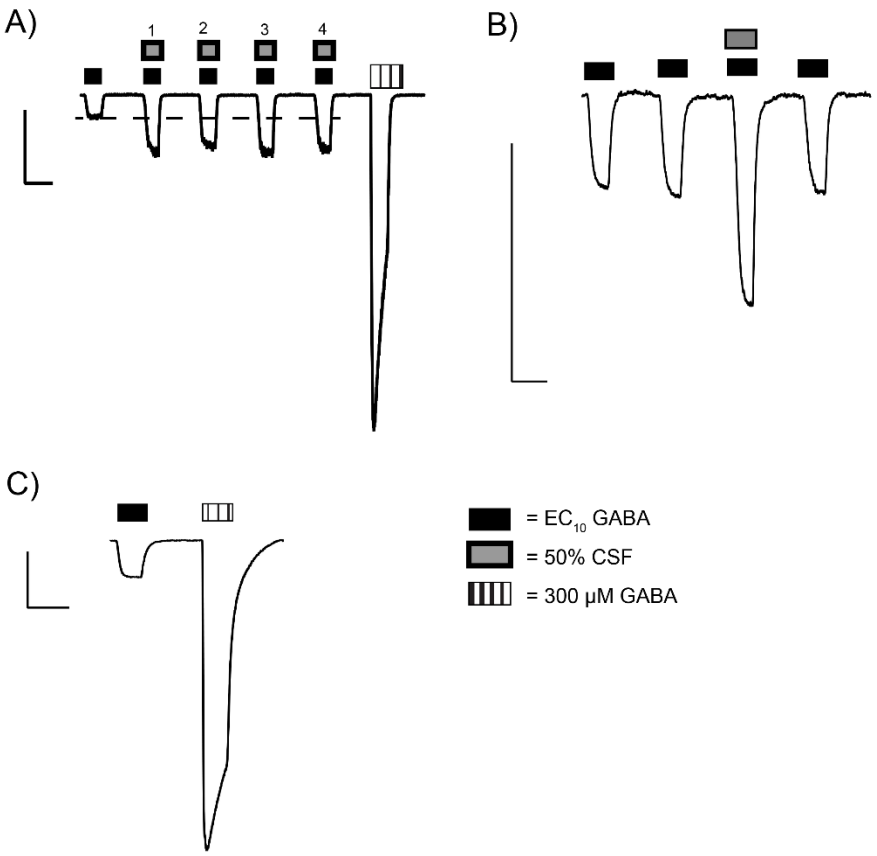

Figure 4.2. Different drug exposure protocols used to measure CSF potentiation depending on the experiment. A) Example whole-cell trace of a protocol used to measure up to 4 different CSF samples. B) Example whole-cell trace of a protocol used to measure the CSF potentiation of pooled CSF for different $\alpha_x\beta_2X$ receptor assemblies. C) Example whole-cell trace of the EC Protocol. This protocol was run before and after ever cell patched and assayed for CSF potentiation. Scale bars: 5 sec, 500pA.

***4.2.4 Whole-Cell Analysis*:** All recordings were baseline corrected and analyzed using MATLAB. Whole-cell peak currents (*I*) were measured from GABA and CSF exposures. CSF potentiation (%) was calculated by the following equation:

$$Pot = (I_{CSF} - I_G)/I_G \, x \, 100\%$$

Where *Pot* was potentiation (%), and I_G and I_{CSF} were the amplitude of peak currents for the EC_{10} GABA and GABA + CSF responses, respectively.

ECn & CSF analysis: Peak currents from each cell for all four GABA concentrations (10, 30, 100, 300) were separated into the control (GABA only) and CSF (GABA + CSF) conditions. The Hill equation was fit twice from the data for one cell. One fit was to the GABA control condition peaks and one fit was to the GABA + CSF condition peaks. The whole-cell peak currents (*I*) were fit using the Hill equation:

$$I = I_{max} * [A]^{nH}/(EC_{50}^{nH} + [A]^{nH})$$

Where *I* was the current peak amplitude recorded, I_{max} was maximum current amplitude, EC_{50} was the half-maximal GABA concentration, *A* was agonist concentration and *nH* was the Hill coefficient. The maximum peak current, EC_{50} and Hill coefficient were estimated for each cell's run.

4.2.4 Statistics

Statistical comparisons of CSF potentiation (%) across receptor conditions (ex. $\alpha_x\beta_2X$ receptors) were evaluated for significant ($p<0.05$) differences using a one-way ANOVA with a Tukey's post-hoc analysis for multiple comparisons. For comparisons of Hill parameters in which there were only two groups (Hill parameters), a paired two-way Student's t-test was performed ($\alpha=0.05$). Statistical analysis was carried out using Prism 7.0 (Graphpad Software, Inc.).

4.3 Results:

4.3.1 Measuring CSF potentiation of $\alpha_1\beta_2\gamma_{2s}$ $GABA_A$ receptors:

Hypersomnolent CSF enhanced the whole-cell current responses of $\alpha_1\beta_2\gamma_{2s}$ $GABA_A$ receptors activated by an EC_{10} GABA concentration (Figure 4.1, 4.2). This enhancement was called potentiation. A 100% potentiation of an EC_{10} GABA response was a doubling in amplitude of the peak current. Whole-cell patch clamp recording of HEK293T cells expressing $\alpha_1\beta_2\gamma_{2s}$ receptors was used to measure the CSF potentiation of 55 patient samples of hypersomnolent CSF (Table 4.1). Hypersomnolent CSF was CSF taken from patients who received a lumbar puncture to better understand the etiology of their sleepiness and who were suspected of having primary idiopathic hypersomnia (IH) (as described in the methods, Chapter 4.2.2).

Different hypersomnolent CSF samples had different degrees of potentiation at $\alpha_1\beta_2\gamma_{2s}$ receptors (Figure 4.2). Across the 55 samples tested (Table 4.1), potentiation measurements ranged from 41-320% with the mean value being 95.6 ± 61.2% (mean ± standard deviation). The standard deviation is shown to highlight the variability within the sample set and how the samples vary from each other. The median value of this dataset was 77.4%.

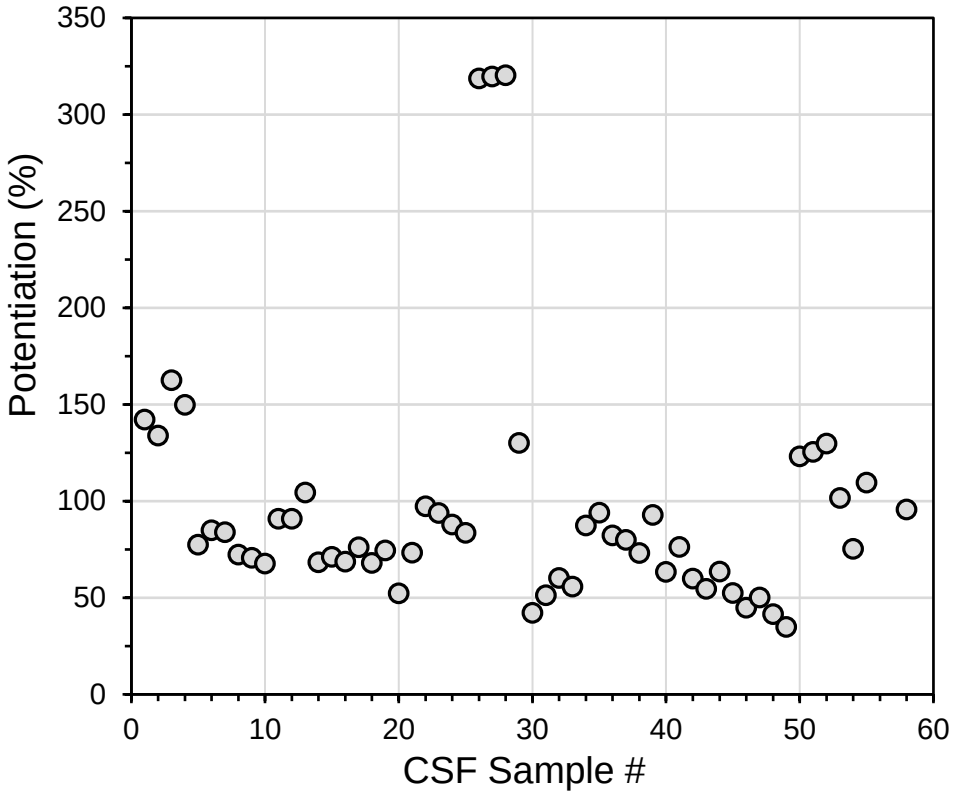

Figure 4.3. Average potentiation (%) of a EC_{10} GABA response by 50% cerebrospinal fluid (CSF) samples from patients with unexplained hypersomnia. CSF sample numbers match the numbers listed in Table 4.1. Measurements were taken using whole-cell patch clamp recording of HEK293T cells expressing $\alpha_1\beta_2\gamma_{2s}$ receptors. Potentiation was calculated as: $Pot = (I_{CSF} - I_G)/I_G \times 100\%$, where *Pot* was potentiation (%), and I_G and I_{CSF} were the amplitude of peak currents for the EC_{10} GABA and GABA + CSF responses, respectively. A 100% potentiation would be a doubling in raw current relative to the GABA control response.

Table 4.1. Average potentiation (%) by CSF samples from patients suspected of having primary idiopathic hypersomnia.

Sample #	CSF Sample Name	Average Potentiation (%)	S.E.M.	StdDev
1	**479 LF**	142.148	16.897	5.974
2	**480 LW**	133.886	38.047	13.452
3	**481 CS**	162.629	43.906	15.523
4	**483 JM**	149.753	32.798	11.596
5	**495 RC**	77.420	21.533	7.178
6	**496 SM**	84.976	22.303	7.434
7	**497 SS**	83.977	26.609	8.870
8	**449 SJ**	72.372	37.504	12.501
9	**535 LC**	70.641	37.590	12.530
10	**536 WB**	67.668	37.724	12.575
11	**488 MB**	90.908	35.083	12.404
12	**490 JL**	90.865	38.904	13.755
13	**492 PW**	104.505	54.416	19.239
14	**498 DN**	68.416	14.362	5.078
15	**499 DB**	71.188	15.114	5.344
16	**500 JK**	68.750	16.425	5.807
17	**501 LC**	76.181	20.019	7.078
18	**502 PF**	68.058	18.474	6.158
19	**503 CS**	74.403	22.997	7.666
20	**504 ZB**	52.200	59.524	19.841
21	**506 DK**	73.231	26.286	8.762
22	**450 JD**	97.309	40.234	13.411
23	**451 JW**	93.909	44.243	14.748
24	**452 JT**	87.809	51.599	17.200
25	**453 ME**	83.534	41.186	13.729
26	**556EK**	318.682	99.898	33.299
27	**554AS***	319.757	98.415	32.805
28	**553CJ***	320.381	82.681	27.560
29	**552HP***	130.183	33.518	11.850
30	**510 LS**	42.184	30.367	10.736
31	**511 JM**	51.364	10.867	3.842
32	**512 WR**	60.247	10.553	3.989
33	**513 NP**	55.735	18.604	7.032
34	**507 EK**	87.324	58.824	20.797
35	**508 RLB**	93.974	55.567	19.646

36	**509 LV**	82.204	48.740	17.232
37	**514 CH**	79.860	42.302	15.989
38	**515 PS**	73.125	40.863	13.621
39	**516 JB**	92.896	36.588	12.196
40	**517 JK**	63.337	24.303	8.592
41	**518 EC**	76.355	34.471	12.187
42	**556 EK**	59.862	23.223	8.211
43	**535 LC**	54.582	22.906	8.098
44	**541 TH**	63.538	25.556	9.659
45	**545 OH**	52.401	26.092	9.862
46	**552 HP***	44.849	8.929	3.157
47	**553 CJ***	50.056	17.499	6.187
48	**554 AS***	41.488	19.877	7.513
49	**521 KP**	34.859	50.340	16.780
50	**351 IM**	123.200	48.834	17.265
51	**519 BF**	125.397	50.952	18.014
52	**547 WK**	129.788	57.280	21.650
53	**560 JI**	101.607	44.332	15.674
54	**OM011**	75.34	24.61	8.20
55	**Pool C_{om}**	109.5	63.38	13.22
	AVERAGE	**95.651**	**61.211**	**8.254**

Table 4.1. Average potentiation (%) of a EC_{10} GABA response by 50% dilution of cerebrospinal fluid (CSF) samples from patients having unexplained hypersomnia. CSF sample numbers match the sample numbers in Figure 4.3. CSF potentiation measured using whole-cell patch clamp recording of HEK293T cells expressing $\alpha_1\beta_2\gamma_{2s}$ receptors. *Denotes samples that were run multiple times from different frozen CSF samples. Pool C_{om} was the pooled CSF sample from five patient samples (453 ME, 459 MM, 474 BC, 477 DG, 503 CS) and used for experiments in Section 4.3.2 and 4.3.3. S.E.M. = standard error of the mean. StdDev = standard deviation.

4.3.2 Ruling out the high-affinity benzodiazepine binding site as a site of action

If the endogenous peptide in hypersomnolent CSF acted through the high-affinity benzodiazepine binding site on $GABA_A$ receptors, then a specific pattern of potentiation would be expected across benzodiazepine sensitive-/insensitive- $\alpha_x\beta_2\gamma_{2s}$ receptor assemblies. The degree of CSF potentiation was measured using a pooled sample of hypersomnolent CSF (Pool C_{om}). Three different mutations within the high-affinity benzodiazepine binding site were also tested (α_1(H102R), α_1(S206) and α_4(R100H)). The receptor assemblies tested that previously showed potentiation by midazolam were $\alpha_1\beta_2\gamma_{2s}$, α_4(R100H)$\beta_2\gamma_{2s}$ and α_1(S206I)$\beta_2\gamma_{2s}$ (Chapter 3.3). These were predicted to show CSF potentiation. The receptors tested that were insensitive to midazolam were $\alpha_1\beta_2$, α_1(H102R)$\beta_2\gamma_{2s}$, and $\alpha_4\beta_2\gamma_{2s}$ receptors. These receptors were predicted to show no CSF potentiation. Overall, all receptor assemblies ($\alpha_1\beta_2\gamma_{2s}$, α_4(R100H)$\beta_2\gamma_{2s}$ α_1(S206I)$\beta_2\gamma_{2s}$, α_1(H102R)$\beta_2\gamma_{2s}$, α_1(S206)$\beta_2\gamma_{2s}$, and α_4(R100H)$\beta_2\gamma_{2s}$) showed CSF potentiation that was reversible and washed out rapidly (Figure 4.4).

The average CSF potentiation measured across all receptor conditions ($\alpha_1\beta_2\gamma_{2s}$, α_4(R100H)$\beta_2\gamma_{2s}$, α_1(S206I)$\beta_2\gamma_{2s}$, $\alpha_1\beta_2$, α_1(H102R)$\beta_2\gamma_{2s}$, and $\alpha_4\beta_2\gamma_{2s}$) ranged from 79-143% (Figure 4.5, Table 4.2). The average CSF potentiation of $GABA_A$ receptor assemblies sensitive to midazolam was 109.5 ± 13.2% ($\alpha_1\beta_2\gamma_{2s}$, n=23), n=22), 79.7 ±5.5% (α_1(S206I)$\beta_2\gamma_{2s}$), and 143.6 ± 8.2% (α_4(R100H)$\beta_2\gamma_{2s}$, n=14). The average CSF potentiation of receptors normally insensitive to midazolam was 100.2 ± 18.6% ($\alpha_1\beta_2$, n=12), 117.7 ± 5.9% (α_1(H102R)$\beta_2\gamma_{2s}$, n=17) and 136.4 ± 14.4% ($\alpha_4\beta_2\gamma_{2s}$, n=16). A one-way ANOVA test revealed a significant difference in the degree of potentiation measured across receptor assemblies ($F(5, 98) = 3.842$, $p=0.0032$). A Tukey's post-hoc test for multiple comparisons revealed a significant ($p<0.05$) difference between α_1(S206I)$\beta_2\gamma_{2s}$ and $\alpha_4\beta_2\gamma_{2s}$ ($p=0.0111$), and also between α_1(S206I)$\beta_2\gamma_{2s}$ and α_4(R100H)$\beta_2\gamma_{2s}$ ($p=0.0048$). Although significant, the

comparisons to $\alpha_1(S206I)\beta_2\gamma_{2s}$ and $\alpha_4(R100H)\beta_2\gamma_{2s}$ would have little physiological relevance to the natural brain because these combinations do not exist naturally.

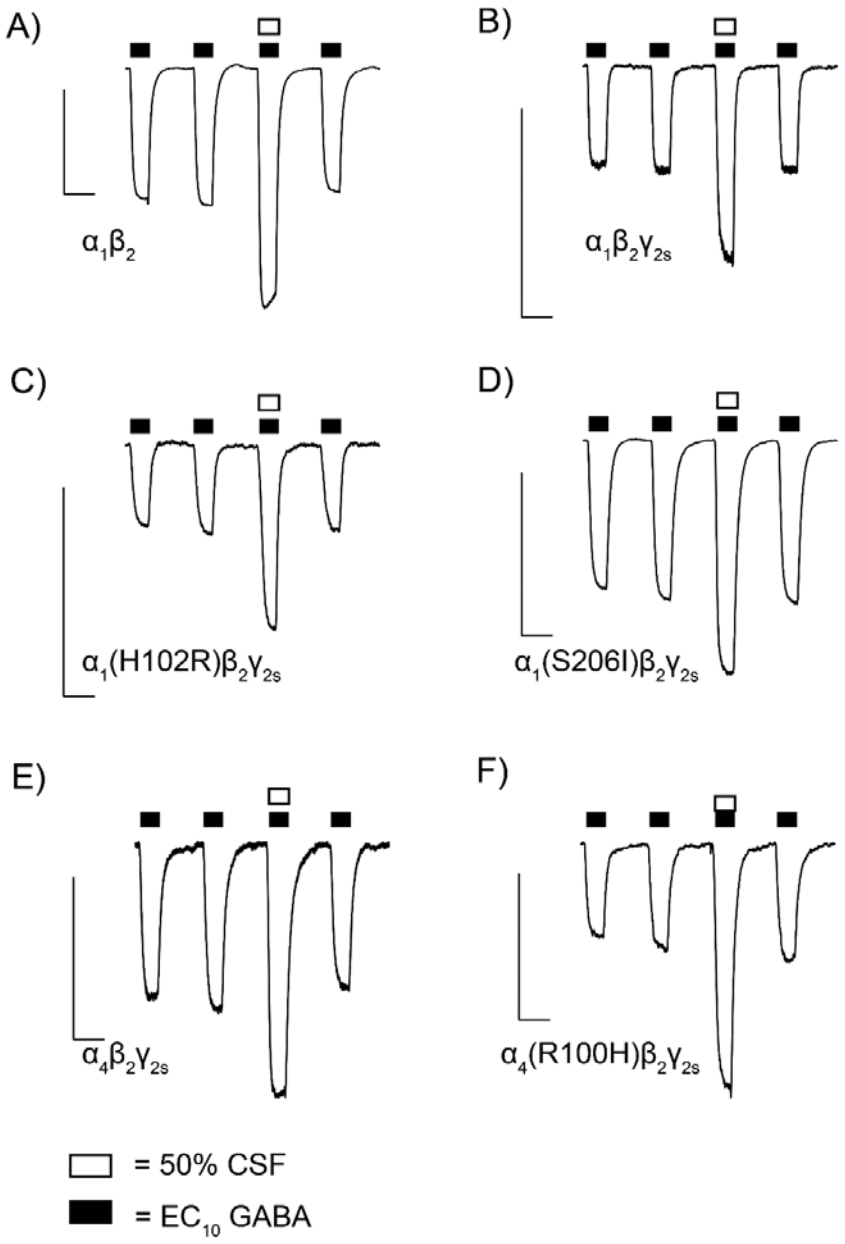

Figure 4.4. Example traces of pooled CSF potentiating EC_{10} GABA-evoked responses for receptor conditions that previously showed differing responses to midazolam. Whole-cell patch clamp recordings from HEK293T cells expressing human $GABA_A$ receptors: A) $\alpha_1\beta_2$, B) $\alpha_1\beta_2\gamma_{2s}$, C) α_1(H102R)$\beta_2\gamma_{2s}$, D) α_1(S206I)$\beta_2\gamma_{2s}$, E) $\alpha_4\beta_2\gamma_{2s}$, F) α_4(R100H)$\beta_2\gamma_{2s}$. Scale bars are 5 sec, 500pA. Pooled CSF (Pool C_{om}) was a 50% dilution and consisted of five CSF samples: 453 ME, 459 MM, 474 BC, 477 DG, and 503 CS.

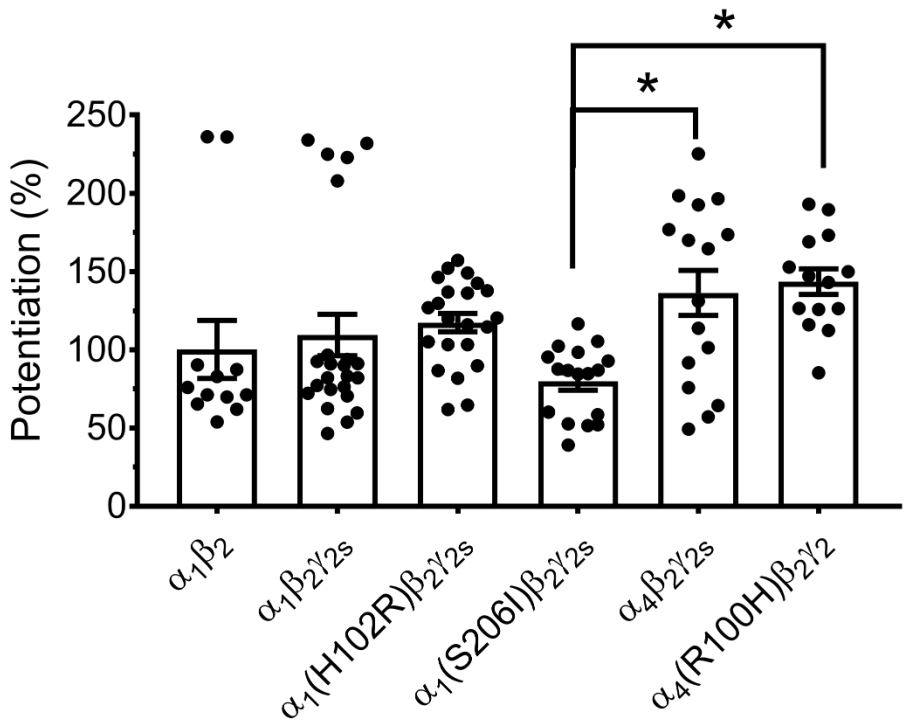

Figure 4.5. Percent of potentiation (%) evoked by pooled CSF for receptor conditions normally showing discriminating responses for midazolam. Potentiation was the degree of enhancement of an EC_{10} GABA response. Bars are mean ± S.E.M. Individual dots are separate runs from 6-12 cells per group. A one-way ANOVA test ($F(5, 98) = 3.842$, $p=0.0032$) revealed a significant difference across groups in the average potentiation measured. A Tukey's post hoc test for multiple comparisons revealed two significant ($p<0.05$, *) differences. Means ± SEM: $\alpha_1\beta_2$: 100.2 ± 18.6% (n=12), $\alpha_1\beta_2\gamma_2$s: 109.5 ± 13.2% (n=23), α_1(H102R)$\beta_2\gamma_2$s: 117.7 ± 5.9% (n=22), α_1(S206I)$\beta_2\gamma_2$s: 79.7 ±5.5% (n=17), $\alpha_4\beta_2\gamma_{2s}$: 136.4 ± 14.4% (n=16), α_4(R100H)$\beta_2\gamma_2$s: 143.6 ± 8.2% (n=14). Pooled CSF (Pool C_{om}) was a 50% dilution and consisted of five CSF samples: 453 ME, 459 MM, 474 BC, 477 DG, and 503 CS.

4.3.3 Alpha- and Delta- subunit specificity of CSF potentiation

Pooled CSF (Pool C_{om}) was also used to measure the $GABA_A$ subunit specificity of CSF potentiation at different receptor combinations (α1-6 and δ). First, the α subunit specificity across the six α isoforms was measured at $\alpha_x\beta_2\gamma_{2s}$ receptors (Figure 4.6A-F). Second, the degree of CSF potentiation at δ-containing $\alpha_x\beta_2\delta$ receptor assemblies was measured (Figure 4.6G-H).

The α subunit affected the degree of CSF potentiation measured. The CSF potentiation for α1-6-containing $\alpha_x\beta_2\gamma_{2s}$ receptors from smallest to largest potentiation was: α1 < α4 < α3 < α5 < α2 < α6. The average potentiation measured was 109.5 ± 13.22 ($\alpha_1\beta_2\gamma_{2s}$, n=23), 129.8 ± 9.74 ($\alpha_4\beta_2\gamma_{2s}$, n=24), 133.6 ± 8.67 ($\alpha_3\beta_2\gamma_{2s}$, n=23), 156.6 ± 14.8 ($\alpha_5\beta_2\gamma_{2s}$, n=18), 171.7 ± 12.03 ($\alpha_2\beta_2\gamma_{2s}$, n=17) and 207.8 ± 16.94 ($\alpha_6\beta_2\gamma_{2s}$, n=19) (Table 4.2). A one-way ANOVA test revealed a significant difference in the degree of potentiation measured across groups ($F(5, 118) = 7.736$, $p<0.0001$). A Tukey's post-hoc test for multiple comparisons revealed several significant (*$p<0.05$) differences (Figure 4.7). The $\alpha_1\beta_2\gamma_{2s}$ receptors showed significantly less potentiation than $\alpha_2\beta_2\gamma_{2s}$ and $\alpha_6\beta_2\gamma_{2s}$ receptors. The $\alpha_6\beta_2\gamma_{2s}$ receptors showed significantly higher potentiation than $\alpha_3\beta_2\gamma_{2s}$ and $\alpha_4\beta_2\gamma_{2s}$ receptors.

The δ-containing receptors, normally found extrasynaptically, both showed large degrees of CSF potentiation (Figure 4.8). The $\alpha_4\beta_2\delta$ receptors showed 360.3 ± 21.80% potentiation (n=21). The $\alpha_6\beta_2\delta$ receptors showed 193.6 ± 7.49% (n=15) potentiation. The $\alpha_4\beta_2\delta$ receptors had the largest percent of CSF potentiation overall, but the raw current amplitudes were relatively small (-51.1 ± 5.19 pA for EC_{10} GABA). The average EC value of cells patched with $\alpha_4\beta_2\delta$ receptors was 8.8 (~EC_9). All values above are mean ± SEM.

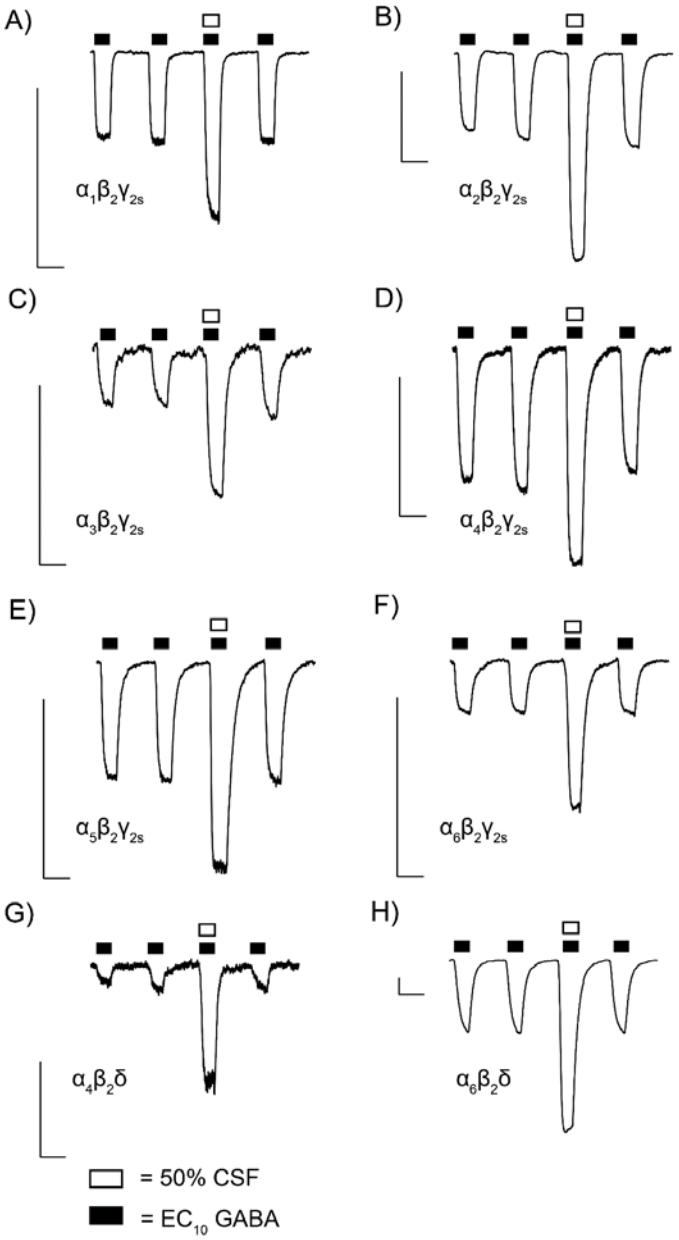

Figure 4.6. Example traces of pooled CSF (Pool C_{om}) potentiating EC_{10} GABA-evoked responses for $\alpha_x\beta_2\gamma_{2s}$ and $\alpha_x\beta_2\delta$ receptors. Recordings were made using whole-cell patch clamp recording of HEK293T cells expressing human $GABA_A$ receptors: A) $\alpha_1\beta_2\gamma_{2s}$, B) $\alpha_2\beta_2\gamma_{2s}$, C) $\alpha_3\beta_2\gamma_{2s}$, D) $\alpha_4\beta_2\gamma_{2s}$, E) $\alpha_5\beta_2\gamma_{2s}$, F) $\alpha_6\beta_2\gamma_{2s}$, G) $\alpha_4\beta_2\delta$, and H) $\alpha_6\beta_2\delta$. Scale bars are 5 sec, 500pA. Pooled CSF (Pool C_{om}) was a 50% dilution and consisted of five CSF samples: 453 ME, 459 MM, 474 BC, 477 DG, and 503 CS.

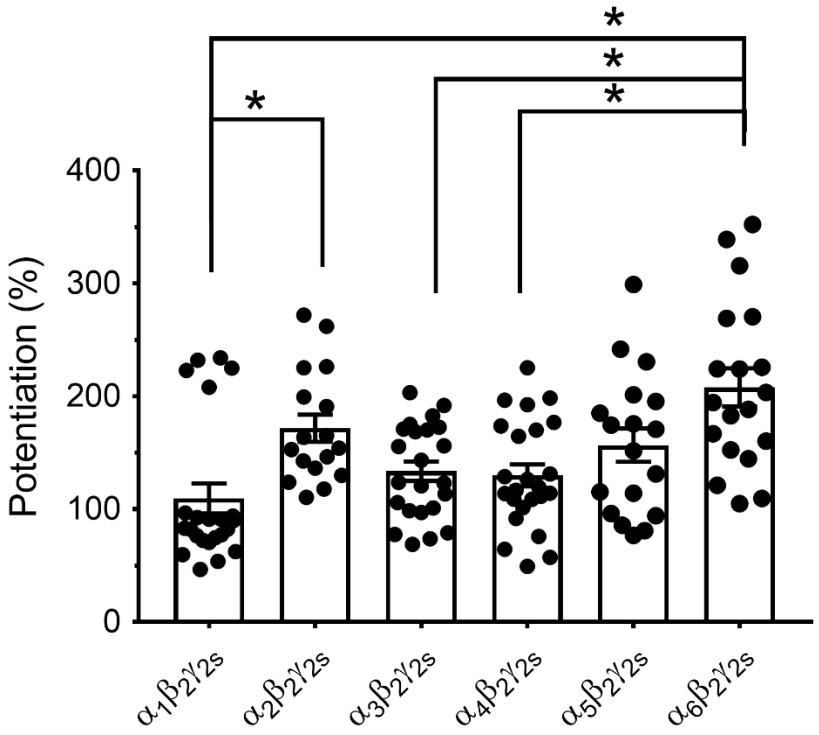

Figure 4.7. The α subunit specificity of potentiation (%) evoked by pooled CSF (Pool C_{om}) for $\alpha_x\beta_2\gamma_{2s}$. Potentiation was the degree of enhancement of an EC_{10} GABA response. A one-way ANOVA test revealed a significant difference in potentiation across groups ($F(5, 118) = 7.736$, $p<0.0001$). A Tukey's post hoc test for multiple comparisons revealed several significant (*$p<0.05$) differences. Bars are mean ± S.E.M. Individual dots are separate replicates from 9-12 cells per group. Pooled CSF (Pool C_{om}) was a 50% dilution and consisted of five CSF samples: 453 ME, 459 MM, 474 BC, 477 DG, and 503 CS.

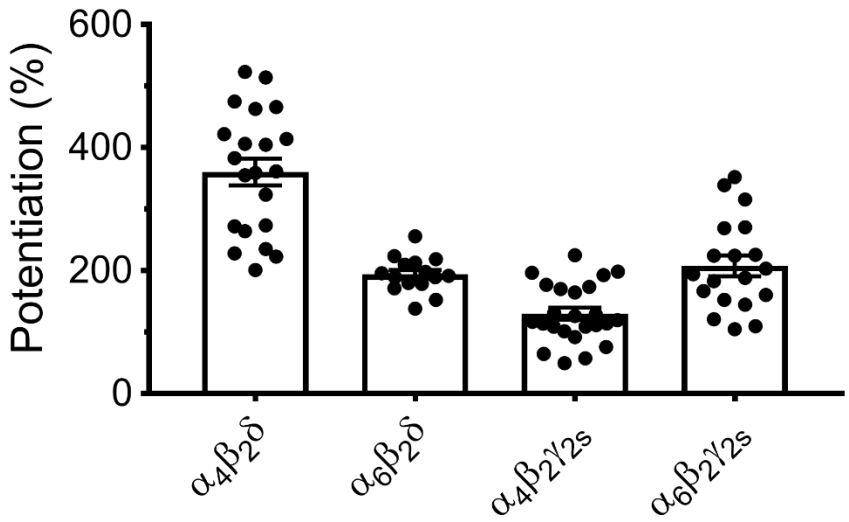

Figure 4.8. The γ and δ subunit specificity of potentiation (%) evoked by pooled CSF (Pool C_{om}) for $\alpha_x\beta_2X$ receptors. Potentiation was the degree of enhancement of an EC_{10} GABA response. Bars are mean ± S.E.M. Individual dots are separate replicates from 7-12 cells per group. Pooled CSF (Pool C_{om}) was a 50% dilution and consisted of five CSF samples: 453 ME, 459 MM, 474 BC, 477 DG, and 503 CS.

Table 4.2. Whole-cell measurements for pooled CSF potentiation

Receptor	Average potentiation (raw current, pA)	Average potentiation % (% of EC_{10} GABA)	N recordings (# cells)	EC_{10} [GABA] μM
$\alpha_1\beta_2$	-842.4 ± 452.5	100.2 ± 18.56	12 (6)	4-5
$\alpha_1\beta_2\gamma_{2s}$	-671.7 ± 56.15	109.5 ± 13.22	23 (12)	4
α_1(H102R)$\beta_2\gamma_{2s}$	-503.2 ± 182.63	117.4 ± 5.90	22 (11)	5
α_1(S206I)$\beta_2\gamma_{2s}$	-734.6 ± 149.84	79.7 ± 5.52	17 (9)	4
$\alpha_2\beta_2\gamma_{2s}$	-977.6 ± 66.76	171.7 ± 12.03	17(10)	0.3
$\alpha_3\beta_2\gamma_{2s}$	-544.1 ± 39.06	133.6 ± 8.67	23 (11)	0.5-0.8
$\alpha_4\beta_2\gamma_{2s}$	-646.3 ± 68.64	129.8 ± 9.74	24 (12)	0.2-0.3
α_4(R100H)$\beta_2\gamma_{2s}$	-589.1 ± 69.77	143.6 ± 8.21	14 (7)	0.25
$\alpha_5\beta_2\gamma_{2s}$	-798.7 ± 152.10	156.6 ± 14.8	18 (9)	0.15-0.2
$\alpha_6\beta_2\gamma_{2s}$	-761.5 ± 81.56	207.8 ± 16.94	19 (10)	0.05-0.15
$\alpha_4\beta_2\delta$	-218.2 ± 28.23	360.3 ± 21.80	21 (11)	0.05-0.1
$\alpha_6\beta_2\delta$	-1100 ± 99.0	193.6 ± 7.49	15 (7)	0.1

Table 4.2. Raw current and percent of potentiation of EC_{10} GABA responses measured at $\alpha_x\beta_2X$ receptors using pooled hypersomnolent CSF (Pool C_{om}). Whole-cell measurements were take using patch clamp recording of HEK293T cells expressing the specified $GABA_A$ receptors. Raw potentiation was the peak current response measured in the presence of EC_{10} GABA + 50% CSF. The percent of potentiation was calculated by: $Pot = (I_{CSF} - I_G)/I_G \times 100\%$, where *Pot* was potentiation (%), and I_G and I_{CSF} were the amplitude of peak currents for the EC_{10} GABA and GABA + CSF responses, respectively. Sample sizes are listed with the number of cells in parentheses. Potentiation values are mean ± S.E.M. Pooled CSF (Pool C_{om}) was a 50% dilution and consisted of five CSF samples: 453 ME, 459 MM, 474 BC, 477 DG, and 503 CS.

4.3.4 CSF shifts GABA concentration-response curve leftwards

Although the hypersomnolent CSF was known to potentiate the whole-cell currents of $\alpha_1\beta_2\gamma_{2s}$ $GABA_A$ receptors, it had not previously been shown directly that CSF potentiation directly depends on the underlying GABA concentration. To better understand how CSF enhances $GABA_A$ receptor activity, a GABA concentration-response assay was carried out in the presence and absence of hypersomnolent CSF. A single hypersomnolent CSF sample was used (562 RM) for all whole-cell measurements at 10, 30, 100 and 300 µM GABA. Each patched cell was measured at all four GABA concentrations in the presence and absence of CSF (n=7 cells, 9 recordings). As with other positive allosteric modulators, the percent of potentiation measured with CSF decreased as the GABA concentration increased (Figure 4.9A). At saturating GABA concentrations, the whole-cell peak currents desensitized quickly and likely were an underestimation of the peak response for that GABA concentration (Figure 4.9B). As a result, the potentiation calculated for these peaks was dramatically reduced to 0.366 ± 6.509% (100 µM GABA) and -11.74 ±4.145% (300 µM GABA).

All whole-cell currents evoked by 10, 30, 100 and 300 µM GABA in the presence and absence of CSF were normalized to the peak current evoked by 300 µM GABA. Then raw current points were plotted on a semi-logarithmic scale and each condition (GABA or GABA + CSF) fit to the Hill equation. The GABA concentration-response relationship was shifted leftwards in the presence of hypersomnolent CSF (Figure 4.9C). The presence of CSF significantly decreased the maximum current evoked (GABA: -3078.8 ± 397.1 pA; GABA + CSF: -2520.3 ± 378.2 pA, t=0.3704, *p*=0.006). There was no significant change in the Hill coefficient (GABA: 1.184 ± 0.118; GABA + CSF: 1.226 ± 0.080, t=0.5711 *p*=0.5836). Hypersomnolent CSF significantly decreased the EC_{50} for GABA (GABA: 66.74 ± 14.63 µM; GABA + CSF: 31.19 ± 5.34 µM; t=2.8424, *p*=0.0224). Overall, these

results confirmed that hypersomnolent CSF increases the apparent-affinity of GABA. Also, measuring potentiation at saturating GABA concentrations can result in measuring CSF-mediated inhibition.

To further examine the above GABA concentration-dependence of CSF potentiation, I examined the CSF potentiation measurements taken from the larger CSF dataset listed in Table 4.1. To confirm that the GABA concentration affected the degree of potentiation measured with hypersomnolent CSF for the other individual patient CSF samples, the EC value of the patched cell was plotted against the potentiation measured. The EC value of a patched cell was the percent of the maximum current response that the specific GABA concentration evoked. Data was plotted for all individual recordings taken from each CSF sample (generally 5-10 recordings per CSF sample). All 437 measurements were plotted (Figure 4.10) and a linear regression line fit. The average EC value of patched cells was 14.4 ± 7.5 (mean ± standard deviation). The average potentiation measured was 95.1 ± 61.2% (mean ± standard deviation). Overall, the CSF potentiation measured decreased slightly as the EC value of the patched cell increased ($y = -2.4584x + 132.62$ and $R^2 = 0.061$). This was consistent with the potentiation data above using a single CSF sample at multiple GABA concentrations.

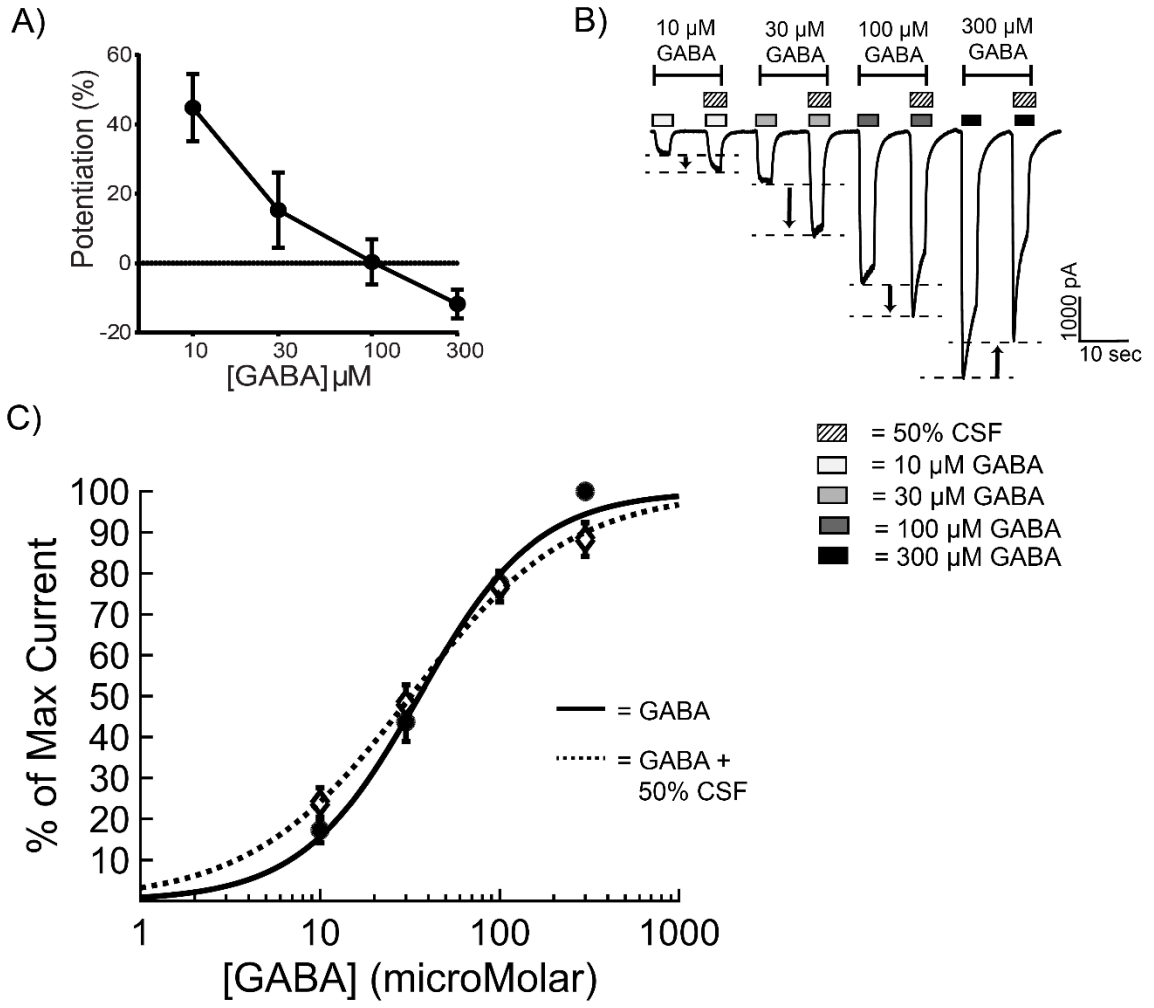

Figure 4.9. Hypersomnolent CSF potentiation (%) of GABA-evoked responses depended on the GABA concentration used. A) The average potentiation (%) of 50% CSF at different GABA concentrations (10, 30, 100 and 300µM). B) Example responses for GABA and GABA + 50% diluted CSF at 10, 30, 100 and 300 µM. Measurements were performed using whole-cell patch clamp recording of HEK293T cells expressing $\alpha_1\beta_2\gamma_{2s}$ receptors. C) Concentration-response curves plotted for the GABA only (solid line, circles) and GABA +50% CSF (dotted line, open diamonds) average responses. Points are mean ± S.E.M. The CSF sample (562 RM) was from a patient suspected of having Idiopathic Hypersomnia.

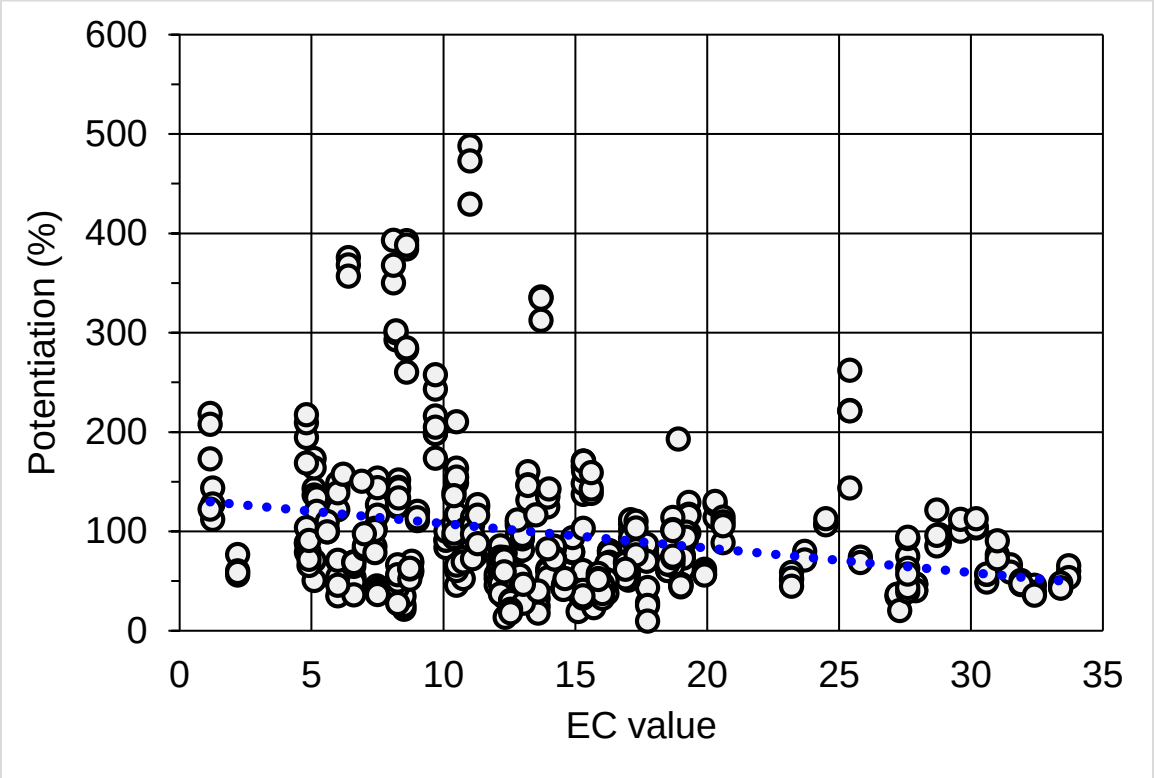

Figure 4.10. EC value of the patched cell compared to the degree of potentiation (%) measured. The dotted blue line is a linear regression showing that as EC value increased, the degree of potentiation measured decreased. The equation of the line is y = -2.4584x + 132.62 and R^2 = 0.061. Measurements taken using whole-cell patch clamp recording of HEK293T cells expressing $\alpha_1\beta_2\gamma_{2s}$ receptors. Data from all single CSF recordings collected from 53 of the CSF samples assayed. A CSF recording consisted of at least one control GABA response, GABA + CSF response and a maximum GABA response. Each dot represents a single recording. Most CSF samples consisted of 8-10 recordings per experiment from 3-5 different cells.

4.4 Discussion

The exact mechanism by which hypersomnolent CSF enhances $GABA_A$ receptor activity remains unknown. This is not due to a lack of evidence, but instead reflects the complexities of studying idiopathic hypersomnia, CSF and sleep. Originally, it was proposed that a small endogenous peptide in the CSF of patients with idiopathic hypersomnia bound the high-affinity benzodiazepine site to enhance receptor activity. The rationale for the experiments in this chapter was that expanding our knowledge of the $GABA_A$ receptor's subunit-specificity for hypersomnolent CSF will inform which known modulatory sites on the $GABA_A$ receptor may be responsible for CSF's PAM actions. Results here show that hypersomnolent CSF potentiates a wide range of $GABA_A$ receptor assemblies, including those that normally do not respond to benzodiazepines. These results highlight the complexity of CSF's actions on $GABA_A$ receptors but also potential overlap this topic may have with many other exciting research areas. The results and their implications are discussed below.

The first set of experiments were performed to determine the role of the high-affinity benzodiazepine site in hypersomnolent CSF's actions. Pooled hypersomnolent CSF that was filtered through a 10 kDa filter was used to measure the potentiation of $GABA_A$ receptors' activity. I measured the CSF potentiation at specific $GABA_A$ receptor assemblies that have either a functional or non-functional high-affinity benzodiazepine site. The high-affinity benzodiazepine site requires both an α and γ subunit to form the pocket (Cromer et al., 2002). $GABA_A$ receptors containing a δ, α4 or α6 are generally insensitive to positive benzodiazepines, as shown with midazolam in Chapter 3. The $\alpha_1\beta_2\gamma_{2s}$ contain a functional high-affinity benzodiazepine site. The α_4(R100H)$\beta_2\gamma_{2s}$ receptors have a mutation that makes them responsive to midazolam (Chapter 3.3) and diazepam (Benson et al., 1998). The receptor assemblies that lack a functional high-affinity benzodiazepine site include $\alpha_1\beta_2$, α_1(H102R)$\beta_2\gamma_{2s}$ and $\alpha_4\beta_2\gamma_{2s}$. My results showed

robust CSF potentiation at $\alpha_1\beta_2\gamma_{2s}$, $\alpha_1\beta_2$, α_1(H102R)$\beta_2\gamma_{2s}$, α_4(R100H)$\beta_2\gamma_{2s}$, and $\alpha_4\beta_2\gamma_{2s}$ receptors. The average CSF potentiation measured across the above-mentioned receptor assemblies ranged from 79-143% (Table 4.2). Specifically, the receptors that normally do not respond to benzodiazepines (α_1(H102R)$\beta_2\gamma_{2s}$, $\alpha_4\beta_2\gamma_{2s}$ and $\alpha_1\beta_2$ receptors) all showed over 100% potentiation by hypersomnolent CSF. These results suggest a mechanism of action not purely acting through the high-affinity benzodiazepine site to explain the actions of the endogenous peptide found in CSF. In the following paragraphs, I will explain how my data supports a non-benzodiazepine site theory in the context of previous data.

Two important differences between the CSF results presented here and those in the Rye, *et al.,* 2012 paper can be explained by the following. First, the high degree of CSF potentiation I measured at α_1(H102R)$\beta_2\gamma_{2s}$ receptors (~117%) is not completely contradictory to the approximately 72% potentiation measured by Rye, *et al.,* 2012. The 2012 results showed that the α_1(H102R) mutation incompletely inhibited CSF potentiation by ~61% of the original potentiation measured at wildtype receptors (Rye et al., 2012). This suggests that the endogenous peptide does not act singularly through the high-affinity benzodiazepine site, a result consistent with data presented here. Second, I measured robust CSF potentiation (~130%) from $\alpha_4\beta_2\gamma_{2s}$ receptors, while previous data from the paper in 2012 measured only 0.20 ± 14.5% potentiation (Rye et al., 2012). As mentioned earlier, the control GABA concentration used to evoke GABA responses critically determines the range of receptor activation within which one can measure potentiation. If a close to saturating GABA concentration was used then a ceiling effect would prevent any further potentiation of activity from being measured (Moody et al., 2017). Previous CSF measurements at $\alpha_4\beta_2\gamma_{2s}$ receptors used a 2 μM GABA concentration. This concentration may have evoked a response closer to the EC_{50} response and could have obscured any potentiation evoked by hypersomnolent CSF. The present CSF results used 0.2-0.3 μM GABA which is well below the EC_{50} of $\alpha_4\beta_2\gamma_{2s}$ receptors (EC_{50} of $\alpha_4\beta_2\gamma_{2s}$ is ~3

μM; Table 3.1) and gave a ~EC_{10} response. The CSF assays performed here on $\alpha_4\beta_2\gamma_{2s}$ receptors also measured responses from 12 different HEK293T cells from two different transfections in two different months. The average potentiation measured from the two different experiments was relatively similar (136 ± 57% and 116 ± 8%). As a final explanation about the $_4\beta_2\gamma_{2s}$ data, the CSF samples used for this study and the one in 2012 were different samples from different patients and so may have had different levels of peptide in them.

Two other pieces of evidence that strongly suggest that the peptide in hypersomnolent CSF may not act primarily through the high-affinity benzodiazepine site are these. First, the potentiation seen at $\alpha_1\beta_2$ vs. the $\alpha_1\beta_2\gamma_{2s}$ receptors provides strong evidence for a non-benzodiazepine site of action. As mentioned previously, the high-affinity benzodiazepine site requires a γ subunit be expressed (Pritchett, Luddens, et al., 1989; Pritchett, Sontheimer, et al., 1989). When assayed in another lab's *in vitro* system (J.W. Lynch lab, The University of Queensland Brisbane, Australia), the hypersomnolent CSF samples had highly correlated degrees of potentiation between the $\alpha_1\beta_2$ receptors compared to those measured at $\alpha_1\beta_2\gamma_{2s}$ receptors in the Jenkins lab (Moody et al., 2017). This is consistent with the γ subunit not being necessary for CSF potentiation. The γ subunit is necessary for benzodiazepine's actions at $GABA_A$ receptors (Pritchett, Sontheimer, et al., 1989). The second piece of evidence supporting a non-benzodiazepines site theory is based on the previous ligand binding assays. Previous ligand binding assays using four individual IH patient CSF samples found that [^{3}H]-flumazenil was not displaced by CSF in binding assays using human cortex tissue samples (Rye et al., 2012). This again suggested that although clinically flumazenil worked in a subset of patients, at the molecular level it might not be acting through the traditional high-affinity benzodiazepine site on the $GABA_A$ receptor. Together, the past and present data suggest that the CSF potentiation needs to be further explored at other $GABA_A$

receptor assemblies to better understand which receptors might contribute to a systemic or behavioral effect of sleepiness.

Next, to evaluate the subunit specificity of hypersomnolent CSF potentiation, different $GABA_A$ receptor assemblies were tested using the same pooled hypersomnolent CSF sample as above. First, the α-specificity of CSF potentiation was tested using $\alpha_x\beta_2\gamma_{2s}$ receptors. The rank-order of CSF potentiation by α subunit expressed was α1 < α4 < α3 < α5 < α2 < α6 (potentiation ranging from 109 to 207%; Table 4.2). The increased sensitivity of $\alpha_2\beta_2\gamma_{2s}$ compared to $\alpha_1\beta_2\gamma_{2s}$ receptors was consistent with past data (Rye et al., 2012). The rank-order for all six α subunits was not consistent with the general order of midazolam's efficacy based on α subunit (α5 < α2 < α1 < α3, Figure 3.17). Second, CSF potentiation was measured at $\alpha_4\beta_2\delta$ and $\alpha_6\beta_2\delta$ receptors, both of which showed dramatic levels of potentiation (Table 4.2). The δ-containing $GABA_A$ receptors are generally found perisynaptically or extrasynaptically, as are $\alpha_5\beta_x\gamma_2$ receptors (Farrant & Nusser, 2005). Normally, δ-containing extrasynaptic $GABA_A$ receptors are not responsive to diazepam or midazolam. Together, this data suggests that the endogenous component of CSF enhancing $GABA_A$ receptor activity may be affecting both synaptic and tonic inhibition levels in the brain.

"Endozepine" is a term referring to the search for the endogenous modulator that acts through the benzodiazepine site on $GABA_A$ receptors. Endozepines are thought to be endogenous benzodiazepines that positively modulate $GABA_A$ receptors (Rothstein et al., 1992). Over the years there have been multiple molecules studied for their potential role as "endozepines", including oleamides, diazepine binding inhibitor, endozepine-2 and endozepine-4 (see Introduction 1.4.2 for detailed discussion) (Farzampour et al., 2015; Granot et al., 2004; Rothstein et al., 1992). Results presented here have ruled out the high-affinity benzodiazepine site as the primary site of action for hypersomnolent CSF.

Based on these results, the term “endozepine” may not be an appropriate term for the active component being studied here from hypersomnolent CSF samples.

There is also low-affinity benzodiazepine site on $GABA_A$ receptors mediating the PAM actions of diazepam at higher concentrations (30-100 μM). It is predicted to be in the transmembrane domain of the α+/β- interface on the $GABA_A$ receptor (Walters et al., 2000). It is unlikely that the active component of hypersomnolent CSF examined here acts at this separate low-affinity benzodiazepine site. The reason for this is based on previous results using flumazenil. Flumazenil was previously shown to inhibit CSF potentiation at $GABA_A$ receptors (Rye et al., 2012). However, other studies have shown that flumazenil does not block benzodiazepine’s PAM actions at the secondary low-affinity benzodiazepine site (Walters et al., 2000; D. S. Wang et al., 2003). Therefore, the inhibitory molecular actions of flumazenil on CSF modulation are also not likely to be a result of flumazenil blocking a modulator acting through the low-affinity benzodiazepine site. The arousal clinical effects produced by flumazenil in IH patients are most likely due to flumazenil’s actions at another molecular site on the $GABA_A$ receptor or another receptor in the brain. For example, flumazenil has been shown to block the hypnotic effects of low doses of the general anesthetic propofol (Tung, Bluhm, & Mendelson, 2001), a PAM than binds the a site in the transmembrane domain of the β $GABA_A$ receptor subunit (Krasowski et al., 2001). Other known modulator sites on the $GABA_A$ receptor include those for etomidate, ethanol, isoflurane and barbiturates (see Figure 1.3 for binding sites). Further studies of the PAM actions of hypersomnolent CSF on $GABA_A$ receptors should consider investigating the role of other modulator sites on $GABA_A$ receptors.

The high levels of potentiation (>100%) measured at $\alpha_5\beta_2\gamma_{2s}$, $\alpha_4\beta_2\delta$ and $\alpha_6\beta_2\delta$ receptors suggest that endogenous PAMs of extrasynaptic $GABA_A$ receptors may be a good next candidate to consider. The $GABA_A$ receptor system is known to interact with the neurosteroids and hormone systems. Progesterone and its neuroactive metabolites

(5α-pregnanolone and 5β-pregnanolone) are known to allosterically modulate $GABA_A$ receptors and are have hypnotic effects clinically (Lancel, Faulhaber, Holsboer, & Rupprecht, 1996). Allopregnanolone (5β-pregnan-3α-ol-20-one), a neuroactive metabolite of progesterone, is known to potentiate extrasynaptic $GABA_A$ receptors (Carver & Reddy, 2016; P. Li et al., 2014) and can alter the expression of the α4 subunit (Sundstrom-Poromaa et al., 2002; Sundstrom Poromaa, Smith, & Gulinello, 2003). Changes in $GABA_A$ receptors have also been linked to certain conditions in which hormone levels are altered. In premenstrual dysphoric disorder, altered $GABA_A$ receptor function and reduced sensitivity to benzodiazepines has been shown (Sundstrom, Ashbrook, & Backstrom, 1997). Given that many of the patients with IH are women (Rye et al., 2012; Trotti et al., 2014), a renewed look at endogenous hormone levels in hypersomnia patients may offer new directions to look for $GABA_A$ receptor PAMs found in CSF. An extension of this would be to re-analyze hypersomnolent CSF samples for levels of endogenous neurosteroids to see if any neurosteroids correlate with higher levels in sleepiness in patients.

It is also possible that multiple components of CSF contribute to receptor enhancement. There may be multiple PAMs and NAMs in the CSF which, depending on the balance, may contribute more or less overall enhancement of $GABA_A$ receptor activity. This will be harder to separate out but as proteomics analysis improves, it could be examined. This would require a large cohort of IH patients with varying degrees of sleepiness and their detailed patient history. Ideally, one molecular component in their CSF would correlate positively with sleepiness while another would negatively correlate with sleepiness. As the proteome of CSF and its analysis using mass spectrometry improves, this kind of experiment will become easier.

Finally, the role of CSF in sleep and the clearance of metabolites from the brain should be considered. The are many hypotheses about the role of sleep in organisms. Lack of sleep can reduce learning, impair cognitive function and slow reaction times. Total

sleep deprivation is fatal to lab animals within days to weeks, and in humans a type of fatal familial insomnia leads to death (Xie et al., 2013). CSF plays an important role in supporting, providing nutrients and clearing proteins and molecules from the brain tissue. CSF also helps maintain neuronal viability (Perez-Alcazar et al., 2016). The glymphatic system refers to the clearance system and exchange between CSF and the interstitial fluid in the CNS (Xie et al., 2013). Recently, it was shown that the rate of clearing proteins from the glymphatic system is almost two-times faster during sleep than during waking periods (Xie et al., 2013). If one purpose of sleep is to clear metabolic waste, then it's possible a dysfunctional clearance system is leading to toxic metabolites building up in the CSF. This would make sense in the context that non-sleepy control CSF samples also potentiate $GABA_A$ receptors but to a lesser degree than hypersomnolent CSF. If the CSF system is not clearing metabolites and toxic proteins properly then their buildup might cause the excessive enhancement of $GABA_A$ receptors in hypersomnia. The excessive GABAergic inhibition could lead to a repressed arousal system. There is still much work to do in understanding how the endogenous peptide's molecular actions are affecting neural circuits at a systems level to cause hypersomnia, but the present results provide good evidence for looking beyond a benzodiazepine-based theory.

4.5 Limitations and Future Directions

Working with human CSF samples presents several limitations that were controlled for as best as possible in present experiments. Assaying 12 different receptor assemblies required a large amount of hypersomnolent CSF (15+ mL compared to 1 mL). Given this requirement, CSF samples were pooled from five affected sleep patients whose CSF had been previously assayed in the Jenkins lab and found to potentiate $\alpha_1\beta_2\gamma_{2s}$ receptors over 50%. Pooling CSF prevents us from understanding the individual variations across patient samples however clinical patient data wat not available for the present experiments and

so those correlations could not be made. If the CSF component is multiple components, then pooling CSF would alter the balance of these components. Pooling CSF, however, should not remove these components, though it may dilute them. Given that the potentiation of the pooled CSF used here (Pool C_{om} = 109%) was similar to the average potentiation across the 50+ CSF samples tested (~94%), it is unlikely that any balance of multiple components was drastically altered in this pooled CSF sample.

Data presented in this chapter provide important evidence supporting a robust and reliable effect of hypersomnolent CSF modulation of $GABA_A$ receptors. A French group recently published a study claiming no CSF potentiation was measured at $\alpha_1\beta_2\gamma_{2s}$ $GABA_A$ receptors (Dauvilliers et al., 2016). A closer look at their methods and experimental design revealed flaws in the patch clamp studies carried out. Most notable was the use of high GABA concentrations that appeared to evoke responses closer to 50-90% of the maximum receptor response before the presence of CSF was even added (Moody et al., 2017). While it is possible that the CSF samples studied by this group represented a novel population of hypersomnia patients, it is more likely that poor experimental design masked the modulatory effects of CSF. The data presented in Table 4.1 shows the robust PAM effects of hypersomnolent CSF across patients with hypersomnia. The failure of Dauvilliers and colleagues to replicate this CSF effect, while possibly due to experimental error, does raise an important point about replication and the complexity of IH. The population of IH patients likely does contain a fair amount of variability, given that this diagnosis is one of exclusion. Future studies of the molecular effects of hypersomnolent CSF would do well to widen the population of CSF samples tested to include a uniform neurological and sleep-controlled population. The hypersomnia population of samples could also be divided into subgroups based on severity of clinical sleepiness or responsiveness to certain medications. Expanding and clarifying the clinical groups from

which CSF samples are taken might help clarify the molecular effects measured at $GABA_A$ receptors, such as the subunit specificity of CSF potentiation.

Future electrophysiology experiments will help refine a new hypothesis. First, the subunit-specificity of CSF potentiation should be repeated using individual CSF samples. Given the high volume of CSF required, this experiment would be challenging but important if the effects at extrasynaptic $GABA_A$ receptor assemblies are to be explored further. The subunit-specificity of CSF potentiation could then be correlated with clinical metrics of individual patients. This would help narrow down the possible brain regions where GABAergic inhibition might be most disrupted. Second, the inhibition of CSF potentiation at non-$\alpha_1\beta_2\gamma_{2s}$ receptors should be measured using known antagonists and negative modulators, such as flumazenil and clarithromycin, which are known to play a role in reversing sedation (Safavynia et al., 2016; Trotti et al., 2014). This could expand our knowledge of flumazenil and clarithromycin may be acting, along with how they interact with hypersomnolent CSF. Although both flumazenil and clarithromycin provide some clinical relief to a subset of hypersomnia patients, alternative treatments are still needed. The ultimate goal of research on Idiopathic hypersomnia is to understand the disease mechanism causing excessive daytime sleepiness and create a platform from which new drug therapies can be developed. The results here have provided important information to redefine the hypersomnia disease mechanism, which will ultimately help advance sleep research.

Chapter 5:

Chapter 5:

Functional consequences of missense mutations in the *GABR* gene linked to early-onset epilepsy

Overview:

Early-onset epilepsies may reflect a miswiring of the brain's balance in neural excitation and inhibition. Mutations within the *GABR* genes (*GABRA1, GABRB2, GABRB3, GABRG2, and GABRD*) have been associated with different forms of epilepsy from mild generalized epilepsies to severe epileptic encephalopathies (Johannesen et al., 2016; Yuan et al., 2015). As genome sequencing of patients increases, the number of mutations found from patients with epilepsy continues to grow. In this chapter, three mutations (two *de novo* and one whose inheritance was unconfirmed) were identified in the *GABRA2, GABRA5,* and *GABRB3* genes from pediatric patients with early-onset epilepsy and developmental delays. Two mutations (α2(T292K) and α5(V294L)) occurred in the second transmembrane domain (M2), and the third mutation (β3(P301L)) occurred in the linker region between the second and third transmembrane domains (M2-M3 linker). Mutations in both regions are predicted to be harmful to receptor function because the M2 domain forms the pore of the channel, and the M2-M3 linker region is important for channel gating (O'Shea, Williams, & Jenkins, 2009; Xu & Akabas, 1996). Whole-cell patch clamp recording was used to assess the impact of each mutation on $\alpha_x\beta_x\gamma_{2s}$ $GABA_A$ receptor function. The results show that the α2(T292K) mutation trapped the receptor in a tonically open state where it was unable to respond to GABA signals. The α5(V294L) mutation increased GABA's apparent-affinity for the receptor and increased its desensitization. The third mutation, β3(P301L), decreased GABA's apparent-affinity. All three mutations disrupted $GABA_A$ receptor function in different ways that would each reduce the receptor's ability to pass GABA-evoked currents. These results are significant because they provide

two novel disease mechanisms for how altering $GABA_A$ receptor function can increase the seizure susceptibility of neurons.

5.1 Introduction:

Epilepsy is a neurological disease characterized by recurrent, unprovoked seizures. It is the fourth most common neurological disease in the U.S. and can affect people of all ages (Shafer, P. & Sirven, J. Epilepsy Statistics [Internet]. Epilepsy Foundation .10/2013. Available from: https://www.epilepsy.com/learn/about-epilepsy-basics/epilepsy-statistics). Although epilepsy can develop secondary to an infection or traumatic event to the brain, the exact cause of the seizures is unknown in approximately 50% of cases. Genetic mutations are increasingly being linked to different forms of epilepsy, such as early onset epileptic encephalopathies, benign neonatal/infantile seizures, and genetic generalized and benign focal epilepsies (Olson et al., 2014). The increased efficiency and lower-cost of whole genome sequencing and exon sequencing (sequencing of the protein coding regions) has resulted in the identification of dozens of rare *de novo* variants in the *GABR* genes to data (Hernandez et al., 2016; Yuan et al., 2015). The goal of many genetic studies is to identify the genetic risk or causal factors at the genome level, but both functional and behavioral data is needed to confirm a direct link.

Although the number of *de novo* and inherited *GABR* mutations with functional data (e.g. electrophysiology, behavior or protein expression assays) is increasing, many mutations still lack functional data. In 2015, there were 27 *GABR* missense mutations with a frequency <1% correlated with epilepsies, most in *GABRA1* and *GABRG2 (Yuan et al., 2015)*. To date, more mutations in *GABRA1, GABRA4, GABRA5, GABRA6*, *GABRB1, GABRB2, GABRB3*, *GABRG1, GABRG3* and *GABRD* genes have been linked to inherited epilepsies (Hernandez et al., 2016; Macdonald, Kang, & Gallagher, 2010; Yuan et al.,

2015). Many of these mutations alter trafficking of the protein or alter the activation of the receptor (Hernandez et al., 2016; Yuan et al., 2015).

Two regions important for proper $GABA_A$ receptor function are the second transmembrane domain (M2) and the extracellular linker region between the second and third transmembrane domains (M2-M3 linker) (Figure 5.1). The M2 region is critical to the normal function of the $GABA_A$ receptor because each M2 domain of the five subunits making up the receptor contributes to forming the pore of the anion channel (Figure 5.2) (Miller & Aricescu, 2014). The M2-M3 linker region is involved in coupling the agonist binding to the gating of the channel, a crucial step for channel activation (Kash et al., 2003). Previous studies have identified multiple residues (Thr6', Thr7', Leu9', Thr10', Thr13') in M2 that are critical to forming the pore and are exposed to the lumen when the channel is open (Xu & Akabas, 1996). The prime numbering system of residues in M2 was designed to allow comparison across different cys-loop receptors (Q. Wang, Pless, & Lynch, 2010).

The M2 domain of $GABA_A$ receptor subunits is critical to channel function. Other mutations in the pore region of M2 have been found to alter $GABA_A$ receptor single channel function (Luu, Cromer, Gage, & Tierney, 2005), gating (Tierney et al., 1998; Tierney et al., 1996), desensitization (Birnir, Tierney, Lim, Cox, & Gage, 1997; Dalziel et al., 1999) and modulation by ethanol (Johnson, Howard, Trudell, & Harris, 2012; Krasowski & Harrison, 1999). M2 pore mutations have also been linked to $GABA_A$ receptor and glycine receptor dysfunction. One mutation turned these anion channels to cation channels (Keramidas, Moorhouse, French, Schofield, & Barry, 2000). The highly conserved M2 region has also been shown to be important in the closely related glycine receptors and nicotinic acetylcholine receptors (Akabas, Stauffer, Xu, & Karlin, 1992; Keramidas et al., 2000). It is not surprising that mutations in M2 and close to M2 might have devastating effects on $GABA_A$ receptor channel function.

In the following study, we report the functional effects of three rare variants in the *GABRA2*, *GABRA5* and *GABRB3* genes. Mutations were identified from pediatric epilepsy patients using trio-based sequencing and a clinical sequencing panel. The mutations were *GABRA2* c.875C>A (p.T292K), *GABRA5* c.880G>C (p.Val294Leu) and *GABRB3* c.902C>T (p.P301L). To date, no functional data or mechanism has been proposed for these mutations. Whole-cell patch clamp recordings from HEK293T cells expressing wildtype and mutant $\alpha_x\beta_x\gamma_{2s}$ $GABA_A$ receptor quantified the functional changes in GABA-evoked currents for each mutant variant. The functional results showed that each mutation altered GABA-evoked responses but through different mechanisms. The data were consistent with all three variants reducing GABAergic inhibition. This is predicted to decrease the threshold for neuronal excitability, leading to an increased susceptibility to seizures in the brain.

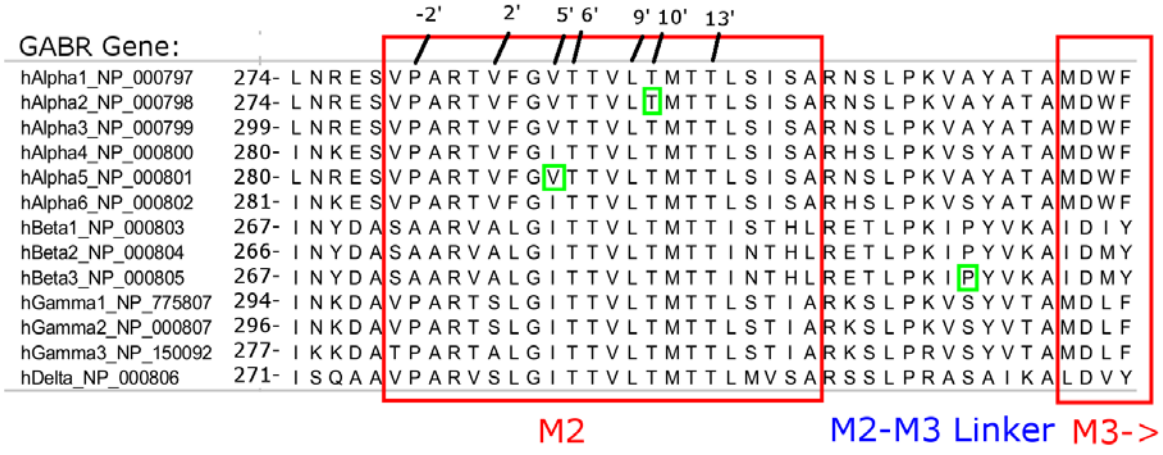

Figure 5.1 Sequence alignment of human immature peptide sequences of α1-6, β1-3, γ1-3, δ GABR subunits with residue prime numbering of the transmembrane 2 (M2) domain. Red boxes identify M2 and M3 transmembrane domains. Green boxes indicate the residues mutated in this study of epilepsy-related mutations. Alignment was performed using Clustral Omega (MegaAlign Pro from DNASTAR, INC.). The length of signal peptides are: α1 = 27, α2 = 28, α3 = 28, α4 = 35, α5 = 31, α6 = 19, β1 = 24, β2 = 24, β3 = 25, γ1 = 35, γ2=39, γ3 = 17, δ = 24. The protein NCBI reference numbers are also listed in the table.

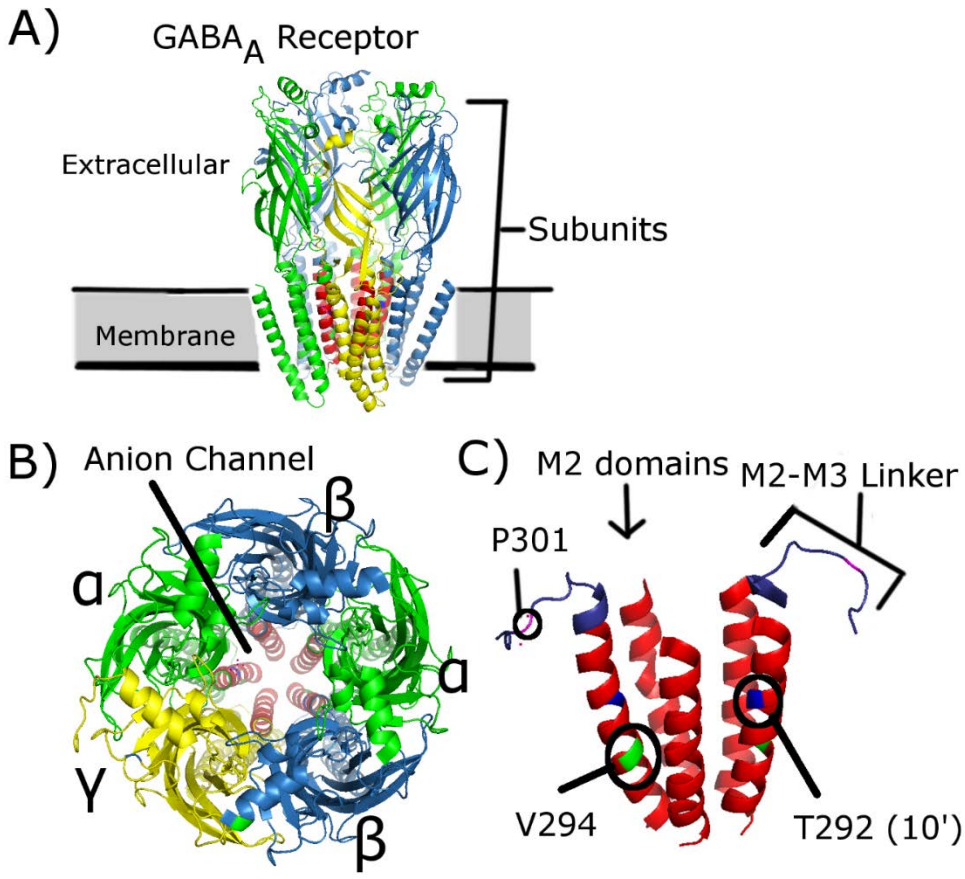

Figure 5.2. Location of three missense mutations identified in *GABRA2, GABRA5,* and *GABRB3*. The location of the second transmembrane domains (M2) is highlighted in red while subunits are colored green (α), blue (β) and yellow (γ). The αβγ $GABA_A$ receptor is viewed from A) the side view in the cell membrane, and B) the top view looking down from the extracellular side of the receptor. C) The location of the three mutations in the M2 region and M2-M3 linker region is shown. The mutations are colored as blue (α2(T292K)), green (α5V294L)), and pink (β3(P301L)). Mutations are highlighted in no particular order of the subunits, except to best visual each residue separately. Each patient only exhibited one mutation but mutations are shown together here for simplicity of the figure. The schematic is based on the beta3 homopentamer crystal structure published by Miller, *et al.,* 2014, and the subunits were highlighted using PyMOL to represent a heteropentameric receptor.

Section 5.2 METHODS:

Cell culture, plasmids and mutagenesis were performed as described in Chapter 2 (Sections 2.1 and 2.3)

5.2.1 Whole-cell patch clamp recording

Whole-cell patch clamp recording of HEK293T cells expressing $\alpha_x\beta_2\gamma_{2s}$ or $\alpha_1\beta_x\gamma_{2s}$ $GABA_A$ receptors was performed as described in Chapter 2 (Section 2.6). GABA concentration-response assays were performed and analyzed as described in Section 2.6.4 and 2.7.2 by exposing each whole-cell patches to increasing concentrations of GABA within a 3.5 logarithmic decade.

Picrotoxin assay

Picrotoxin assays were performed on HEK293T cells expressing $\alpha_2\beta_2\gamma_{2s}$ or α_2(T292K)$\beta_2\gamma_{2s}$ receptors. Picrotoxin was dissolved in DMSO and then diluted in extracellular solutions to the final concentrations of 1 μM, 10 μM and 100μM (0.1% DMSO). Picrotoxin solutions were applied in increasing concentrations to patched cells for 3 seconds with 8 seconds of washout between concentrations.

5.2.2 Whole-cell Analysis

Whole-cell analysis of recordings were baseline corrected and GABA concentration-response relationships fit using the Hill equation as described in Section 2.7.

Measurement of baseline leak current and picrotoxin block

Baseline leak current for α_2(T292K)-containing receptors was measured from GABA concentration-response assays. The first 41 points (0.2 sec) of whole-cell baseline current in extracellular solution was averaged for each patch to give a measurement of baseline leak. This was performed for all 8 concentrations in that concentration assay and the value averaged for each cell. A two-way unpaired *t*-test (α=0.05) with Welch's correction was used to evaluate group differences.

The picrotoxin assay results were analyzed similar to responses with GABA, except that the peak currents went in the positive direction (upwards). This was because picrotoxin blocked the tonic leak current. The amplitude of peak currents was measured from the baseline leak current measured when no picrotoxin was present. The peak current amplitudes were measured for each picrotoxin concentration and plotted using Prism.

Measurement of desensitization

Desensitization was measured for α_5(V294L)- and α_5-containing receptors from the whole-cell recordings of GABA concentration-response assays based on analysis methods previously described by Moody and colleagues (Moody et al., 2017). Briefly, desensitization was measured across 2 second GABA exposures as follows: $(I_{peak} - I_{end})/I_{peak}*100$ where I_{Peak} was the amplitude of the total peak current response and I_{end} was the amplitude of the peak current response at the end of the drug exposure (at 2 s). For each cell's assay, desensitization was measured for each of the 8 GABA concentration responses. The average desensitization for each GABA concentration was plotted on a semilogarithmic scale (GABA concentrations converted to Log[GABA]) and a linear regression fit to estimate a slope (rate of desensitization) and y-intercept.

5.2.3 Statistics

Changes in Hill parameters from GABA concentration-response curves were evaluated for significant (p<0.05) differences using two-way *t*-tests between mutant and wildtype conditions. The effect of picrotoxin on baseline leak current was evaluated by a two-way ANOVA with repeated measures on the concentration. Where significance was found (p<0.05), a Sidak's post-hoc analysis was performed for multiple comparisons.

Desensitization was evaluated in Prism using an ANOVA. Statistics were performed using Graphpad Prism 7.0.

5.3 RESULTS

5.3.1 Identification of *GABR* mutations from patients with epilepsy

The three *de novo* mutations were identified in the *GABRA5, GABRA2* and G*ABRB3* genes (see Butler, Moody, *et al.,* 2017 (manuscript submitted) for extended sequencing details). Briefly, the α5(V294L) mutation *(GABRA5* c.880G>C (p.Val294Leu) was identified from trio-based whole genome sequencing of a pediatric patient with severe epilepsy and developmental delay. The other two mutations, α2(T292K) and β3(P301L), were identified from sequence data available from 279 clinically-referred epilepsy patients screened at EGL Genetics (Tucker, GA). The sequencing panel contained approximately 4800 genes that included the *GABRA1, GABRA2, GABRA6, GABRB3, GABRG1, GABRG2, GABBR1, GABRD,* and *GABRR2 genes* but not *GABRA5.* The *GABRA2* and *GABRB3* variants were both heterozygous missense mutations with a frequency less than 1%. The *GABRA2* mutation and *GABRA5* mutations were confirmed as *de novo* mutations. Sequencing of parental DNA was not available from the patient with the *GABRB3* mutation (*GABRB3* c.902C>T (p.Pro301Leu)) to confirm if it was *de novo*. However, this same mutation was identified recently in another pediatric patient with epilepsy (Moller et al., 2017) where it was *de novo*.

5.3.2 Functional characterization of α2(T292K) mutation

The α_2(T292K) mutation, when co-expressed with β_2 and γ_{2s} subunits, produced dysfunctional $GABA_A$ receptors. Under bright-field and fluorescence microscopy, the HEK293T cells expressing α_2(T292K)$\beta_2\gamma_{2s}$ receptors were healthy-looking cells with normal GFP brightness of expression. However, the mutant receptors did not produce GABA-evoked currents within the GABA concentration range of 0.3-1000μM that normally evoked up to several nanoamps of current with wildtype $\alpha_2\beta_2\gamma_{2s}$ receptors (Figure 5.3). The average current responses to 300, 1000 and 3000 μM GABA for α_2(T292K)$\beta_2\gamma_{2s}$

receptors were: -22.32 ± 7.11, -23.57 ± 76.27 and -7.33 ± 1.82 pA (n=9 cells). Wildtype $\alpha_2\beta_2\gamma_{2s}$ receptors had normal GABA concentration-response relationships with an EC_{50} of 5.97 ± 1.16 μM, Hill coefficient of 1.344 ± 0.069, and a maximum current of -3340 ± 392 pA. It was also noted that the basal leak current of patches from mutant α_2(T292K)$\beta_2\gamma_{2s}$ receptors was twice as large as that of wildtype receptors ($t(24.45)=3.37$, $p<0.05$, unpaired *t*-test with Welch's correction). This led us to hypothesize that the mutant channels might be trapped in an open state, even in the absence of GABA, given that the mutation is in the receptor's pore-forming region within the M2 domain.

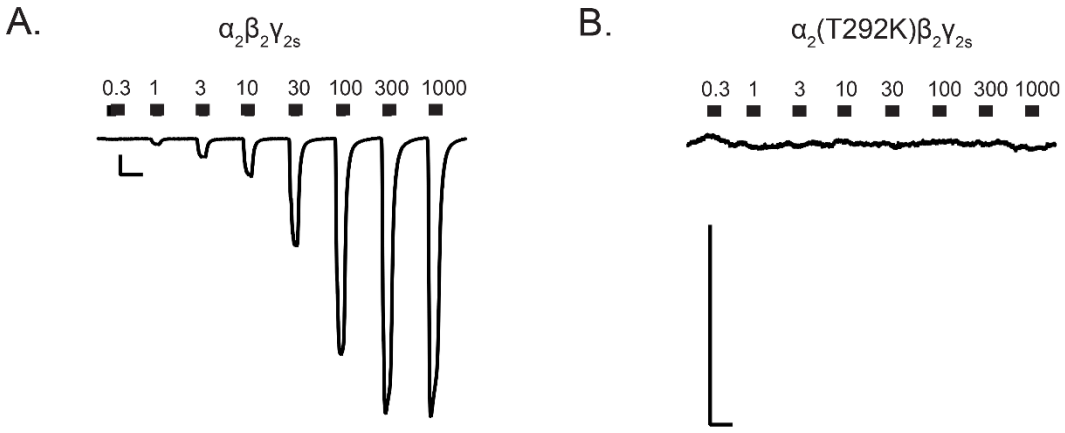

Figure 5.3. Example whole-cell recordings of GABA concentration-response assays for: (A) wildtype $\alpha_2\beta_2\gamma_{2s}$ receptors and (B)mutant α_2(T292K)$\beta_2\gamma_{2s}$ receptors. Scale bars are 5sec, 500pA. Traces are baseline corrected and normalized to zero for easier visualization. Raw traces would show that the basal leak current of patches from mutant α_2(T292K)$\beta_2\gamma_{2s}$ receptors was twice as large as that of wildtype receptors.

Next, a picrotoxin inhibition assay was performed to determine if mutant α_2(T292K)$\beta_2\gamma_{2s}$ receptors were passing tonic current in the absence of GABA. Picrotoxin is a GABA antagonist that acts as a channel blocker (Xu, Covey, & Akabas, 1995). Mutant α_2(T292K)$\beta_2\gamma_{2s}$ receptors showed increasing inhibition of the basal leak current when exposed to increasing concentrations of picrotoxin (1, 10, 100 μM) in the absence of GABA (Figure 5.4). This resulted in upwards current responses during picrotoxin exposures that reflected the suppression of the tonic leak current being passed by the mutant receptors. The wildtype receptors showed only slight responses to picrotoxin inhibition of the leak current (Figure 5.4). A two-way ANOVA was conducted on the influence of receptor condition (wildtype or mutant) and picrotoxin concentration on the block of tonic leak current. All main and interaction effects were statistically significant (picrotoxin concentration $F(2, 68) = 40.14$; receptor condition $F(1, 34) = 25.44$; interaction $F(2, 68) = 32.14$) at the 0.05 significance level. The α_2(T292K) mutant receptors showed significantly larger picrotoxin block of tonic leak current than wildtype receptors at both 10 μM (p=0.0017) and 100 μM (p<0.0001) picrotoxin concentrations. At a saturating concentration, 100μM picrotoxin blocked an average of 255.0 ± 26.1 pA of current in cells expressing α_2(T292K)$\beta_2\gamma_{2s}$ receptors (n=10 cells), while only 24.6 ± 5.8pA was blocked with wildtype $\alpha_2\beta_2\gamma_{2s}$ receptors (n=4 cells) at the same concentration. Overall, the mutant α_2(T292K)$\beta_2\gamma_{2s}$ receptors failed to respond to GABA, but picrotoxin blocked a large tonic baseline current which was not seen with wildtype receptors (Table 5.1).

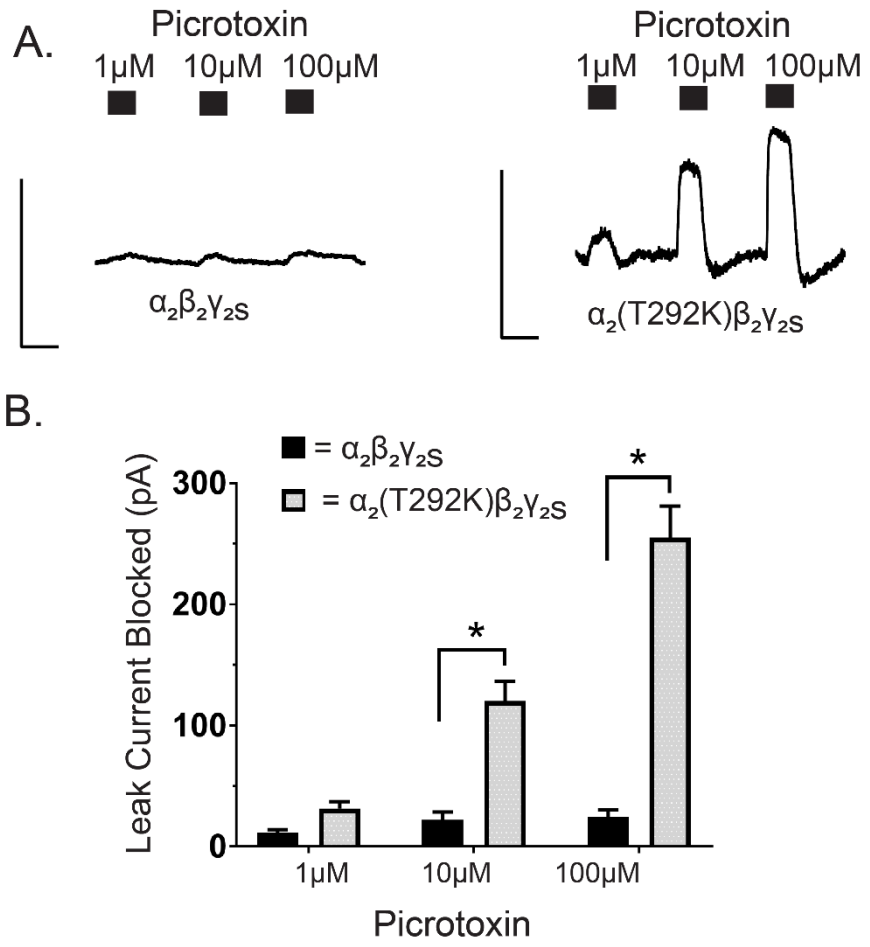

Figure 5.4. Picrotoxin blocks baseline leak current for mutant $\alpha_2(T292K)\beta_2\gamma_{2s}$ receptors but not of wildtype $\alpha_2\beta_2\gamma_{2s}$ receptors. A) 1, 10 and 100 μM picrotoxin was applied to whole-cell patches in the absence of GABA. Scale bar: 5sec, 300pA. B) Quantification of inhibition of leak current (pA) by picrotoxin. Picrotoxin block was significantly larger for mutant receptors at concentrations 10 μM (p=0.0017) and 100 μM (p<0.0001) (two-way repeated-measures ANOVA, Sidak post-hoc test). Bars represent mean ± SEM. *p<0.05. Sample sizes were: wildtype $\alpha_2\beta_2\gamma_{2s}$ (n=4 cells) and $\alpha_2(T292K)\beta_2\gamma_{2s}$ (n=10 cells).

	GABA Assay		Picrotoxin Assay			
Mutation	**Basal Leak current (pA)**	**N**	**1 μM Picrotoxin**	**10 μM Picrotoxin**	**100 μM Picrotoxin**	**N**
$\alpha_2\beta_2\gamma_{2s}$	-665 ± 105	9 (20)	11.5 ± 2.5 pA	21.9 ± 6.5 pA	24.6 ± 5.8 pA	4 (11)
α_2(T292K)$\beta_2\gamma_{2s}$	-1370 ± 185*	9 (18)	31.4 ± 5.7 pA	120.2 ±16.3 pA*	255.0 ± 26.1 pA*	10 (25)

Table 5.1. Table of whole-cell current measurements from α_2(T292K)$\beta_2\gamma_{2s}$ and $\alpha_2\beta_2\gamma_{2s}$ receptors. Data from GABA concentration-response assays was used to measure basal leak current from wildtype and mutant receptors, showing that mutant receptors had greater basal leak current (p<0.05, t(24.45)=3.37; unpaired t-test with Welch's correction). Picrotoxin assays were performed separately with the amount of basal leak current blocked by 1, 10, and 100 μM picrotoxin measured on each patch in the absence of GABA. Picrotoxin blocked significantly more basal leak current in mutant receptors (p<0.05, F(1,34)=25.44, p<0.0001; two-way ANOVA with Sidak post-hoc test for multiple comparisons). Sample sizes are the number of cells patched and the total number of runs in parentheses. Values are Mean ± SEM. *p<0.05 significance.

5.3.3 Functional characterization of the α5(V294L) mutation

Whole-cell patch clamp recording of HEK293T cells was used to evaluate the functional consequences of the α_5(V294L) mutation in the second transmembrane domain of the subunit. GABA concentration-response assays revealed a leftward shift for cells expressing the mutant α_5(V294L)$\beta_2\gamma_{2s}$ receptors (n=22 cells) relative to wildtype $\alpha_5\beta_2\gamma_{2s}$ receptors (n=18 cells) (Figure 5.5 and 5.6A). The maximum GABA-evoked current of mutant receptors was significantly lower than that of wildtype receptors (α_5(V294L): -2717 ± 324 pA vs. α_5: -4165 ± 314 pA, p=0.0024). The Hill coefficient of the mutant receptors was significantly higher than that of wildtype receptors (α_5(V294L): 1.562 ± 0.071 vs. α_5: 1.120 ± 0.061 p<0.0001). The α_5(V294L)$\beta_2\gamma_{2s}$ receptors also had an EC_{50} that was approximately one tenth the size of wildtype receptors (α_5(V294L): 0.238 ± 0.028 vs. α_5: 2.041 ± 0.314 μM, p=0.0024). It was noted that on average, the mutant receptors neared maximal activation around 1 μM GABA.

Desensitization was measured from the peak responses of whole-cell recordings taken from the GABA concentration-response assays. The rate of desensitization as GABA concentration increased was enhanced for the mutant α_5(V294L)$\beta_2\gamma_{2s}$ receptors compared to wildtype receptors ($F_{1,7}$ = 15.03, *p*=0.0061) (Figure 5.6B). The relationship between GABA concentration and the degree of desensitization could be described by lines of: Y=5.508X + 0.909 (wildtype receptors) and Y = 9.584X – 6.277 (α_5(V294L)$\beta_2\gamma_{2s}$ receptors), where Y is the percent of desensitization and X is the log[GABA] using concentrations in micromolar. Overall, the α_5(V294L)$\beta_2\gamma_{2s}$ receptors enhanced the GABA apparent-affinity and increased the degree of desensitization at high GABA concentrations.

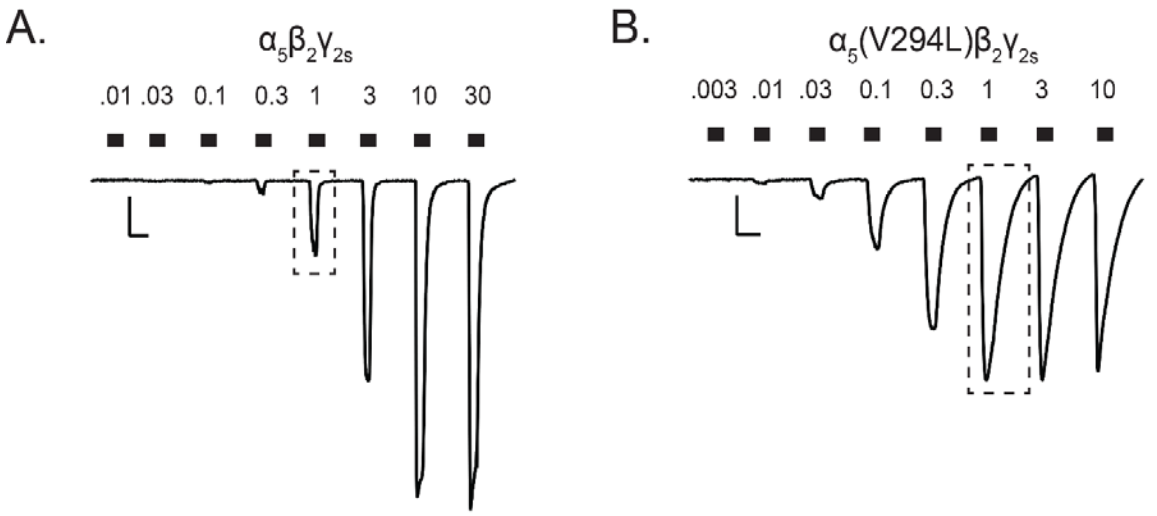

Figure 5.5. Example whole-cell recordings of GABA concentration-response assays (0.003-30 μM) for: (A) wildtype $\alpha_5\beta_2\gamma_{2s}$ receptors, and (B) mutant α_5(V294L)$\beta_2\gamma_{2s}$ receptors. Scale bars are 5sec, 500pA. Dotted box highlights the peak current response at 1 μM GABA.

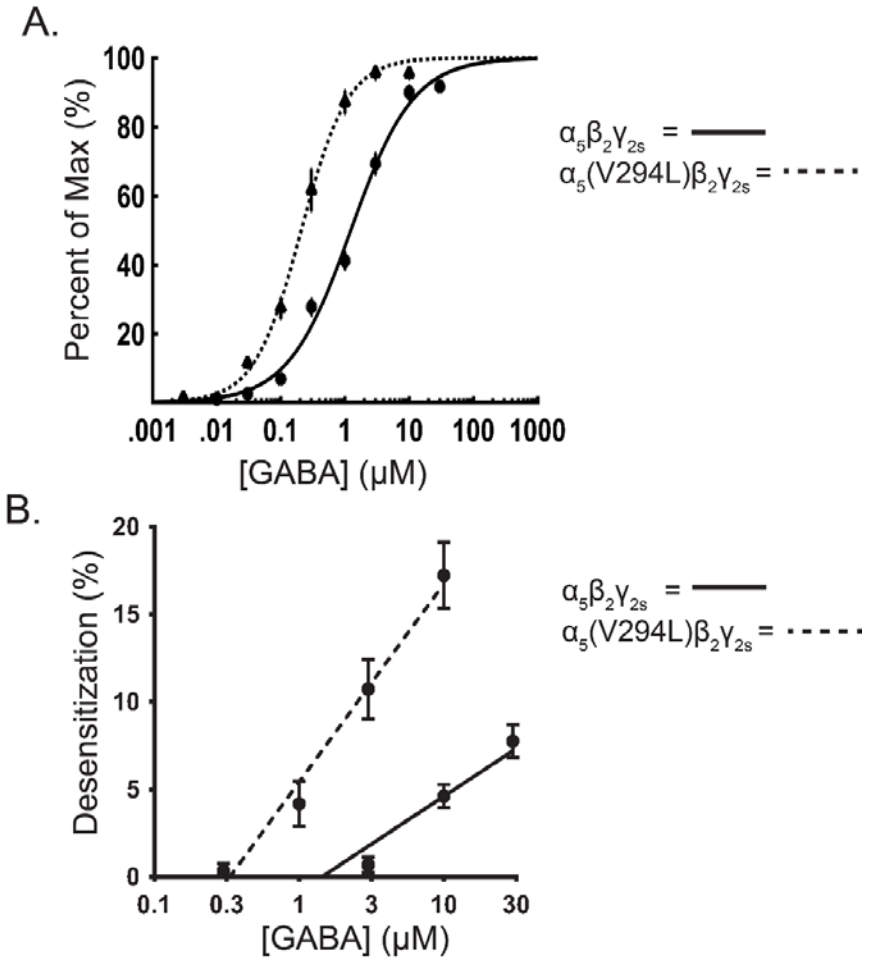

Figure 5.6. Effect of the α_5(V294L) mutation on GABA-evoked responses. A) The GABA concentration-response relationship for mutant α_5(V294L)$\beta_2\gamma_{2s}$ receptors shifted leftwards compared to that of wildtype $\alpha_5\beta_2\gamma_{2s}$ receptors (EC_{50}: α_5(V294L) = 0.238 ± 0.028; α_5: 2.041 ± 0.314 μM, p=0.0024). B) The percent of desensitization occurring during whole-cell GABA concentration-response assays for wildtype and mutant α_5(V294L)$\beta_2\gamma_{2s}$ receptors. Desensitization was calculated as the difference in amplitude between the peak current and the amplitude at the end of each GABA exposure. Linear regressions to calculate desensitization were: Y=5.508X + 0.909 ($\alpha_5\beta_2\gamma_{2s}$, solid line) and Y = 9.584X – 6.277 (α_5(V294L), dotted line), where Y is the percent of desensitization and X is the log[GABA] in micromolar. Slopes were significantly different ($F_{1,7}$ = 15.03, *p*=0.0061), indicating mutant receptors desensitized more frequently at higher GABA concentrations than wildtype receptors. Points represent mean ± SEM. Sample sizes were n=18 cells ($\alpha_5\beta_2\gamma_{2s}$) and n=22 cells ($\alpha_5$(V294L)$\beta_2\gamma_{2s}$).

5.3.4 Functional characterization of β3(P301L) mutation

Expression of the β_3(P301L) variant with α_1 and γ_{2s} subunits shifted the GABA concentration-response curve (1-3000μM) rightwards relative to wildtype receptors (Figure 5.7; β_3(P301L): n=20 cells vs. β_3: n=21 cells). The EC_{50} for β_3(P301L) mutant receptors was significantly higher than wildtype receptors (β_3(P301L): 298.10 ± 16.51 vs. β_3: 120 ± 14.37 μM, p<0.0001). The maximum GABA-evoked current was significantly lower than wildtype receptors (β_3(P301L): -540.2 ± 43.0 vs. β_3: -1742.0 ± 157.1 pA, p<0.0001). The Hill coefficient was significantly higher for mutant receptors (β_3(P301L): 1.474 ± 0.050 vs. β_3: 1.235 ± 0.046, p=0.0007). These results were consistent with the β_3(P301L) mutation decreasing the sensitivity to GABA and reducing the receptor's capacity to pass current in response to GABA events.

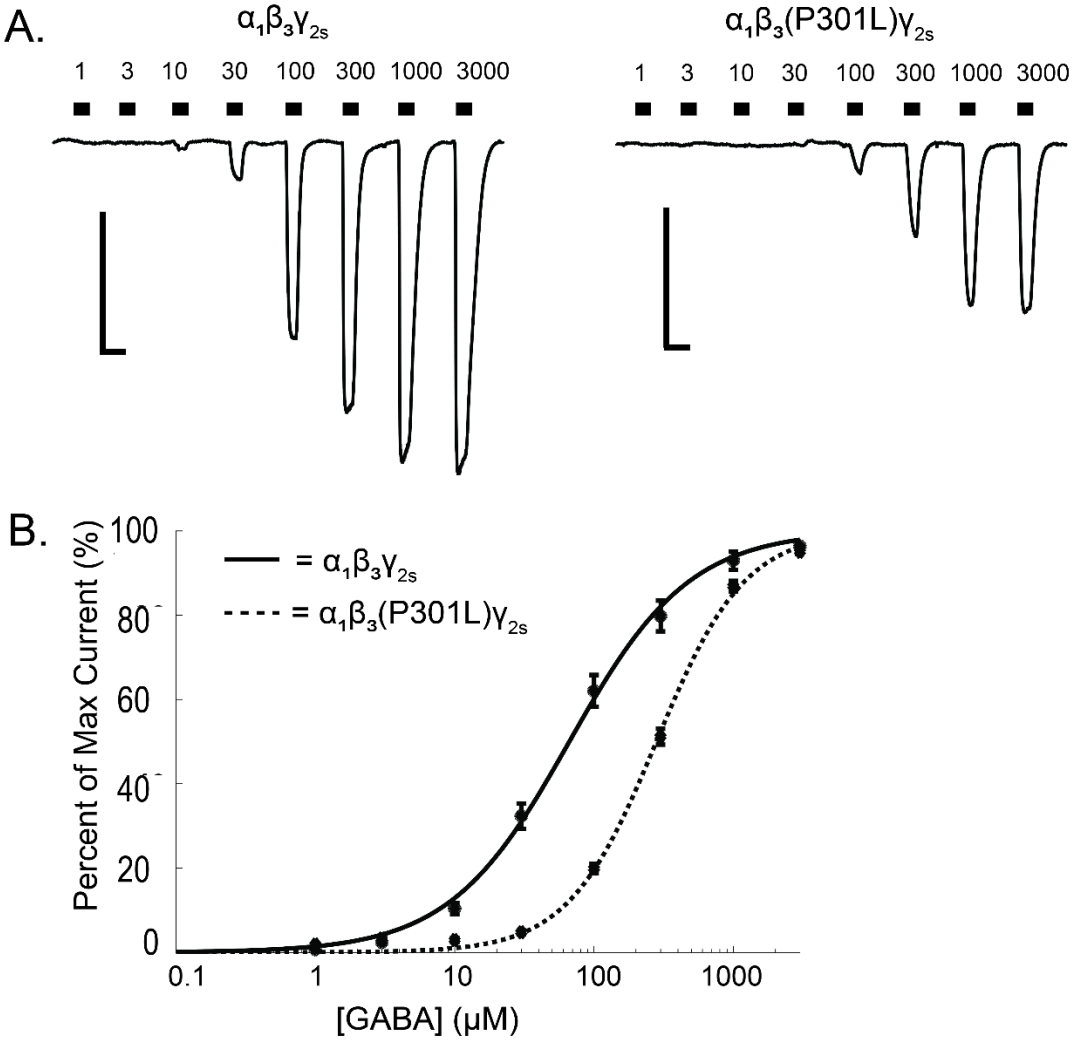

Figure 5.7. The mutated $\alpha_1\beta_3(P301L)\gamma_{2s}$ receptors are less sensitive to GABA activation. (A) Example trace of GABA concentration-response assays (1-3000 μM) for $\alpha_1\beta_3\gamma_{2s}$ and $\alpha_1\beta_3(P301L)\gamma_{2s}$ receptors expressed in HEK293T cells. Scale bar: 5sec, 500pA. (B) GABA concentration-response curves for $\alpha_1\beta_3\gamma_{2s}$ (black line, n=21 cells) and $\alpha_1\beta_3(P301L)\gamma_{2s}$ (dotted line, n=20 cells) receptors. Points are mean ± SEM and error bars are not shown where bars are smaller than points.

5.4 DISCUSSION

An increasing number of mutations in the *GABR* gene have been found in cases of rare epilepsies. For example, 24 non-synonymous (altering the amino acid sequence) mutations were identified in *GABR* genes (*GABRA, GABRB* and *GABRG*) from patients with monogenetic epilepsy (Hernandez et al., 2016). Mutations that mapped to the N-terminal or transmembrane domains were found to be deleterious to $GABA_A$ receptor function. The mutations that mapped to the β+/α- GABA binding interface specifically were associated with impaired receptor gating (Hernandez et al., 2016). Given that none of these variants significantly reduced protein surface expression, the authors conclude that the primary mechanism through which mutations affect the $GABA_A$ receptor function is through gating deficiencies and not altered receptor expression. However, there were multiple ways gating could be altered (slowed activation, accelerated deactivation, reduced current amplitudes). Different alterations in gating could call for drugs that target the $GABA_A$ receptors in different ways to treat disease. If different dysfunctional gating mechanisms are a theme of severe *GABR* mutations linked to epilepsy, there is an increased need for the functional characterization of *GABR* mutations linked to epilepsy to understand these dysfunctions and provide improved personalized treatments.

In our study, we examined two new *de novo* missense mutations and one previously uncharacterized mutation across the *GABRA2, GABRA5* and *GABRB3* genes. These mutations were identified from three different pediatric patients with early-onset epilepsies and developmental delays. The α_5(V294L) mutation was a heterozygous, *de novo* variant in *GABRA5,* confirmed by trio-based whole genome sequencing. The patient's seizures began at four months of age progressed to up to 100 seizures/day. The patient became seizure-free at 14 months of age on a combination of zonisamide, levetiracetam, and oxcarbazepine, but now the patient now (24-months) has both mental and motor developmental delays. The other two mutations were rare variants in *GABRA2*

and *GABRB3* genes. They were identified from sequencing data of nine *GABR* genes from 279 epilepsy patients screened using a clinical sequencing panel (Butler, Moody, et al., 2017, manuscript submitted). The α_2(T292K) mutation was found in a pediatric patient whose seizures began at 6 weeks and continue to the present age of 11. Now at age 11, the patient exhibits microcephaly, cerebral palsy with severe central hypotonia and asymmetric lower extremity spasticity, and cortical visual impairment. This patient is nonambulatory, nonverbal, and has profound intellectual disability. She is currently treated with a combination of valproic acid, phenobarbital, and clobazam, but still experiences seizures. The β_3(P301L) mutation was identified from a 6-year-old male referred for genetic testing due to intractable seizures, developmental delay, and an unspecified psychiatric abnormality. Clinical history and genetic data from the parents was unavailable, preventing the hereditary nature of this mutation from being analyzed. A previous study by another group identified this same mutation (β_3(P301L)) as *de novo* in another pediatric patient with focal epilepsy that started at 15 months of age, but did not functionally characterize the mutation (Moller et al., 2017).

Whole-cell patch clamp experiments were performed with $\alpha_x\beta_x\gamma_{2s}$ $GABA_A$ receptors to assess the effects of the α_2(T292K), α_5(V294L), and β_3(P301L) mutations on receptor function. Results show that each mutation altered channel function by a different mechanism. First, the α_2(T292K) mutation created a non-functional receptor trapped in the open channel state, incapable of producing GABA-evoked responses and passing indiscriminate tonic current. Second, the α_5(V294L) mutation increased the GABA apparent-affinity of receptors by ~10x, making the receptor much more sensitive to GABA but more prone to desensitization. Third, the β_3(P301L) mutation reduced GABA apparent-affinity by ~2.4-fold and reduced the maximum current amplitude passed. As discussed below, the three mutations are predicted to reduce the inhibitory neurotransmission in the brain and lowering the seizure threshold.

The α_2(T292K) mutation

Threonine292, also called Thr(10'), is highly conserved across the human α1-6, β1-3, and γ1-3 *GABR* genes (Figure 5.1). It is one of the conserved residues (2', 6', 10') in he second transmembrane domain (M2) that becomes exposed to the lumen when the pore is opened (Luu et al., 2005; Tierney et al., 1998; Xu et al., 1995). Thr(10') has been studied previously in mutagenesis studies examining the channel pore. Tryptophan and alanine mutations of the Thr(10') produced spontaneously opening channels with no detectable GABA-evoked responses (Ueno et al., 2000) or with rapidly decaying currents (Tierney et al., 1998). Other mutations in M2 have also produced spontaneously opening channels, consistent with this region being important for proper channel function (Buhr, Wagner, Fuchs, Sieghart, & Sigel, 2001; Tierney et al., 1996; Ueno et al., 2000; Williams, Bell, & Jenkins, 2010). Another threonine *GABR* mutation in M2 was identified in an infant patient with early myoclonic encephalopathy epilepsy. The patient had a β2(T287P) mutation of Thr(13') (Ishii et al., 2017). Surface expression assays showed that $\alpha_1\beta2(T287P)\gamma_{2s}$ receptors had reduced surface expression. Patch clamp analysis of mutant $\alpha_1\beta2(T287P)\gamma_{2s}$ receptors showed reduced GABA-evoked responses to a single GABA concentration, but further patch clamp experiments were not performed. Disease causing mutations of Thr(10') have not been previously reported, but M2's important function in channel pore formation suggests they would be deleterious to $GABA_A$ receptor function.

Experiments here examined the effect of a *de novo* α_2(T292K) mutation in M2 found in a patient with severe early-onset epilepsy. When expressed as $\alpha_2(T292K)\beta_2\gamma_{2s}$ receptors, the α_2(T292K) mutation produced no GABA-evoked responses. Even at saturating concentrations of 1-3 mM GABA, no current responses above 25 pA were detected (Figure 5.3). Surprisingly, there was an increase in basal leak current from

patched cells expressing the mutated receptor. The leak current is the current that passes in the absence of GABA or other stimulation when a patched cell is exposed to extracellular solution. Usually the leak current is set by the tightness of the seal between the patch pipette and the cell membrane, although the spontaneous single channel opening rate can also contribute a low level of current. Leak current from cells expressing the α_2(T292K) mutant was dramatically blocked by picrotoxin, a $GABA_A$ receptor channel blocker, in the absence of GABA (Figure 5.4). The α_2(T292K) mutant blocked approximately 10x the amount of current blocked by wildtype receptors. As a side note, the α_2(Thr292) (also called Thr(10')) is not one of the M2 residues known to disrupt picrotoxin block , which are Val(2') and Thr(6') (Gurley, Amin, Ross, Weiss, & White, 1995; Martin & Olsen, 2000; Xu et al., 1995). These data are consistent with a receptor being trapped in the open conformation, during which tonic current can pass in the absence of GABA. This would reduce the receptor's ability to respond to temporally-specific GABAergic signals. Instead the receptor would pass continual, non-specific hyperpolarization signals. Surface expression measurements of the α_2(T292K) subunit showed that mutant α_2(T292K)$\beta_3\gamma_2$ receptors had reduced total protein expression (~60% of WT levels, $p<0.0001$) and reduced surface protein expression (~27% of WT levels, $p<0.0001$) compared to wildtype receptors (Butler, Moody, *et al.,* 2017, manuscript submitted). However, the functional data for this mutation in the context of the previous mutagenesis literature strongly implicates that disrupted gating is responsible for the dysfunctional channel and not altered surface expression levels.

The *GABRA2* gene is highly expressed throughout the brain. Areas with high α2 expression include the forebrain, dentate molecular layer, CA3 of the hippocampus, the central and lateral amygdala, septum, striatum, accumbens and hypothalamus (Pirker et al., 2000). The $\alpha_2\beta_3\gamma_2$ receptors are a major $GABA_A$ receptor assembly in the brain (J. M.

Fritschy & H. Mohler, 1995). The $\alpha_2\beta_{2/3}\gamma_2$ receptors are also sensitive to modulation by benzodiazepines, a drug often used to treat seizures (Benson et al., 1998).

During embryonic and early postnatal development, α2 is highly expressed across the thalamus and cortical regions before its expression reduces later in development (Laurie et al., 1992). There is also a shift in expression levels from α2 to α1 in the basolateral amygdala in early postnatal development that affects the time course of postsynaptic $GABA_A$ receptor-mediated currents there (Ehrlich, Ryan, Hazra, Guo, & Rainnie, 2013). During the development period, there is a shift from excitatory to inhibitory GABAergic currents which correlates with the switch in the chloride transporter expression from NKCC1 (sodium-potassium-chloride cotransporter 1) to KCC2 (potassium-chloride transporter 2) (Watanabe & Fukuda, 2015). During development, high intercellular chloride concentrations causes depolarization when $GABA_A$ receptors are activated. Excitatory GABAergic signals are important for neuronal growth, neuronal differentiation, proliferation, migration, proper synapse formation and calcium influx to the neurons (Ben-Ari, Khazipov, Leinekugel, Caillard, & Gaiarsa, 1997; Zhao et al., 2011). GABAergic synapses also precede glutamatergic synapses in development, making them an important mediator in development (Ben-Ari, 2006).

The tonic activation of the mutant α2(T292K) receptors during the period when GABA is depolarizing could cause excitotoxicity. During development, depolarizing signals by GABA can activate voltage-dependent calcium channels leading to an influx in calcium (Ben-Ari, 2002). Excitotoxicity and cell death are commonly linked to excessive calcium influx into the neuron (Lipton & Nicotera, 1998). In cultured immature hippocampal neurons causes, exposure of the $GABA_A$ receptors to isoflurane caused increased Ca^{2+} influx which activated the voltage-dependent calcium channels (Zhao et al., 2011). This example of the overactivation of $GABA_A$ receptors causing excessive calcium influx, suggests that during development, the overactivation of $GABA_A$ receptors can have

deleterious effects. Since increased calcium is a critical factor of excitotoxic cell damage, it's possible that the mutation could also be causing increased cell death during development. Excessive cell death during development would have detrimental effects on the developing neuronal circuitry, even before the seizures begin postnatally. A transgenic animal model of the α2(T292K) mutation would be needed to explore these mechanisms further.

The excess excitation caused by the α2(T292K) mutation could also increase the seizure susceptibility of neurons during development. If seizures occurred in early development, they could have long-lasting consequences. The normal neonatal brain appears more susceptible to seizures, but individual neurons are more resilient to them (Ben-Ari, 2006). Specifically, immature neurons appear to be less vulnerable to cell death following prolonged seizures than in adults (Holmes & Ben-Ari, 2001). As a result, the consequences of neonatal seizures are more likely to be changes in neuronal function and circuitry rather than direct neuronal death (Ben-Ari, 2006). Seizures can also change the expression of other $GABA_A$ receptor subunits. In P9 rats (developmentally similar to a full-term neonate), inducing status epilepticus altered the expression of the α1, α2, β3, and γ2 $GABA_A$ subunit mRNAs in the hippocampus (Holopainen, 2008). The α2(T292K) mutation could be leading to compensatory changes in the expression of other $GABA_A$ receptor subunits, altering the GABAergic system.

Given that the α2 subunit is more highly expressed during development than other subunits like α1 (Laurie et al., 1992), this α2(T292K) mutation would be highly impactful during development. The seizures caused by the α2(T292K) mutation would likely have long-lasting effects on the development of neuronal circuits. As the child got older, tonic inhibitory current could even disrupt the chloride concentration gradient. This might even shift GABA signals to become excitatory in regions of high α2 expression. This shift to depolarizing GABA signals has been seen in tissue resected from patients with chronic

temporal lobe epilepsy (Huberfeld et al., 2007). Aside from disrupted GABAergic signals during development, the α2(T292K) mutation would also have long-lasting effects on the neuronal circuits as the patient got older.

The α5(V294L) mutation

The second mutation, α5(V294L), had three interesting effects on $GABA_A$ receptor function. First, the mutation enhanced the GABA apparent-affinity of $\alpha_5(V294L)\beta_2\gamma_{2s}$ receptors by approximately 10 times compared to the wildtype receptors (Figure 5.5, 5.6). Second, saturating GABA concentrations evoked whole-cell current responses with decreased amplitude. Third, GABA-evoked responses displayed an increased rate of desensitization at high GABA concentrations. In general, increases in GABA apparent-affinity (equivalent to decreased EC_{50}) can be due to enhanced binding affinity or enhanced gating. Given that this mutation is located near the channel pore in a region known to affect gating, the change in apparent-affinity is most likely due to enhanced gating, as discussed below. The results are consistent with the $\alpha_5(V294L)\beta_2\gamma_{2s}$ receptors becoming more sensitive to GABA, but due to the increased rate of desensitization, the receptors pass less current in response to GABA signals.

The α5(V294L) mutation is located in the M2 transmembrane domain. This valine (Val5', Figure 5.1) is part of the M2 sequence important to forming the pore, but the valine is not directly exposed to the lumen when the channel opens (Ueno et al., 2000; Xu & Akabas, 1996). It is conserved across the human α1-3,5 subunits, but in the other human subunits (α4, α6, β1-3, γ2 and δ) this residue is an isoleucine (Figure 5.1 for sequence alignment). Another genetic study identified a similar mutation in the α1 subunit (α1(V287L)). The patient had early-onset epileptic encephalopathy (Kodera et al., 2016). However, the only functional data showed that the α1(V287L) mutation did not alter surface expression of the receptors. Patient history for this α1(V287L) mutation showed that the seizures were not controlled by either clobazam (a 1,5-benzodiazepine) or

clorazepate (a classical 1,4-benzodiazepine). $\alpha_1\beta\gamma_2$ receptors, even with the α1(V287L) mutation should have an intact benzodiazepine site, but if this mutation caused the receptors to be overly sensitive to GABA, than further enhancement of $GABA_A$ receptors by benzodiazepines would likely not be beneficial to the patient. This patient was responsive to gabapentin. Gabapentin was first developed to mimic GABA, but acts through voltage-gated calcium channels and possibly $GABA_B$ receptors (Alles & Smith, 2016; Cheng et al., 2004; Kodera et al., 2016). This suggests that the patient in our study, with the α5(V294L) mutation, might also benefit from non-benzodiazepine treatments.

Two other *in vitro* studies of the Val5' residue in the M2 domain found changes in the GABA-evoked responses. One study performed tryptophan scanning mutagenesis of M2, including a homologous mutation of the 5' valine (α_2(V260W)). The α_2(V260W) mutation increased the GABA apparent-affinity by ~12-fold relative to wildtype receptors (Ueno et al., 2000). Another study showed that mutating this same valine (5') to a threonine in combination with the homologous residue in β1 (α1(V260T)β_1(I255T)) caused a decreased rate of desensitization (Birnir et al., 1997). Both these studies suggest that mutations of the 5' valine in M2 can alter the kinetics of the receptor's response to GABA. The electrophysiology data presented here, along with the past literature, is consistent with the α5(V263L) mutation altering the channel's gating function.

During development, the expression patterns of α5 vary by brain region. In the thalamus and diencephalon, α5 has a period of higher expression levels during development that drops adulthood (Laurie et al., 1992). In the hippocampus, α5 expression is high in development and stays high in adult rats (Laurie et al., 1992). It is possible that the α_5(V294L) mutation affected the expression of $GABA_A$ receptor subunits during development, and this contributed to a more seizure prone environment.

The α5 subunit is expressed most highly in the pyramidal hippocampal cells but also in layer 5 cortical neurons (Lee & Maguire, 2014; Pirker et al., 2000; Serwanski et al.,

2006; Winsky-Sommerer, 2009). Hippocampal pyramidal neurons express $\alpha_5\beta_3\gamma_2$ receptors that mediate extrasynaptic tonic inhibition (Caraiscos et al., 2004). Tonic inhibition is important for setting the threshold for excitability of neurons. The extrasynaptic concentrations of GABA are estimated to be in the hundreds of nanomolar range (Egawa & Fukuda, 2013; Farrant & Nusser, 2005). My experiments found that α_5(V294L)$\beta_2\gamma_2$ $GABA_A$ receptors had a GABA EC_{50} of approximately 0.24 μM. It is likely that α_5(V294L)$\beta\gamma_2$ receptors would become activated from the nanomolar concentrations of GABA in the extrasynaptic space. Since the α_5(V294L) mutated receptors desensitize faster at saturating GABA concentrations, the mutated receptors would likely enter a desensitized state rapidly in the presence of extrasynaptic GABA. Desensitization represents a GABA-bound state in which the channel is closed in the continued presence of agonist, and cannot pass current (Jones & Westbrook, 1996). Populations of desensitized receptors would not be able to pass current or respond properly to new GABA signals. This would be detrimental to α5-mediated tonic inhibition.

The α_5(V294L) mutation may make the brain more prone to seizures. Since the α5(V294L) mutation increased the receptor's sensitivity to GABA but also increased the receptor's rate of desensitization, it could cause a large portion of receptors to enter the desensitization state. This would prevent the receptors from contributing to the normal hyperpolarizing tonic current that sets the baseline threshold of excitability in the hippocampus (Farrant & Nusser, 2005). Overall, this could reduce the tonic inhibitory current and increasing the neuronal excitability in the brain. Since the hippocampus is a highly susceptible region to seizures (Holmes & Ben-Ari, 2001), an alteration that increased the excitability of the neurons would increase the chance of seizures even more.

Benzodiazepines are a common first-line treatment of seizure patients that have developed status epilepticus (Grover, Nazzal, & Hirsch, 2016). This is because seizures are caused by overexcitation, and benzodiazepines enhance $GABA_A$ receptor-mediated

inhibition. Like the other epilepsy patient with the α1(V287L) mutation (Kodera et al., 2016), benzodiazepines would probably not be therapeutically beneficial to a patient with an α5(V263L) mutation. Benzodiazepines, like midazolam, would enhance the current passed by $\alpha_5\beta_x\gamma_2$ receptors already activated by GABA in the extrasynaptic space. Enhancing the activation of receptors that are already extremely sensitive to GABA would lead to increased desensitization and reduced GABAergic current. Benzodiazepines can also alter the diffusion of $GABA_A$ receptors (Levi, Le Roux, Eugene, & Poncer, 2015). Diazepam specifically has been reported to increase the synaptic clustering of $GABA_A$ receptors (Gouzer, Specht, Allain, Shinoe, & Triller, 2014; Levi et al., 2015). Prolonged exposure to benzodiazepine therapies could further alter the synaptic clustering and further disrupt GABAergic inhibition in the affected brain. Currently, the patient with the α5(V263L) mutation has been seizure-free for 6-months a combination of zonegrane (a sulfonamide), levetiracetam (a racetam), and oxcarbazepine (blocks voltage-sensitive sodium channels), none of which directly target the $GABA_A$ receptors. Patients with similar mutations in the *GABR* genes that increase the sensitivity and rate of desensitization of the $GABA_A$ receptors might respond better to non-$GABA_A$-receptor-targeted antiepileptic drugs.

The β3(P301L) mutation

The third mutation (β3(P301L)) was identified from a 6-year-old male referred for intractable seizures and developmental delay. GABA concentration-response curves showed that the β3(P301L) mutation significantly reduced the maximum current amplitude, the Hill coefficient and the EC_{50} (Figure 5.7). Specifically, the mutation reduced the GABA apparent-affinity for $\alpha_1\beta_3$(P301L)γ_{2s} receptors by 2.4-fold. Changes in apparent-affinity can be due to altered ligand binding or gating of the channel. The mutation is located in the highly conserved region of the M2-M3 linker. The M2-M3 linker is known to be involved in coupling the agonist binding to the gating of the channel, a crucial step for

channel activation (O'Shea & Harrison, 2000; O'Shea et al., 2009). Overall, data were consistent with a mutated receptor that would pass reduced GABA-evoked currents. Based on the location of the mutation, it likely caused dysfunctional gating that reduced receptor function, but further experiments with a partial GABA agonist would confirm this.

Mutations in the M2-M3 linker have been identified in other epilepsy patients as well (Baulac et al., 2001; Janve et al., 2016; Moller et al., 2017). One study found a mutation in the M2-M3 linker region (γ2(K289M)) in a family with a type of generalized epilepsy. The $\alpha_1\beta_2\gamma_2$(K289M) receptors showed reduced GABA-evoked currents when expressed in oocytes (Baulac et al., 2001). When expressed in HEK293 cells, these receptors had faster deactivation rates and a shorter mean duration of single channel openings (M. T. Bianchi, Song, Zhang, & Macdonald, 2002). These observations are consistent with the γ2(K289M) mutation altering gating. The conserved proline in the M2-M3 linker that was mutated in my studies has been previously identified (β3(P301L)) in a female epilepsy patient with focal seizures that began at 16 months (Moller et al., 2017). However, this group showed no functional data for the β3(P301L) mutation. They did show limited functional data for the residue next to this proline, β3(Y302C), from a patient with focal seizures that began at 7 months. The $\alpha_1\beta_3$(Y302C)γ_2 receptor showed reduced GABA-evoked responses in oocytes with a GABA EC_{50} of 326μM, an EC_{50} 13-fold larger than that for wildtype $\alpha_5\beta_3\gamma_{2s}$ receptors (Moller et al., 2017). Janve and colleagues also reported a *de novo* β3(Y302C) mutation from a patient with Lennox-Geastaut epilepsy encephalopathy (Janve et al., 2016). Functional data showed reduced GABA-evoked responses from $\alpha_1\beta_3$(Y302C)γ_{2L} receptors. Single channel data showed decreased P_o, decreased frequency of openings and decreased single channel conductance, all of which would reduce channel function (Janve et al., 2016). For a mechanism, they proposed that this mutation caused dysfunctional coupling between the binding and gating domains, consistent with the role of the M2-M3 linker region (Janve et al., 2016).

The overall reduction of function in $GABA_A$ receptors containing the β3(P301L) mutation could have widespread implications in the brain. The β3 subunit is abundant in the brain. The $\alpha_1\beta_{2/3}\gamma_2$ receptors, specifically, are one of most abundant synaptic $GABA_A$ receptors in the brain (Benke et al., 1991). The β3 subunit is expressed highly in the cortex and thalamus during embryonic and early postnatal development (Laurie et al., 1992). The β3 subunit is also expressed in regions known to be involved in seizure generation (cortex, hippocampus and thalamic reticular nucleus) (Janve et al., 2016). As the brain develops into the mature brain, the β3 subunit expression is reduced as β2 expression increases (Laurie et al., 1992). A mutant receptor with dysfunctional binding-to-gating coupling could be devastating during development and tip the balance towards unbalanced excitation in the system.

5.5 Conclusions and Future Directions

The three rare mutations characterized in this chapter were α_5(V294L), α_2(T292K) and β3(P301L). They represent a growing group of *GABR* mutations linked to epilepsy. The functional data presented here provides a mechanism consistent with a link between receptor dysfunction and seizure susceptibility. However, *in vitro* data only provides molecular information about the receptor mechanism that underlies a mutation. To definitively link a mutation to the behavioral symptoms of a disease, a knock-in mouse or other transgenic model would need to be tested. Also, epilepsy is a diverse category of seizures disorders. The mutations described here represent rare variants, and at least two of which are *de novo*. This limits how the specific mechanism of action can be generalized to other epilepsy phenotypes. To examine the behavior and seizure susceptibility caused by epilepsy mutations, knock-in mice carrying the heterozygous or homozygous mutation should be created. Another reason to create transgenic animals with specific mutations is that the regional brain expression profiles of subunits can be measured.

Each *GABR* gene has a distinct expression profile in the brain. Depending on the regions where a *GABR* gene product is expressed, the effects of a mutation could have different effects on the GABAergic inhibition for that brain region. Both α2 and β3 subunits have widespread expression patterns in the brain. This makes it difficult to predict which neuronal populations affected by the mutation might lead to seizures or if the mutation only affects specific receptor populations. A mutation could also lead to altered expression patterns of the other subunits to compensate for the dysfunction subunit. This would again require a transgenic animal to explore unless human brain tissue could be acquired from the patients.

Some $GABA_A$ subunits are expressed in both synaptic and extrasynaptic receptor assemblies. If the mutant α5 and β3 subunits can associate with both synaptic and extrasynaptic $GABA_A$ receptors, then predicting how the balance of phasic and tonic

inhibition in the brain would be specifically altered to cause seizures would be complex. A future study of these mutations could take fibroblasts from the patients with these mutations and reprogram them to express as neurons. Although not the same as a brain slice from a human brain, something difficult to acquire if a mutation is rare, it would allow the subunit expression patterns to be explored.

Human epilepsy patients with rare mutations often develop seizure disorders in early childhood. Some $GABA_A$ receptor subunits are present in higher levels during development (ex. α2). Mutations in these subunits might have earlier consequences than for other subunits that increase expression later in life. For example, microRNA from human cortical samples at 8-12 weeks post-conception showed high levels of β3 and α5, suggesting a role of these subunits in development (Al-Jaberi, Lindsay, Sarma, Bayatti, & Clowry, 2015). Other studies have examined whether the development of neural circuits is changed by disease. One study examined human brain samples from patients with tuberous sclerosis complex (TSC), a complex genetic disorder including refractory epilepsy. They found evidence that the immature brain circuits persisted rather than mature and develop (Ruffolo et al., 2016).. For example, the switch from NKCC1 to KCC2 chloride transporters that underlies the switch in the $GABA_A$ receptor reversal potential, did not occur in these brain samples. This suggested that depolarizing GABA currents, a feature of immature neural circuits, remained in the affected circuits. This could have important implications for how these disease circuits respond to medications The neonatal brain is known to be highly seizure prone, and high neuronal excitability during development is important for triggering proper synaptic formation (Cellot & Cherubini, 2013). However, the lack of switching from immature to mature brain circuits will impair brain function long-term. Examining these *GABR* mutations during developmental periods might provide greater insight into which drug therapies would better treat seizures.

Each mutation studied here might benefit from slightly different pharmacological treatments. The simplest mechanism examined here was for β3(P301L) because the mutation caused the reduced GABA apparent-affinity. To enhance the mutated receptor's activity, a PAM, like benzodiazepines, would likely be a good first GABAergic treatment option. The other two mutations had mechanisms that affected the receptor's function in a way that might be harder to treat with GABAergic drugs. For example, the patient with α_5(V294L) mutation would likely not respond well to a simple $GABA_A$ receptor PAM because it would increase the number of receptor becoming desensitized, which would ultimately lower inhibition. A partial α5-targeted agonist might increase the α_5(V294L)-mutated receptor's activity without inducing large amounts of desensitization, but further studies would need to test the efficacy of such a drug. The patient with the α_2(T292K) mutation would be best treated with a non-$GABA_A$ drug because the affected receptors do not have the ability to open and close properly to begin with. These results highlight how studying novel *GABR* mutations can reveal very different mechanisms but also help personalize and improve the medical treatments for patients. Ultimately, studying these mutations will help develop new therapies to reestablish the balance between excitation and inhibition in the brain.

Chapter 6: Discussion

Chapter 6: Discussion

6.1 Summary of findings

$GABA_A$ receptors play an important role in tuning the excitability of neurons and neural circuits. Because $GABA_A$ receptors are expressed widely throughout the brain, it is not surprising that drugs targeting $GABA_A$ receptors have a wide range of effects. These effects can include altered consciousness, sedation, reduced seizures, anxiolytic effects or altered cognition. Drugs that target $GABA_A$ receptors can modulate receptor activity through different binding sites on the receptor. PAMs are a common type of modulator that enhance the activity of $GABA_A$ receptors. Examples of PAMs acting at $GABA_A$ receptors include benzodiazepines, ethanol, neuroactive steroids, and etomidate (See Introduction 1.2). The subunit composition of $GABA_A$ receptors can affect how receptors respond to PAMs and other modulators. The rationale for this thesis is that understanding the mechanisms of different PAM actions on $GABA_A$ receptors will provide a better insight to improving pharmacological therapies used to treat neurological disease.

This dissertation took steps towards understanding the subunit-specificity of the PAM actions of midazolam and hypersomnolent CSF at $GABA_A$ receptors. It also characterized three novel missense mutations found in three different pediatric cases of epilepsy. Two of these mutations provided novel characterizations of epilepsy-related mutations in the *GABRA2* and *GABRA5* genes. Since benzodiazepines are a common anti-epileptic drug, understanding how these mutations alter receptor function provides insight into whether $GABA_A$-targeted therapies will be useful or not to patients. Overall, results from this dissertation have advanced our knowledge of the pharmacological profiles of synaptic $GABA_A$ receptors and how their activity can be altered by PAMs and gene manipulations. Results from Chapters 3-5 can be summarized in the following three paragraphs.

In Chapter 3, the efficacy of midazolam was characterized across the six α subunits. Three different mutations were made within the benzodiazepine binding site of the $GABA_A$ receptor in loops A, B and C of the α subunit. Across all 18 mutations, only subtle changes were seen in the apparent-affinity of GABA for $\alpha_x\beta_2\gamma_{2s}$ receptors, as expected. When the benzodiazepine, midazolam, was applied to the mutated receptors, the mutations did, however, alter midazolam's ability to allosterically modulate the mutated $GABA_A$ receptors. The loop A mutations across α1-6 were able to dramatically abolish (R100H) or confer (H102R) midazolam responsiveness depending on the substituted residue. The presence of an arginine in the homologous position of α1(His102) within α1, α2, α3, and α5 abolished the receptor's ability to be positively modulated by midazolam. The opposite mutation (R100H) in α4 and α6 subunits could make previously insensitive receptors responsive to midazolam with up to ~100% potentiation measured for GABA-evoked currents. The loop B mutations (threonine-to-proline or proline-to-threonine) had only subtle effects on the efficacy of midazolam potentiation across α1-6. Interestingly, the loop C mutations had an α-specific pattern of effects on the efficacy of midazolam. The α1(S206I) and α2(S205I) loop C mutations decreased the efficacy of midazolam, while the α3(S230I) and α5(S209I) mutations increased the efficacy of midazolam. This novel pattern of α-specific effects on midazolam's efficacy provides new information about how loop C may play a role in determining the efficacy of benzodiazepine ligands. Novel PAM benzodiazepine site ligands that aim to discriminate α3- or α5-selective receptors might be improved by altering the ligand's ability to interact with loop C within the benzodiazepine pocket. These experiments also provided the first complete panel, to our knowledge, measuring the potentiation of midazolam at all $\alpha_x\beta_2\gamma_{2s}$ receptors containing α1-6.

Chapter 4, examined the PAM actions of hypersomnolent CSF at synaptic and extrasynaptic assemblies of the $GABA_A$ receptor. An endogenous peptide within

hypersomnolent CSF is predicted to potentiate the activity of $GABA_A$ receptors, but the molecular binding site of this activity remains unknown. Results presented here are not consistent with the active component of hypersomnolent CSF acting through the high-affinity benzodiazepine site of the $GABA_A$ receptor. For example, three key $GABA_A$ receptor assemblies ($\alpha_1\beta_2$, α_1(H102R)$\beta_2\gamma_{2s}$ and $\alpha_4\beta_2\gamma_{2s}$) showed robust CSF potentiation but normally do not show potentiation for benzodiazepines. Further measurements of the CSF potentiation at other synaptic α1-6-containing $\alpha_x\beta_2\gamma_{2s}$ receptors and extrasynaptic $\alpha_x\beta_2\delta$ receptors showed robust potentiation at all these assemblies (>100%) but with different efficacies. This new pattern of $GABA_A$ receptors sensitivity to hypersomnolent CSF modulation did not match any obvious pattern of common allosteric modulators (ex. benzodiazepines, neurosteroids, ethanol) for $GABA_A$ receptors. These results reflect the complexity of studying the molecular actions of hypersomnolent CSF on $GABA_A$ receptors and highlights the continued need for careful and systematic examination of these actions.

Until the active component in CSF is identified, multiple active components are still a possibility. The widespread potentiation seen across different combinations of α1-6-, δ- and γ-containing receptors could reflect multiple components with different overlapping patterns of subunit-specificity. A new hypothesis for how the active component of hypersomnolent CSF modulates $GABA_A$ receptors should consider the binding sites of modulators that can act at extrasynaptic receptors, like neurosteroids, or those that occur more generally in a single subunit domain. Another direction to consider should be how tonic $GABA_A$ receptor activity can be involved in sleep and consciousness. $GABA_A$ receptors found in many sleep-related centers of the brain tend to be synaptic assemblies (Table 1.1), but the thalamic relay neurons also have δ-containing receptors that mediate tonic inhibition (Jean-Marc Fritschy & Hanns Mohler, 1995). These neurons produce the thalamocortical oscillations important to various aspects of sleep architecture and consciousness (Franks & Zecharia, 2011). The potential modulation of tonic GABAergic

inhibition by hypersomnolent CSF should be considered, especially since general anesthetics like etomidate have been shown to affect tonic inhibition (Herd, Lambert, & Belelli, 2014). Finally, the PAM actions of hypersomnolent CSF may reflect a secondary effect of other molecular disruptions in the brain underlying idiopathic hypersomnia (IH). This does not rule out these actions are a potential biomarker for hypersomnia or the value of future findings that studying these actions might provide. Overall, the results in Chapter 4 highlight the complexity of studying IH, and further isolation of the CSF active component will be an important step to better understanding these molecular actions.

Finally, in Chapter 5, three novel missense *de novo* mutations in *GABRA2, GABRA5* and *GABRB3* were characterized from pediatric patients with severe forms of early-onset epilepsy. The α2(T292K) mutation disrupted $GABA_A$ receptor function by restricting the channel gating and trapping the receptor in a tonically open conformation. These receptors would be incapable of responding to a synaptic GABA event. The α5(V294L) mutation enhanced the GABA apparent-affinity of the receptors while increasing the receptor's tendency to become desensitized. In α5-extrasynaptic receptors that are already sensitive to nanomolar GABA, this would decrease the overall $GABA_A$ receptor-mediated currents. The β3(P301L) mutation decreased the GABA apparent-affinity and reduced the amplitude of GABA-evoked currents. Findings from two of these mutations, α2(T292K) and α5(V294L), provided novel mechanisms for how disrupting $GABA_A$-mediated currents in the epileptic brain can increasing seizure susceptibility. Overall, mutations in the M2 and M2-M3 linker domains appear to be harmful to $GABA_A$ receptor function and may reflect rare genetic causes for severe early-onset epilepsies.

6.2 Implications of findings for pharmacology and studying neurological disease

Results presented in this dissertation have important implications for how $GABA_A$ receptor function can be altered and modulated pharmacologically. Studying the pharmacological profile of different $GABA_A$ receptor assemblies can provide important insights into the GABAergic signaling occurring in different brain regions where those specific assemblies can be found. For example, results here found that α_3-containing receptors were very sensitive to being modulated by both midazolam (Chapter 3.3.3.3) and hypersomnolent CSF (Chapter 4.3.3). The $\alpha_3\beta_{2/3}\gamma_2$ receptors are expressed in several regions of the brain, including the thalamic reticular nucleus. The thalamic reticular nucleus provides an important inhibitory input to the thalamic relay neurons that generate the thalamocortical oscillations important to sleep (Winsky-Sommerer, 2009). The sensitivity of α3-containing receptors to allosteric modulation reflects the important role of these receptors in modulating consciousness and sleep. Alternatively, α4-containing receptors, while insensitive to midazolam's modulatory effects, can be robustly enhanced by an active component within hypersomnolent CSF samples. Since α4-containing receptors generally mediate tonic inhibition, investigating modulators that alter the activity of these exrasynaptic receptors will have important implications for how pharmacologically altering tonic inhibition may alter brain activity, sleep and consciousness.

The pharmacological results measured with midazolam across different $GABA_A$ receptors have also contributed important information about the relationship between structure and drug efficacy. His102 in loop A has been previously shown to affect the binding of benzodiazepines (H A Wieland et al., 1992), but the relationship between efficacy and other residues in loops A-C has been less studied. Efficacy is an important property affecting the overall effect of a drug. Although loop C is known to play an important role in the ligand binding of both of GABA and benzodiazepine site ligands, only recently have specific residues in loop C been linked directly to drug efficacy (Morlock &

Czajkowski, 2011). Results presented here are consistent with previous studies showing that mutations in loop C can alter benzodiazepine's efficacy. The relationship between loop C mutations, α-subunit and midazolam efficacy highlights the importance of systematically examining drugs across multiple $GABA_A$ receptor assemblies. Better understanding how benzodiazepines alter the activity of $GABA_A$ receptors is important because benzodiazepines are still widely used clinically as sedatives and anxiolytics. Novel drugs that are specifically designed to interact with loop C might provide a new method of altering drug efficacy.

Data presented in this dissertation also had important implications for how the molecular mechanisms of diseases involving ion channels are studied. The diagnosis of IH is an exclusionary diagnosis in which all other diseases and conditions must be ruled out. It is possible that the excessive daytime sleepiness across patients given a IH diagnosis may reflect different biological mechanisms, as suggested by the division of IH patients into subcategories by medication-responsiveness (Khan & Trotti, 2015). There could be two ways to approach this potential problem. One method would be to pick the most homogenous population of IH patients to study. This is based on the rationale that clinically-similar patients would likely belong to the same disease subcategory. A second method would be to accept the heterogeneity in the IH population and instead try to study the largest unbiased group of IH patients as possible and look for factors that correlate across the group to symptoms like excessive daytime sleepiness or sleep drunkenness. Both approaches have benefits. The first method has an increased probability of finding a specific biological mechanism that all patients in that subset of a IH population share. A limitation is that the mechanism might not generalize to *all* IH patients as a cause of their daytime sleepiness. The second method is more likely to uncover a more general mechanism underlying excessive sleepiness or hypersomnia that may or may not be

specific to IH patients. This would however provide novel insights to the neurobiology of sleep.

The majority of results presented in Chapter 4 used a single pooled CSF sample. It was created from randomly selected patient CSF samples that had been previously assays for $GABA_A$ receptor potentiation and had 4-5 mLs of sample available for use. While unbiased, this selection criteria did not take into account the clinical symptoms of the patients. As a result, the argument could be made that the results using the pooled CSF provided more information about the molecular actions of modulators in hypersomnolent CSF than about IH or hypersomnolence specifically. The results are still useful because the mechanism underlying the robust PAM effect of hypersomnolent CSF at $GABA_A$ receptors remains unknown. The results here provide new and important information about the molecular actions of CSF modulation at $GABA_A$ receptors. Recently, a French group published a study claiming to find no potentiation of hypersomnolent CSF samples at $GABA_A$ receptors. A closer look at their data and methods revealed factors in their experimental design that obscured their ability to measure the CSF potentiation that our group measures consistently (Moody et al., 2017). Results presented here provide a robust example of the PAM actions of CSF on $GABA_A$ receptors. The next step to understanding the molecular actions of CSF at $GABA_A$ receptors will be to isolate the active components using mass spectrometry and proteomic analysis. This will also help locate a biomarker for IH that could correlate with sleepiness or the disease severity.

It should be noted that in the seminal 2012 paper on idiopathic hypersomnia, the biological activity of CSF at $GABA_A$ receptors did not correlate with the severity of sleepiness or other sleep metrics of hypersomnia patients (Rye et al., 2012). This suggests that the enhanced biological activity in hypersomnolent CSF samples may not be a direct cause of sleepiness but may be a secondary effect of another disease-causing mechanism. This does not exclude $GABA_A$ receptor potentiation as a potential biomarker

for hypersomnia, but acknowledges the complexity of studying CSF and searching for biomarkers of disease. For example, amyloid-β protein levels have been studied extensively in Alzheimer's disease and yet the plaque load in the brain does not correlated directly with cognitive dysfunction (Morris, Clark, & Vissel, 2014). This highlights the difference between a direct molecular mechanism and a biomarker for disease. A good biomarker should be reliable, easy to measure, correlate with disease progression and is relatively cheap. A major step forward in the research of primary hypersomnia disorders would be to locate such a biomarker for IH patients. Low hypocretin levels are often measured from CSF of patients with narcolepsy type 1. Hypocretin levels provide a strong indication of narcolepsy in conjunction with certain clinical symptoms (Khan & Trotti, 2015). Until IH has a clear and reliable biomarker for disease, it will be difficult to ensure that research groups across different countries are studying homogenous IH populations.

Epilepsy is another neurological disease with a spectrum of subcategories. Identifying specific mutations in genes, like SCN1A, that correlate with specific types of epilepsy has helped expand the knowledge of how seizures and epilepsy can develop in the brain (Dravet, 2011). Unlike hypersomnia disorders, measurements from an electroencephalogram (EEG) provide distinct profiles of seizure activity across different brain regions. This combined with a list of genetic mutations that can be screened for have expanded the ability of doctors to provide both a specific diagnosis or cause for more patients than in previous decades. However, the growing list of genetic mutations found across a variety of genes (*SCN1A, SCN1B, KCNQ, SLC2A1, GABR*) has also highlighted the complexity of different types of seizures and the multiple molecular mechanisms that can cause seizures (Dhiman, 2017; Helbig, 2015).

As the number of genetic mutations linked to epilepsies increases, the simplified view of epilepsy being a disease of imbalanced excitation and inhibition in the brain becomes more complex. Examining just the mutations in a single gene family like the

GABR genes have revealed a wide variety of mechanisms for impairing protein function. Mutations in the *GABR* gene can disrupt the protein synthesis, trafficking of receptors, assembly of subunits into receptors or the direct function of receptors (Hernandez et al., 2016). Mutations that alter receptor function can disrupt function in multiple ways. For example, several *GABR* gene mutations linked to genetic epilepsy have been shown to reduce $GABA_A$ receptor function by altering the receptor gating despite being located in different structural regions of the $GABA_A$ receptor (Hernandez et al., 2016).

Results presented in Chapter 5, highlight how three different *GABR* mutations located in similar structural domains can alter GABA-evoked currents in different ways. The α2(T292K) and α5(V294L) mutations were both located in M2, while β3(P301L) was located nearby in the M2-M3 linker domain. Of the α5(V294L) and α2(T292K) mutations, only α2(T292K) appeared to lock the channel in an open position. The α5(V294L) and β3(P301L) mutations instead altered the apparent-affinity of GABA. The β3(P301L) mutation reduced the GABA apparent-affinity, and α5(V294L) enhanced it. At first glance, these mutations appear to have opposing effects on $GABA_A$ receptor function, but a closer look at the increased desensitization of the α5(V294L) mutation suggests that both mutations would likely reduce the GABA-evoked currents at the synaptic level. These results highlight how many different ways $GABA_A$ receptor function can be altered to causes even a single type of neurological disease.

When measuring the molecular effects of mutations on $GABA_A$ receptors, other factors should also be considered when predicting the effects of the mutation at the neuronal excitability level. The expression patterns and the tendency of each subunit to assemble with other subunits affects the contributions of the mutated subunit to $GABA_A$ receptor function and the overall inhibition. For example, the α5 subunit is expressed on the pyramidal cells of the hippocampus and tends to form extrasynaptic receptors that mediate tonic GABAergic current. A dysfunctional α5 subunit might disrupt the tonic

inhibition in the hippocampus and raise the level of excitability of these neurons. The β3 subunit is widely expressed in the brain in both synaptic and extrasynaptic assemblies of $GABA_A$ receptors. A dysfunctional β3 subunit would likely have wide spread effects on both synaptic and tonic inhibition. Even if both the β3(P301L) and α5(V294L) mutations reduced GABA-evoked currents *in vitro*, further studies would be needed to measure how these mutations alter the balance of synaptic and extrasynaptic of inhibition in the epileptic brain and alter neuronal excitability.

Predicting the effects of *GABR* mutations on the GABAergic neurotransmission during development is even more complicated. During development, the *GABR* gene expression patterns are different from those in the mature brain. For example, a mutation in a *GABR* gene like *GABRA2* (α2) is more likely to affect GABAergic signaling early on because its expression levels are higher during development in regions like the thalamus and cortex (Laurie et al., 1992). Taking into account that $GABA_A$ receptors mediate depolarizing currents at the ealry stages of development, also complicates the predictions of these *GABR* mutations on the development of the neural circuitry. Early-onset epilepsies can be severe, as seen in two of the cases of the pediatric patients whose mutations were described here (Chapter 5.3.1). Whether these severe seizure phenotypes are caused by a mutation that affects the GABAergic signaling when it is depolarizing or hyperpolarizing is difficult to predict without a transgenic animal model. A *GABR* mutation of a subunit highly expressed during development does not immediately suggest that extensive neuronal death would occur. Immature neurons are slightly more resilient to neuronal death caused by overexcitation than mature neurons (Ben-Ari, 2002), but depending on the mutation, neuronal death might still occur. Such a *GABR* mutation could have complex effects on the development of the neuronal circuitry and possibly the excitability of the developing neurons. Also, a mutation in one *GABR* subunit might affect the expression of other subunits, which could have compensatory effects on the

GABAergic system. Again, a transgenic animal model would be needed to better understand how severe *GABR* mutations alter the developing neuronal circuitry of the brain and causes a more seizure prone brain. Treating an epileptic brain in which genetic mutations and prolonged seizure activity have altered the neuronal circuitry from development onwards can be complicated when most drugs actions are tested *in vitro* or on normal brain circuitry. By understanding how the developing brain is changed by such a mutation, new therapies can be developed based on the altered neural circuitry.

Finally, investigating the GABAergic molecular mechanisms underlying hypersomnia and epilepsy highlights the important relationship between sleep and epilepsy. Pool sleep quality, difficulty sleeping or excessive daytime sleepiness are 2-3 times more common in adults with epilepsy than healthy people (Grigg-Damberger & Ralls, 2014). Sleep disturbances have also been shown to be linked to insufficiently controlled epilepsy (Unterberger et al., 2015). In addition, sleep deprivation is a known trigger for seizures, dependent on the type of seizure, type of epilepsy and the individual's susceptibility (Grigg-Damberger & Ralls, 2014).On the other hand, excessive daytime sleepiness is also a common complaint among people with epilepsy and is sometimes blamed on antiepileptic drugs (Grigg-Damberger & Ralls, 2014). However, a recent clinical trial found that the antiepileptic drug, lacosamide, did not affect daytime sleepiness (Foldvary-Schaefer et al., 2017). The sleep disturbances reported in epilepsy underline the relationship between seizure state, consciousness and arousal state.

There are different changes in sleep architecture reported in people with epilepsy. These include reduced REM sleep, increased wake after sleep and reduced sleep efficiency (Grigg-Damberger & Ralls, 2014). Because there are certain types of epilepsy that occur during sleep (ex. nocturnal frontal lobe epilepsy) and others that occur primarily upon awakening from sleep (ex. juvenile myoclonic epilepsy), the arousal state of a person clearly affects the brain's susceptibility to different types of seizures. For example, sleep

spindles, K-complexes and slow wave activity in non-REM sleep can promote interictal epileptiform discharges or seizure propagation (Grigg-Damberger & Ralls, 2014). However, seizure activity, even in sleep-related epilepsy, represents a different state of consciousness than sleep. Drugs like benzodiazepines, that alter consciousness and induce sedation-hypnosis, can be used to treat seizures, but benzodiazepines and general anesthetics do not induce natural sleep (Brown, Lydic, & Schiff, 2010). This highlights the common theme in which enhancing GABAergic inhibition can alter consciousness, as seen with benzodiazepines, general anesthetics, and *GABR* mutations reported in seizure disorders. Yet, it is important to recognize that the GABAergic balance in the brain is complex, and mechanisms that increase GABAergic inhibition and alter arousal/consciousness (ex. benzodiazepines and *GABR* mutations) can have very different effects on brain function and consciousness.

6.3 Final Conclusions

The mechanisms by which $GABA_A$ receptor activity can be altered vary widely from pharmacological intervention to mutations. Results from this dissertation have examined the mechanisms of $GABA_A$ receptors involved in benzodiazepine modulation, hypersomnolent CSF modulation and rare genetic mutations of the *GABR* genes from patients with epilepsy. Major findings include the role of specific mutations in the benzodiazepine site that affect midazolam's efficacy at $GABA_A$ receptors. Second, the endogenous modulator in hypersomnolent CSF is not acting through the high-affinity benzodiazepine-site of the $GABA_A$ receptor. Third, seizure disorders have multiple mechanisms through which $GABA_A$-mediated currents can be disrupted. Overall, these findings underline the complexity of $GABA_A$ receptor pharmacology and function across the many different receptor assemblies. Since many drug therapies target the $GABA_A$ receptors, it is also not surprising that when $GABA_A$-mediated inhibition is disrupted it can

result in neurological disease. Understanding the actions of modulators and genetic mutations across multiple $GABA_A$ receptors can offer new ways to improve existing pharmacological therapies to treat neurological disease.

Appendices A-D:

Appendix A:

Drug exposure protocols and Clampex protocols:

Included in Appendix A:

1. Protocol 1. GABA concentration-response curves (8 concentrations at 3.5 logarithmic intervals)
2. Protocol 2. Midazolam concentration-response curves (5 midazolam concentrations, 2 GABA control peaks)
3. Protocol 3. Measuring the effective GABA concentration (EC_n)of the patched cell:
4. Protocol 4: Measuring potentiation with CSF (2mL of 50% CSF) (4 CSF samples)
5. Protocol 5: Measuring CSF potentiation with pre- and post-GABA exposures
6. Images of patch clamp rigs

GABA Concentration-Response Curve:

Protocol 1. GABA concentration-response curves (8 concentrations at 3.5 logarithmic intervals)

Setup of Drug Solutions:

Tubes	Drug Solution
1	Extracellular solution
2	[GABA] 1
3	[GABA] 2
4	[GABA] 3
5	[GABA] 4
6	[GABA] 5
7	[GABA] 6
8	[GABA] 7
9	[GABA] 8
10	Extracellular solution

Clampex Protocol Name: "DRC_10secupsweep"			
Step	A	B	C
First level	1	2	1
Delta level	0	1	0
Duration (ms)	200	400	200
200=1sec 400 samples = 2000ms			
Sweeps/run = 8			
Samples/sweep/signal	2048 pts = 10.24 sec		
Interval (µs): 5000 = 200Hz			

Which rig set up used: Rig 1

Midazolam Concentration-Response Curve

Protocol 2. Midazolam concentration-response curves (5 midazolam concentrations, 2 GABA control peaks)

To measure peak currents at increasing concentrations of midazolam (5 concentrations from 10-1000nM). The extra GABA step after midazolam exposure makes for cleaner and faster decay/washout of peaks (seconds not minutes). For receptors with higher GABA sensitivities (A4-6) sometimes the washout period was extended by lengthening the sweep length to 15-16sec.

Setup of drug solutions:

Tubes	Drug Solution	Pump
1	Extracellular solution	Pump 1 – 10 syringe
2	EC_{10} GABA	
3	EC_{10} GABA	
4	EC_{10} GABA + [MDZ] 1	
5	EC_{10} GABA + [MDZ] 2	
6	EC_{10} GABA + [MDZ] 3	
7	EC_{10} GABA + [MDZ] 4	
8	EC_{10} GABA + [MDZ] 5	
9	Extracellular solution	
10	Extracellular solution	
11	Extracellular solution	Pump 2 – 10 syringe
12	EC_{10} GABA	
13	Max GABA	
14	Extracellular solution	
15	Extracellular solution	Pump 3 – 2 syringe
16	Extracellular solution	

*MDZ = midazolam

Clampex Protocol Name: "MDZ_DRC"				
Step	A	B	C	D
First level	1	2	2	1
Delta level	0	1	0	0
Duration (ms)	200			
200=1sec 400 samples = 2000ms				
Sweeps/run = _____				
Samples/sweep/signal	_____= _____sec			
Interval (µs): 5000 = 200Hz				

Which rig set up used: Rig 1

Protocol 3. Measuring the effective GABA concentration (EC_n)of the patched cell:

Clampex Protocol Name: EC_11-14			
Step	A	B	C
First level	11	12	11
Delta level	0	1	0
Duration (ms)	200	400	200
200=1sec 400 samples = 2000ms			
Sweeps/run = 2			
Samples/sweep/signal	2800 = 14 sec		
Interval (µs): 5000 = 200Hz			

Which rig set up used: Rig 1

*Same drug setup as above for midazolam concentration-response curves

Midazolam Drug Preparation for *in vitro* Experiments:

Note: "Stock" MZD refers to "pure" midazolam from bottle.

MW	= 362.23	g/mol
Water solubility	= 0.024	mg/ml
Stock concentration	= 5 mg/ml	= 0.0138M

10uM (0.010mM) stock

5mL Slosh + 3.62uL Midazolam (13.8mM bottle)

Solution #	**Stock MZD (M)**	**Final concentration (uM)**	**final volume (ml)**	**Stock to add(uL)**
1	10uM dilution	10 nM	100	100uL
2	10uM dilution	20 nM	100	200uL
3	10uM dilution	50 nM	100	500uL
4	0.0138 M	100 nM	100	0.72
5	0.0138 M	200 nM	100	1.45
6	0.0138 M	500 nM	100	3.62
7	0.0138 M	1 uM	50	3.62
8	0.0138 M	2 uM	40	5.80
9	0.0138 M	5 uM	40	14.49
6	0.0138 M	10 uM	40	28.9

Cerebrospinal fluid assay – Setup Version 1

Protocol 4: Measuring potentiation with CSF (2mL of 50% CSF) (4 CSF samples)

Set up of drug solutions:

Tubes	Drug Solution
14	Extracellular solution
13	EC_{10} GABA
12	Extracellular solution
11	EC_{10} GABA + CSF #1
10	Extracellular solution
9	EC_{10} GABA + CSF #2
8	Extracellular solution
7	EC_{10} GABA + CSF #3
6	Extracellular solution
5	EC_{10} GABA + CSF #4
4	Extracellular solution
3	Max GABA
2	Extracellular solution
1	Extracellular solution

Clampex Protocol Name: AJCSFep7			
Step	A	B	C
First level	14	13	12
Delta level	-2	-2	-2
Duration (ms)	300	3000	1000
200=1sec 400 samples = 2000ms			
Sweeps/run = 6			
Samples/sweep/signal	2048 = 10.24 sec		
Interval (µs): 5000 = 200Hz			

Goal: To measure the potentiation of 4 different CSF samples.
Which rig set up used: Rig 2 (CSF rig)

Clampex Protocol Name: AJCSFep7_EC			
Step	A	B	C
First level	14	13	12
Delta level	0	-10	0
Duration (ms)	300	3000	1000
200=1sec 400 samples = 2000ms			
Sweeps/run = 2			
Samples/sweep/signal	2048 = 10.24 sec		
Interval (µs): 5000 = 200Hz			

Goal: Measuring EC_n value of the cell for pre-/post CSF assay
Which rig set up used: Rig 2 (CSF rig)

Cerebrospinal fluid assay – Setup Version 2

Protocol 5: Measuring CSF potentiation with pre- and post-GABA exposures

Set up of drug solutions:

Tubes	Drug Solution
14	Extracellular solution
13	EC_{10} GABA
12	EC_{10} GABA
11	EC_{10} GABA + CSF #1
10	EC_{10} GABA
9	EC_{10} GABA
8	Extracellular solution
7	Max [GABA]

Clampex Protocol Name: CSF mutations_EC			
Step	A	B	C
First level	14	13	14
Delta level	0	-5	0
Duration (ms)	300	3000	1000
200=1sec 400 samples = 2000ms			
Sweeps/run = 2			
Samples/sweep/signal	2048 = 10.24 sec		
Interval (µs): 5000 = 200Hz			

Which rig set up used: Rig 2 (CSF rig)

Clampex Protocol Name: CSF mutations_EC			
Step	A	B	C
First level	14	13	14
Delta level	0	-1	0
Duration (ms)	300	3000	1000
200=1sec 400 samples = 2000ms			
Sweeps/run = 4 or 5			
Samples/sweep/signal	2048 = 10.24 sec		
Interval (µs): 5000 = 200Hz			

Which rig set up used: Rig 2 (CSF rig)

Patch clamp rig setups:

Rig 1 = consists of 2 10-infusion KD Scientific pumps (holding 10mL syringes) and one 2-infusion pump (holding 60mL syringes).

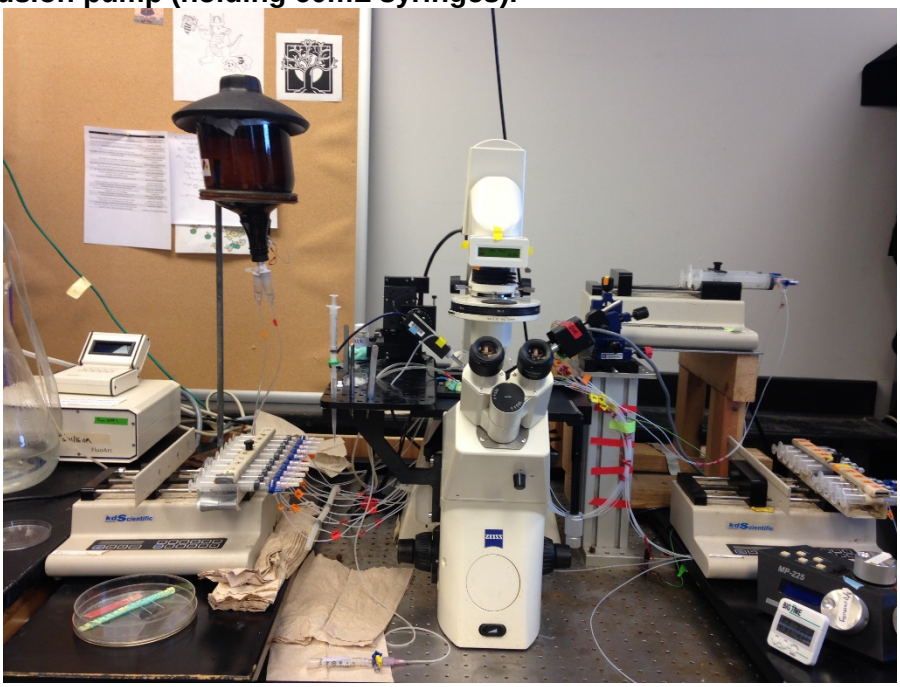

Rig 2 = consists of one 10-infusion pump (holding 10mL syringes) and two 2-infusion pumps (holding 3mL syringes).

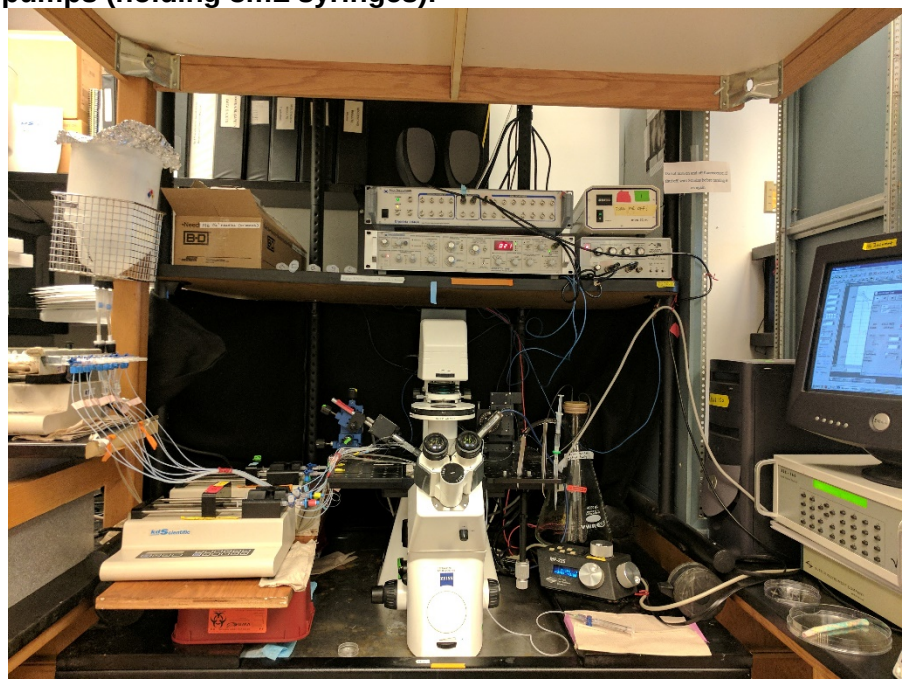

Appendix B:
Matlab scripts

Matlab scripts included below:

1. DRC_thesis
2. MDZ_trace
3. MDZ_ECpeaks
4. DRC_thesis_desensitizationMeasure_epilepsyV294L
5. CSF_mutations_4peaks
6. Picrotoxin_a2T292K_v2

Script 1:

Name: DRC_thesis

Function of code: To analyze and create GABA concentration-response curves using the Hill equation

```
%Code used to produce identical graphs of Averaged Trace and a DRC Curve
%for each hA1-A6 GABA DRC to be used in thesis/posters... March 31, 2016 OM
close ALL
clear ALL

%directories for programs and data
homedir='C:\Users\Olivia Moody\Documents\MATLAB';
datadir='C:\Users\Olivia Moody\Desktop\Analyze_This';
%counters reset / constants:
episodexaxis=(1:2048)';
%concentrations=[0.3 1 3 10 30 100 300 1000];  %A1 uM   %Pick concentration range
concentrations=[0.1 0.3 1 3 10 30 100 300]; %A2-A3 uM
%concentrations=[0.01 0.03 0.1 0.3 1 3 10 30];   %A5-A6
%concentrations=[0.003 0.01 0.03 0.1 0.3 1 3 10];   %A5(V294L)
%concentrations=[0.03 0.1 0.3 1 3 10 30 100]; %A4 uM
episode = 1;
resultrowcounter=1;
results=[];
dataz=[];
rawdataz=[];
%how many files to analyze? = filetotal
cd (datadir);
filestoanalyze=dir('*.abf');
filetotal=length(filestoanalyze);
for filecounter = 1:filetotal;
   filenumber=strtok(filestoanalyze(filecounter).name, '.');
   [d, si, h] = abfload(filestoanalyze(filecounter).name);
   sizeoffile=size(d);
    episodexaxis=(1:sizeoffile(1,1))';
%    A1=sizeoffile(1,1);
   episod=sizeoffile(3);
   for episode = 1:episod;
      rawcurrent=d(:,1,episode);
      startmean=mean(rawcurrent(1:21));
      endmean=mean(rawcurrent(2028:2048));
      mgrad = (endmean-startmean)/2028;

%       endmean=mean(rawcurrent(2779:2800));
%       mgrad = (endmean-startmean)/2779;

      c=startmean - (mgrad*10);
      leak=c + mgrad*episodexaxis;
      LScurrent=rawcurrent - leak;
      [lspeaki, lspeakpsn]=min(LScurrent);
      LSpeak=mean(LScurrent((lspeakpsn-10):(lspeakpsn+10)));
      %results(resultrowcounter, 1)=filenumber;
      results(resultrowcounter, 2)=episode;
      results(resultrowcounter, 3)=LSpeak;
      results(resultrowcounter, 4)=filecounter;
      dataz=cat(1,dataz, LScurrent);
```

```
        rawdataz=cat(1, rawdataz, rawcurrent);
        resultrowcounter=resultrowcounter+1;
        filelist(filecounter,:)=filenumber;
    end
    conc=concentrations';
    wcc= results(resultrowcounter-8:resultrowcounter-1, 3);
    modelFun= @(p,x) p(1).*( x.^p(2))./(x.^p(2) + p(3).^p(2));
    startingVals = [-4000, 1.5, 8];
    coefEsts = nlinfit(conc, wcc, modelFun, startingVals);
    crcrez=coefEsts;
    %crcfits(filecounter, 1) = real(filenumber);
    crcfits(filecounter, 2) = real(crcrez(1));
    crcfits(filecounter, 3) = real(crcrez(2));
    crcfits(filecounter, 4) = real(crcrez(3));
    crcfits(filecounter, 5) = filecounter;
    results(resultrowcounter-8:resultrowcounter-1,5)=100*results(resultrowcounter-
8:resultrowcounter-1,3)/crcfits(filecounter,2);

end
%r=results(:,3);
EC50=mean(crcfits(:,4))
raw_results = reshape(results(:,3),8,filetotal);
rn=results(:,5);
rnn=reshape(rn,8,filetotal);
normalized_results = mean(rnn,2)';
normalized_std = std(rnn');
SEM = normalized_std/sqrt(filetotal);
GABA = concentrations;
time= 5e-3:5e-3:81.92*filetotal;
error = std(rnn')/sqrt(filetotal); %calculate SEM
current= (reshape(results(:,3),8,filecounter));
%%%%%%%% Averaged trace of all files %%%%%%%%
avg_dataz=reshape(dataz(:,1),2048*8,filetotal);
AVG_dataz = mean(avg_dataz,2);

figure2 = figure(2);
set(figure(2), 'units', 'inches', 'pos', [0 0 8 10])
axes2 = axes('Parent',figure2,'XColor','w','YColor','w','ZColor','w');
hold(axes2,'on');

plot(AVG_dataz,'k');

% Create xlabel     %xlabel('Time (sec)','FontSize',14);
% Create ylabel     %ylabel('Current (pA)','FontSize',14);

% Create title
title('Averaged Trace','FontSize',16);

hold on
calx=[2000 2000 3000];% 5sec
caly=[-1000 -1500 -1500];%500pA
plot(calx, caly,'k','lineWidth',3)
saveas(gcf,'Avg_trace')
%%print -depsc   %trying to save as vector-based file
print -djpeg -r600 -f2 Avg_trace
```

```
%%%%%%%%%%%%%%%%%%%%%%%%%%%%%%%%%%%%%%%%%%%%%% Fit sigmoidal
(Hill equation) to
% DRC curve of normalized DRC ("curve fit by eye and has no theoretical value"
norm_points= normalized_results;
omp_error= SEM;
conc=concentrations;   %GABA concentrations.
hillfn= @(p,x) 100.*(x.^p(1))./(x.^p(1)+p(2).^(p(1)));  %Hill equation that MATLAB is going to use
to try and fit
startvals=[2, 30];  %these are the starting values MATLAB will use when trying to fit a line to. "fit
by eye line"
logxaxis=-4:0.005:4;
xaxes=10.^logxaxis; %creates an x-axis with enough dots when plotted on log scale.
loop=1;
   echill=nlinfit(conc, norm_points(loop,:), hillfn, startvals);
   fitline1=100.*xaxes.^echill(1)./(xaxes.^echill(1)+echill(2).^echill(1));

figure3=figure(3);
set(figure(3), 'units', 'inches', 'pos', [0 0 8 6])
% Create axes
axes3 = axes('Parent',figure3,'YGrid','on','ZColor',[0 0 0],...
   'YColor',[0 0 0],'XMinorTick','on','XScale','log','XTick',[0.001 0.01 0.1 1 10 100 1000 10000],...
   'XTickLabel',['0.001', '0.01', '0.1', '1', '10', '100', '1000', '10000'],...
   'XColor',[0 0 0],'YTick', [20 40 60 80 100 120],'FontSize',16);
xlim(axes3,[0.001 10000])

hold(axes3,'on');
%Add Error bars with SEM
errorbar(GABA,normalized_results,SEM,'ko','MarkerFaceColor','k','MarkerSize',6,'LineWidth',2)
hold on
semilogx(xaxes,fitline1,'k','LineWidth',3)

xlabel('[GABA] (microMolar)','FontSize',16);            % Create xlabel
ylabel('Percent of Maximum Current (%)','FontSize',16);    % Create ylabel
%title('Concentration-Response Curve','FontSize',16);   % Create title
saveas(gcf,'Curve')
print -djpeg -r600 -f3 Sigmoidal
```

Script 2:

Name: MDZ_trace

Function of code: To analyze midazolam traces from concentration-response curves (only calculates peak current amplitudes)

```
%Goal: For Matlab to plot Dataz from multiple files with different episode lengths.
clear ALL
close ALL

%directories for programs and data
homedir='C:\Users\Olivia Moody\Documents\MATLAB';
datadir='C:\Users\Olivia Moody\Desktop\Analyze_This';
cd (datadir);
filestoanalyze=dir('*.abf');
filetotal=length(filestoanalyze);
A1=2379; %12 sec
A2=2400;
%B1=2979;    %15 sec sweep
%B2=3000;
%counters reset / constants:
%episodexaxis=(1:2048)';
episode = 1;
resultrowcounter=1;
results=[];
dataz=[];
rawdataz=[];
for filecounter = 1:filetotal;
   filenumber=strtok(filestoanalyze(filecounter).name, '.');
   [d, si, h] = abfload(filestoanalyze(filecounter).name);
   sizeoffile=size(d);
   episod=sizeoffile(3);
   A=size(d(:,1)); %Episode Length determined
   A=A(1,1);
   episodeax=(1:A)';
   for episode = 1:episod;
      rawcurrent=d(:,1,episode);
      startmean=mean(rawcurrent(1:21));
      endmean=mean(rawcurrent(A1:A2));
      mgrad = (endmean-startmean)/(A1);
      c=startmean - (mgrad*10);
      leak=c + mgrad*episodeax;
      LScurrent=rawcurrent - leak;
      [lspeaki, lspeakpsn]=min(LScurrent);
      LSpeak=mean(LScurrent((lspeakpsn-10):(lspeakpsn+10)));
      results(resultrowcounter, 2)=episode;
      results(resultrowcounter, 3)=LSpeak;
      results(resultrowcounter, 4)=filecounter;
      dataz=cat(1,dataz, LScurrent);
      rawdataz=cat(1, rawdataz, rawcurrent);
      resultrowcounter=resultrowcounter+1;
      %filelist(filecounter,:)=filenumber;
   end
end
table_raw = reshape(results(:,3),episod,filecounter)';
```

Script 3:

Name of code: MDZ_ECpeaks

Function of code: Measure two peaks (EC_{10} and Max GABA) to determine EC_n value.

```
clear ALL
close ALL

%directories for programs and data
homedir='C:\Users\Olivia Moody\Documents\MATLAB';
datadir='C:\Users\Olivia Moody\Desktop\Analyze_This';
%counters reset / constants:
episodexaxis=(1:2048)'; %10.24 sec
%episodexaxis=(1:2800)';  %14 sec
%episodexaxis=(1:3000)';  %15 sec
%episodexaxis=(1:2400)'; %12 sec

episode = 1;
resultrowcounter=1;
results=[];
dataz=[];
rawdataz=[];
%how many files to analyze? = filetotal
cd (datadir);
filestoanalyze=dir('*.abf');
filetotal=length(filestoanalyze);
A1=2048;
A2=2028;
%B1=2800;
%B2=2779;
%CC1=3000;
%CC2=2979;
%D1=2400;
%D2=2379;

for filecounter = 1:filetotal;
    filenumber=strtok(filestoanalyze(filecounter).name, '.');
    [d, si, h] = abfload(filestoanalyze(filecounter).name);
    sizeoffile=size(d);
    episod=sizeoffile(3);
    for episode = 1:episod;
        rawcurrent=d(:,1,episode);
        startmean=mean(rawcurrent(1:21));
        endmean=mean(rawcurrent(A2:A1));
        mgrad = (endmean-startmean)/A2;
        c=startmean - (mgrad*10);
        leak=c + mgrad*episodexaxis;
        LScurrent=rawcurrent - leak;
        [lspeaki, lspeakpsn]=min(LScurrent);
        LSpeak=mean(LScurrent((lspeakpsn-10):(lspeakpsn+10)));
        %results(resultrowcounter, 1)=filenumber;
        results(resultrowcounter, 2)=episode;
        results(resultrowcounter, 3)=LSpeak;
        results(resultrowcounter, 4)=filecounter;
        dataz=cat(1,dataz, LScurrent);
```

```
        rawdataz=cat(1, rawdataz, rawcurrent);
        resultrowcounter=resultrowcounter+1;
        filelist(filecounter,:)=filenumber;
    end
    %%%% Andy's code to normalize the peaks to the final peak (MAX).

    norman=results(resultrowcounter-1,3);
    lastprotocolpeaks=results(resultrowcounter-episod:resultrowcounter-1,3);
    normprotocolpeaks=100*lastprotocolpeaks/norman;
    results(resultrowcounter-episod:resultrowcounter-1,5)=normprotocolpeaks;

end
time= 5e-3:5e-3:81.92*filetotal;
%plot(time,dataz)
results(:,5)
table=reshape(results(:,5),episode,filecounter)';

table_raw=reshape(results(:,3),episode,filecounter)';
```

Script 4:

Name: DRC_thesis_desensitizationMeasure_epilepsyV294L

Function of code: to analyze desensitization of α5(V294L)-receptors from GABA concentration-response curve data.

```
%Goal: to measure desensitization on Epilepsy mutation a5(V294L) which has
%very spiky peaks. June 28 2017 OM
close ALL
clear ALL

%directories for programs and data
homedir='C:\Users\Olivia Moody\Documents\MATLAB';
datadir='C:\Users\Olivia Moody\Desktop\Analyze_This';
%counters reset / constants:
episodexaxis=(1:2048)';
%concentrations=[0.01 0.03 0.1 0.3 1 3 10 30];   %A5-A6
concentrations=[0.003 0.01 0.03 0.1 0.3 1 3 10];   %A5(V294L)

episode = 1;
resultrowcounter=1;
results=[];
dataz=[];
rawdataz=[];
%how many files to analyze? = filetotal
cd (datadir);
filestoanalyze=dir('*.abf');
filetotal=length(filestoanalyze);
for filecounter = 1:filetotal;
   filenumber=strtok(filestoanalyze(filecounter).name, '.');
   [d, si, h] = abfload(filestoanalyze(filecounter).name);
   sizeoffile=size(d);
   episodexaxis=[1:sizeoffile(1,1)]';   %this is length of sweep
   lengthSweep=sizeoffile(1,1);
   Sweeps(filecounter,1)=lengthSweep;
   episod=sizeoffile(3);
   for episode = 1:episod;
      rawcurrent=d(:,1,episode);
      startmean=mean(rawcurrent(1:21));
      endmean=mean(rawcurrent((lengthSweep-21):lengthSweep));
      mgrad = (endmean-startmean)/(lengthSweep-21);
      c=startmean - (mgrad*10);
      leak=c + mgrad*episodexaxis;
      LScurrent=rawcurrent - leak;
      [lspeaki, lspeakpsn]=min(LScurrent);
      LSpeak=mean(LScurrent((lspeakpsn-10):(lspeakpsn+10)));
      % Isolate the beginning of peak and end of peak during GABA exposure
      Peakstart=min(LScurrent(400:500)); %Ignore the positive gains btw start and end because
we are currently only interested in desensitization
      Peakend = min(LScurrent(650:750)); %assume 2.5 sec drug exposure
      %results(resultrowcounter, 1)=filenumber;
      %PeakMeasures: resultrowcounter, Peakstart, Peakend,
      %Peakstart-Peakend, LSpeak, (Peakstart-Peakend)/LSpeak*100, episode
      results(resultrowcounter, 2)=episode;
      results(resultrowcounter, 3)=LSpeak;
      results(resultrowcounter, 4)=filecounter;
      PeakMeasures(resultrowcounter,1)=resultrowcounter;
```

```
        PeakMeasures(resultrowcounter,2)=Peakstart;
        PeakMeasures(resultrowcounter,3)=LSpeak;
        PeakMeasures(resultrowcounter,4)=Peakend;
        PeakMeasures(resultrowcounter,5)= LSpeak-Peakend;
        PeakMeasures(resultrowcounter,6)=LSpeak;
        PeakMeasures(resultrowcounter,7)=(LSpeak-Peakend)/LSpeak*100;    %Must normalize to
each GABA peak to account for differences in Whole-cell Current Amplitudes
        PeakMeasures(resultrowcounter,8)=episode;
        %PeakMeasures(resultrowcounter,9)=(LSpeak-Peakstart);
        %PeakMeasures(resultrowcounter,10)=(LSpeak-Peakstart)/LSpeak*100;
        dataz=cat(1,dataz, LScurrent);
        rawdataz=cat(1, rawdataz, rawcurrent);


        resultrowcounter=resultrowcounter+1;
        filelist(filecounter,:)=filenumber;
    end
    conc=concentrations';
    wcc= results(resultrowcounter-8:resultrowcounter-1, 3);
    modelFun= @(p,x) p(1).*( x.^p(2))./(x.^p(2) + p(3).^p(2));
    startingVals = [-4000, 1.5, 8];
    coefEsts = nlinfit(conc, wcc, modelFun, startingVals);
    crcrez=coefEsts;
    %crcfits(filecounter, 1) = real(filenumber);
    crcfits(filecounter, 2) = real(crcrez(1));
    crcfits(filecounter, 3) = real(crcrez(2));
    crcfits(filecounter, 4) = real(crcrez(3));
    crcfits(filecounter, 5) = filecounter;
    results(resultrowcounter-8:resultrowcounter-1,5)=100*results(resultrowcounter-
8:resultrowcounter-1,3)/crcfits(filecounter,2);

end

%r=results(:,3);
EC50=mean(crcfits(:,4))
rn=results(:,5);
rnn=reshape(rn,8,filetotal);
normalized_results = mean(rnn,2)';
normalized_std = std(rnn');
SEM = normalized_std/sqrt(filetotal);
GABA = concentrations;
time= 5e-3:5e-3:81.92*filetotal;
error = std(rnn')/sqrt(filetotal); %calculate SEM
current= (reshape(results(:,3),8,filecounter));
XX=reshape(PeakMeasures(:,7),8,filecounter);
XXX=XX';
```

Script 5:

Name: CSF_mutations_4peaks

Function of code: To analyze CSF modulation (two pre-control GABA, 1 CSF+GABA peak, 1 post-control GABA peak)

```
clear ALL; close ALL
  %Jan 10, 2017 OM
% This code assumes you are running CSF files from mutations +CSF
% experiments where CSF run = GABA, GABA, GABA+CSF, GABA peaks
homedir='C:\Users\Olivia Moody\Documents\MATLAB';
datadir='C:\Users\Olivia Moody\Desktop\Analyze_This';
episodexaxis=(1:2048)';
episode = 1; resultrowcounter=1; results=[]; dataz=[]; rawdataz=[];
cd (datadir);
filestoanalyze=dir('*.abf');
filetotal=length(filestoanalyze);
for filecounter = 1:filetotal;
   filenumber=strtok(filestoanalyze(filecounter).name, '.');
   [d, si, h] = abfload(filestoanalyze(filecounter).name);
   sizeoffile=size(d);
   episod=sizeoffile(3);
   A=size(d(:,1)); %Episode Length determined
   A=A(1,1);
   for episode = 1:episod;
      rawcurrent=d(:,1,episode);
      startmean=mean(rawcurrent(1:21));
       endmean=mean(rawcurrent((2048-21):2048));
      mgrad = (endmean-startmean)/(2048-21);
      c=startmean - (mgrad*10);
      leak=c + mgrad*(1:2048)'; % must be in 1:2048 form to avoid square step btw sweeps
      LScurrent=rawcurrent - leak;
      [lspeaki, lspeakpsn]=min(LScurrent);
      LSpeak=mean(LScurrent((lspeakpsn-10):(lspeakpsn+10)));
      %results(resultrowcounter, 1)=filenumber;
      results(resultrowcounter, 2)=episode;
      results(resultrowcounter, 3)=LSpeak;
      results(resultrowcounter, 4)=filecounter;
      dataz=cat(1,dataz, LScurrent);
      rawdataz=cat(1, rawdataz, rawcurrent);
      resultrowcounter=resultrowcounter+1;
      filelist(filecounter,:)=filenumber;
   end
   %%%% Andy's code to normalize the peaks to the final peak (MAX).
   norman=results(resultrowcounter-1,3);
   lastprotocolpeaks=results(resultrowcounter-episod:resultrowcounter-1,3);
   normprotocolpeaks=100*lastprotocolpeaks/norman;
   results(resultrowcounter-episod:resultrowcounter-1,5)=normprotocolpeaks;
end
results(:,5)
table=reshape(results(:,5),episode,filecounter)';
table_raw = zeros(episode,filecounter);
table_raw=reshape(results(:,3),episode,filecounter)'; %reshaping peak currents into table
AAA=table_raw';
```

Script 6:

Name: Picrotoxin_a2T292K_v2

Function of code: Measure size of peaks where picrotoxin blocked leak current (upwards peaks)

```
clear ALL; close ALL  %March 31, 2017 OM   Epilepsy Mutation
% This is for picrotoxin that blocks leak current of tonically open
% a2(T292K) receptors - so peaks are going upwards - 1, 10, 100uM (3peaks)
homedir='C:\Users\Olivia Moody\Documents\MATLAB';
datadir='C:\Users\Olivia Moody\Desktop\Analyze_This';
episodexaxis=(1:240)';      %Sweeps = 12sec (3 sec drugs)
episode = 1; resultrowcounter=1; results=[]; dataz=[]; rawdataz=[];
cd (datadir);
filestoanalyze=dir('*.abf');
filetotal=length(filestoanalyze);
for filecounter = 1:filetotal;
   filenumber=strtok(filestoanalyze(filecounter).name, '.');
   [d, si, h] = abfload(filestoanalyze(filecounter).name);
   sizeoffile=size(d);
   episod=sizeoffile(3);
   A=size(d(:,1)); %Episode Length determined
   A=A(1,1);
   for episode = 1:episod;
      rawcurrent=d(:,1,episode);
      startmean=mean(rawcurrent(1:21));
       endmean=mean(rawcurrent((2400-21):2400));
      mgrad = (endmean-startmean)/(2400-21);
      c=startmean - (mgrad*10);
      leak=c + mgrad*(1:2400)';    % must be in 1:2048 form to avoid square step btw sweeps
      LScurrent=rawcurrent - leak;
      [lspeaki, lspeakpsn]=max(LScurrent);
      LSpeak=mean(LScurrent((lspeakpsn-10):(lspeakpsn+10)));
      %results(resultrowcounter, 1)=filenumber;
      results(resultrowcounter, 2)=episode;
      results(resultrowcounter, 3)=LSpeak;
      results(resultrowcounter, 4)=filecounter;
      dataz=cat(1,dataz, LScurrent);
      rawdataz=cat(1, rawdataz, rawcurrent);
      resultrowcounter=resultrowcounter+1;
      filelist(filecounter,:)=filenumber;
   end
   %%%% Andy's code to normalize the peaks to the final peak (MAX).
   norman=results(resultrowcounter-1,3);
   lastprotocolpeaks=results(resultrowcounter-episod:resultrowcounter-1,3);
   normprotocolpeaks=100*lastprotocolpeaks/norman;
   results(resultrowcounter-episod:resultrowcounter-1,5)=normprotocolpeaks;
end
results(:,5)
table=reshape(results(:,5),episode,filecounter)';
table_raw = zeros(episode,filecounter);
table_raw=reshape(results(:,3),episode,filecounter)'; %reshaping peak currents into table
AAA=table_raw';
```

Appendix C:
Pipette pulling program

Sutter P-97 micropipette puller
Pipettes for whole-cell recordings of HEK293T:

	Heat	**Pull**	**Velocity**	**Time**
Pressure = 500				
	710	5	95	250
	710	5	95	250
	710	5	95	250
	710	35	129	250

Pipettes gave resistances of 2-8 MΩ when filled and placed in extracellular solution.

Appendix D:

Example of sequencing a mutated cDNA plasmid to confirm successful site-directed mutagenesis

Example from a sequencing file of the α1(H102R) mutation when sequenced by the T7 forward primer:

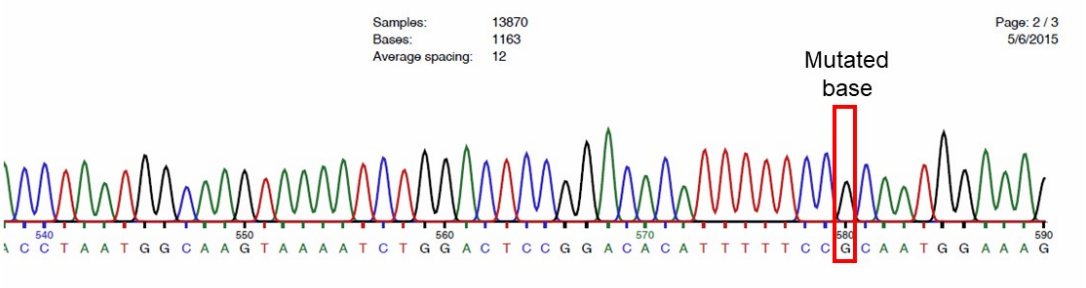

α1(H102R) mutation:

	Peptide sequence	Nucleotide sequence
Wildtype	dtffHngkk	ccg gac aca ttt ttc cAc aat gga aag aag tca gtg gc
Mutated	dtffRngkk	ccg gac aca ttt ttc cGc aat gga aag aag tca gtg gc

Figure D. Example of the sequencing file received from Eurofins MWG Operon. The sequence was acquired by sequencing the pcDNA 3.1+ plasmid containing an insert for the α1 open reading frame. In this example, the α1(H102R) mutation was produced by mutating an alanine to a guanine. This sequencing file was acquired by sequencing the insert using the forward T7 primer. Mutated inserts were also sequenced from the reverse direction to confirm the full fidelity of the insert.

References:

Abramian, A. M., Comenencia-Ortiz, E., Vithlani, M., Tretter, E. V., Sieghart, W., Davies, P. A., & Moss, S. J. (2010). Protein kinase C phosphorylation regulates membrane insertion of GABAA receptor subtypes that mediate tonic inhibition. *J Biol Chem, 285*(53), 41795-41805. doi:10.1074/jbc.M110.149229

Achermann, G., Ballard, T. M., Blasco, F., Broutin, P. E., Buttelmann, B., Fischer, H., . . . Wichmann, J. (2009). Discovery of the imidazo[1,5-a][1,2,4]-triazolo[1,5-d][1,4]benzodiazepine scaffold as a novel, potent and selective GABA(A) alpha5 inverse agonist series. *Bioorg Med Chem Lett, 19*(19), 5746-5752. doi:10.1016/j.bmcl.2009.07.153

Akabas, M. H., Stauffer, D. A., Xu, M., & Karlin, A. (1992). Acetylcholine receptor channel structure probed in cysteine-substitution mutants. *Science, 258*(5080), 307-310.

Al-Jaberi, N., Lindsay, S., Sarma, S., Bayatti, N., & Clowry, G. J. (2015). The early fetal development of human neocortical GABAergic interneurons. *Cereb Cortex, 25*(3), 631-645. doi:10.1093/cercor/bht254

Alles, S. R., & Smith, P. A. (2016). The Anti-Allodynic Gabapentinoids: Myths, Paradoxes, and Acute Effects. *Neuroscientist*. doi:10.1177/1073858416628793

Amin, J., Brooks-Kayal, A., & Weiss, D. S. (1997). Two tyrosine residues on the alpha subunit are crucial for benzodiazepine binding and allosteric modulation of gamma-aminobutyric acidA receptors. *Mol Pharmacol, 51*(5), 833-841.

Anderson, K. N., Pilsworth, S., Sharples, L. D., Smith, I. E., & Shneerson, J. M. (2007). Idiopathic hypersomnia: a study of 77 cases. *Sleep, 30*(10), 1274-1281.

Angelotti, T. P., & Macdonald, R. L. (1993). Assembly of GABAA receptor subunits: alpha 1 beta 1 and alpha 1 beta 1 gamma 2S subunits produce unique ion channels with dissimilar single-channel properties. *J Neurosci, 13*(4), 1429-1440.

Atack, J. R. (2011). GABAA receptor subtype-selective modulators. II. alpha5-selective inverse agonists for cognition enhancement. *Curr Top Med Chem, 11*(9), 1203-1214.

Atack, J. R., Wafford, K. A., Tye, S. J., Cook, S. M., Sohal, B., Pike, A., . . . McKernan, R. M. (2006). TPA023 [7-(1,1-dimethylethyl)-6-(2-ethyl-2H-1,2,4-triazol-3-ylmethoxy)-3-(2-fluorophenyl)-1,2,4-triazolo[4,3-b]pyridazine], an agonist selective for alpha2- and alpha3-containing GABAA receptors, is a nonsedating anxiolytic in rodents and primates. *J Pharmacol Exp Ther, 316*(1), 410-422. doi:10.1124/jpet.105.089920

Barnard, E. A., Skolnick, P., Olsen, R. W., Mohler, H., Sieghart, W., Biggio, G., . . . Langer, S. Z. (1998). International Union of Pharmacology. XV. Subtypes of gamma-aminobutyric acidA receptors: classification on the basis of subunit structure and receptor function. *Pharmacol Rev, 50*(2), 291-313.

Bassetti, C. L., Baumann, C. R., Dauvilliers, Y., Croyal, M., Robert, P., & Schwartz, J. C. (2010). Cerebrospinal fluid histamine levels are decreased in patients with narcolepsy and excessive daytime sleepiness of other origin. *J Sleep Res, 19*(4), 620-623. doi:10.1111/j.1365-2869.2010.00819.x

Baulac, S., Huberfeld, G., Gourfinkel-An, I., Mitropoulou, G., Beranger, A., Prud'homme, J. F., . . . LeGuern, E. (2001). First genetic evidence of GABA(A) receptor dysfunction in epilepsy: a mutation in the gamma2-subunit gene. *Nat Genet, 28*(1), 46-48. doi:10.1038/88254

Ben-Ari, Y. (2002). Excitatory actions of gaba during development: the nature of the nurture. *Nat Rev Neurosci, 3*(9), 728-739. doi:10.1038/nrn920

Ben-Ari, Y. (2006). Basic developmental rules and their implications for epilepsy in the immature brain. *Epileptic Disord, 8*(2), 91-102.

Ben-Ari, Y., Khazipov, R., Leinekugel, X., Caillard, O., & Gaiarsa, J. L. (1997). GABAA, NMDA and AMPA receptors: a developmentally regulated 'menage a trois'. *Trends Neurosci, 20*(11), 523-529.

Benke, D., Fritschy, J. M., Trzeciak, A., Bannwarth, W., & Mohler, H. (1994). Distribution, prevalence, and drug binding profile of gamma-aminobutyric acid type A receptor subtypes differing in the beta-subunit variant. *J Biol Chem, 269*(43), 27100-27107.

Benke, D., Mertens, S., Trzeciak, A., Gillessen, D., & Mohler, H. (1991). GABAA receptors display association of gamma 2-subunit with alpha 1- and beta 2/3-subunits. *J Biol Chem, 266*(7), 4478-4483.

Benson, J. A., Low, K., Keist, R., Mohler, H., & Rudolph, U. (1998). Pharmacology of recombinant gamma-aminobutyric acidA receptors rendered diazepam-insensitive by point-mutated alpha-subunits. *FEBS Lett, 431*(3), 400-404.

Bera, A. K., & Akabas, M. H. (2005). Spontaneous thermal motion of the GABA(A) receptor M2 channel-lining segments. *J Biol Chem, 280*(42), 35506-35512. doi:10.1074/jbc.M504645200

Berezhnoy, D., Nyfeler, Y., Gonthier, A., Schwob, H., Goeldner, M., & Sigel, E. (2004). On the benzodiazepine binding pocket in GABAA receptors. *J Biol Chem, 279*(5), 3160-3168. doi:10.1074/jbc.M311371200

Berjukow, S., Doring, F., Froschmayr, M., Grabner, M., Glossmann, H., & Hering, S. (1996). Endogenous calcium channels in human embryonic kidney (HEK293) cells. *Br J Pharmacol, 118*(3), 748-754.

Bianchi, M. T., Botzolakis, E. J., Lagrange, A. H., & Macdonald, R. L. (2009). Benzodiazepine modulation of GABA(A) receptor opening frequency depends on activation context: A patch clamp and simulation study. *Epilepsy research, 85*(2-3), 212-220. doi:10.1016/j.eplepsyres.2009.03.007

Bianchi, M. T., Song, L., Zhang, H., & Macdonald, R. L. (2002). Two different mechanisms of disinhibition produced by GABAA receptor mutations linked to epilepsy in humans. *J Neurosci, 22*(13), 5321-5327. doi:20026554

Billiard, M., & Sonka, K. (2016). Idiopathic hypersomnia. *Sleep Med Rev, 29*, 23-33. doi:10.1016/j.smrv.2015.08.007

Birnir, B., Tierney, M. L., Lim, M., Cox, G. B., & Gage, P. W. (1997). Nature of the 5' residue in the M2 domain affects function of the human alpha 1 beta 1 GABAA receptor. *Synapse, 26*(3), 324-327. doi:10.1002/(sici)1098-2396(199707)26:3<324::aid-syn13>3.0.co;2-v

Blair, L. A., Levitan, E. S., Marshall, J., Dionne, V. E., & Barnard, E. A. (1988). Single subunits of the GABAA receptor form ion channels with properties of the native receptor. *Science, 242*(4878), 577-579.

Bloom, F. E., & Iversen, L. L. (1971). Localizing 3H-GABA in nerve terminals of rat cerebral cortex by electron microscopic autoradiography. *Nature, 229*(5287), 628-630.

Boileau, A. J., Li, T., Benkwitz, C., Czajkowski, C., & Pearce, R. A. (2003). Effects of gamma2S subunit incorporation on GABAA receptor macroscopic kinetics. *Neuropharmacology, 44*(8), 1003-1012.

Boillot, M., Morin-Brureau, M., Picard, F., Weckhuysen, S., Lambrecq, V., Minetti, C., . . . Baulac, S. (2015). Novel GABRG2 mutations cause familial febrile seizures. *Neurol Genet, 1*(4), e35. doi:10.1212/nxg.0000000000000035

Bormann, J. (1988). Electrophysiology of GABAA and GABAB receptor subtypes. *Trends Neurosci, 11*(3), 112-116.

Bormann, J. (1991). Electrophysiological characterization of diazepam binding inhibitor (DBI) on GABAA receptors. *Neuropharmacology, 30*(12B), 1387-1389.

Bormann, J., Hamill, O. P., & Sakmann, B. (1987). Mechanism of anion permeation through channels gated by glycine and gamma-aminobutyric acid in mouse cultured spinal neurones. *J Physiol, 385*, 243-286.

Botzolakis, E. J., Gurba, K. N., Lagrange, A. H., Feng, H. J., Stanic, A. K., Hu, N., & Macdonald, R. L. (2016). Comparison of gamma-Aminobutyric Acid, Type A (GABAA), Receptor alphabetagamma and alphabetadelta Expression Using Flow Cytometry and Electrophysiology: EVIDENCE FOR ALTERNATIVE SUBUNIT STOICHIOMETRIES AND ARRANGEMENTS. *J Biol Chem, 291*(39), 20440-20461. doi:10.1074/jbc.M115.698860

Bracamontes, J. R., Li, P., Akk, G., & Steinbach, J. H. (2014). Mutations in the main cytoplasmic loop of the GABA(A) receptor alpha4 and delta subunits have opposite effects on surface expression. *Mol Pharmacol, 86*(1), 20-27. doi:10.1124/mol.114.092791

Brejc, K., van Dijk, W. J., Klaassen, R. V., Schuurmans, M., van Der Oost, J., Smit, A. B., & Sixma, T. K. (2001). Crystal structure of an ACh-binding protein reveals the ligand-binding domain of nicotinic receptors. *Nature, 411*(6835), 269-276. doi:10.1038/35077011

Brinker, T., Stopa, E., Morrison, J., & Klinge, P. (2014). A new look at cerebrospinal fluid circulation. *Fluids Barriers CNS, 11*, 10. doi:10.1186/2045-8118-11-10

Brown, E. N., Lydic, R., & Schiff, N. D. (2010). General Anesthesia, Sleep, and Coma. *New England Journal of Medicine, 363*(27), 2638-2650. doi:doi:10.1056/NEJMra0808281

Buhr, A., Schaerer, M. T., Baur, R., & Sigel, E. (1997). Residues at positions 206 and 209 of the alpha1 subunit of gamma-aminobutyric AcidA receptors influence affinities for benzodiazepine binding site ligands. *Mol Pharmacol, 52*(4), 676-682.

Buhr, A., & Sigel, E. (1997). A point mutation in the gamma2 subunit of gamma-aminobutyric acid type A receptors results in altered benzodiazepine binding site specificity. *Proc Natl Acad Sci U S A, 94*(16), 8824-8829.

Buhr, A., Wagner, C., Fuchs, K., Sieghart, W., & Sigel, E. (2001). Two novel residues in M2 of the gamma-aminobutyric acid type A receptor affecting gating by GABA and picrotoxin affinity. *J Biol Chem, 276*(11), 7775-7781. doi:10.1074/jbc.M008907200

Caraiscos, V. B., Elliott, E. M., You-Ten, K. E., Cheng, V. Y., Belelli, D., Newell, J. G., . . . Orser, B. A. (2004). Tonic inhibition in mouse hippocampal CA1 pyramidal neurons is mediated by alpha5 subunit-containing gamma-aminobutyric acid type A receptors. *Proc Natl Acad Sci U S A, 101*(10), 3662-3667. doi:10.1073/pnas.0307231101

Carver, C. M., & Reddy, D. S. (2016). Neurosteroid Structure-Activity Relationships for Functional Activation of Extrasynaptic deltaGABA(A) Receptors. *J Pharmacol Exp Ther, 357*(1), 188-204. doi:10.1124/jpet.115.229302

Cellot, G., & Cherubini, E. (2013). Functional role of ambient GABA in refining neuronal circuits early in postnatal development. *Front Neural Circuits, 7*, 136. doi:10.3389/fncir.2013.00136

Cheng, J. K., Lee, S. Z., Yang, J. R., Wang, C. H., Liao, Y. Y., Chen, C. C., & Chiou, L. C. (2004). Does gabapentin act as an agonist at native GABA(B) receptors? *J Biomed Sci, 11*(3), 346-355. doi:10.1159/000077103

Christian, C. A., Herbert, A. G., Holt, R. L., Peng, K., Sherwood, K. D., Pangratz-Fuehrer, S., . . . Huguenard, J. R. (2013). Endogenous positive allosteric modulation of GABA(A) receptors by diazepam binding inhibitor. *Neuron, 78*(6), 1063-1074. doi:10.1016/j.neuron.2013.04.026

Colquhoun, D. (1998). Binding, gating, affinity and efficacy: the interpretation of structure-activity relationships for agonists and of the effects of mutating receptors. *Br J Pharmacol, 125*(5), 924-947.

Comenencia-Ortiz, E., Moss, S. J., & Davies, P. A. (2014). Phosphorylation of GABAA receptors influences receptor trafficking and neurosteroid actions. *Psychopharmacology (Berl), 231*(17), 3453-3465. doi:10.1007/s00213-014-3617-z

Cortelli, P., Avallone, R., Baraldi, M., Zeneroli, M. L., Mandrioli, J., Corsi, L., . . . Montagna, P. (2005). Endozepines in recurrent stupor. *Sleep Med Rev, 9*(6), 477-487. doi:10.1016/j.smrv.2005.07.003

Cravatt, B. F., Prospero-Garcia, O., Siuzdak, G., Gilula, N. B., Henriksen, S. J., Boger, D. L., & Lerner, R. A. (1995). Chemical characterization of a family of brain lipids that induce sleep. *Science, 268*(5216), 1506-1509.

Crestani, F., Keist, R., Fritschy, J. M., Benke, D., Vogt, K., Prut, L., . . . Rudolph, U. (2002). Trace fear conditioning involves hippocampal alpha5 GABA(A) receptors. *Proc Natl Acad Sci U S A, 99*(13), 8980-8985. doi:10.1073/pnas.142288699

Crestani, F., Low, K., Keist, R., Mandelli, M., Mohler, H., & Rudolph, U. (2001). Molecular targets for the myorelaxant action of diazepam. *Mol Pharmacol, 59*(3), 442-445.

Crestani, F., Martin, J. R., Mohler, H., & Rudolph, U. (2000). Mechanism of action of the hypnotic zolpidem in vivo. *Br J Pharmacol, 131*(7), 1251-1254. doi:10.1038/sj.bjp.0703717

Cromer, B. A., Morton, C. J., & Parker, M. W. (2002). Anxiety over GABA(A) receptor structure relieved by AChBP. *Trends Biochem Sci, 27*(6), 280-287.

Dalziel, J. E., Birnir, B., Everitt, A. B., Tierney, M. L., Cox, G. B., & Gage, P. W. (1999). A threonine residue in the M2 region of the beta1 subunit is needed for expression of functional alpha1beta1 GABA(A) receptors. *Eur J Pharmacol, 370*(3), 345-348.

Dauvilliers, Y., Delallee, N., Jaussent, I., Scholz, S., Bayard, S., Croyal, M., . . . Robert, P. (2012). Normal cerebrospinal fluid histamine and tele-methylhistamine levels in hypersomnia conditions. *Sleep, 35*(10), 1359-1366. doi:10.5665/sleep.2114

Dauvilliers, Y., Evangelista, E., Lopez, R., Barateau, L., Jaussent, I., Cens, T., . . . Charnet, P. (2016). Absence of gamma-aminobutyric acid-a receptor potentiation in central hypersomnolence disorders. *Ann Neurol*. doi:10.1002/ana.24710

Davies, P. A., Hoffmann, E. B., Carlisle, H. J., Tyndale, R. F., & Hales, T. G. (2000). The influence of an endogenous beta3 subunit on recombinant GABA(A) receptor assembly and pharmacology in WSS-1 cells and transiently transfected HEK293 cells. *Neuropharmacology, 39*(4), 611-620.

Derry, J. M., Dunn, S. M., & Davies, M. (2004). Identification of a residue in the gamma-aminobutyric acid type A receptor alpha subunit that differentially affects diazepam-sensitive and -insensitive benzodiazepine site binding. *J Neurochem, 88*(6), 1431-1438.

Dhiman, V. (2017). Molecular Genetics of Epilepsy: A Clinician's Perspective. *Ann Indian Acad Neurol, 20*(2), 96-102. doi:10.4103/aian.AIAN_447_16

Dias, R., Sheppard, W. F., Fradley, R. L., Garrett, E. M., Stanley, J. L., Tye, S. J., . . . Reynolds, D. S. (2005). Evidence for a significant role of alpha 3-containing GABAA receptors in mediating the anxiolytic effects of benzodiazepines. *J Neurosci, 25*(46), 10682-10688. doi:10.1523/jneurosci.1166-05.2005

Diviney, M., Reynolds, J. P., & Henshall, D. C. (2015). Comparison of short-term effects of midazolam and lorazepam in the intra-amygdala kainic acid model of status epilepticus in mice. *Epilepsy Behav, 51*, 191-198. doi:10.1016/j.yebeh.2015.07.038

Dixon, C., Sah, P., Lynch, J. W., & Keramidas, A. (2014). GABAA receptor alpha and gamma subunits shape synaptic currents via different mechanisms. *J Biol Chem, 289*(9), 5399-5411. doi:10.1074/jbc.M113.514695

Draguhn, A., Verdorn, T. A., Ewert, M., Seeburg, P. H., & Sakmann, B. (1990). Functional and molecular distinction between recombinant rat GABAA receptor subtypes by Zn2+. *Neuron, 5*(6), 781-788.

Draguhn, A., Verdorn, T. A., Ewert, M., Seeburg, P. H., & Sakmann, B. (1990). Functional and molecular distinction between recombinant rat GABAA receptor subtypes by Zn2+. *Neuron, 5*(6), 781-788. doi:http://dx.doi.org/10.1016/0896-6273(90)90337-F

Dravet, C. (2011). Dravet syndrome history. *Dev Med Child Neurol, 53 Suppl 2*, 1-6. doi:10.1111/j.1469-8749.2011.03964.x

DuBridge, R. B., Tang, P., Hsia, H. C., Leong, P. M., Miller, J. H., & Calos, M. P. (1987). Analysis of mutation in human cells by using an Epstein-Barr virus shuttle system. *Molecular and Cellular Biology, 7*(1), 379-387. Retrieved from http://www.ncbi.nlm.nih.gov/pmc/articles/PMC365079/

Duncalfe, L. L., Carpenter, M. R., Smillie, L. B., Martin, I. L., & Dunn, S. M. (1996). The major site of photoaffinity labeling of the gamma-aminobutyric acid type A receptor by [3H]flunitrazepam is histidine 102 of the alpha subunit. *J Biol Chem, 271*(16), 9209-9214.

Eaton, M. M., Bracamontes, J., Shu, H. J., Li, P., Mennerick, S., Steinbach, J. H., & Akk, G. (2014). gamma-aminobutyric acid type A alpha4, beta2, and delta subunits assemble to produce more than one functionally distinct receptor type. *Mol Pharmacol, 86*(6), 647-656. doi:10.1124/mol.114.094813

Egawa, K., & Fukuda, A. (2013). Pathophysiological power of improper tonic GABA(A) conductances in mature and immature models. *Front Neural Circuits, 7*, 170. doi:10.3389/fncir.2013.00170

Eghbali, M., Curmi, J. P., Birnir, B., & Gage, P. W. (1997). Hippocampal GABA(A) channel conductance increased by diazepam. *Nature, 388*(6637), 71-75. doi:10.1038/40404

Ehrlich, D. E., Ryan, S. J., Hazra, R., Guo, J. D., & Rainnie, D. G. (2013). Postnatal maturation of GABAergic transmission in the rat basolateral amygdala. *J Neurophysiol, 110*(4), 926-941. doi:10.1152/jn.01105.2012

Essrich, C., Lorez, M., Benson, J. A., Fritschy, J. M., & Luscher, B. (1998). Postsynaptic clustering of major GABAA receptor subtypes requires the gamma 2 subunit and gephyrin. *Nat Neurosci, 1*(7), 563-571. doi:10.1038/2798

Farrant, M., & Nusser, Z. (2005). Variations on an inhibitory theme: phasic and tonic activation of GABA(A) receptors. *Nat Rev Neurosci, 6*(3), 215-229. doi:10.1038/nrn1625

Farzampour, Z., Reimer, R. J., & Huguenard, J. (2015). Endozepines. *Adv Pharmacol, 72*, 147-164. doi:10.1016/bs.apha.2014.10.005

Foldvary-Schaefer, N., Neme-Mercante, S., Andrews, N., Bruton, M., Wang, L., Morrison, S., . . . Grigg-Damberger, M. (2017). Wake up to sleep: The effects of lacosamide on daytime sleepiness in adults with epilepsy. *Epilepsy Behav, 75*, 176-182. doi:10.1016/j.yebeh.2017.08.002

Foote, S. L., Bloom, F. E., & Aston-Jones, G. (1983). Nucleus locus ceruleus: new evidence of anatomical and physiological specificity. *Physiological Reviews, 63*(3), 844-914. Retrieved from http://physrev.physiology.org/content/physrev/63/3/844.full.pdf

Franks, N. P. (2008). General anaesthesia: from molecular targets to neuronal pathways of sleep and arousal. *Nat Rev Neurosci, 9*(5), 370-386. doi:10.1038/nrn2372

Franks, N. P., & Zecharia, A. Y. (2011). Sleep and general anesthesia. *Can J Anaesth, 58*(2), 139-148. doi:10.1007/s12630-010-9420-3

Fritschy, J. M., & Mohler, H. (1995). GABAA-receptor heterogeneity in the adult rat brain: differential regional and cellular distribution of seven major subunits. *J Comp Neurol, 359*(1), 154-194. doi:10.1002/cne.903590111

Fritschy, J. M., & Mohler, H. (1995). GABAA-receptor heterogeneity in the adult rat brain: Differential regional and cellular distribution of seven major subunits. *Journal of Comparative Neurology, 359*(1), 154-194.

Fuchs, K., Zezula, J., Slany, A., & Sieghart, W. (1995). Endogenous [3H]flunitrazepam binding in human embryonic kidney cell line 293. *Eur J Pharmacol, 289*(1), 87-95.

Gingrich, K. J., Roberts, W. A., & Kass, R. S. (1995). Dependence of the GABAA receptor gating kinetics on the alpha-subunit isoform: implications for structure-function relations and synaptic transmission. *J Physiol, 489 (Pt 2)*, 529-543.

Glass, P. S., Bloom, M., Kearse, L., Rosow, C., Sebel, P., & Manberg, P. (1997). Bispectral analysis measures sedation and memory effects of propofol, midazolam, isoflurane, and alfentanil in healthy volunteers. *Anesthesiology, 86*(4), 836-847.

Gouzer, G., Specht, C. G., Allain, L., Shinoe, T., & Triller, A. (2014). Benzodiazepine-dependent stabilization of GABA(A) receptors at synapses. *Mol Cell Neurosci, 63*, 101-113. doi:10.1016/j.mcn.2014.10.004

Graham, F. L., Smiley, J., Russell, W. C., & Nairn, R. (1977). Characteristics of a human cell line transformed by DNA from human adenovirus type 5. *J Gen Virol, 36*(1), 59-74. doi:10.1099/0022-1317-36-1-59

Granot, R., Berkovic, S. F., Patterson, S., Hopwood, M., Drummer, O. H., & Mackenzie, R. (2004). Endozepine stupor: disease or deception? A critical review. *Sleep, 27*(8), 1597-1599.

Gravielle, M. C. (2016). Activation-induced regulation of GABAA receptors: Is there a link with the molecular basis of benzodiazepine tolerance? *Pharmacol Res, 109*, 92-100. doi:10.1016/j.phrs.2015.12.030

Griebel, G., Perrault, G., Simiand, J., Cohen, C., Granger, P., Decobert, M., . . . Scatton, B. (2001). SL651498: an anxioselective compound with functional selectivity for alpha2- and alpha3-containing gamma-aminobutyric acid(A) (GABA(A)) receptors. *J Pharmacol Exp Ther, 298*(2), 753-768.

Grigg-Damberger, M. M., & Ralls, F. (2014). Sleep disorders in adults with epilepsy: past, present, and future directions. *Curr Opin Pulm Med, 20*(6), 542-549. doi:10.1097/mcp.0000000000000101

Grover, E. H., Nazzal, Y., & Hirsch, L. J. (2016). Treatment of Convulsive Status Epilepticus. *Curr Treat Options Neurol, 18*(3), 11. doi:10.1007/s11940-016-0394-5

Gundry, R. L., White, M. Y., Murray, C. I., Kane, L. A., Fu, Q., Stanley, B. A., & Van Eyk, J. E. (2009). Preparation of proteins and peptides for mass spectrometry analysis in a bottom-up proteomics workflow. *Curr Protoc Mol Biol, Chapter 10*, Unit10.25. doi:10.1002/0471142727.mb1025s88

Gurley, D., Amin, J., Ross, P. C., Weiss, D. S., & White, G. (1995). Point mutations in the M2 region of the alpha, beta, or gamma subunit of the GABAA channel that abolish block by picrotoxin. *Receptors Channels, 3*(1), 13-20.

Hadingham, K. L., Garrett, E. M., Wafford, K. A., Bain, C., Heavens, R. P., Sirinathsinghji, D. J., & Whiting, P. J. (1996). Cloning of cDNAs encoding the human gamma-aminobutyric acid type A receptor alpha 6 subunit and characterization of the pharmacology of alpha 6-containing receptors. *Mol Pharmacol, 49*(2), 253-259.

Han, S., Tai, C., Jones, C. J., Scheuer, T., & Catterall, W. A. (2014). Enhancement of inhibitory neurotransmission by GABAA receptors having alpha2,3-subunits ameliorates

behavioral deficits in a mouse model of autism. *Neuron, 81*(6), 1282-1289. doi:10.1016/j.neuron.2014.01.016

Hanson, S. M., & Czajkowski, C. (2008). Structural mechanisms underlying benzodiazepine modulation of the GABA(A) receptor. *J Neurosci, 28*(13), 3490-3499. doi:10.1523/jneurosci.5727-07.2008

Hanson, S. M., Morlock, E. V., Satyshur, K. A., & Czajkowski, C. (2008). Structural requirements for eszopiclone and zolpidem binding to the gamma-aminobutyric acid type-A (GABAA) receptor are different. *J Med Chem, 51*(22), 7243-7252. doi:10.1021/jm800889m

Harrison, N. L. (2007). Mechanisms of sleep induction by GABA(A) receptor agonists. *J Clin Psychiatry, 68 Suppl 5*, 6-12.

He, B., & Soderlund, D. M. (2010). Human embryonic kidney (HEK293) cells express endogenous voltage-gated sodium currents and Na v 1.7 sodium channels. *Neurosci Lett, 469*(2), 268-272. doi:10.1016/j.neulet.2009.12.012

Heidelberg, L. S., Warren, J. W., & Fisher, J. L. (2013). SB-205384 is a positive allosteric modulator of recombinant GABAA receptors containing rat alpha3, alpha5, or alpha6 subunit subtypes coexpressed with beta3 and gamma2 subunits. *J Pharmacol Exp Ther, 347*(1), 235-241. doi:10.1124/jpet.113.207324

Helbig, I. (2015). Genetic Causes of Generalized Epilepsies. *Semin Neurol, 35*(3), 288-292. doi:10.1055/s-0035-1552922

Herd, M. B., Lambert, J. J., & Belelli, D. (2014). The general anaesthetic etomidate inhibits the excitability of mouse thalamocortical relay neurons by modulating multiple modes of GABAA receptor-mediated inhibition. *Eur J Neurosci, 40*(3), 2487-2501. doi:10.1111/ejn.12601

Hernandez, C. C., Klassen, T. L., Jackson, L. G., Gurba, K., Hu, N., Noebels, J. L., & Macdonald, R. L. (2016). Deleterious Rare Variants Reveal Risk for Loss of GABAA Receptor Function in Patients with Genetic Epilepsy and in the General Population. *PLoS One, 11*(9), e0162883. doi:10.1371/journal.pone.0162883

Hernandez, C. C., Kong, W., Hu, N., Zhang, Y., Shen, W., Jackson, L., . . . Macdonald, R. L. (2017). Altered Channel Conductance States and Gating of GABAA Receptors by a Pore Mutation Linked to Dravet Syndrome. *eNeuro, 4*(1). doi:10.1523/eneuro.0251-16.2017

Holewinski, R. J., Jin, Z., Powell, M. J., Maust, M. D., & Van Eyk, J. E. (2013). A fast and reproducible method for albumin isolation and depletion from serum and cerebrospinal fluid. *Proteomics, 13*(5), 743-750. doi:10.1002/pmic.201200192

Holmes, G. L., & Ben-Ari, Y. (2001). The neurobiology and consequences of epilepsy in the developing brain. *Pediatr Res, 49*(3), 320-325. doi:10.1203/00006450-200103000-00004

Holopainen, I. E. (2008). Seizures in the developing brain: cellular and molecular mechanisms of neuronal damage, neurogenesis and cellular reorganization. *Neurochem Int, 52*(6), 935-947. doi:10.1016/j.neuint.2007.10.021

Horsburgh, A., & Massoud, T. F. (2013). The circumventricular organs of the brain: conspicuity on clinical 3T MRI and a review of functional anatomy. *Surg Radiol Anat, 35*(4), 343-349. doi:10.1007/s00276-012-1048-2

Huberfeld, G., Wittner, L., Clemenceau, S., Baulac, M., Kaila, K., Miles, R., & Rivera, C. (2007). Perturbed chloride homeostasis and GABAergic signaling in human temporal lobe epilepsy. *J Neurosci, 27*(37), 9866-9873. doi:10.1523/jneurosci.2761-07.2007

Hubner, C. A., & Holthoff, K. (2013). Anion transport and GABA signaling. *Front Cell Neurosci, 7*, 177. doi:10.3389/fncel.2013.00177

Ishii, A., Kang, J. Q., Schornak, C. C., Hernandez, C. C., Shen, W., Watkins, J. C., . . . Hirose, S. (2017). A de novo missense mutation of GABRB2 causes early myoclonic encephalopathy. *J Med Genet, 54*(3), 202-211. doi:10.1136/jmedgenet-2016-104083

Janve, V. S., Hernandez, C. C., Verdier, K. M., Hu, N., & Macdonald, R. L. (2016). Epileptic encephalopathy de novo GABRB mutations impair GABAA receptor function. *Ann Neurol*. doi:10.1002/ana.24631

Jaremko, M., Jaremko, L., Jaipuria, G., Becker, S., & Zweckstetter, M. (2015). Structure of the mammalian TSPO/PBR protein. *Biochem Soc Trans, 43*(4), 566-571. doi:10.1042/bst20150029

Jin, N., Guo, Y., Sun, P., Bell, A., Chintagari, N. R., Bhaskaran, M., . . . Liu, L. (2008). Ionotropic GABA receptor expression in the lung during development. *Gene Expr Patterns, 8*(6), 397-403. doi:10.1016/j.gep.2008.04.008

Johannesen, K., Marini, C., Pfeffer, S., Moller, R. S., Dorn, T., Niturad, C. E., . . . Maljevic, S. (2016). Phenotypic spectrum of GABRA1: From generalized epilepsies to severe epileptic encephalopathies. *Neurology, 87*(11), 1140-1151. doi:10.1212/wnl.0000000000003087

Johnson, W. D., 2nd, Howard, R. J., Trudell, J. R., & Harris, R. A. (2012). The TM2 6' position of GABA(A) receptors mediates alcohol inhibition. *J Pharmacol Exp Ther, 340*(2), 445-456. doi:10.1124/jpet.111.188037

Jones, M. V., & Westbrook, G. L. (1996). The impact of receptor desensitization on fast synaptic transmission. *Trends Neurosci, 19*(3), 96-101.

Kanbayashi, T., Kodama, T., Kondo, H., Satoh, S., Inoue, Y., Chiba, S., . . . Nishino, S. (2009). CSF histamine contents in narcolepsy, idiopathic hypersomnia and obstructive sleep apnea syndrome. *Sleep, 32*(2), 181-187.

Kash, T. L., Jenkins, A., Kelley, J. C., Trudell, J. R., & Harrison, N. L. (2003). Coupling of agonist binding to channel gating in the GABA(A) receptor. *Nature, 421*(6920), 272-275. doi:10.1038/nature01280

Kash, T. L., Trudell, J. R., & Harrison, N. L. (2004). Structural elements involved in activation of the gamma-aminobutyric acid type A (GABAA) receptor. *Biochem Soc Trans, 32*(Pt3), 540-546. doi:10.1042/bst0320540

Kemp, J. A., Marshall, G. R., Wong, E. H., & Woodruff, G. N. (1987). The affinities, potencies and efficacies of some benzodiazepine-receptor agonists, antagonists and inverse-agonists at rat hippocampal GABAA-receptors. *Br J Pharmacol, 91*(3), 601-608.

Keramidas, A., Moorhouse, A. J., French, C. R., Schofield, P. R., & Barry, P. H. (2000). M2 pore mutations convert the glycine receptor channel from being anion- to cation-selective. *Biophys J, 79*(1), 247-259. doi:10.1016/s0006-3495(00)76287-4

Khan, Z., & Trotti, L. M. (2015). Central Disorders of Hypersomnolence: Focus on the Narcolepsies and Idiopathic Hypersomnia. *Chest, 148*(1), 262-273. doi:10.1378/chest.14-1304

Kilpatrick, G. J., McIntyre, M. S., Cox, R. F., Stafford, J. A., Pacofsky, G. J., Lovell, G. G., . . . Tilbrook, G. S. (2007). CNS 7056A Novel Ultra–short-acting Benzodiazepine. *Anesthesiology, 107*(1), 60-66. doi:10.1097/01.anes.0000267503.85085.c0

Kim, Y. S., & Yoon, B. E. (2017). Altered GABAergic Signaling in Brain Disease at Various Stages of Life. *Exp Neurobiol, 26*(3), 122-131. doi:10.5607/en.2017.26.3.122

Kleingoor, C., Wieland, H. A., Korpi, E. R., Seeburg, P. H., & Kettenmann, H. (1993). Current potentiation by diazepam but not GABA sensitivity is determined by a single histidine residue. *Neuroreport, 4*(2), 187-190.

Knoflach, F., Benke, D., Wang, Y., Scheurer, L., Luddens, H., Hamilton, B. J., . . . Benson, J. A. (1996). Pharmacological modulation of the diazepam-insensitive recombinant gamma-

aminobutyric acidA receptors alpha 4 beta 2 gamma 2 and alpha 6 beta 2 gamma 2. *Mol Pharmacol, 50*(5), 1253-1261.

Knoflach, F., Drescher, U., Scheurer, L., Malherbe, P., & Mohler, H. (1993). Full and partial agonism displayed by benzodiazepine receptor ligands at recombinant gamma-aminobutyric acidA receptor subtypes. *J Pharmacol Exp Ther, 266*(1), 385-391.

Knoflach, F., Hernandez, M. C., & Bertrand, D. (2016). GABAA receptor-mediated neurotransmission: Not so simple after all. *Biochem Pharmacol, 115*, 10-17. doi:10.1016/j.bcp.2016.03.014

Kodera, H., Ohba, C., Kato, M., Maeda, T., Araki, K., Tajima, D., . . . Matsumoto, N. (2016). De novo GABRA1 mutations in Ohtahara and West syndromes. *Epilepsia, 57*(4), 566-573. doi:10.1111/epi.13344

Kopp, C., Rudolph, U., Keist, R., & Tobler, I. (2003). Diazepam-induced changes on sleep and the EEG spectrum in mice: role of the alpha3-GABA(A) receptor subtype. *Eur J Neurosci, 17*(10), 2226-2230.

Krasowski, M. D., & Harrison, N. L. (1999). General anaesthetic actions on ligand-gated ion channels. *Cell Mol Life Sci, 55*(10), 1278-1303.

Krasowski, M. D., Nishikawa, K., Nikolaeva, N., Lin, A., & Harrison, N. L. (2001). Methionine 286 in transmembrane domain 3 of the GABAA receptor beta subunit controls a binding cavity for propofol and other alkylphenol general anesthetics. *Neuropharmacology, 41*(8), 952-964.

Krishek, B. J., Moss, S. J., & Smart, T. G. (1996). Homomeric beta 1 gamma-aminobutyric acid A receptor-ion channels: evaluation of pharmacological and physiological properties. *Mol Pharmacol, 49*(3), 494-504.

Kristiansen, U., & Lambert, J. D. (1996). Benzodiazepine and barbiturate ligands modulate responses of cultured hippocampal neurones to the GABAA receptor partial agonist, 4-PIOL. *Neuropharmacology, 35*(9-10), 1181-1191.

Kucken, A. M., Teissere, J. A., Seffinga-Clark, J., Wagner, D. A., & Czajkowski, C. (2003). Structural requirements for imidazobenzodiazepine binding to GABA(A) receptors. *Mol Pharmacol, 63*(2), 289-296.

Kucken, A. M., Wagner, D. A., Ward, P. R., Teissere, J. A., Boileau, A. J., & Czajkowski, C. (2000). Identification of benzodiazepine binding site residues in the gamma2 subunit of the gamma-aminobutyric acid(A) receptor. *Mol Pharmacol, 57*(5), 932-939.

Labrakakis, C., Patt, S., Hartmann, J., & Kettenmann, H. (1998). Functional GABA(A) receptors on human glioma cells. *Eur J Neurosci, 10*(1), 231-238.

Lancel, M., Faulhaber, J., Holsboer, F., & Rupprecht, R. (1996). Progesterone induces changes in sleep comparable to those of agonistic GABAA receptor modulators. *Am J Physiol, 271*(4 Pt 1), E763-772.

Laurie, D. J., Wisden, W., & Seeburg, P. H. (1992). The distribution of thirteen GABAA receptor subunit mRNAs in the rat brain. III. Embryonic and postnatal development. *J Neurosci, 12*(11), 4151-4172.

Lavoie, A. M., & Twyman, R. E. (1996). Direct evidence for diazepam modulation of GABAA receptor microscopic affinity. *Neuropharmacology, 35*(9-10), 1383-1392.

Lee, V., & Maguire, J. (2014). The impact of tonic GABAA receptor-mediated inhibition on neuronal excitability varies across brain region and cell type. *Front Neural Circuits, 8*(3). doi:10.3389/fncir.2014.00003

Levi, S., Le Roux, N., Eugene, E., & Poncer, J. C. (2015). Benzodiazepine ligands rapidly influence GABAA receptor diffusion and clustering at hippocampal inhibitory synapses. *Neuropharmacology, 88*, 199-208. doi:10.1016/j.neuropharm.2014.06.002

Levitan, E. S., Blair, L. A., Dionne, V. E., & Barnard, E. A. (1988). Biophysical and pharmacological properties of cloned GABAA receptor subunits expressed in Xenopus oocytes. *Neuron, 1*(9), 773-781.

Lewter, L. A., Fisher, J. L., Siemian, J. N., Methuku, K. R., Poe, M. M., Cook, J. M., & Li, J. X. (2017). Antinociceptive Effects of a Novel alpha2/alpha3-Subtype Selective GABAA Receptor Positive Allosteric Modulator. *ACS Chem Neurosci, 8*(6), 1305-1312. doi:10.1021/acschemneuro.6b00447

Li, G. D., Chiara, D. C., Sawyer, G. W., Husain, S. S., Olsen, R. W., & Cohen, J. B. (2006). Identification of a GABAA receptor anesthetic binding site at subunit interfaces by photolabeling with an etomidate analog. *J Neurosci, 26*(45), 11599-11605. doi:10.1523/jneurosci.3467-06.2006

Li, P., Bracamontes, J. R., Manion, B. D., Mennerick, S., Steinbach, J. H., Evers, A. S., & Akk, G. (2014). The neurosteroid 5beta-pregnan-3alpha-ol-20-one enhances actions of etomidate as a positive allosteric modulator of alpha1beta2gamma2L GABAA receptors. *Br J Pharmacol, 171*(23), 5446-5457. doi:10.1111/bph.12861

Lin, Y. C., Boone, M., Meuris, L., Lemmens, I., Van Roy, N., Soete, A., . . . Callewaert, N. (2014). Genome dynamics of the human embryonic kidney 293 lineage in response to cell biology manipulations. *Nat Commun, 5*, 4767. doi:10.1038/ncomms5767

Lipton, S. A., & Nicotera, P. (1998). Calcium, free radicals and excitotoxins in neuronal apoptosis. *Cell Calcium, 23*(2-3), 165-171.

Low, K., Crestani, F., Keist, R., Benke, D., Brunig, I., Benson, J. A., . . . Rudolph, U. (2000). Molecular and neuronal substrate for the selective attenuation of anxiety. *Science, 290*(5489), 131-134.

Luddens, H., Pritchett, D. B., Kohler, M., Killisch, I., Keinanen, K., Monyer, H., . . . Seeburg, P. H. (1990). Cerebellar GABAA receptor selective for a behavioural alcohol antagonist. *Nature, 346*(6285), 648-651. doi:10.1038/346648a0

Luddens, H., Seeburg, P. H., & Korpi, E. R. (1994). Impact of beta and gamma variants on ligand-binding properties of gamma-aminobutyric acid type A receptors. *Mol Pharmacol, 45*(5), 810-814.

Luscher, B. P., Baur, R., Goeldner, M., & Sigel, E. (2012). Influence of GABA(A) receptor alpha subunit isoforms on the benzodiazepine binding site. *PLoS One, 7*(7), e42101. doi:10.1371/journal.pone.0042101

Luu, T., Cromer, B., Gage, P. W., & Tierney, M. L. (2005). A role for the 2' residue in the second transmembrane helix of the GABA A receptor gamma2S subunit in channel conductance and gating. *J Membr Biol, 205*(1), 17-28. doi:10.1007/s00232-005-0759-2

Macdonald, R. L., Kang, J. Q., & Gallagher, M. J. (2010). Mutations in GABAA receptor subunits associated with genetic epilepsies. *J Physiol, 588*(Pt 11), 1861-1869. doi:10.1113/jphysiol.2010.186999

Macdonald, R. L., Kang, J. Q., & Gallagher, M. J. (2012). GABAA Receptor Subunit Mutations and Genetic Epilepsies. In J. L. Noebels, M. Avoli, M. A. Rogawski, R. W. Olsen, & A. V. Delgado-Escueta (Eds.), *Jasper's Basic Mechanisms of the Epilepsies*. Bethesda (MD): National Center for Biotechnology Information (US)

Michael A Rogawski, Antonio V Delgado-Escueta, Jeffrey L Noebels, Massimo Avoli and Richard W Olsen.

Malamed, S. F. (2010). chapter 25 - Pharmacology *Sedation (Fifth Edition)* (pp. 316-354). Saint Louis: Mosby.

Martin, D. L., & Olsen, R. W. (2000). *GABA in the Nervous System: The View at Fifty Years*: Lippincott Williams & Wilkins.

Mayer, G., Benes, H., Young, P., Bitterlich, M., & Rodenbeck, A. (2015). Modafinil in the treatment of idiopathic hypersomnia without long sleep time--a randomized, double-blind, placebo-controlled study. *J Sleep Res, 24*(1), 74-81. doi:10.1111/jsr.12201

McClellan, A. M., & Twyman, R. E. (1999). Receptor system response kinetics reveal functional subtypes of native murine and recombinant human GABAA receptors. *J Physiol, 515 (Pt 3)*, 711-727.

McKernan, R. M., Rosahl, T. W., Reynolds, D. S., Sur, C., Wafford, K. A., Atack, J. R., . . . Whiting, P. J. (2000). Sedative but not anxiolytic properties of benzodiazepines are mediated by the GABA(A) receptor alpha1 subtype. *Nat Neurosci, 3*(6), 587-592. doi:10.1038/75761

Mendelson, W. B., & Basile, A. S. (2001). The hypnotic actions of the fatty acid amide, oleamide. *Neuropsychopharmacology, 25*(5 Suppl), S36-39. doi:10.1016/s0893-133x(01)00341-4

Michalowski, M. A., Kraszewski, S., & Mozrzymas, J. W. (2017). Binding site opening by loop C shift and chloride ion-pore interaction in the GABAA receptor model. *Phys Chem Chem Phys*. doi:10.1039/c7cp00582b

Miller, P. S., & Aricescu, A. R. (2014). Crystal structure of a human GABAA receptor. *Nature, 512*(7514), 270-275. doi:10.1038/nature13293

Mohler, H. (2006). GABA(A) receptor diversity and pharmacology. *Cell Tissue Res, 326*(2), 505-516. doi:10.1007/s00441-006-0284-3

Mohler, H. (2015). The legacy of the benzodiazepine receptor: from flumazenil to enhancing cognition in Down syndrome and social interaction in autism. *Adv Pharmacol, 72*, 1-36. doi:10.1016/bs.apha.2014.10.008

Moller, R. S., Wuttke, T. V., Helbig, I., Marini, C., Johannesen, K. M., Brilstra, E. H., . . . Maljevic, S. (2017). Mutations in GABRB3: From febrile seizures to epileptic encephalopathies. *Neurology, 88*(5), 483-492. doi:10.1212/wnl.0000000000003565

Moody, O. A., Talwar, S., Jenkins, M. A., Freeman, A. A., Trotti, L. M., Garcia, P. S., . . . Jenkins, A. (2017). Rigor, Reproducibility and in vitro CSF assays: The Devil in the Details. *Ann Neurol*. doi:10.1002/ana.24940

Morlock, E. V., & Czajkowski, C. (2011). Different residues in the GABAA receptor benzodiazepine binding pocket mediate benzodiazepine efficacy and binding. *Mol Pharmacol, 80*(1), 14-22. doi:10.1124/mol.110.069542

Morris, G. P., Clark, I. A., & Vissel, B. (2014). Inconsistencies and controversies surrounding the amyloid hypothesis of Alzheimer's disease. *Acta Neuropathol Commun, 2*, 135. doi:10.1186/s40478-014-0135-5

Nardou, R., Ferrari, D. C., & Ben-Ari, Y. (2013). Mechanisms and effects of seizures in the immature brain. *Semin Fetal Neonatal Med, 18*(4), 175-184. doi:10.1016/j.siny.2013.02.003

O'Shea, S. M., & Harrison, N. L. (2000). Arg-274 and Leu-277 of the gamma-aminobutyric acid type A receptor alpha 2 subunit define agonist efficacy and potency. *J Biol Chem, 275*(30), 22764-22768. doi:10.1074/jbc.M001299200

O'Shea, S. M., Williams, C. A., & Jenkins, A. (2009). Inverse effects on gating and modulation caused by a mutation in the M2-M3 Linker of the GABA(A) receptor gamma subunit. *Mol Pharmacol, 76*(3), 641-651. doi:10.1124/mol.109.055111

O'Toole, K. K., & Jenkins, A. (2011). Discrete M3-M4 intracellular loop subdomains control specific aspects of gamma-aminobutyric acid type A receptor function. *J Biol Chem, 286*(44), 37990-37999. doi:10.1074/jbc.M111.258012

O'Toole, K. K., & Jenkins, A. (2012). The apparent voltage dependence of GABAA receptor activation and modulation is inversely related to channel open probability. *Mol Pharmacol, 81*(2), 189-197. doi:10.1124/mol.111.074476

Olfson, M., King, M., & Schoenbaum, M. (2015). Benzodiazepine use in the United States. *JAMA Psychiatry, 72*(2), 136-142. doi:10.1001/jamapsychiatry.2014.1763

Olkkola, K. T., & Ahonen, J. (2008). Midazolam and other benzodiazepines. *Handb Exp Pharmacol*(182), 335-360. doi:10.1007/978-3-540-74806-9_16

Olsen, R. W., & Sieghart, W. (2008). International Union of Pharmacology. LXX. Subtypes of gamma-aminobutyric acid(A) receptors: classification on the basis of subunit composition, pharmacology, and function. Update. *Pharmacol Rev, 60*(3), 243-260. doi:10.1124/pr.108.00505

Olson, H. E., Poduri, A., & Pearl, P. L. (2014). Genetic forms of epilepsies and other paroxysmal disorders. *Semin Neurol, 34*(3), 266-279. doi:10.1055/s-0034-1386765

Ong, J., & Kerr, D. I. (1990). GABA-receptors in peripheral tissues. *Life Sci, 46*(21), 1489-1501.

Oreskovic, D., & Klarica, M. (2010). The formation of cerebrospinal fluid: nearly a hundred years of interpretations and misinterpretations. *Brain Res Rev, 64*(2), 241-262. doi:10.1016/j.brainresrev.2010.04.006

Otis, T. S., & Mody, I. (1992). Modulation of decay kinetics and frequency of GABAA receptor-mediated spontaneous inhibitory postsynaptic currents in hippocampal neurons. *Neuroscience, 49*(1), 13-32.

Owens, D. F., & Kriegstein, A. R. (2002). Is there more to GABA than synaptic inhibition? *Nat Rev Neurosci, 3*(9), 715-727. doi:10.1038/nrn919

Papandreou, A., McTague, A., Trump, N., Ambegaonkar, G., Ngoh, A., Meyer, E., . . . Kurian, M. A. (2016). GABRB3 mutations: a new and emerging cause of early infantile epileptic encephalopathy. *Dev Med Child Neurol, 58*(4), 416-420. doi:10.1111/dmcn.12976

Perez-Alcazar, M., Culley, G., Lyckenvik, T., Mobarrez, K., Bjorefeldt, A., Wasling, P., . . . Illes, S. (2016). Human Cerebrospinal Fluid Promotes Neuronal Viability and Activity of Hippocampal Neuronal Circuits In Vitro. *Front Cell Neurosci, 10*, 54. doi:10.3389/fncel.2016.00054

Persson, M. P., Nilsson, A., & Hartvig, P. (1988). Relation of sedation and amnesia to plasma concentrations of midazolam in surgical patients. *Clin Pharmacol Ther, 43*(3), 324-331.

Persson, P., Nilsson, A., Hartvig, P., & Tamsen, A. (1987). Pharmacokinetics of midazolam in total i.v. anaesthesia. *Br J Anaesth, 59*(5), 548-556.

Petroski, R. E., Pomeroy, J. E., Das, R., Bowman, H., Yang, W., Chen, A. P., & Foster, A. C. (2006). Indiplon is a high-affinity positive allosteric modulator with selectivity for alpha1 subunit-containing GABAA receptors. *J Pharmacol Exp Ther, 317*(1), 369-377. doi:10.1124/jpet.105.096701

Pieri, L. (1983). Preclinical pharmacology of midazolam. *Br J Clin Pharmacol, 16 Suppl 1*, 17s-27s.

Pirker, S., Schwarzer, C., Wieselthaler, A., Sieghart, W., & Sperk, G. (2000). GABA A receptors: immunocytochemical distribution of 13 subunits in the adult rat brain. *Neuroscience, 101*(4), 815-850.

Pompeiano, M., Cirelli, C., Arrighi, P., & Tononi, G. (1995). c-Fos expression during wakefulness and sleep. *Neurophysiol Clin, 25*(6), 329-341. doi:10.1016/0987-7053(96)84906-9

Poncer, J. C., Durr, R., Gahwiler, B. H., & Thompson, S. M. (1996). Modulation of synaptic GABAA receptor function by benzodiazepines in area CA3 of rat hippocampal slice cultures. *Neuropharmacology, 35*(9-10), 1169-1179.

Pritchett, D. B., Luddens, H., & Seeburg, P. H. (1989). Type I and type II GABAA-benzodiazepine receptors produced in transfected cells. *Science, 245*(4924), 1389-1392.

Pritchett, D. B., & Seeburg, P. H. (1990). Gamma-aminobutyric acidA receptor alpha 5-subunit creates novel type II benzodiazepine receptor pharmacology. *J Neurochem, 54*(5), 1802-1804.

Pritchett, D. B., Sontheimer, H., Gorman, C. M., Kettenmann, H., Seeburg, P. H., & Schofield, P. R. (1988). Transient expression shows ligand gating and allosteric potentiation of GABAA receptor subunits. *Science, 242*(4883), 1306-1308.

Pritchett, D. B., Sontheimer, H., Shivers, B. D., Ymer, S., Kettenmann, H., Schofield, P. R., & Seeburg, P. H. (1989). Importance of a novel GABAA receptor subunit for benzodiazepine pharmacology. *Nature, 338*(6216), 582-585. doi:10.1038/338582a0

Puia, G., Vicini, S., Seeburg, P. H., & Costa, E. (1991). Influence of recombinant gamma-aminobutyric acid-A receptor subunit composition on the action of allosteric modulators of gamma-aminobutyric acid-gated Cl- currents. *Mol Pharmacol, 39*(6), 691-696.

Quirk, K., Gillard, N. P., Ragan, C. I., Whiting, P. J., & McKernan, R. M. (1994). gamma-Aminobutyric acid type A receptors in the rat brain can contain both gamma 2 and gamma 3 subunits, but gamma 1 does not exist in combination with another gamma subunit. *Mol Pharmacol, 45*(6), 1061-1070.

Renard, S., Olivier, A., Granger, P., Avenet, P., Graham, D., Sevrin, M., . . . Besnard, F. (1999). Structural elements of the gamma-aminobutyric acid type A receptor conferring subtype selectivity for benzodiazepine site ligands. *J Biol Chem, 274*(19), 13370-13374.

Richter, C., Woods, I. G., & Schier, A. F. (2014). Neuropeptidergic control of sleep and wakefulness. *Annu Rev Neurosci, 37*, 503-531. doi:10.1146/annurev-neuro-062111-150447

Rio, D. C., Clark, S. G., & Tjian, R. (1985). A mammalian host-vector system that regulates expression and amplification of transfected genes by temperature induction. *Science, 227*(4682), 23-28.

Rogers, C. J., Twyman, R. E., & Macdonald, R. L. (1994). Benzodiazepine and beta-carboline regulation of single GABAA receptor channels of mouse spinal neurones in culture. *J Physiol, 475*(1), 69-82.

Roth, B. (1976). Narcolepsy and hypersomnia: review and classification of 642 personally observed cases. *Schweiz Arch Neurol Neurochir Psychiatr, 119*(1), 31-41.

Rothstein, J. D., Guidotti, A., Tinuper, P., Cortelli, P., Avoni, P., Plazzi, G., . . . Montagna, P. (1992). Endogenous benzodiazepine receptor ligands in idiopathic recurring stupor. *Lancet, 340*(8826), 1002-1004.

Rovira, C., & Ben-Ari, Y. (1999). Developmental study of miniature IPSCs of CA3 hippocampal cells: modulation by midazolam. *Brain Res Dev Brain Res, 114*(1), 79-88.

Rudolph, U., Crestani, F., Benke, D., Brunig, I., Benson, J. A., Fritschy, J. M., . . . Mohler, H. (1999). Benzodiazepine actions mediated by specific gamma-aminobutyric acid(A) receptor subtypes. *Nature, 401*(6755), 796-800. doi:10.1038/44579

Rudolph, U., Crestani, F., & Mohler, H. (2001). GABA(A) receptor subtypes: dissecting their pharmacological functions. *Trends Pharmacol Sci, 22*(4), 188-194.

Rudolph, U., & Knoflach, F. (2011). Beyond classical benzodiazepines: novel therapeutic potential of GABAA receptor subtypes. *Nat Rev Drug Discov, 10*(9), 685-697. doi:10.1038/nrd3502

Rudolph, U., & Mohler, H. (2004). Analysis of GABAA receptor function and dissection of the pharmacology of benzodiazepines and general anesthetics through mouse genetics. *Annu Rev Pharmacol Toxicol, 44*, 475-498. doi:10.1146/annurev.pharmtox.44.101802.121429

Ruffolo, G., Iyer, A., Cifelli, P., Roseti, C., Muhlebner, A., van Scheppingen, J., . . . Palma, E. (2016). Functional aspects of early brain development are preserved in tuberous sclerosis complex (TSC) epileptogenic lesions. *Neurobiol Dis, 95*, 93-101. doi:10.1016/j.nbd.2016.07.014

Rusch, D., & Forman, S. A. (2005). Classic benzodiazepines modulate the open-close equilibrium in alpha1beta2gamma2L gamma-aminobutyric acid type A receptors. *Anesthesiology, 102*(4), 783-792.

Rye, D. B., Bliwise, D. L., Parker, K., Trotti, L. M., Saini, P., Fairley, J., . . . Jenkins, A. (2012). Modulation of vigilance in the primary hypersomnias by endogenous enhancement of GABAA receptors. *Sci Transl Med, 4*(161), 161ra151. doi:10.1126/scitranslmed.3004685

Safavynia, S. A., Keating, G., Speigel, I., Fidler, J. A., Kreuzer, M., Rye, D. B., . . . Garcia, P. S. (2016). Effects of gamma-Aminobutyric Acid Type A Receptor Modulation by Flumazenil on Emergence from General Anesthesia. *Anesthesiology, 125*(1), 147-158. doi:10.1097/aln.0000000000001134

Sakka, L., Coll, G., & Chazal, J. (2011). Anatomy and physiology of cerebrospinal fluid. *Eur Ann Otorhinolaryngol Head Neck Dis, 128*(6), 309-316. doi:10.1016/j.anorl.2011.03.002

Sancar, F., Ericksen, S. S., Kucken, A. M., Teissere, J. A., & Czajkowski, C. (2007). Structural determinants for high-affinity zolpidem binding to GABA-A receptors. *Mol Pharmacol, 71*(1), 38-46. doi:10.1124/mol.106.029595

Sanger, D. J., Morel, E., & Perrault, G. (1996). Comparison of the pharmacological profiles of the hypnotic drugs, zaleplon and zolpidem. *Eur J Pharmacol, 313*(1-2), 35-42.

Sawyer, G. W., Chiara, D. C., Olsen, R. W., & Cohen, J. B. (2002). Identification of the bovine gamma-aminobutyric acid type A receptor alpha subunit residues photolabeled by the imidazobenzodiazepine [3H]Ro15-4513. *J Biol Chem, 277*(51), 50036-50045. doi:10.1074/jbc.M209281200

Schaerer, M. T., Buhr, A., Baur, R., & Sigel, E. (1998). Amino acid residue 200 on the alpha1 subunit of GABA(A) receptors affects the interaction with selected benzodiazepine binding site ligands. *Eur J Pharmacol, 354*(2-3), 283-287.

Scharfman, H. E. (2007). The neurobiology of epilepsy. *Curr Neurol Neurosci Rep, 7*(4), 348-354.

Sengupta, S., Weeraratne, S. D., Sun, H., Phallen, J., Rallapalli, S. K., Teider, N., . . . Cho, Y. J. (2014). alpha5-GABAA receptors negatively regulate MYC-amplified medulloblastoma growth. *Acta Neuropathol, 127*(4), 593-603. doi:10.1007/s00401-013-1205-7

Serwanski, D. R., Miralles, C. P., Christie, S. B., Mehta, A. K., Li, X., & De Blas, A. L. (2006). Synaptic and nonsynaptic localization of GABAA receptors containing the alpha5 subunit in the rat brain. *J Comp Neurol, 499*(3), 458-470. doi:10.1002/cne.21115

Shen, D., Hernandez, C. C., Shen, W., Hu, N., Poduri, A., Shiedley, B., . . . Macdonald, R. L. (2017). De novo GABRG2 mutations associated with epileptic encephalopathies. *Brain, 140*(Pt 1), 49-67. doi:10.1093/brain/aww272

Sieghart, W. (1995a). Structure and pharmacology of gamma-aminobutyric acidA receptor subtypes. *Pharmacol Rev, 47*(2), 181-234.

Sieghart, W. (1995b). Structure and pharmacology of γ-aminobutyric acidA receptor subtypes. *Pharmacol Rev, 47*(2), 181-234. Retrieved from https://www.scopus.com/inward/record.uri?eid=2-s2.0-0028981088&partnerID=40&md5=f81378f23bb11e755445cbfd5fd9595e

Sieghart, W., Fuchs, K., Tretter, V., Ebert, V., Jechlinger, M., Hoger, H., & Adamiker, D. (1999). Structure and subunit composition of GABA(A) receptors. *Neurochem Int, 34*(5), 379-385.

Sigel, E., & Baur, R. (1988). Allosteric modulation by benzodiazepine receptor ligands of the GABAA receptor channel expressed in Xenopus oocytes. *J Neurosci, 8*(1), 289-295.

Sigel, E., Schaerer, M. T., Buhr, A., & Baur, R. (1998). The benzodiazepine binding pocket of recombinant alpha1beta2gamma2 gamma-aminobutyric acidA receptors: relative orientation of ligands and amino acid side chains. *Mol Pharmacol, 54*(6), 1097-1105.

Sigel, E., Stephenson, F. A., Mamalaki, C., & Barnard, E. A. (1983). A gamma-aminobutyric acid/benzodiazepine receptor complex of bovine cerebral cortex. *J Biol Chem, 258*(11), 6965-6971.

Siso, S., Jeffrey, M., & Gonzalez, L. (2010). Sensory circumventricular organs in health and disease. *Acta Neuropathol, 120*(6), 689-705. doi:10.1007/s00401-010-0743-5

Sizemore, G. M., Sizemore, S. T., Seachrist, D. D., & Keri, R. A. (2014). GABA(A) receptor pi (GABRP) stimulates basal-like breast cancer cell migration through activation of extracellular-regulated kinase 1/2 (ERK1/2). *J Biol Chem, 289*(35), 24102-24113. doi:10.1074/jbc.M114.593582

Smith, G. B., & Olsen, R. W. (1995). Functional domains of GABAA receptors. *Trends Pharmacol Sci, 16*(5), 162-168.

Smith, T. A. (2001). Type A gamma-aminobutyric acid (GABAA) receptor subunits and benzodiazepine binding: significance to clinical syndromes and their treatment. *Br J Biomed Sci, 58*(2), 111-121.

Spector, R., Robert Snodgrass, S., & Johanson, C. E. (2015). A balanced view of the cerebrospinal fluid composition and functions: Focus on adult humans. *Exp Neurol, 273*, 57-68. doi:10.1016/j.expneurol.2015.07.027

Stephenson, F. A., Watkins, A. E., & Olsen, R. W. (1982). Physicochemical characterization of detergent-solubilized gamma-aminobutyric acid and benzodiazepine receptor proteins from bovine brain. *Eur J Biochem, 123*(2), 291-298.

Stevenson, A., Wingrove, P. B., Whiting, P. J., & Wafford, K. A. (1995). beta-Carboline gamma-aminobutyric acidA receptor inverse agonists modulate gamma-aminobutyric acid via the loreclezole binding site as well as the benzodiazepine site. *Mol Pharmacol, 48*(6), 965-969.

Strakhova, M. I., Harvey, S. C., Cook, C. M., Cook, J. M., & Skolnick, P. (2000). A single amino acid residue on the alpha(5) subunit (Ile215) is essential for ligand selectivity at alpha(5)beta(3)gamma(2) gamma-aminobutyric acid(A) receptors. *Mol Pharmacol, 58*(6), 1434-1440.

Study, R. E., & Barker, J. L. (1981). Diazepam and (--)-pentobarbital: fluctuation analysis reveals different mechanisms for potentiation of gamma-aminobutyric acid responses in cultured central neurons. *Proc Natl Acad Sci U S A, 78*(11), 7180-7184.

Sundstrom-Poromaa, I., Smith, D. H., Gong, Q. H., Sabado, T. N., Li, X., Light, A., . . . Smith, S. S. (2002). Hormonally regulated alpha(4)beta(2)delta GABA(A) receptors are a target for alcohol. *Nat Neurosci, 5*(8), 721-722. doi:10.1038/nn888

Sundstrom, I., Ashbrook, D., & Backstrom, T. (1997). Reduced benzodiazepine sensitivity in patients with premenstrual syndrome: a pilot study. *Psychoneuroendocrinology, 22*(1), 25-38.

Sundstrom Poromaa, I., Smith, S., & Gulinello, M. (2003). GABA receptors, progesterone and premenstrual dysphoric disorder. *Arch Womens Ment Health, 6*(1), 23-41. doi:10.1007/s00737-002-0147-1

Tan, K. R., Gonthier, A., Baur, R., Ernst, M., Goeldner, M., & Sigel, E. (2007). Proximity-accelerated chemical coupling reaction in the benzodiazepine-binding site of gamma-

aminobutyric acid type A receptors: superposition of different allosteric modulators. *J Biol Chem, 282*(36), 26316-26325. doi:10.1074/jbc.M702153200

Thomas, P., & Smart, T. G. (2005). HEK293 cell line: a vehicle for the expression of recombinant proteins. *J Pharmacol Toxicol Methods, 51*(3), 187-200. doi:10.1016/j.vascn.2004.08.014

Thomas, P., & Smart, T. G. (2012). Use of electrophysiological methods in the study of recombinant and native neuronal ligand-gated ion channels. *Curr Protoc Pharmacol, Chapter 11*, Unit 11.14. doi:10.1002/0471141755.ph1104s59

Thompson, S. A., Whiting, P. J., & Wafford, K. A. (1996). Barbiturate interactions at the human GABAA receptor: dependence on receptor subunit combination. *Br J Pharmacol, 117*(3), 521-527.

Tierney, M. L., Birnir, B., Cromer, B., Howitt, S. M., Gage, P. W., & Cox, G. B. (1998). Two threonine residues in the M2 segment of the alpha 1 beta 1 GABAA receptor are critical for ion channel function. *Receptors Channels, 5*(2), 113-124.

Tierney, M. L., Birnir, B., Pillai, N. P., Clements, J. D., Howitt, S. M., Cox, G. B., & Gage, P. W. (1996). Effects of mutating leucine to threonine in the M2 segment of alpha1 and beta1 subunits of GABAA alpha1beta1 receptors. *J Membr Biol, 154*(1), 11-21.

Tobias, J. D., & Leder, M. (2011). Procedural sedation: A review of sedative agents, monitoring, and management of complications. *Saudi Journal of Anaesthesia, 5*(4), 395-410. doi:10.4103/1658-354X.87270

Trotti, L. M., Saini, P., Freeman, A. A., Bliwise, D. L., Garcia, P. S., Jenkins, A., & Rye, D. B. (2013). Improvement in daytime sleepiness with clarithromycin in patients with GABA-related hypersomnia: Clinical experience. *J Psychopharmacol, 28*(7), 697-702. doi:10.1177/0269881113515062

Trotti, L. M., Saini, P., Freeman, A. A., Bliwise, D. L., Garcia, P. S., Jenkins, A., & Rye, D. B. (2014). Improvement in daytime sleepiness with clarithromycin in patients with GABA-related hypersomnia: Clinical experience. *J Psychopharmacol, 28*(7), 697-702. doi:10.1177/0269881113515062

Trotti, L. M., Saini, P., Koola, C., LaBarbera, V., Bliwise, D. L., & Rye, D. B. (2016). Flumazenil for the Treatment of Refractory Hypersomnolence: Clinical Experience with 153 Patients. *J Clin Sleep Med, 12*(10), 1389-1394. doi:10.5664/jcsm.6196

Trudell, J. R., Yue, M. E., Bertaccini, E. J., Jenkins, A., & Harrison, N. L. (2008). Molecular modeling and mutagenesis reveals a tetradentate binding site for Zn2+ in GABA(A) alphabeta receptors and provides a structural basis for the modulating effect of the gamma subunit. *J Chem Inf Model, 48*(2), 344-349. doi:10.1021/ci700324a

Tung, A., Bluhm, B., & Mendelson, W. B. (2001). Sleep inducing effects of propofol microinjection into the medial preoptic area are blocked by flumazenil. *Brain Res, 908*(2), 155-160.

Ueno, S., Lin, A., Nikolaeva, N., Trudell, J. R., Mihic, S. J., Harris, R. A., & Harrison, N. L. (2000). Tryptophan scanning mutagenesis in TM2 of the GABA(A) receptor alpha subunit: effects on channel gating and regulation by ethanol. *Br J Pharmacol, 131*(2), 296-302. doi:10.1038/sj.bjp.0703504

Unterberger, I., Gabelia, D., Prieschl, M., Chea, K., Hofer, M., Hogl, B., . . . Frauscher, B. (2015). Sleep disorders and circadian rhythm in epilepsy revisited: a prospective controlled study. *Sleep Med, 16*(2), 237-242. doi:10.1016/j.sleep.2014.09.021

Unwin, N. (1995). Acetylcholine receptor channel imaged in the open state. *Nature, 373*(6509), 37-43. Retrieved from http://dx.doi.org/10.1038/373037a0

Unwin, N. (2005). Refined structure of the nicotinic acetylcholine receptor at 4A resolution. *J Mol Biol, 346*(4), 967-989. doi:10.1016/j.jmb.2004.12.031

van Rijnsoever, C., Tauber, M., Choulli, M. K., Keist, R., Rudolph, U., Mohler, H., . . . Crestani, F. (2004). Requirement of alpha5-GABAA receptors for the development of tolerance to the sedative action of diazepam in mice. *J Neurosci, 24*(30), 6785-6790. doi:10.1523/jneurosci.1067-04.2004

Verdoorn, T. A., Draguhn, A., Ymer, S., Seeburg, P. H., & Sakmann, B. (1990). Functional properties of recombinant rat GABAA receptors depend upon subunit composition. *Neuron, 4*(6), 919-928.

Wafford, K. A., Thompson, S. A., Thomas, D., Sikela, J., Wilcox, A. S., & Whiting, P. J. (1996). Functional characterization of human gamma-aminobutyric acidA receptors containing the alpha 4 subunit. *Mol Pharmacol, 50*(3), 670-678.

Walters, R. J., Hadley, S. H., Morris, K. D., & Amin, J. (2000). Benzodiazepines act on GABAA receptors via two distinct and separable mechanisms. *Nat Neurosci, 3*(12), 1274-1281. doi:10.1038/81800

Wang, D. S., Lu, S. Y., Hong, Z., & Zhu, H. L. (2003). Biphasic action of midazolam on GABAA receptor-mediated responses in rat sacral dorsal commissural neurons. *Biochem Biophys Res Commun, 309*(4), 893-899.

Wang, J., Shen, D., Xia, G., Shen, W., Macdonald, R. L., Xu, D., & Kang, J. Q. (2016). Differential protein structural disturbances and suppression of assembly partners produced by nonsense GABRG2 epilepsy mutations: implications for disease phenotypic heterogeneity. *Sci Rep, 6*, 35294. doi:10.1038/srep35294

Wang, Q., Pless, S. A., & Lynch, J. W. (2010). Ligand- and subunit-specific conformational changes in the ligand-binding domain and the TM2-TM3 linker of {alpha}1 {beta}2 {gamma}2 GABAA receptors. *J Biol Chem, 285*(51), 40373-40386. doi:10.1074/jbc.M110.161513

Watanabe, M., & Fukuda, A. (2015). Development and regulation of chloride homeostasis in the central nervous system. *Front Cell Neurosci, 9*, 371. doi:10.3389/fncel.2015.00371

Whiting, P., McKernan, R. M., & Iversen, L. L. (1990). Another mechanism for creating diversity in gamma-aminobutyrate type A receptors: RNA splicing directs expression of two forms of gamma 2 phosphorylation site. *Proc Natl Acad Sci U S A, 87*(24), 9966-9970.

Whiting, P. J., McKernan, R. M., & Wafford, K. A. (1995). Structure and pharmacology of vertebrate GABAA receptor subtypes. *Int Rev Neurobiol, 38*, 95-138.

Whittemore, E. R., Yang, W., Drewe, J. A., & Woodward, R. M. (1996). Pharmacology of the human gamma-aminobutyric acidA receptor alpha 4 subunit expressed in Xenopus laevis oocytes. *Mol Pharmacol, 50*(5), 1364-1375.

Wieland, H. A., & Luddens, H. (1994). Four amino acid exchanges convert a diazepam-insensitive, inverse agonist-preferring GABAA receptor into a diazepam-preferring GABAA receptor. *J Med Chem, 37*(26), 4576-4580.

Wieland, H. A., Lüddens, H., & Seeburg, P. H. (1992). A single histidine in GABAA receptors is essential for benzodiazepine agonist binding. *Journal of Biological Chemistry, 267*(3), 1426-1429. Retrieved from http://www.jbc.org/content/267/3/1426.abstract

Wieland, M., & Hartig, J. S. (2007). RNA quadruplex-based modulation of gene expression. *Chem Biol, 14*(7), 757-763. doi:10.1016/j.chembiol.2007.06.005

Williams, C. A., Bell, S. V., & Jenkins, A. (2010). A residue in loop 9 of the beta2-subunit stabilizes the closed state of the GABAA receptor. *J Biol Chem, 285*(10), 7281-7287. doi:10.1074/jbc.M109.050294

Wingrove, P. B., Safo, P., Wheat, L., Thompson, S. A., Wafford, K. A., & Whiting, P. J. (2002). Mechanism of alpha-subunit selectivity of benzodiazepine pharmacology at gamma-aminobutyric acid type A receptors. *Eur J Pharmacol, 437*(1-2), 31-39.

Winsky-Sommerer, R. (2009). Role of GABAA receptors in the physiology and pharmacology of sleep. *Eur J Neurosci, 29*(9), 1779-1794. doi:10.1111/j.1460-9568.2009.06716.x

Wisden, W., Herb, A., Wieland, H., Keinanen, K., Luddens, H., & Seeburg, P. H. (1991). Cloning, pharmacological characteristics and expression pattern of the rat GABAA receptor alpha 4 subunit. *FEBS Lett, 289*(2), 227-230.

Xie, L., Kang, H., Xu, Q., Chen, M. J., Liao, Y., Thiyagarajan, M., . . . Nedergaard, M. (2013). Sleep drives metabolite clearance from the adult brain. *Science, 342*(6156), 373-377. doi:10.1126/science.1241224

Xu, M., & Akabas, M. H. (1996). Identification of channel-lining residues in the M2 membrane-spanning segment of the GABA(A) receptor alpha1 subunit. *J Gen Physiol, 107*(2), 195-205.

Xu, M., Covey, D. F., & Akabas, M. H. (1995). Interaction of picrotoxin with GABAA receptor channel-lining residues probed in cysteine mutants. *Biophys J, 69*(5), 1858-1867. doi:10.1016/s0006-3495(95)80056-1

Yakushiji, T., Fukuda, T., Oyama, Y., & Akaike, N. (1989). Effects of benzodiazepines and non-benzodiazepine compounds on the GABA-induced response in frog isolated sensory neurones. *Br J Pharmacol, 98*(3), 735-740.

Yee, B. K., Hauser, J., Dolgov, V. V., Keist, R., Mohler, H., Rudolph, U., & Feldon, J. (2004). GABA receptors containing the alpha5 subunit mediate the trace effect in aversive and appetitive conditioning and extinction of conditioned fear. *Eur J Neurosci, 20*(7), 1928-1936. doi:10.1111/j.1460-9568.2004.03642.x

Yip, G. M., Chen, Z. W., Edge, C. J., Smith, E. H., Dickinson, R., Hohenester, E., . . . Franks, N. P. (2013). A propofol binding site on mammalian GABAA receptors identified by photolabeling. *Nat Chem Biol, 9*(11), 715-720. doi:10.1038/nchembio.1340

Yoon, B. E., & Lee, C. J. (2014). GABA as a rising gliotransmitter. *Front Neural Circuits, 8*, 141. doi:10.3389/fncir.2014.00141

Yost, C. S., Hampson, A. J., Leonoudakis, D., Koblin, D. D., Bornheim, L. M., & Gray, A. T. (1998). Oleamide potentiates benzodiazepine-sensitive gamma-aminobutyric acid receptor activity but does not alter minimum alveolar anesthetic concentration. *Anesth Analg, 86*(6), 1294-1300.

Yu, S. P., & Kerchner, G. A. (1998). Endogenous voltage-gated potassium channels in human embryonic kidney (HEK293) cells. *J Neurosci Res, 52*(5), 612-617. doi:10.1002/(sici)1097-4547(19980601)52:5<612::aid-jnr13>3.0.co;2-3

Yuan, H., Low, C. M., Moody, O. A., Jenkins, A., & Traynelis, S. F. (2015). Ionotropic GABA and Glutamate Receptor Mutations and Human Neurologic Diseases. *Mol Pharmacol, 88*(1), 203-217. doi:10.1124/mol.115.097998

Zhang, P., Zhang, W., Liu, R., Harris, B., Skolnick, P., & Cook, J. M. (1995). Synthesis of novel imidazobenzodiazepines as probes of the pharmacophore for "diazepam-insensitive" GABAA receptors. *J Med Chem, 38*(10), 1679-1688.

Zhang, X., Zhang, R., Zheng, Y., Shen, J., Xiao, D., Li, J., . . . Zhang, H. (2013). Expression of gamma-aminobutyric acid receptors on neoplastic growth and prediction of prognosis in non-small cell lung cancer. *J Transl Med, 11*, 102. doi:10.1186/1479-5876-11-102

Zhao, Y. L., Xiang, Q., Shi, Q. Y., Li, S. Y., Tan, L., Wang, J. T., . . . Luo, A. L. (2011). GABAergic excitotoxicity injury of the immature hippocampal pyramidal neurons' exposure to isoflurane. *Anesth Analg, 113*(5), 1152-1160. doi:10.1213/ANE.0b013e318230b3fd

Zurek, A. A., Yu, J., Wang, D. S., Haffey, S. C., Bridgwater, E. M., Penna, A., . . . Orser, B. A. (2014). Sustained increase in alpha5GABAA receptor function impairs memory after anesthesia. *J Clin Invest, 124*(12), 5437-5441. doi:10.1172/jci76669